

**U.S. GEOLOGICAL SURVEY PROGRAM ON TOXIC
WASTE – GROUND-WATER CONTAMINATION:**

**Proceedings of the second technical meeting,
Cape Cod, Massachusetts, October 21–25, 1985**

Stephen E. Ragone, editor

U.S. GEOLOGICAL SURVEY

Open-File Report 86–481

Reston, Virginia

1988

REPRODUCED FROM BEST AVAILABLE COPY

**DEPARTMENT OF THE INTERIOR
DONALD PAUL HODEL, Secretary**

**U.S. GEOLOGICAL SURVEY
Dallas L. Peck, Director**

For additional information write to:

**Toxic Waste–Ground-Water
Contamination Program
U.S. Geological Survey
410 National Center
Reston, Virginia 22092**

Copies of this report can be purchased from:

**U.S. Geological Survey
Books and Open-File Reports
Box 25425, Bldg. 41
Denver Federal Center
Lakewood, Colorado 80225**

IMPORTANT NOTICE
PRINTED IN THE "NEW PUBLICATIONS OF THE U.S. GEOLOGICAL SURVEY"
LIST 992 - ISSUED IN MARCH 1991

One of the articles listed in Open-file report 86-0481, U.S. Geological Survey program on toxic waste-ground-water contamination; proceedings of the Second technical meeting, Cape Cod, Massachusetts, October 21-25, 1985, edited by S.E. Ragone. 1988. 169 p. (NC, Da, M, Wb.) Microfiche \$4; paper copy \$25.50, announced in the November 1990 New Publications of the U.S. Geological Survey, has been withdrawn by the U.S. Geological Survey.

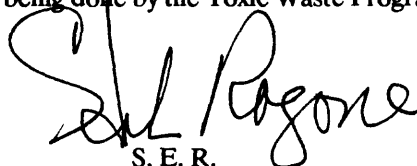
Hydrogeochemistry of uranium and associated elements at abandoned uranium mines in western North Dakota, by R.L. Houghton (senior author) and others, p. E19-E22 is based on falsified data and related technical findings. The falsified data and related technical errors are the responsibility of Mr. Houghton and not the other authors. As is the case with all other U.S. Geological Survey works by Mr. Houghton previously withdrawn, we bring it to your attention because of the possibility that researchers in the field of geochemistry might refer to the data or conclusions.

PREFACE

In October 1985, a meeting was held on Cape Cod, Mass., to review the technical progress of the U.S. Geological Survey's Toxic Waste - Ground-Water Contamination Program. This report provides a brief description of the major components of the program and includes selected abstracts of presentations made that meeting.

The Cape Cod meeting was the Toxic Waste Program's second technical review meeting. The

first meeting was held in Tucson, Ariz., in March 1984; results are described in reports by Hult (1984); Mattraw and Franks (1986); LeBlanc (1984); and Ragone and Sulam (1986). Two other publications (Ragone, 1984, 1986) describe the research being done by the Toxic Waste Program.



S. E. R.

Disclaimer

The use of trade and product names in this report is for identification purposes only and does not constitute endorsement by the U.S. Geological Survey.

REPRODUCED FROM BEST AVAILABLE COPY

CONTENTS

	Page
Preface.....	iii
Toxic Waste – Ground-Water Contamination Program.....	xiii
Basic Research.....	xiii
Point-Source Contamination Research.....	xiii
NonPoint-Source Contamination Research.....	xiv
References Cited.....	xiv
Selected abstracts presented at the Toxic-Waste Meeting.....	xvii

CHAPTER A. – MOVEMENT AND FATE OF CREOSOTE WASTE IN GROUND WATER NEAR AN ABANDONED WOOD-PRESERVING PLANT NEAR PENSACOLA, FLORIDA

Introduction.....	A-3
Preliminary three-dimensional simulation of ground-water flow, by B.J. Franks.....	A-5
Geophysical methods of contaminant detection, by G.R. Olhoeft.....	A-7
Clay mineralogy of sediments associated with a plume of creosote-contaminated ground water, by M.W. Bodine, Jr.....	A-9
Geochemistry of a shallow aquifer contaminated with creosote products, by M.J. Baedecker, B.J. Franks, D.F. Goerlitz, and J.A. Hopple.....	A-17
Reexamination of the occurrence and distribution of creosote compounds in ground water, by D.F. Goerlitz.....	A-21
Determination of the rates of anaerobic degradation of the water-soluble fraction of creosote, by E.M. Godsy and D.F. Goerlitz	
Introduction.....	A-27
Anaerobic degradation.....	A-27
Modeling substrate utilization.....	A-28
Contamination, bioaccumulation, and ecological effects of creosote-derived compounds in the nearshore estuarine environment of Pensacola Bay, Florida, by P.V. Dresler and J.F. Elder ...	A-33

CHAPTER B – FATE AND TRANSPORT OF CONTAMINANTS IN SEWAGE-CONTAMINATED GROUND WATER ON CAPE COD, MASSACHUSETTS

	Page
Introduction.....	B-3
Hydrogeologic controls on solute transport in a plume of sewage-contaminated ground water, by D.R. LeBlanc, S.P. Garabedian, R.D. Quadri, R.H. Morin, W.E. Teasdale, and F.L. Paillet.....	B-7
Design and implementation of a large-scale natural-gradient tracer test, by S.P. Garabedian, D.R. Leblanc, R.D. Quadri, K.M. Hess, K.G. Stollenwerk, and W.W. Wood.....	B-13
Identification of trace organic substances in sewage- contaminated ground water, by L.B. Barber, II, E.M. Thurman, and M.P. Schroeder.....	B-19
Sampling and analysis of volatile organic compounds in a plume of sewage-contaminated ground water, by E.M. Thurman, M.G. Brooks, and L.B. Barber, II.....	B-21

Movement and fate of detergents in sewage-contaminated ground water, by E.M. Thurman and L.B. Barber, II	B-23
Bacterial distribution and transport in a plume of sewage-contaminated ground water, by R.W. Harvey and Leah George	B-25
Nitrate reduction in a sewage-contaminated aquifer, by R.L. Smith and J.H. Duff.....	B-27
Fate of ammonium in a sewage-contaminated ground water, by M.L. Ceazan, R.L. Smith, and E.M. Thurman	B-29

CHAPTER C. – GROUND-WATER CONTAMINATION BY CRUDE OIL AT BEMIDJI, MINNESOTA

	Page
Introduction	C-3
Surficial and subsurface distribution of aquifer sediments at the Bemidji, Minnesota, research site, by D.A. Franzi	
Surficial geomorphology	C-5
Stratigraphy	C-5
Hydrologic aspects	C-9
Hydrogeology and preliminary regional flow modeling at the Bemidji, Minnesota, research site, by R.T. Miller.....	C-11
Inorganic geochemistry of ground water and aquifer matrix: First-year results, by D.I. Siegel, P.C. Bennett, M.J. Baedecker, M.P. Berndt, and D.A. Franzi	C-17
Distribution of gases and hydrocarbon vapors in the unsaturated zone, by M.F. Hult and R.R. Grabbe.....	C-21
Composition and alteration of hydrocarbons in ground water, by R.P. Eganhouse, M.J. Baedecker, Curtis Phinney, and Jessica Hopple.....	C-27
Mass transfer at the alkane-water interface in laboratory columns of porous media, by H.O. Pfannkuch, S.N. Nourse, and M.F. Hult	C-29
Objectives and hypotheses.....	C-29
Experimental apparatus and methods	C-29
Data and results	C-29
Discussion.....	C-31
Microbial degradation of crude oil and some model hydrocarbons, by F.H. Chang, N.N. Noben, Danny Brand, and M.F. Hult	C-33

CHAPTER D. – FATE OF HEAVY METALS NEAR ABANDONED LEAD AND ZINC MINES IN NORTHEASTERN OKLAHOMA AND SOUTHEASTERN KANSAS

	Page
Introduction	D-3
Mine-water discharge, metal loading, and chemical reactions, by D.L. Parkhurst	D-5
Water discharge and metal loading.....	D-5
Major chemistry of the mine water.....	D-8
Distribution of microorganisms and selected metals in mine drainage, stream water, and sediment, by K.S. Smith, L.H. Filipek, D.M. Updegraff, and C.S.E. Papp	D-11

Problems associated with analyses of plant samples in the Tar Creek study, by B.M. Erickson, T.F. Harms, and L.H. Filipek.....	D-17
--	------

CHAPTER E. – METALS IN GROUND WATER

	Page
Geohydrologic setting of the Miami Wash-Pinal Creek acidic ground-water study area near Globe, Arizona, by J.H. Eychaner.....	E-3
Neutralization of acidic ground water in eastern Arizona, by K.G. Stollenwerk.....	E-7
Arsenic species in ground water and pore waters in stream sediments affected by mine drainage in Montana and Colorado, by W.H. Ficklin and J.L. Ryder	E-9
Arsenic in an alluvial-lacustrine aquifer, Carson Desert, western Nevada, by A.H. Welch and M.S. Lico	E-13
Hydrogeochemistry of uranium and associated elements at abandoned uranium mines in western North Dakota, by R.L. Houghton, R.L. Hall, J.D. Unseth, J.D. Wald, G.S. Anderson, and S.R. Hill	E-19

CHAPTER F. – ORGANIC COMPOUNDS IN GROUND WATER

	Page
Field comparison of ground-water sampling devices for recovery of purgeable organic compounds, by T.E. Imbrigiotta, Jacob Gibs, T.V. Fusillo, J.J. Hochreiter, and G.R. Kish	F-5
Recent developments in downhole samplers for organic and volatile compounds in ground water, by J.H. Fickin, W.H. Sonntag, and A.J. Boettcher	F-5
Screening for volatile organic compounds in ground water by gas chromatography with photoionization and hall detectors, by T.V. Fusillo, Jacob Gibs, J.A. Kammer, and T.E. Imbrigiotta	F-9
Application of the gas chromatographic/flame ionization detector analysis, by H.R. Feltz, J.A. Lewis, and F.L. Cardinali	F-11
Methodology	F-11
Detector sensitivity	F-11
Sample analysis, reporting procedures, and quality control	F-12
Application of GC/FID scans	F-13
Use of gas chromatograph/flame ionization detector to identify organic substances in ground water, by R.C. Buchmiller	F-17
Evaluation of four field-determined characteristics used as water-quality indicators during aquifer sampling for purgeable organic compounds, by Jacob Gibs and T.E. Imbrigiotta.....	F-19

ILLUSTRATIONS

Figure	Page
A-1. Map showing major features of study area at abandoned wood-preserving plant near Pensacola, Florida	A-3
A-2. Plan views of modeled area showing potentiometric-surface altitudes and model-boundary conditions.....	A-5
A-3. North-south vertical section through flow-model area showing directions of ground-water movement.....	A-6
A-4. Map showing location of drilling sites from which sediment samples were collected	A-9
A-5. Generalized vertical section B-B' showing dissolved iron concentrations in ground water	A-10
A-6. X-ray diffractometer traces of 001 spacings of representative clay-mineral assemblages from oriented < 2- μ m samples that were air dried, ethylene glycol-saturated, or heated to 550 °C	A-11
A-7. X-ray diffractometer traces of 001 spacings from ethylene glycol-saturated, oriented mounts for 2.0- to 0.5- μ m, 0.5- to 0.2- μ m, and < 0.2- μ m particale-size fractions.....	A-12
A-8. X-ray diffractometer traces of 060 spacings from four randomly oriented, < 2- μ m mounts with differing aluminum-to-iron atom ratios.....	A-13
A-9. Map showing extent of shallow (6-m depth) methane plume at an abandoned creosote works near Pensacola, Florida, 1985	A-17
A-10. Plots showing concentrations of dissolved iron, hydrogen sulfide, sulfate, organic carbon, total carbon dioxide, and methane along transect A-A'	A-18
A-11. Map showing extent of deeper (17-m to 35-m depth) methane plume at an abandoned creosote works near Pensacola, Florida, 1985	A-18
A-12. Plots showing concentrations of dissolved iron, hydrogen sulfide, sulfate, oxygen, organic carbon, total carbon dioxide, and methane with depth.....	A-19
A-13. Plot showing concentrations of dissolved organic carbon and total carbon dioxide along section B-B'	A-20
A-14. Map showing locations of drilling sites and wells in abandoned creosote-works area near Pensacola, Florida	A-23
A-15. Plot showing degradation of organic acids, phenolic compounds, and heterocyclic compounds in anaerobic digestors	A-29
A-16. Plots showing calculated carbon balance for identified compounds in water-soluble fraction in anaerobic digester	A-30
A-17. Plot showing total carbon values obtained by mass-balance computation and by dissolved organic carbon analysis	A-30
A-18. Plot showing comparison of best-fit mathematical models to calculated carbon substrate-disappearance curve	A-31
A-19. Map showing location of sampling sites in Pensacola Bay, Bayou Chico, and along drainage channel near abandoned creosote works, Pensacola, Florida	A-34
A-20. Vertical profiles for three creosote-compound concentrations in drainage-channel sediments at site 1, August 30, 1984	A-35
B-1. Map showing location of study area at Otis Air Base on Cape Cod, Massachusetts	B-4
B-2. Map showing path of sewage-contaminated ground-water plume and water-table altitude downgradient from sewage- infiltration beds.....	B-8
B-3. Geologic section along axis of sewage plume and vertical profiles of specific conductance at four sites along plume, 1983-85.....	B-9

ILLUSTRATIONS – Continued

Figure	Page
B-4. Plot of observed drawdown in observation wells 20 feet from pumping well and screened above, opposite, and below pumping interval, July 7-14, 1984	B-10
B-5. Plot of bromide-tracer concentration during pumping test at pumping well 20 feet from injection point, July 1984	B-10
B-6. Plot of bromide-tracer concentration at top, middle, and bottom of injection zone in divergent-flow tracer test, September 1984, at points 5 and 10 feet from injection well	B-11
B-7. Map showing water-table altitude, location of injection and monitoring wells, and projected path of tracer cloud at abandoned gravel pit used for solute- dispersion test, Cape Cod, Massachusetts.....	B-14
B-8. Map showing vertically averaged bromide concentrations in aquifer 13 days after injection of tracer	B-15
B-9. Map showing vertically averaged bromide concentrations in aquifer 32 days after injection of tracer	B-16
B-10. Plot of vertical distribution of bromide cloud along section A-A' 32 days after injection of tracer	B-17
C-1. Map showing location of crude-oil spill near Bemidji, Minnesota	C-4
C-2. Map showing surficial geology of Bemidji crude-oil spill site and vicinity.....	C-6
C-3. Composite stratigraphic column of the principal lithofacies at the Bemidji crude-oil spill site	C-7
C-4. Fence diagram of ground-water flow-model area near Bemidji, Minnesota.....	C-8
C-5. Map showing observed steady-state water-table altitude, 1983-85, and locations of observation wells and model-area boundary.....	C-12
C-6. Areal view of: A. three-dimensional model area, location of section A-A', and well locations, B. two-dimensional vertical model grid.....	C-13
C-7. Map and vertical section showing comparison of observed and simulated steady-state water levels for 1983-85 in: A. three-dimensional flow model, and B. two-dimensional vertical-section model.....	C-14
C-8. Map and vertical section showing comparison of observed water levels resulting from applied 1.0-foot increase and decrease in level of unnamed lake with simulated levels in: A. three-dimensional model, and B. two-dimensional vertical-section model	C-15
C-9. Map showing comparison of observed with simulated water-table levels at end of 90-day spring recharge period, 1984	C-16
C-10. Maps showing areal distributions of selected ground-water constituents or properties at water table downgradient of crude-oil spill, August 1985: A. pH, B. silicon, and C. iron and magnesium	C-18
C-11. Scanning electron photomicrographs of feldspar: A. Unetched sample from uncontaminated zone; B. Etched sample from contaminated zone.....	C-20
C-12. Maps showing areal distribution of: A. organic carbon in upper meter of saturated zone, and B. methane in lower meter of saturated zone.....	C-22
C-13. Examples of chromatograms used to detect presence of organic compounds, carbon dioxide, oxygen, and nitrogen in gas samples from lower meter of the saturated zone.....	C-24
C-14. Vertical sections showing distribution of selected constituents within the unsaturated zone	C-25
C-15. Diagram of laboratory-column setup.....	C-30
C-16. Plot showing mass transfer of pure liquid hydrocarbons to formation water in relation to Sherwood and Peclet numbers	C-31

ILLUSTRATIONS – Continued

	Page
Figure	
C-17. Graph showing mass-transfer rates for selected hydrocarbons obtained from published values and those obtained in this study in relation to Sherwood numbers and Peclet numbers.....	C-32
C-18. Plot of oxygen uptake by indigenous microorganisms in sediment and ground-water mixture mixed with hexadecane or crude oil and incubated at 12 °C and 2 °C.....	C-34
C-19. Graphs showing heterotrophic bacterial counts in sediment and ground-water microcosms with varied amounts of selected nutrients: A. at 2 °C, and B. 7 °C.....	C-36
C-20. Graphs showing heterotrophic bacterial counts in sediment and ground-water microcosms with varied amounts of selected nutrients: A. at 12 °C, and B. 17 °C.....	C-37
C-21. Plot of cumulative carbon mineralization of hexadecane mixed with sediment and ground water with varied amounts of selected nutrients and antibacterial or antifungal agents	C-38
C-22. Plot of bacterial and fungal counts with varied amounts of selected nutrients or antifungal agent at 17 °C	C-41
D-1. Map showing location of Tar Creek sampling sites near Picher, Oklahoma	D-4
D-2. Map showing location of mine workings of the Picher Field and selected features.....	D-6
D-3. Plots of mine discharge against: (a) water level in air shaft, and (b) mean daily discharge of Tar Creek	D-7
D-4. Histogram showing amounts of minerals and gases that must react with rainwater to evolve the chemical composition of mine water.....	D-8
D-5. Map showing location of mine-tributary sampling sites.....	D-12
D-6. Plot of total microbial counts in Tar Creek water and sediment on nutrient agar, 1984 and 1985	D-14
D-7. Plots of total microbial counts in 1985 water and sediment on nutrient agar and minimal yeast extract agar: (a) Tar Creek sites, and (b) mine tributary sites	D-15
D-8. Map showing Tar Creek study area and location of sampling sites	D-18
D-9. Map showing location of sampling sites near borehole discharge.....	D-19
E-1. Map showing major geographic features of Miami Wash-Pinal Creek study site near Globe, Arizona.....	E-4
E-2. Map showing locations of study sites on Clark Fork River, Montana, and Clear Creek, Colorado.....	E-10
E-3. Graph showing arsenic concentrations in pore water at 10-cm intervals in two sediment cores from Clark Fork River, Montana	E-11
E-4. Map showing location of Dodge Ranch site in Carson Desert, western Nevada.....	E-14
E-5. Map showing location of wells, piezometers, soil-water samplers, and staff gages at Dodge Ranch	E-15
E-6. Vertical section A-A' showing: (A) lithology with dissolved arsenic concentrations in February 1985, and (B) ground-water zones at Dodge Ranch	E-16
E-7. Map showing location of abandoned uraniferous lignite mines and associated uraniferous lignite deposits in Montana, North Dakota, and South Dakota	E-20
E-8. Gamma-ray log of subsurface in uraniferous lignite area, western North Dakota	E-22
F-1. Photographs of samplers described in text:	
(A) Pump-type sampler	F-5
(B) Small-diameter flow-through sampler	F-6
(C) Small-diameter sampler that collects a sealed sample	F-7
F-2. Chromatograms showing comparison of detector sensitivity.....	F-13

F-3. Sample GC/FID analytical report: (A) chromatogram, and (B) table showing retention times (RT), peak (AREA), area integration codes (TYPE), compound identification number (CAL), calculated concentration ($\mu\text{g/L}$) (AMOUNT), and names of compounds present (NAME).....	F-14
F-4. Graph showing Northern New Jersey well, August 14, 1984, purgeable organic compounds concentration time history during well purging.....	F-21

TABLES

	Page
Table	
A-1. Chemical analyses of clay-size ($< 2 \mu\text{m}$) fraction in core samples from creosote-works area, Pensacola, Florida, with lithic description of whole sediment	A-14
A-2. Concentrations of polynuclear aromatic hydrocarbons and phenolics found in water samples collected at sites 16 and 17 from the 30-m depth.....	A-21
A-3. Concentrations of polynuclear aromatic hydrocarbons and phenolics found in water samples collected at site 18	A-22
A-4. Concentrations of polynuclear aromatic hydrocarbons and phenolics found in water samples collected at the 20-m depth at site 19.....	A-22
A-5. Comparison of on-site high performance liquid chromatographic (HPLC) analysis for naphthalene with laboratory gas-chromatographic (GC) analysis for naphthalene	A-24
A-6. Concentrations of heterocyclic nitrogen compounds in a water sample taken at site 3.....	A-24
A-7. Concentrations of polynuclear aromatic hydrocarbon compounds, phenolic compounds, and nitrogen compounds in samples taken at the water table and 6 m below the water table ...	A-25
A-8. Species list including seasonally averaged benthic invertebrate distributions and abundances by sampling site, Pensacola, Florida, 1983-84.....	A-35
C-1. Metal oxide distribution in uncontaminated drift near the water table	C-17
C-2. Peclet numbers, Sherwood numbers, and mass-transfer coefficients obtained in laboratory column experiments with alkane over aquifer sand in distilled water	C-31
C-3. Rates of oxygen uptake before and after 10 °C temperature change, and values for Q_{10} with sediment nutrients.....	C-34
C-4. Cumulative CO_2 evolution and carbon mineralization from oil-contaminated topsoil samples.....	C-35
C-5. Cumulative CO_2 evolution and carbon mineralization from crude oil in aquifer-sediment samples.....	C-39
C-6. Cumulative CO_2 evolution and carbon mineralization from $^{14}\text{C}_1$ through C_{10} (hexadecane) in control sediment- and ground-water mixture by indigenous microbes.....	C-40
C-7. Degradation of model hydrocarbons by bacteria and fungi	C-42
D-1. Analysis of two samples of vegetation and their duplicate by inductively coupled plasma-emission spectroscopy.....	D-17
D-2. Zinc analysis of three samples of grass, one sample of sumac, and their duplicates by atomic absorption spectrophotometry.....	D-20
E-1. Speciation of elements in contaminated ground water	E-7
E-2. Concentration of radioactive and selected associated constituents in mine-affected and unaffected aquifer settings.....	E-21
F-1. Characteristics of gas-chromatographic detectors.....	F-12
F-2. Chemical quality of ground water at two sites in New Jersey.....	F-20

CONVERSION FACTORS AND ABBREVIATIONS

The following factors may be used to convert the International System (SI) units of measure used in this report to inch-pound units:

Multiply	By	To Obtain
centimeter (cm)	0.394	inch (in.)
meter (m)	3.281	foot (ft.)
kilometer (km)	0.621	mile (mi.)
square meter (m ²)	10.76	square foot (ft ²)
square kilometer (km ²)	0.386	square mile (mi ²)
cubic meter (m ³)	35.31	cubic foot (ft ³)
gram (g)	0.035	ounce avoirdupois (oz avdp)
kilogram (kg)	2.205	pound (lb)
megagram (Mg)	1.102	short ton (2000 lb)
liter (L)	0.2642	gallon
micrometer (μm)	0.00003937	inch
nanometer (nm)	3.937x10 ⁻⁸	inch
milligram (mg)	0.0000353	ounce (oz)
 Degrees Celsius (°C)	 (1.8 x °C) + 32	 Degrees Fahrenheit

OTHER ABBREVIATIONS USED IN THIS REPORT

μS/cm	microsiemens per centimeter	mo	month
μCi	microcurie	yr	year
mv	millivolt	d	day
MPN	most probable number		
CFU	colony-forming units		

TOXIC WASTE--GROUND-WATER CONTAMINATION PROGRAM

The U.S. Geological Survey's Program on Toxic Waste – Ground-Water Contamination (hereinafter called the Toxic Waste Program) provides a focus for ongoing and the opportunity for new, earth-science research on the fate and transport of toxic wastes in ground water. In fiscal year 1986¹, the Toxic Waste Program consisted of three research activities: (1) Basic research of the physical, chemical, and microbiological factors affecting the fate of contaminants in ground water, (2) point source field research at sites where ground-water contamination has occurred, and (3) nonpoint-source-contamination research to understand the influence of human activities on regional ground-water quality. Although many of these studies represent independent efforts by Survey scientists, it is the intention of the Toxic Waste Program to provide the opportunity for the individual researchers to exchange information with the broader technical community. One way to accomplish this is to encourage scientists to share research opportunities at field sites. In many cases, scientists conducting process research also are directly involved in the point- and nonpoint-source contamination research or serve as consultants to these studies. Such involvement brings new perspectives and state-of-the-science techniques to the field and provides useful feedback concerning the applicability of basic research to real-world problems.

Information obtained through basic and field research will help in the description of regional ground-water quality. Improved sampling and analytical methods developed as part of the field-research efforts will help to ensure that the water sample being analyzed is representative of ground water from which it was obtained. Research findings will help to provide the earth-sciences information needed to explain the occurrence (or absence) and distribution of organic and inorganic contaminants in ground water.

Basic Research

Knowledge of the physical, chemical, and microbiological processes that affect the subsur-

face movement of contaminants and their ultimate fate must be factored into the complex equation to solve the toxic-waste and ground-water contamination problems of the Nation. Earlier studies have helped to characterize the basic processes that affect contaminant transport in the subsurface, but, at the same time, they have demonstrated how complex natural systems can be. Thus, the objective of the Toxic Waste Program is to extend current understanding of earth-science processes to better describe the fate of contaminants in the complex multiphase and multicomponent systems found in nature. Some study of processes occurring in the unsaturated zone and surface water also are being conducted to evaluate their impact on ground-water transport of contaminants.

Point-Source Contamination Research

To evaluate how well current earth-science knowledge can be used to quantitatively describe real-world problems and to advance that state of that knowledge, teams of scientists from the U.S. Geological Survey and universities representing all major earth-science disciplines began studies in Federal Fiscal Year (FY) 1983 at four ground-water contamination sites. Sites were selected to study ground-water contamination that resulted from a crude-oil pipeline break near Bemidji, Minnesota; from the infiltration of creosote and pentachlorophenol from waste-disposal pits near Pensacola, Florida; from the infiltration of sewage-treatment effluent on Cape Cod, Massachusetts; and from the migration of zinc, lead, and cadmium from abandoned zinc mines near Tar Creek, Oklahoma. In FY 1985 three additional sites were selected to study ground-water contamination that resulted from the infiltration of chlorinated hydrocarbons and gasoline in New Jersey and Washington, and an acid-contamination plume in Arizona. The contaminants at the seven sites commonly are associated with ground-water contamination problems throughout the Nation. The field studies are intended to test and develop the understanding of the processes affect-

¹Federal fiscal year extends from October 1 to September 30.

ing contaminant transport rather than to solve the specific problems at the sites. Thus, the knowledge gained through these studies will have transfer value to other sites where similar contamination has occurred in similar hydrogeologic and climatic settings.

Although research at the seven sites is focused on ground water, some of the sites include study of the unsaturated zone and surface water as possible "sinks" or "sources" of organic or inorganic constituents.

Nonpoint-Source Contamination Research

About half of the population of the Nation relies on ground water as a source of drinking water. In some places (for example, Florida, New Mexico, and Long Island) ground water supplies more than 90 percent of the population. Although it has been estimated that only a small percentage of ground water has been affected by point-sources of contaminants (Lehr, 1982), the billions of gallons of wastes infiltrating the ground annually from a variety of industrial and domestic point sources (Miller, 1980) indicate that the potential exists for widespread ground-water contamination. In addition, nonpoint, or diffuse, sources of contamination from a variety of human activities also may affect ground-water quality. Pesticides, for instance, have been found in ground waters in many states owing to widespread agricultural usage (Cohen and others, 1984).

Although there is evidence that ground water has been affected by human activities in virtually every State of the Nation (U.S. Geological Survey, 1984), our knowledge of these problems has come after the fact and unsystematically. There are several reasons for this: (1) the inaccessibility, complexity and vastness of the resource, and the relatively slow rate of ground-water movement, (2) the relative newness of many sampling and analytical methodologies, and (3) the high spatial and temporal variability of anthropogenic sources. Because of these complexities, the Toxic Waste Program began, in fiscal year 1984, the evaluation of a procedure to identify the types of hydrogeologic, land-use, and water-quality data necessary to assess the effect of human activities on ground-water quality (Helsel and Ragone, 1984). The objective of the protocol is to establish a systematic approach to: (1) Clearly define that part

of the ground-water system that is subject to contamination through human activities, (2) design, using existing and new wells, a ground-water sampling network that allows collection of samples that are representative of water in system of interest, (3) identify in an economical manner the constituents or groups of constituents that are present, and (4) establish a statistically sound relationship between these constituents and the causes of their introduction into the ground-water reserve.

To develop an appropriate procedure, 14 reconnaissance studies were completed throughout the nation to determine the type and scale of information that would be required. The studies were limited to parts of the ground-water system in which the ground water is less than 100 years old, generally at or near the water table or near the recharge zone of confined aquifers, to maximize the opportunity to observe the effect of human activity on ground-water quality.

Human activities were represented by a variety of land uses which were in turn characterized by type (suburban, agricultural, industrial, for instance) and intensity. Intensity was estimated on the basis of population density (for suburban land use) or chemical loadings (for agricultural and industrial land uses). Other information about climate, soil types, depth to water, and available water-quality data were also used. Results of selected studies are given Cain and Edelmann (1986) and Eckhart (1986).

REFERENCES CITED

- Cain, Douglas, and Edelmann, Patrick, 1986, A reconnaissance water-quality appraisal of the Fountain Creek alluvial aquifer between Colorado Springs and Pueblo, Colorado, including trace elements and organic constituents; U.S. Geological Survey Toxic Waste—Ground-Water Contamination Program: U.S. Geological Survey Water Resources Investigations Report 86-4085 (in press).
- Cohen, S.Z., Creeger, S.M., Carsel, R.F., Enfield, C.G., 1984, Potential for pesticide contamination of ground water resulting from agricultural uses, *in* Kruger, R. F., and Selver, J. N., eds., Treatment and disposal of pesticide wastes: American Chemical Society Symposium Series 259, p. 297-326.

- Eckhardt, D.A., Flipse, W.J., Jr., and Oaksford, E.T., 1986, Relationship between land use and ground-water quality in the upper glacial aquifer in Nassau and Suffolk Counties, Long Island, New York: U.S. Geological Survey Water Resources Investigations Report 86-4142 (in press).
- Helsel, D.R. and Ragone, S.E., 1984, Evaluation of regional ground-water quality in relation to land use: U.S. Geological Survey Toxic Waste—Ground-Water Contamination Program: U.S. Geological Survey Water-Resources Investigations Report 84-4217, 33 p.
- Hult, M.F., (ed), 1984, Ground-water contamination by petroleum at the Bemidji, Minnesota research site: U.S. Geological Survey Toxic Waste—Ground-Water Contamination Program: U.S. Geological Survey Water Resources Investigations Report 84-4188, 107 p.
- LeBlanc, D.R., (ed.), 1984, Movement and fate of solutes in a plume of sewage-contaminated ground water, Cape Cod, Massachusetts: U.S. Geological Survey Toxic Waste—Ground-Water Contamination Program: U.S. Geological Survey Open-File Report 84-475, 180 p.
- Lehr, J.H., 1982, How much ground water have we really polluted?: Ground Water Monitoring Review, winter, p. 4-5.
- Mattraw, H.C., Jr., and Franks, B.J., (eds.), 1986, Movement and fate of creosote waste in ground water, Pensacola, Florida: U.S. Geological Survey Toxic Waste—Ground-Water Contamination Program: U.S. Geological Survey Water Supply Paper 2285, 63 p.
- Miller, D.W., 1980, Waste disposal effects on ground water: Berkeley, Premier Press, 512 p.
- Ragone, S.E., 1984, U.S. Geological Survey Toxic Waste—Ground-Water Contamination Program—Fiscal Year 1983: U.S. Geological Survey Open-File Report 84-474, 56 p.
- Ragone, S.E., 1986, U.S. Geological Survey Toxic Waste—Ground-Water Contamination Program—Fiscal Year 1985: Environmental Geology Water Science, v. 8, no. 2, p. 129-132.
- Ragone, S.E., and Sulam, D.J., (eds.), 1987, U.S. Geological Survey Toxic Waste—Ground-Water Contamination Program—Fiscal Year 1984: Program Overview and Selected Papers from the first Toxic Waste Technical Meeting in Tucson, Arizona, March 20-22, 1984: U.S. Geological Survey Open-File Report 86-324, 116 p.
- U.S. Geological Survey, 1984, National Water Summary, 1983, hydrologic events and issues: U.S. Geological Survey Water-Supply Paper 2250, 243 p.

SELECTED ABSTRACTS PRESENTED AT THE TOXIC WASTE PROGRAM TECHNICAL MEETING

The abstracts in this report are grouped by chapters. The abstracts in chapters A, B, C, and D summarize findings of point-source studies being conducted at field sites in Pensacola, Fla.; Cape Cod, Mass.; Bemidji, Minn.; and Tar Creek, Okla., respectively. Abstracts in chapter E

describe the fate and transport of metals in the subsurface at several sites, and those in chapter F describe techniques to sample ground water or screen samples for the presence of organic substances.

CHAPTER A. – MOVEMENT AND FATE OF CREOSOTE WASTE IN GROUND WATER NEAR AN ABANDONED WOOD-PRESERVING PLANT NEAR PENSACOLA, FLORIDA

Introduction.....	A-3
Preliminary three-dimensional simulation of ground-water flow, by B.J. Franks	A-5
Geophysical methods of contaminant detection, by G.R. Olhoeft	A-7
Clay mineralogy of sediments associated with a plume of creosote-contaminated ground water, by M.W. Bodine, Jr.....	A-9
Geochemistry of a shallow aquifer contaminated with creosote products, by M.J. Baedecker, B.J. Franks, D.F. Goerlitz, and J.A. Hopple.....	A-17
Reexamination of the occurrence and distribution of creosote compounds in ground water, by D.F. Goerlitz	A-21
Determination of the rates of anaerobic degradation of the water-soluble fraction of creosote, by E.M. Godsy and D.F. Goerlitz	
Introduction.....	A-27
Anaerobic degradation	A-27
Modeling substrate utilization.....	A-28
Contamination, bioaccumulation, and ecological effects of creosote-derived compounds in the nearshore estuarine environment of Pensacola Bay, Florida, by P.V. Dresler and J.F. Elder ...	A-33

ILLUSTRATIONS

	Page
Figure	
A-1. Map showing major features of study area at abandoned wood-preserving plant near Pensacola, Florida	A-3
A-2. Plan views of modeled area showing potentiometric-surface altitudes and model-boundary conditions.....	A-5
A-3. North-south vertical section through flow-model area showing directions of ground-water movement.....	A-6
A-4. Map showing location of drilling sites from which sediment samples were collected	A-9
A-5. Generalized vertical section B-B' showing dissolved iron concentrations in ground water.....	A-10
A-6. X-ray diffractometer traces of 001 spacings of representative clay-mineral assemblages from oriented < 2- μ m samples that were air dried, ethylene glycol-saturated, or heated to 550 °C	A-11
A-7. X-ray diffractometer traces of 001 spacings from ethylene glycol-saturated, oriented mounts for 2.0- to 0.5- μ m, 0.5- to 0.2- μ m, and <0.2- μ m particale-size fractions.....	A-12
A-8. X-ray diffractometer traces of 060 spacings from four randomly oriented, < 2- μ m mounts with differing aluminum-to-iron atom ratios	A-13
A-9. Map showing extent of shallow (6-m depth) methane plume at an abandoned creosote works near Pensacola, Florida, 1985	A-17
A-10. Plots showing concentrations of dissolved iron, hydrogen sulfide, sulfate, organic carbon, total carbon dioxide, and methane along transect A-A'	A-18
A-11. Map showing extent of deeper (17-m to 35-m depth) methane plume at an abandoned creosote works near Pensacola, Florida, 1985	A-18
A-12. Plots showing concentrations of dissolved iron, hydrogen sulfide, sulfate, oxygen, organic carbon, total carbon dioxide, and methane with depth.....	A-19

A-13. Plot showing concentrations of dissolved organic carbon and total carbon dioxide along section B-B'	A-20
A-14. Map showing locations of drilling sites and wells in abandoned creosote-works area near Pensacola, Florida	A-23
A-15. Plot showing degradation of organic acids, phenolic compounds, and heterocyclic compounds in anaerobic digestors	A-29
A-16. Plots showing calculated carbon balance for identified compounds in water-soluble fraction in anaerobic digester	A-30
A-17. Plot showing total carbon values obtained by mass-balance computation and by dissolved organic carbon analysis	A-30
A-18. Plot showing comparison of best-fit mathematical models to calculated carbon substrate-disappearance curve	A-31
A-19. Map showing location of sampling sites in Pensacola Bay, Bayou Chico, and along drainage channel near abandoned creosote works, Pensacola, Florida	A-34
A-20. Vertical profiles for three creosote-compound concentrations in drainage-channel sediments at site 1, August 30, 1984	A-35

TABLES

	Page
Table	
A-1. Chemical analyses of clay-size (< 2 μm) fraction in core samples from creosote-works area, Pensacola, Florida, with lithic description of whole sediment	A-14
A-2. Concentrations of polynuclear aromatic hydrocarbons and phenolics found in water samples collected at sites 16 and 17 from the 30-m depth.....	A-21
A-3. Concentrations of polynuclear aromatic hydrocarbons and phenolics found in water samples collected at site 18	A-22
A-4. Concentrations of polynuclear aromatic hydrocarbons and phenolics found in water samples collected at the 20-m depth at site 19.....	A-22
A-5. Comparison of on-site high performance liquid chromatographic (HPLC) analysis for naphthalene with laboratory gas-chromatographic (GC) analysis for naphthalene	A-24
A-6. Concentrations of heterocyclic nitrogen compounds in a water sample taken at site 3.....	A-24
A-7. Concentrations of polynuclear aromatic hydrocarbon compounds, phenolic compounds, and nitrogen compounds in samples taken at the water table and 6 m below the water table ...	A-25
A-8. Species list including seasonally averaged benthic invertebrate distributions and abundances by sampling site, Pensacola, Florida, 1983-84.....	A-35

CHAPTER A. – MOVEMENT AND FATE OF CREOSOTE WASTE IN GROUND WATER NEAR AN ABANDONED WOOD-PRESERVING PLANT NEAR PENSACOLA, FLORIDA

INTRODUCTION

From 1902 to 1981, an estimated 53 m³/mon (cubic meters per month) of residual wastewater containing creosote, pentachlorophenol, and diesel fuel were discharged to unlined surface im-

poundments at a wood-preserving plant in Pensacola, Fla. (Matraw and Franks, 1986) (fig. A-1).

The impoundments are hydraulically connected to the surficial sand aquifer. Wastewater infiltrating the ground created a plume, as defined

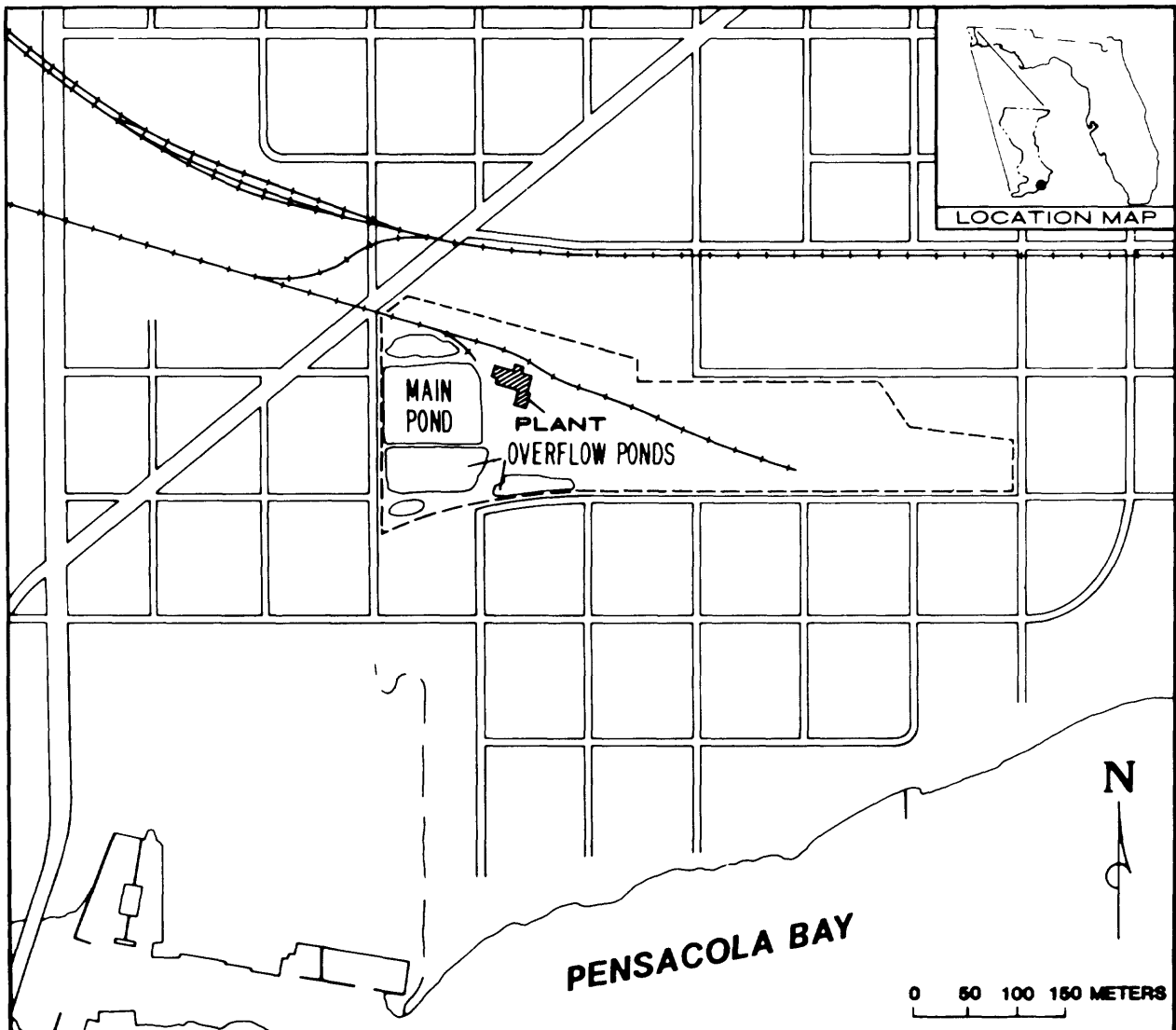


Figure A-1 – Major features of study area at abandoned wood-preserving plant near Pensacola, Florida.

by total phenol, that is less than 9 m (meters) deep in a 27-m-thick sand and gravel aquifer, and extends less than 300 m downgradient (south toward Pensacola Bay). Reports published since the inception of the U.S. Geological Survey's interdisciplinary research effort in 1983 describe:

- Chemical transformations due to microbial action occurring in soil, ground water, and aquifer material at the site and in the ground water downgradient of the site,
- A sequence of five water-quality zones as indicated by the distribution of unstable (reactive) organic and inorganic compounds,
- The inorganic geochemistry and mineralogy of contaminated aquifer sediments, and
- A procedure to isolate organic compounds from water for analysis by gas chromatography-mass spectrometry.

The seven abstracts presented in this chapter present additional information on changes that result from the interaction between aquifer sediments, ground water, and the waste infiltrating from the wood-treatment plant.

Franks describes the geology and preliminary ground-water flow simulation. Olhoeft reviews

and compares surface geophysical techniques used in helping to locate the contaminant plume. Bodine presents details of clay mineralogy associated with the contaminant plumes. Baedecker and others discuss the geochemistry of the shallow aquifer, including distributions of dissolved gases (methane and carbon dioxide) and selected inorganic constituents (sulfate-sulfide and iron). Goerlitz reexamines the occurrence and distribution of organic contaminants in the aquifer using laboratory techniques in conjunction with field sampling. Godsy and Goerlitz determine rates of anaerobic degradation of selected organic compounds in the water-soluble fraction of creosote. Dresler and Elder discuss possible effects of organic compounds on aquatic fauna in the near-shore estuarine environment.

REFERENCES

- Matraw, H.C., Jr., and Franks, B.J., eds., 1986, Movement and fate of creosote waste in ground water, Pensacola, Florida: U.S. Geological Survey Toxic Waste—Ground-Water Contamination Program: U.S. Geological Survey Water-Supply Paper 2285, 63 p.

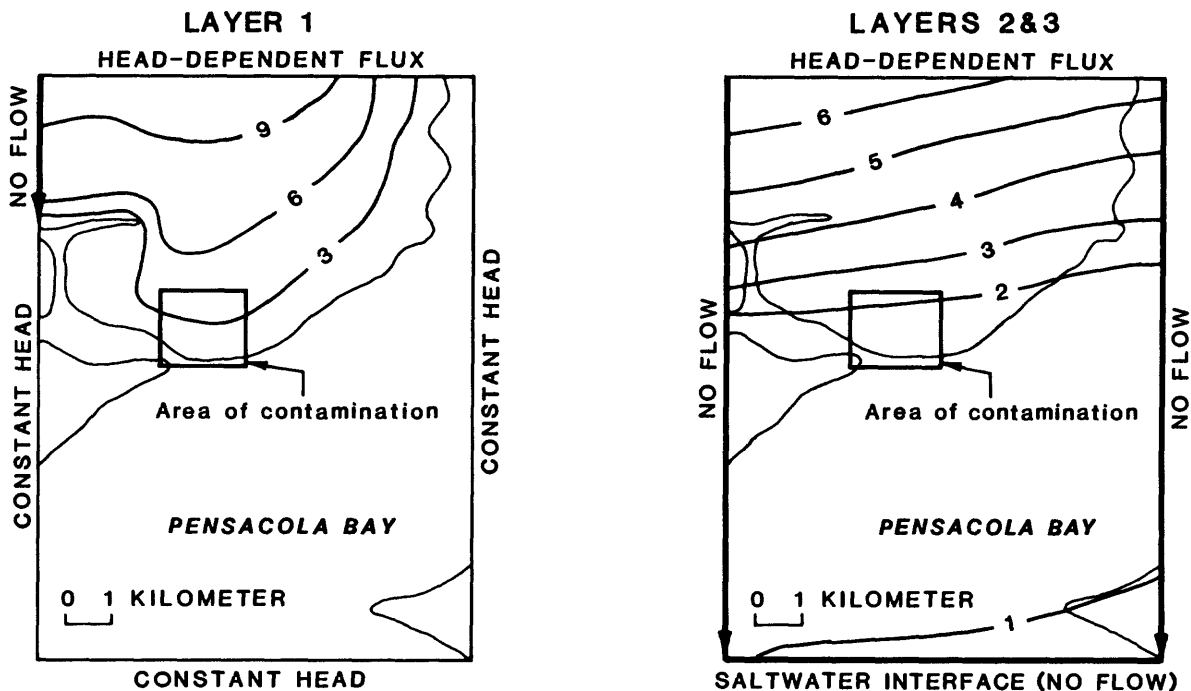
PRELIMINARY THREE-DIMENSIONAL SIMULATION OF GROUND-WATER FLOW

By Bernard J. Franks¹

Preparatory to evaluating the transport of contaminants that are infiltrating ground water from an abandoned wood-preserving plant near Pensacola, Fla. (fig. A-1), the surficial sand and gravel aquifer flow system is being simulated with a three-dimensional finite-difference ground-water flow model. Although the area of contamination occupies less than 0.7 km² (square kilometer), the simulation involves an area of about 80 km². The larger area is needed to include several natural hydrologic boundaries in the model simulations

(fig. A-2). Model nodes near the site represent 60 m² (square meters), to incorporate detailed hydrogeologic information near the contaminant plumes, whereas regional model nodes are 450 m². The entire grid (32x38 nodes) represents a 7.8x10.4-km (kilometer) area.

The sand and gravel aquifer consists of middle Miocene through Holocene fine-to-coarse quartz sand deposits, interbedded with locally confining discontinuous silts and clays. The aquifer is a



EXPLANATION
 — 3 — Potentiometric contour. Number is meters above sea level.

Figure A-2.— Plan views of modeled area showing potentiometric-surface altitudes and model-boundary conditions: left, layer 1; right, layers 2 and 3.

¹U.S. Geological Survey, Tallahassee, Fla.

wedge-shaped deposit extending over the western half of the Florida Panhandle and northward into Alabama. It is over 200 m (meters) thick in the west, gradually pinching out to the east. The top of the aquifer is land surface, and the base corresponds to the top of the Miocene Pensacola Clay. In the Pensacola area, the aquifer is the principal source of drinking water.

Underlying the site, ground-water flow is generally southward toward Pensacola Bay, with flow velocities of about 5 cm/d (centimeters per day). The aquifer is simulated by three horizontal layers: a water-table zone 15 m thick, a shallow semiconfined zone 20 m thick, and a deeper semi-confined to confined zone 50 m thick (fig. A-3). Preliminary simulations based on the following hydrologic values have been completed: hydraulic conductivity, 25 m/d (meters per day) (in all layers); recharge, 20 cm/yr (centimeters per year); pumping (from layer 3 only) 1.8×10^4 m³/d

(cubic meters per day); and vertical hydraulic conductivity of 0.3×10^{-6} to 0.3×10^{-4} m/d. The model was calibrated for steady-state conditions through comparison of observed with simulated water levels, the position of the saltwater interface (southern boundary of layers 2 and 3), and downward leakage between model layers.

Preliminary simulations have helped to improve the conceptual model of the aquifer and have provided information on the sensitivity of the model to factors that affect ground-water flow. The model is sensitive to reasonable variations in hydraulic conductivity and recharge and highly sensitive to variations in vertical fluxes between layers. Each of these and other hydrologic factors that affect flow in the aquifer will be varied further in future model runs to minimize differences between the observed and simulated potentiometric surfaces.

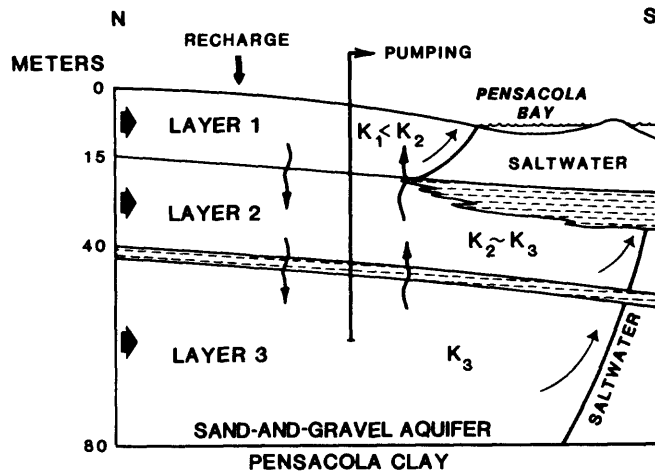


Figure A-3. — North-south vertical section through flow-model area showing directions of ground-water movement.

GEOPHYSICAL METHODS OF CONTAMINANT DETECTION

By Gary R. Olhoeft¹

At the Pensacola, Fla., research site, and also at the Cape Cod, Mass., and Bemidji, Minn., sites discussed in chapters B and C, geophysics has provided useful information about contaminant plumes. On Cape Cod, electromagnetic induction has been used to map electrical conductivity to delineate the areal extent of a sewage plume. Electromagnetic induction also located secondary plumes associated with contamination from temporary storage of road salt. Ground-penetrating radar provided detailed information for preparing stratigraphic sections and for describing the hydrology to depths of 30 m (meters), but failed to provide information on the location of the sewage plume. Complex resistivity added no information to that supplied by electromagnetic induction, and seismic techniques failed because of high attenuation in the soft, sandy soils.

In Pensacola, Fla., the electromagnetic induction technique could not be used to map the creosote plume because of interference from nearby city utilities and the masking effect of the nearby highly conductive saltwater in Pensacola Bay. However, ground-penetrating radar was used to map the stratigraphy, hydrology, and the location of the creosote plume. The radar data were particularly useful in mapping the location of sporadic clay layers that occurred in the subsurface.

Near Bemidji, Minn., electromagnetic induction was used to crudely outline a plume from a petroleum pipeline spill. However, no anomaly related to the plume remained after correcting the electromagnetic data for the effects of surface topography. Ground-penetrating radar was used to map the stratigraphy, hydrology, and extent of the plume in greater detail. The radar data indicated that the oil layer floating on the water table had sharp lateral boundaries.

Electromagnetic induction techniques are inexpensive, easy to interpret, and are most effective in locating inorganic contaminants. Although they may be insensitive to organic compounds, they should be tried first at all sites. Ground-penetrating radar, seismic, and complex resistivity techniques are more expensive and more difficult to interpret. Ground-penetrating radar achieves no useful depth penetration in low resistivity soils or high clay soils. If electromagnetic induction finds the average resistivity to be above 30 ohm-m (ohm-meter), ground-penetrating radar may be useful, and organic contaminants may be directly mappable. Otherwise, seismic techniques will probably be more successful in stratigraphic and hydrologic mapping. If clay is present, complex resistivity has the potential to directly map organic contaminants from the electrical signature of clay-organic reactions.

¹U.S. Geological Survey, Denver, Colo.

CLAY MINERALOGY OF SEDIMENTS ASSOCIATED WITH A PLUME OF CREOSOTE-CONTAMINATED GROUND WATER

By Marc W. Bodine, Jr.¹

This study characterizes the clay minerals in sediments associated with a plume of creosote-contaminated ground water (fig. A-1). The plume of contaminated ground-water near Pensacola, Fla. (fig. A-4), is in shallow, permeable, Miocene-to-Holocene quartz sand and flows southward toward Pensacola Bay (Matraw and Franks, 1986). An apparently lenticular, sandy-to-silty mud unit that locally exceeds 10 m (meters) in thickness, divides the

ground-water system into upper and lower aquifers (fig. A-5), both of which show extensive contamination. In addition to the clays in the mud unit, clay minerals also occur in the permeable sand as coatings on quartz grains (Hearn and others, 1986), as rounded clay galls from 0.5 to 2.0 cm (centimeters) diameter, in sands approaching contacts with the mud lens, and as sparsely distributed interstitial particulates throughout the sands.

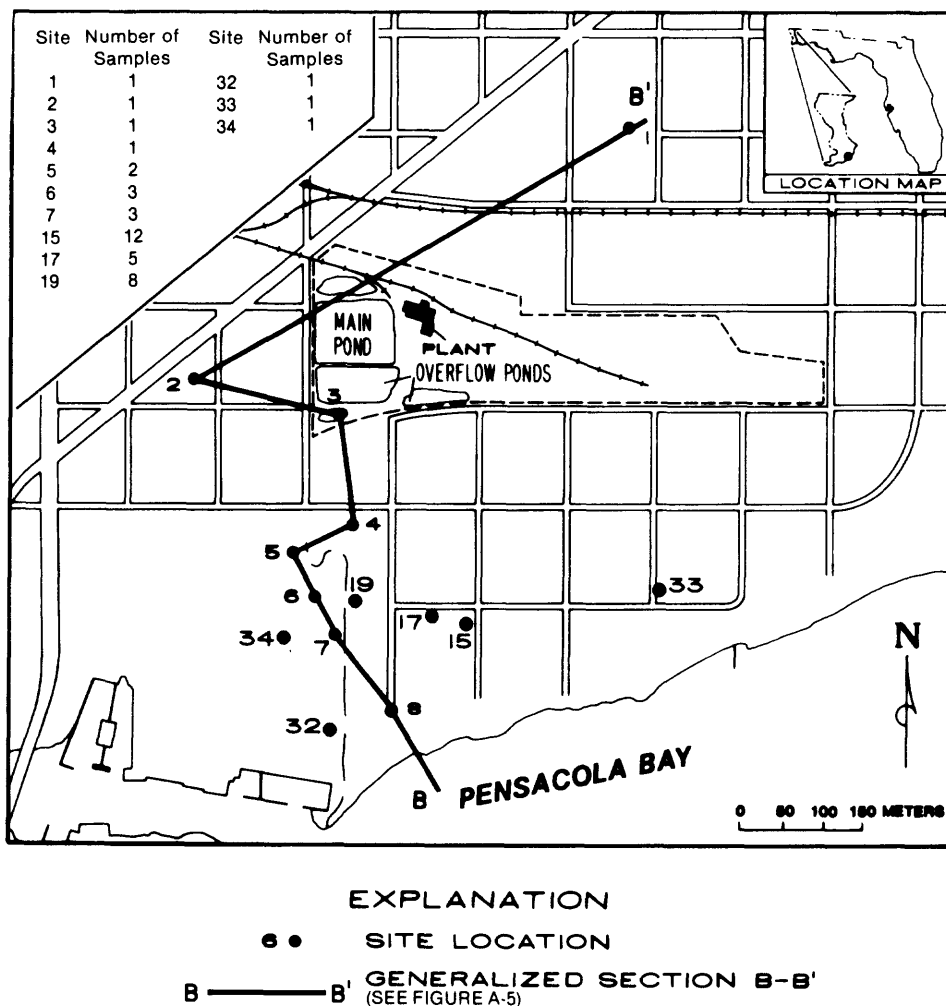


Figure A-4.— Location of drilling sites from which sediment samples were collected. (Inset shows number of samples from each site.)

¹U.S. Geological Survey, Denver, Colo.

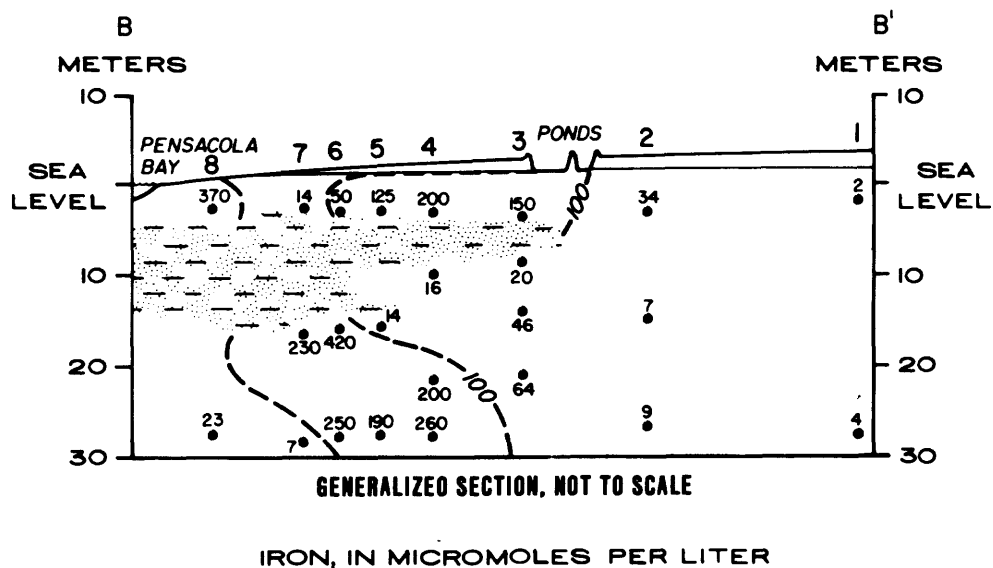
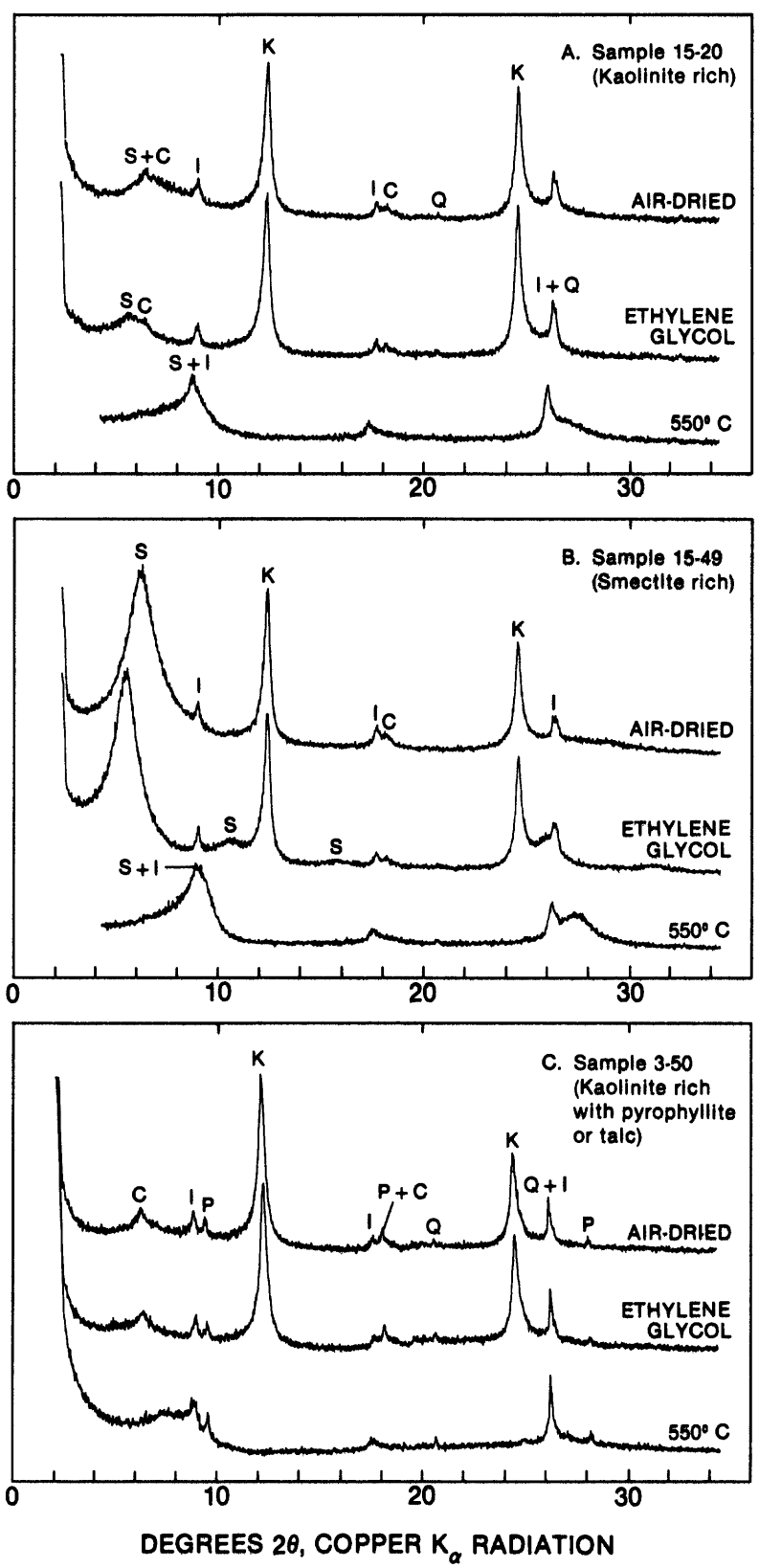


Figure A-5.—Generalized vertical section B-B' showing dissolved iron concentrations in ground water. Location is shown in figure A-4. (Modified from Baedecker and Lindsay, 1986, p. 16.)

Clay-size fractions were separated from 41 cores, chiefly split-spoon samples at 13 drill sites (fig. A-4). The sample numbers, for example 2-40, identify drill hole location (site 2 on fig. A-4) and sampling depth (40 feet). The $< 2\text{-}\mu\text{m}$ (micrometer) effective spherical diameter fraction and, for many, the 2.0 to 0.5, 0.5 to 0.2, and $< 2\text{-}\mu\text{m}$ -splits, were isolated by disaggregation of the sediment in a water suspension, repeated washings with distilled water, thorough dispersion with an ultrasonic probe, and size separation with timed, speed-controlled centrifugation. Each clay fraction was analyzed by x-ray diffraction. The 001 spacings were determined from oriented, glass-slide, sedimented sample mounts that were prepared by the filter-membrane peel technique. Mounts of each sample were analyzed after air-drying at room temperature, after solvation with ethylene glycol, and after heating to 350 °C then 550 °C. An air-dried, randomly oriented, conventional packed-powder mount also was prepared for determining the 060 spacings. Clay-mineral characterization from diffraction data relied chiefly on criteria given in Brindley and Brown (1980). Chemical analysis of the clay-size fractions by x-ray fluorescence is underway; only a few were completed in time for this report.

Relative mineral abundances within the $< 2\text{-}\mu\text{m}$ fractions vary considerably from sample to sample, although, for the most part, they form a continuum from kaolinite-rich to smectite-rich. X-ray diffractometer traces from oriented mounts of a kaolinite-rich assemblage with minor smectite, chlorite, and illite (fig. A-6a), and a smectite-rich assemblage with kaolinite, and minor illite and chlorite (fig. A-6b) illustrate their 001 spacings. Minor 001 spacings in two of the samples (for example, fig. A-6c) are attributed to either pyrophyllite or talc; however, the mineral's low abundance precludes definition of its 060 spacing identification. The relative clay-mineral abundance among the three clay-size fractions in a given sample is similar throughout all samples, as illustrated by sample 15-27 in figure A-7, a kaolinite-rich assemblage, and 19-69, a smectite-rich assemblage. The relative abundance of illite, quartz, and chlorite, as well as that of kaolinite, decreases with decreasing particle size, whereas that of the smectite increases.

Representative 060 spacings (fig. A-8) illustrate the dominance of dioctahedral clays (kaolinite, aluminous smectite, illite) by the strong spacing at 1.49 to 1.50 Å ($\sim 62.1^\circ 2\theta$), as contrasted with the weaker trioctahedral (chlorite)



EXPLANATION
 S, Smectite
 K, Kaolinite
 I, Illite
 C, Chlorite
 P, Pyrophyllite/Talc
 Q, Quartz

Figure A-6. — X-ray diffractometer traces of 001 spacings of representative clay-mineral assemblages from oriented <2- μ m samples that were air dried, ethylene glycol-saturated, or heated to 550 °C.

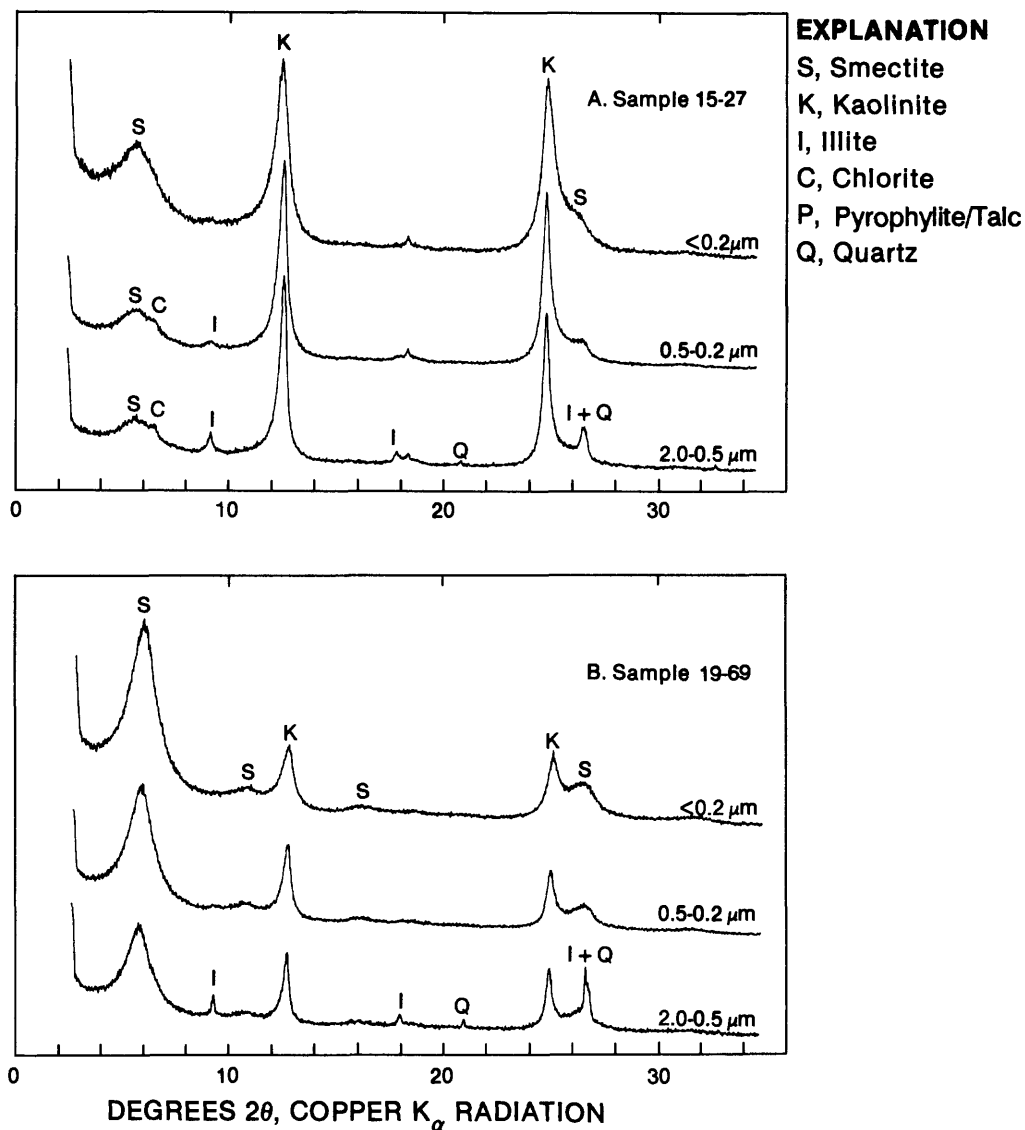


Figure A-7. — X-ray diffractometer traces of 001 spacings from ethylene glycol-saturated, oriented mounts for 2.0- to 0.5- μm , 0.5- to 0.2- μm , and <math><0.2\text{-}\mu\text{m}</math> particle-size fractions. Intensity for each trace was assigned to maintain approximately constant kaolinitic-peak height.

spacing at 1.53 to 1.54 Å ($\sim 60.0^{\circ} 2\theta$). An additional contributor to the low-angle reflection ($\sim 60.0^{\circ} 2\theta$) that is probably responsible for the sharp spikes at $\sim 60^{\circ} 2\theta$ on traces C and D is the presence of quartz in the $<2\ \mu\text{m}$ fraction. Figure A-8 shows a progression from the absence in trace A of a low-angle shoulder on the dioctahedral 060 spacing (1.49–1.50 Å) to its pronounced development in trace D. This shoulder, 1.51 to 1.52 Å

(60.8 to $61.3^{\circ} 2\theta$), is attributed to a nontronite-rich dioctahedral smectite interstratified with or discretely coexisting with the aluminous dioctahedral smectite. Nontronite, a dioctahedral smectite with ferric iron substituting for aluminum in octahedral sites, and generating a 060 spacing of 1.52 Å ($\sim 60.8^{\circ} 2\theta$), forms a dioctahedral series from end member montmorillonite-beidellite to nontronite. The occurrence of the 1.51 to 1.52 Å shoulder is

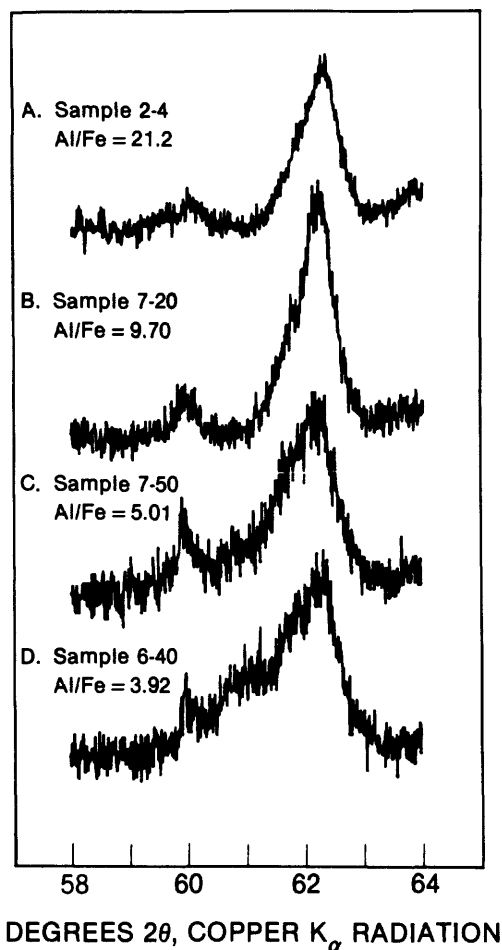


Figure A-8. — X-ray diffractometer traces of 060 spacings from four randomly oriented, $< 2 \mu\text{m}$ mounts with differing aluminum-to-iron ratios.

prevalent, albeit of variable intensity, throughout assemblages from drill sites within the waste plume and is least apparent or absent in those few samples peripheral to the plume.

The most striking feature of the chemical analyses of the clay fractions from uncontaminated site 2 and contaminated sites 4, 5, 6, and 7 (locations shown in fig. A-4) is the variability of

iron oxide (specified in some samples as Fe_2O_3); total iron oxide abundance is lowest (2.5 percent) in uncontaminated sample 2-40, but is greater than 4.5 percent (4.5 to 8.5 percent) in the remaining assemblages (table A-1). The increasing iron abundance, also expressed as the Al/Fe atom ratio in table A-1, parallels the appearance and development of the low-angle shoulder on the dioctahedral 060 spacing (fig. A-8); the Al/Fe atom ratio (table A-1) decreases from 21.2 in the samples with an undetected low-angle shoulder (trace A) to 3.92 in the samples with the most pronounced low-angle shoulder (trace D). The positive correlation between iron content and the intensity of the low-angle shoulder on the dioctahedral 060 spacing is good evidence for the presence of nontronite.

In general, these assemblages are typical of Cenozoic fluvial and marine clays found in the region. The kaolinite-dominant assemblages chiefly reflect local detrital fluvial influx, whereas the smectite-rich assemblages are most likely physical mixtures of the characteristic smectite-rich modern Gulf Coast marine muds with varying amounts of the locally derived detritus.

One feature suggesting interaction between the indigenous clays and the waste plume is the presence of nontronite-rich smectite. Nontronite commonly has been identified as the product of hydrothermal alteration and deep-sea weathering of submarine basalts; it is not a common constituent of Cenozoic Gulf Coast sediments. At the Pensacola site, relatively abundant nontronitic smectite is confined to contaminated sands or associated muds (sites 4-7, 17, 19, 32, and 34; fig. A-4), based on Baedecker and Lindsay's (1986) data for ground-water contamination; it is least abundant or absent in sands and muds peripheral to the waste plume (sites 2, 15, and 33; fig. A-4). Finally, the geochemistry of the waste plume, that is, its substantial (up to $> 20 \text{ mg/L}$ (milligrams per liter)) dissolved, chiefly ferrous iron (fig. A-5), mildly acidic pH (5-6), and low redox composition (Baedecker and Lindsay, 1986), provides an environment similar to that determined by Harder (1978) for the low-temperature synthesis of nontronite.

Table A-1.—Chemical analyses of clay-size (< 2 μm) fraction in core samples from creosote-works area, Pensacola, Florida, with lithic description of whole sediment

A. WEIGHT PERCENT

[Analyzed by J.E. Taggart, U.S. Geological Survey Analytical Laboratory, Denver, Colo.
nd = insufficient sample for analysis]

Com- pound	Sample number								
	2-40	4-20	4-40	5-60	6-20	6-40	7-20	7-50	7-60
SiO ₂	40.5	44.8	36.5	42.7	44.0	45.8	44.0	44.1	44.3
TiO ₂	1.23	.88	1.27	.78	.90	.65	.91	.83	.77
Al ₂ O ₃	34.2	28.3	27.3	24.6	29.7	21.9	30.3	25.0	24.5
Fe ₂ O ₃	¹ 2.53	¹ 5.63	¹ 5.53	6.53	¹ 4.91	7.80	4.16	6.85	¹ 8.51
FeO				.73		.60	.31	.55	
² FeS ₂	nd	.64	nd	.37	.73	.43	.58	.52	.73
MnO	<.02	<.02	<.02	<.02	<0.2	<.02	<.02	<.02	<.02
MgO	.87	1.09	.87	1.99	.95	3.05	.89	1.67	1.65
CaO	.23	.02	.11	2.05	.03	.55	.04	.14	.18
Na ₂ O	.25	.16	.22	.28	.28	.30	.20	.20	.18
K ₂ O	1.00	1.01	.86	.83	.95	.76	.89	.99	.95
P ₂ O ₅	.16	.08	.21	.44	.36	.50	.30	.24	.20
H ₂ O	nd	nd	nd	13.2	nd	12.2	12.9	12.0	nd
H ₂ O	nd	nd	nd	5.94	nd	5.49	3.62	4.88	nd
⁴ LOI	18.9	18.5	27.4	³ 18.8	17.9	³ 17.7	³ 17.7	³ 18.9	18.4
Total	99.9	101.1	100.3	100.4	100.7	100.0	99.1	98.0	100.4
⁵ Al/Fe	21.2	7.36	7.73	5.08	8.61	3.92	9.70	5.01	4.26

¹Total iron oxides as Fe₂O₃.

²Fe required to form FeS₂ excluded from appropriate FeO or Fe₂O₃ abundance.

³Not included in summation of total.

⁴Loss on ignition at 900 °C.

⁵Atom ratio (excludes Fe assigned to FeS₂).

B. LITHIC DESCRIPTIONS, Al₂O₃ WEIGHT PERCENT (WHOLE SAMPLE), AND
DOMINANT CLAY IN <2-μm FRACTION

[Data from Hearn and others, 1986]

Sample number	Sample description	Al ₂ O ₃ weight percent	Dominant clay
2-40	Uncontaminated grain-coated sand	0.7	Kaolinite-rich
4-20	Contaminated clayey sand	8.8	Smectite-kaolinite
4-40	Contaminated grain-coated sand, pyritic	.6	Kaolinite-rich
5-60	Contaminated clayey sand	6.6	Smectite-rich
6-20	Contaminated clayey sand	3.1	Kaolinite-rich
6-40	Silty clay	20.0	Smectite-rich
7-20	Silty clay	22.0	Kaolinite-rich
7-50	Contaminated grain-coated sand, pyritic	.8	Smectite-rich
7-60	Silty clay	24.0	Smectite-rich

Data from clay-size fractions confirm Hearn and others' (1986) conclusion that neofomed pyrite in some grain coatings (samples 4-40 and 7-50) occurs in an assemblage with excess iron over that required in the pyrite. Fractionation to $< 2\mu\text{m}$ effectively removed pyrite from sample 7-50 (table A-1) but greater than 7 percent total iron oxide remains in the assemblage. It is likely that iron-enrichment of the silicate fraction (non-tronitization) and precipitation of authigenic pyrite are contemporaneous and occurred in response to the atypical geochemical environment imposed by the waste plume.

Continuing studies to evaluate these tentative conclusions include: (1) chemical analysis of clay fractions from remaining sites to further examine the apparent relation between iron content and abundance of nontronitic smectite; (2) clay separation and analysis, and pore fluid extraction (squeezing or ultracentrifugation) and analysis from a continuous core through the mud lens to determine pore-fluid composition (presence or absence of waste fluid), and character of associated clay minerals; and (3) clay separation and analysis in both permeable sands and the intervening mud lens that are clearly outside the limits of the waste plume to further document the effects of the plume.

REFERENCES

- Baedecker, M.J., and Lindsay, Sharon, 1986, Distribution of unstable constituents in ground water near a creosote works, Pensacola, Florida, *in* Mattraw, H.C., Jr., and Franks, B.J., eds., Movement and fate of creosote waste in ground water, Pensacola, Florida: U.S. Geological Survey Toxic Waste - Ground-Water Contamination Program: U.S. Geological Survey Water-Supply Paper 2285, p. 1-8.
- Brindley, G.W., and Brown, George, eds., 1980, Crystal structures of clay minerals and their x-ray identification: Mineralogical Society (London), Monograph 5, 495 p.
- Harder, Hermann, 1978, Synthesis of iron layer silicate minerals under natural conditions: *Clays and Minerals*, v. 26, p. 65-72.
- Hearn, P.P., Brown, Z.A., and Dennen, K.O., 1986, Analysis of sand grain coatings and major-oxide composition of samples from a creosote works, Pensacola, Florida, *in* Mattraw, H.C., Jr., and Franks, B.J., eds., Movement and fate of creosote waste in ground water, Pensacola, Florida: U.S. Geological Survey Toxic Waste - Ground-Water Contamination Program: U.S. Geological Survey Water-Supply Paper 2285, p. 19-26.
- Mattraw, H.C., Jr., and Franks, B.J., 1986, Description of hazardous waste research at a creosote works, Pensacola, Florida, *in* Mattraw, H.C., Jr., and Franks, B.J., eds., Movement and fate of creosote waste in ground water, Pensacola, Florida: U.S. Geological Survey Toxic Waste - Ground-Water Contamination Program: U.S. Geological Survey Water-Supply Paper 2285, p. 1-8.

GEOCHEMISTRY OF A SHALLOW AQUIFER CONTAMINATED WITH CREOSOTE PRODUCTS

By Mary Jo Baedecker¹, Bernard J. Franks², Donald F. Goerlitz³, and Jessica A. Hopple¹

The geochemistry of water in a surficial sand and gravel aquifer in Pensacola, Fla. (fig. A-1), has been significantly altered by buried creosote products from a wood-treatment plant. South of the contaminated area, a silt and clay lens about 11 m (meters) thick separates the leachate into a shallow plume (2 to 6 m below land surface) and a deeper plume (17 to 35 m below land surface) (Mattraw and Franks, 1986).

The leachate plume in the shallow system, as indicated by the distribution of dissolved methane, flows southward to Pensacola Bay in several lobes (fig. A-9). The distributions of organic carbon, inorganic carbon (total carbon dioxide calculated from pH and alkalinity), methane, iron, hydrogen sulfide, and sulfate on transect A-A' are shown in figure A-10. An initial increase in concentrations of iron and sulfide followed by a decrease is consistent with their removal by the formation of iron sulfides. The water is supersaturated with respect to several forms of iron sulfides. The initial concentration of sulfate is low because of reduction to hydrogen sulfide. The increase of sulfate 500 m downgradient from the source (fig. A-10) is due to the influence of the saltwater interface; the concentration of chloride also increases. At 180 m from the source on transect A-A', the concentrations of identified polyaromatic hydrocarbons, phenols, and nitrogen heterocyclics (1.1, 2.8, and 1.5 mmol/L (millimole per liter), respectively) account for 59 percent of the organic carbon (9.2 mmol/L). An underground creosote phase southwest of the original ponds (fig. A-11) is the source of the high concentrations of organic compounds. The concentration of organic carbon 350 m from the source is 0.7 mmol/L, and polyaromatic hydrocarbons, phenols, and nitrogen heterocyclics are not present.

¹U.S. Geological Survey, Reston, Va.

²U.S. Geological Survey, Tallahassee, Fla.

³U.S. Geological Survey, Menlo Park, Calif.

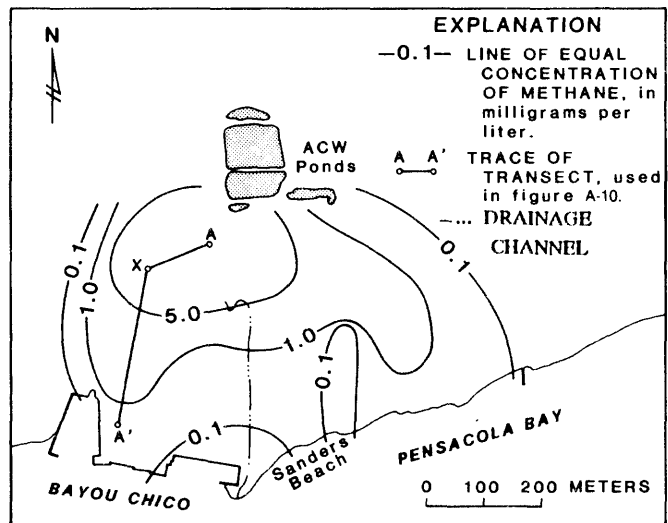


Figure A-9.—Extent of shallow (6-m depth) methane plume at an abandoned creosote works near Pensacola, Florida, 1985. (Location is shown in fig. A-1.)

The rapid decrease in concentrations of organic compounds downgradient may be related to several processes, including (1) sorption of organic compounds on aquifer materials, (2) aerobic degradation by oxygen from the atmosphere, (3) fermentative degradation, and (4) reduction of iron oxides. In this part of the aquifer, the first two processes are not likely to attenuate large concentrations of organic carbon. These organic compounds are not readily sorbed, and the large concentration of oxygen required to oxidize the organic material could not circulate to a depth of 6 m. Organic carbon is attenuated by the latter two processes. Godsy and Goerlitz (1986) demonstrated that certain phenolic compounds

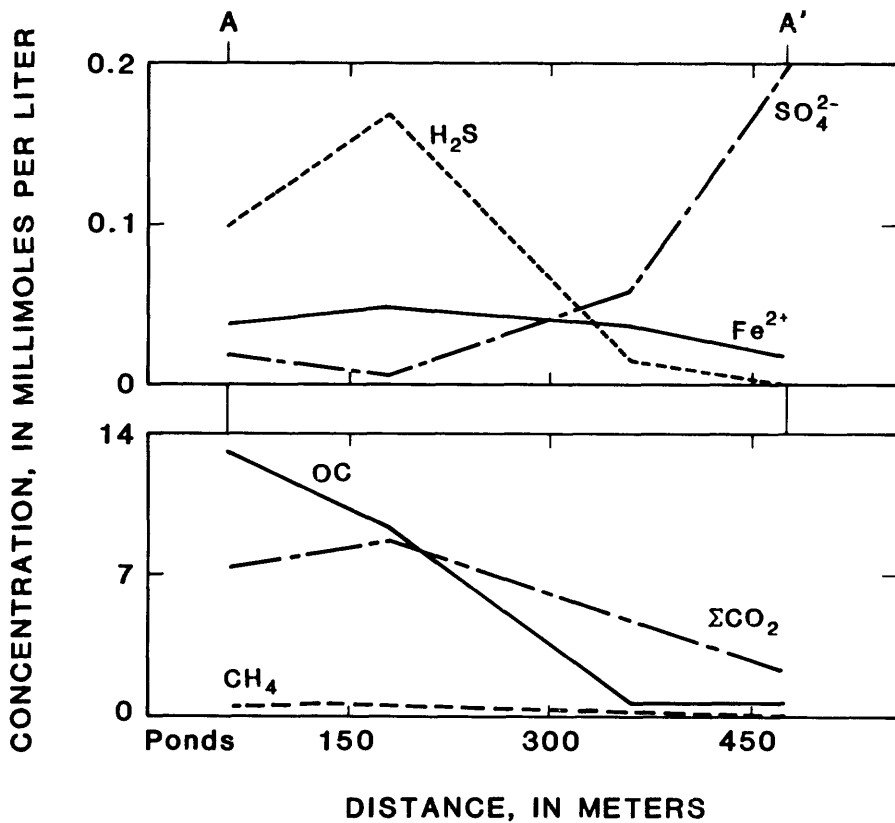


Figure A-10.—Concentrations of dissolved iron, hydrogen sulfide, sulfate, organic carbon, total carbon dioxide, and methane along transect A-A'. (Location is shown in fig. A-9.)

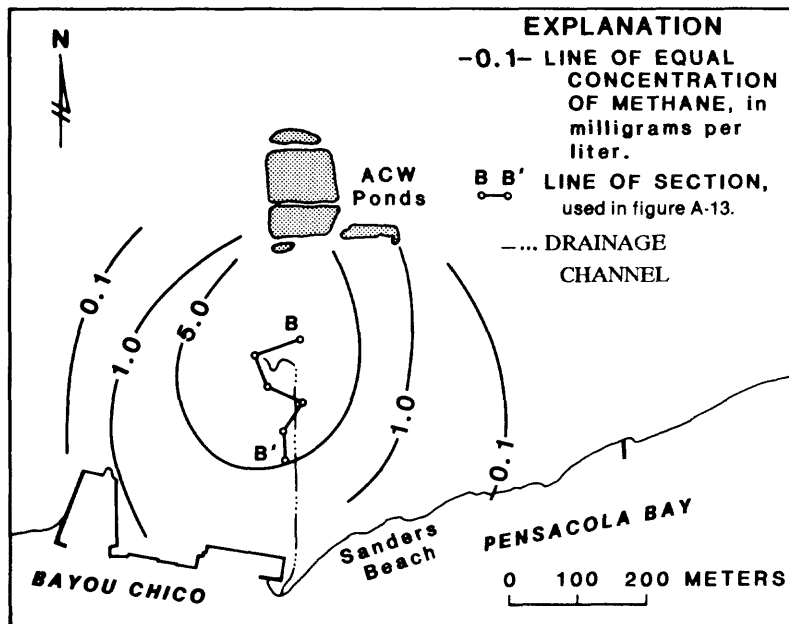


Figure A-11.—Extent of deeper (17-m to 35-m depth) methane plume at an abandoned creosote works near Pensacola, Florida, 1985. (Location is shown in fig. A-1.)

are degraded to carbon dioxide and methane by anaerobic microbial processes. The reduction of iron oxides, which are present throughout the aquifer, and the oxidation of organic compounds, generate ferrous iron and carbon dioxide. The concentrations of iron in solution are not large (0.04 mmol/L), so that the iron that is solubilized is reprecipitated as iron sulfides or incorporated into clays. Bodine (chapter A, this report) suggests that a nontronite-rich clay is formed in the waste plume. In a mass balance, processes (3) and (4) generate carbon dioxide in amounts that exceed concentrations in water, and, because carbonate minerals do not precipitate, carbon dioxide outgasses. In addition, smaller amounts of methane outgas.

The shallow system becomes anoxic a meter or two below the water table. The concentration of dissolved oxygen in a vertical profile decreases with depth from 0.2 mmol/L at the water table (2 m below land surface) to 0.04 mmol/L (3 m below land surface) (fig. A-12). The concentration of dissolved sulfide increases when oxygen is depleted. Initially, the concentrations of iron and sulfate increase as rainwater interacts with the aquifer matrix; however, their concentrations decrease as sulfide is generated. The most abundant dissolved constituents are organic compounds and carbon dioxide, plotted respectively as organic and inorganic carbon (fig. A-12). Both constituents increase gradually to a depth of 4 m, then increase

to about 9 mmol/L where the plume is encountered. The concentration of methane increases gradually to 0.6 mmol/L. Its presence at the water table in water with high oxygen indicates that methane is outgassing from a lower anaerobic zone.

The flow system of the deeper plume is more complicated because of the presence of silt and clay lenses. The deeper plume, as delineated by the distribution of methane, flows directly south and does not spread as extensively to the east and west as does the shallow plume (fig. A-11). On a smaller scale, the movement of contaminants is through the porous layers of silty sand and clayey sand. On section B-B' (fig. A-13), the greatest concentrations of organic and inorganic carbon are in a zone between two small clay lenses. The concentrations are as high as 2.8 mmol/L organic carbon and 6.9 mmol/L inorganic carbon (total carbon dioxide). The high concentrations may be caused by contaminants trapped between the clay lenses from the previous movement of a creosote phase. The concentrations of other dissolved constituents, including methane and $\delta^{13}\text{C}$ values of the inorganic carbon, show similar distributions. An exception is iron, which is ubiquitous in the deeper aquifer, partly because of naturally occurring processes.

Concentrations of most dissolved inorganic constituents in the leachate are low because creosote contaminants are primarily organic com-

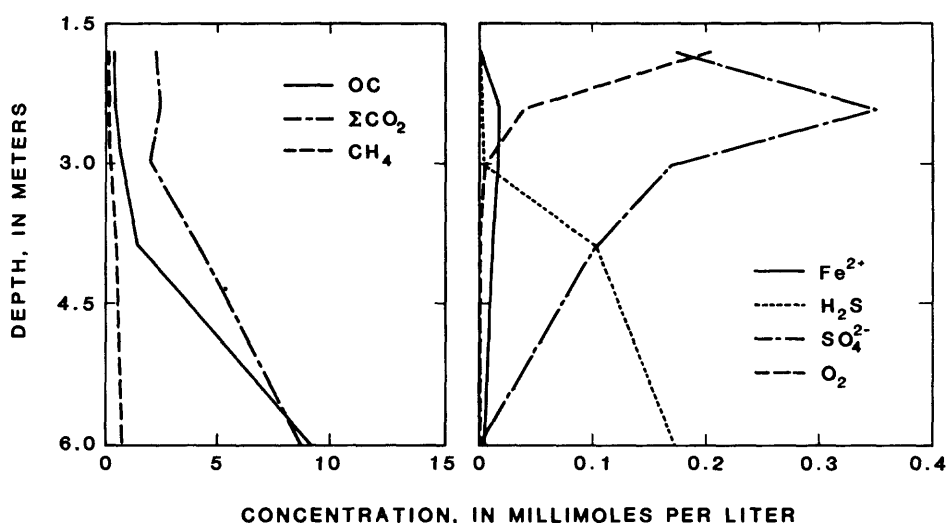


Figure A-12.— Concentrations of dissolved iron, hydrogen sulfide, sulfate, oxygen, organic carbon, total carbon dioxide, and methane with depth. (Location is marked X in fig. A-9.)

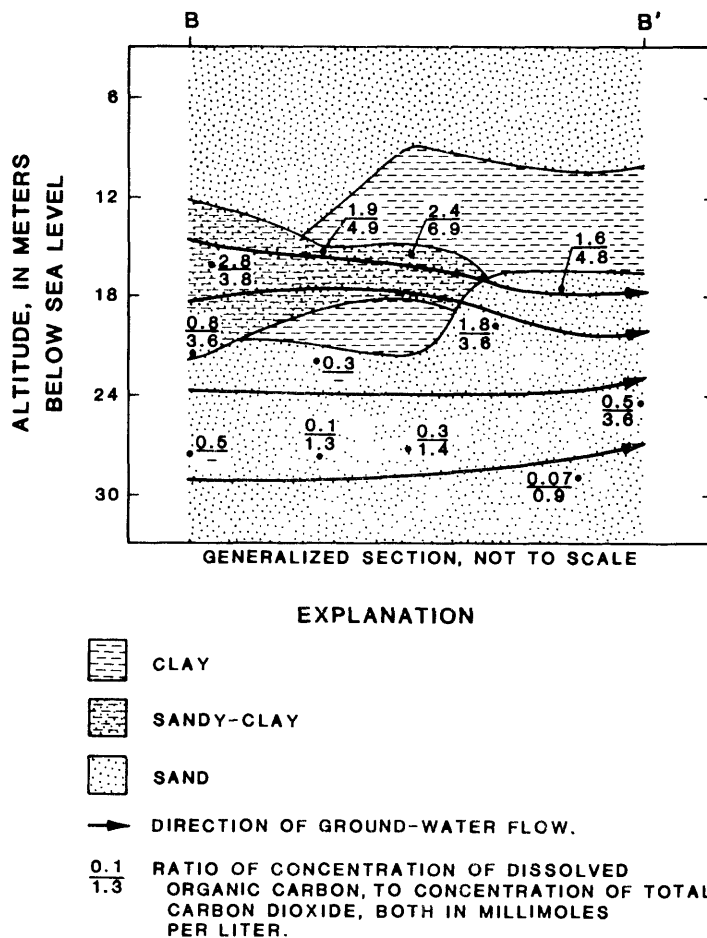


Figure A-13. — Concentrations of dissolved organic carbon and total carbon dioxide along section B-B'. (Location is shown in fig. A-11.)

pounds and because the leachate is in contact with an aquifer matrix of clean quartz sand with small amounts of clay and oxide coatings on sand grains. High concentrations of carbon dioxide result from the degradation of organic compounds, and high iron results from its mobilization in an anoxic environment. Carbon dioxide and methane outgas from the shallow aquifer. The interaction of leachate with silt and clay and the solubilization, generation, and reprecipitation of iron and sulfide phases are important processes as the leachate moves downgradient.

REFERENCES

Godsy, E.M., and Goerlitz, D.F., 1986, Anaerobic microbial transformations of phenolic and other selected compounds in contaminated ground water at a creosote works, Pensacola,

Florida, in Mattraw, H.C., Jr., and Franks, B.J., eds., Movement and fate of creosote waste in ground water, Pensacola, Florida: U.S. Geological Survey Toxic Waste—Ground-Water Contamination Program: U.S. Geological Survey Water-Supply Paper 2285, p. 55-58.

Mattraw, H.C., Jr., and Franks, B.J., 1986, Description of hazardous waste research at a creosote works, Pensacola, Florida, in Mattraw, H.C., Jr., and Franks, B.J., eds., Movement and fate of creosote waste in ground water, Pensacola, Florida: U.S. Geological Survey Toxic Waste—Ground-Water Contamination Program: U.S. Geological Survey Water-Supply Paper 2285, p. 1-8.

REEXAMINATION OF THE OCCURRENCE AND DISTRIBUTION OF CREOSOTE COMPOUNDS IN GROUND WATER

By Donald F. Goerlitz¹

In October 1984, a finding of creosote contamination in the ground water, about 300 m (meters) southeast of an abandoned wood-treatment plant at Pensacola, Fla. (fig. A-1), prompted a reconsideration of previous evaluations of the study site (Troutman and others, 1984; Matraw and Franks, 1986; Goerlitz and others, 1985). The purpose of the October drilling was to augment ground-water data not previously obtained, and the wells at sites 15, 16, and 17 (fig. A-14) were presumed to be in an uncontaminated zone and were to be used for standard aquifer tests. Analysis revealed that the deeper water samples from sites 16 and 17 (table A-2) were heavily contaminated. Analysis of samples from sites 18 (table A-3) and 19 (table A-4) revealed the plume to be much larger than originally thought.

Recent investigations at this and other sites have demonstrated that locating contaminated ground water by hydrologic considerations only is unreliable. Also, as observed at Pensacola, use of nonspecific chemical determinations, such as dissolved organic carbon, colorimetric phenols, and selected inorganic analysis, is unsatisfactory for adequately delineating the volume of contamination. The most definitive approach is specific chemical testing. Because the accurate location of the contamination is essential to understanding the transport and fate of the contaminants, and because this had not been achieved at Pensacola, a decision was made not only to resample the contaminated area, but also to perform onsite, definitive chemical analysis during the drilling.

Table A-2.—Concentrations of polynuclear aromatic hydrocarbons and phenolics found in water samples collected at sites 16 and 17 from the 30-m depth

[Site locations are shown in figure A-14. Concentrations in milligrams per liter. Samples collected on October 26, 1984, and analyzed on November 1, 1984]

Compound	Concentration	
	Site 16	Site 17
Polynuclear aromatic hydrocarbon compounds		
Indene	0.038	0.250
Naphthalene	.200	2.320
Benzothiophene	.030	.258
2-methylnaphthalene	.014	.152
1-methylnaphthalene	.021	.140
1,2-dihydroacenaphthalene	.025	.176
Phenolic compounds		
2,6-dimethylphenol	0	0.033
2,4-dimethylphenol	0	.055
3,5-dimethylphenol	0	.041
2,4,6-trimethylphenol	0	.025
2,3,5-trimethylphenol	0	.025
Naphthol (1 and 2)	0	.053
Pentachlorophenol	2.060	0

¹U.S. Geological Survey, Menlo Park, Calif.

Table A-3. — Concentrations of polynuclear aromatic hydrocarbons and phenolics found in water samples collected at site 18

[Site location shown in figure A-14. Samples collected on October 23, 1984. Concentrations in milligrams per liter; sample depths in meters]

Compound	Concentration at sample depth:		
	10	20	30
Polynuclear aromatic hydrocarbon compounds			
Indene	0.976	1.010	0.015
Naphthalene	14.100	1.180	.385
Benzothiophene	.596	.061	.035
2-methylnaphthalene	1.020	.082	.027
1-methylnaphthalene	.529	.050	.019
Carbazole	.691	.063	.014
Phenolic compounds			
Phenol	1.640	0.249	0.046
2-methylphenol	5.800	.549	.180
3-methylphenol	8.630	.830	.227
4-methylphenol	3.660	.410	.113
2,6-dimethylphenol	1.690	.133	.043
2-ethylphenol	.596	.056	.024
2,4-dimethylphenol	8.680	7.350	.192
2,5-dimethylphenol	3.720	3.150	.082
3,5-dimethylphenol	9.900	.913	.261
2,3-dimethylphenol	1.460	.123	.044
3,4-dimethylphenol	2.180	.197	.059

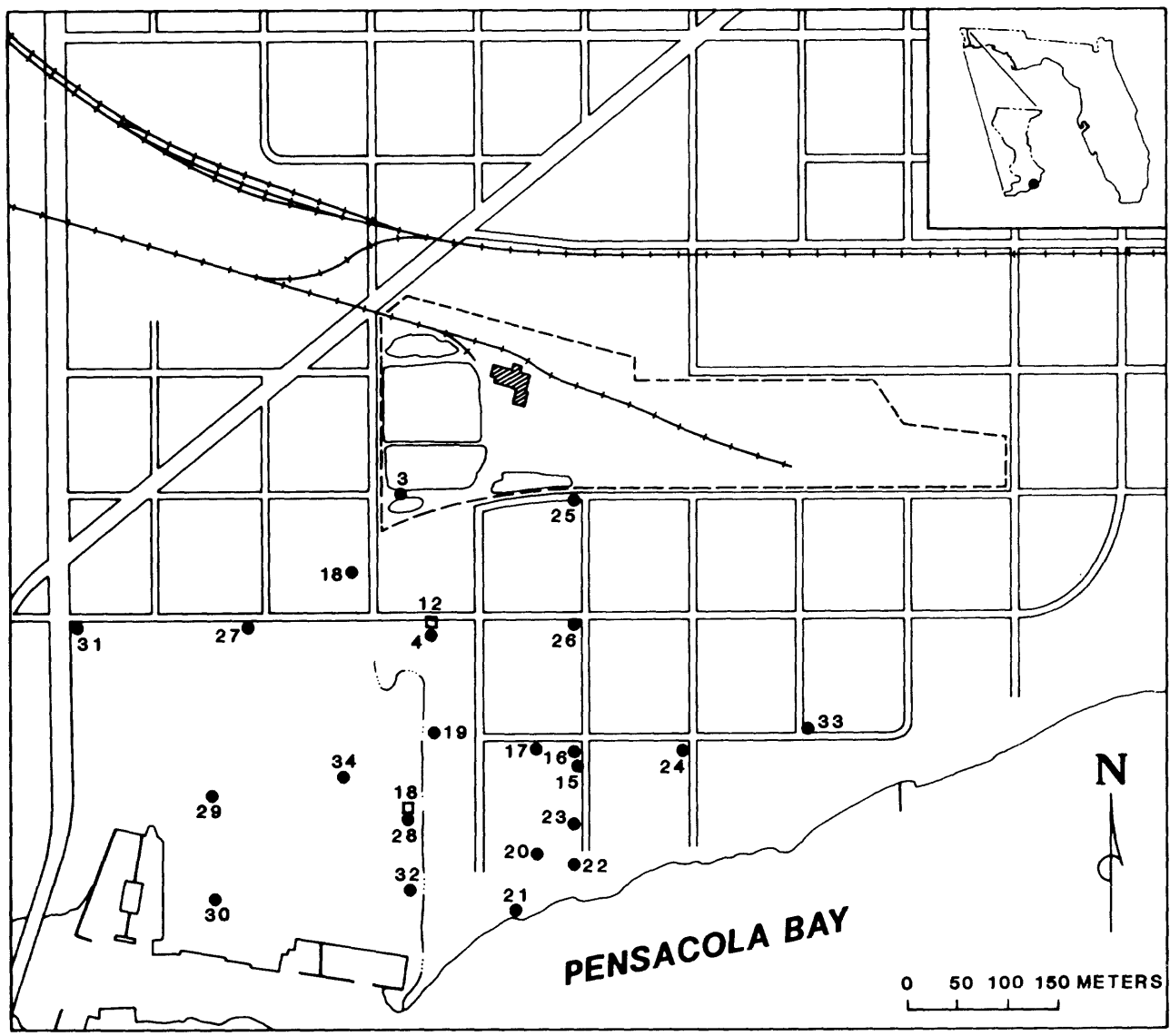
Drilling, sampling, and analysis were done March 15-27, 1985. A total of 26 test holes were drilled at 14 sites, several of which were cased for retention as observation wells. The sampling-site locations are shown in figure A-14 along with the other sites discussed herein. High-performance liquid chromatography (HPLC) was used at the site to determine the soluble components of creosote in the ground water. The determinations were completed within 1 hour of sample collection. HPLC provided accurate determination of naphthalene, other polynuclear aromatic hydrocarbons (PAH), phenols, and pentachlorophenol. Samples were retained and preserved for later, more comprehensive laboratory examinations and for comparison with the field data. As discussed later, preservation of samples for shipment to the laboratory was necessary. Use of HPLC with the sampling enabled accurate delineation of the plume at the time of drilling and of the distribution of specific organic solutes within the aquifer.

Table A-4. — Concentrations of polynuclear aromatic hydrocarbons and phenolics found in water samples collected at the 20-m depth at site 19

[Site location shown in figure A-14. Samples collected on October 26, 1984, and analyzed on November 6, 1984. Concentrations in milligrams per liter]

Compound	Concentration
Polynuclear aromatic hydrocarbon compounds	
Indene	0.612
Naphthalene	7.720
Benzothiophene	.718
2-methylnaphthalene	.585
1-methylnaphthalene	.330
Carbazole	.304
Phenolic compounds	
Phenol	0
2-methylphenol	.023
3-methylphenol	.049
4-methylphenol	.023
2,6-dimethylphenol	.251
2,4-dimethylphenol	.996
2,5-dimethylphenol	.039
3,5-dimethylphenol	.804
2,3-dimethylphenol	.095
3,4-dimethylphenol	.128

HPLC is suitable for use in the field and may be used to determine solutes directly in aqueous samples (Goerlitz, 1982). Little or no sample preparation is required, and the samples may be analyzed immediately after collection. A comparison of field HPLC with laboratory gas chromatographic determinations of naphthalene is given in table A-5. The HPLC field determinations on samples taken near the source of contamination revealed the presence of more than just the phenolic and PAH compounds found in the 1983-84 sampling. Subsequent laboratory investigations by mass spectrometry identified these substances as nitrogen heterocycles in concentrations much higher than previously reported (Pereira and Rostad, 1986). Samples collected in March 1985 contained as much as 88 mg/L (milligrams per liter) of nitrogen heterocycles, as shown in table A-6. The presence of these readily degradable compounds at such high concentrations would not have been revealed in unpreserved samples without on-site HPLC.



EXPLANATION

31● SITE AND SITE NUMBER

12□ WELL AND WELL NUMBER

Figure A-14. – Locations of drilling sites and wells in abandoned creosote-works area near Pensacola, Florida. (Location is shown in fig. A-1.)

Table A-5.—Comparison of on-site high performance liquid chromatographic (HPLC) analysis for naphthalene with laboratory gas-chromatographic (GC) analysis for naphthalene

[Site locations shown in figure A-14. Samples are from 24-m to 30-m depth. Concentrations in milligrams per liter]

Site number	Method	
	HPLC	GC
16	0.200	0.046
17	1.56	1.56
20	.865	.750
21	0	.001
22	.514	.529
23	0.041	0.058
26	.056	.036
27	1.75	1.82
32	0	.031

Table A-6.—Concentrations of heterocyclic nitrogen compounds in a water sample taken at site 3

[Site location is shown in figure A-14. Sample collected on March 25, 1985, from 6-m depth. Concentrations in milligrams per liter]

Compound	Concentration
Pyridine	0.274
2-methylpyridine	.953
4-methylpyridine	.930
3-methylpyridine	.760
2,6-dimethylpyridine	.495
2,5-dimethylpyridine	.680
2,4-dimethylpyridine	2.110
2,3-dimethylpyridine	.501
2,4,6-trimethylpyridine	1.100
2,3,6-trimethylpyridine	.379
Quinoline	11.200
Isoquinoline	3.610
2-methylquinoline	4.320
6-methylquinoline	.800
2,6-dimethylquinoline	.878
4-methylquinoline	.778
2,4-dimethylquinoline	.846
2-quinolinone	27.600
1-isoquinolinone	29.710
Acridine	.111
Carbazole	.264
Total	88.299

Comparison of preserved (65 mg/L mercuric chloride) to unpreserved water samples from the site 3 well showed nearly total degradation of both the phenol and nitrogen base fractions within 11 days of sampling, even though the samples were kept chilled. Further, it was found that the major component originally reported in this fraction, the degradation product of quinoline, 2-quinolinone, is really two compounds. The other compound is 1-isoquinolinone, presumably an alteration product of isoquinoline. Together they are present at nearly an order of magnitude greater concentrations than previously reported, and are the most abundant of the individual solutes found in the ground water near the source. Although quinoline is 5 to 10 times more abundant in creosote than isoquinoline, the isoquinolinone alteration product was found to be the preponderate nitrogen heterocycle remaining. This suggests that isoquinolinone is more stable than the quinolinone isomer. Further, these oxidized derivatives and the other nitrogen heterocycles are evidently degraded in the anaerobic environment. Relatively low concentrations of transformation products, less than 5 mg/L, and none of the other nitrogen heterocycles were found at site 4, which is about 150 m downgradient from the former holding ponds.

Chemical analyses of water samples taken at the shallow (6 m) depth indicate that solute transport was not the only mechanism for movement of contamination from the site. Examination of a 1950's aerial photograph of the area shows a railway passing south of the site on an arc, intercepting sites 18 and 27, on the way to Bayou Chico. The high levels of creosote contaminants in the shallow wells appear to be associated with the abandoned railway. Because the holding ponds are reported to have occasionally overflowed after heavy rainstorms, the contaminated mixture probably flowed from the ponds along drainage features such as the railway drainage ditches, toward Bayou Chico and the bay. In the area immediately south of the former holding ponds and in the vicinity of other drainage features, the relation between overland flow and aquifer contamination is evident. Apparently, the overland flow pooled in lowlands and extended more than 300 m toward the bay.

After the Clean Water Act of 1970, remedial action was taken to halt the overflow from the ponds, and the contaminated wetlands were cov-

ered with fill. Hand-auger borings showed that the area of the former wetlands is indeed covered to a depth of about 1 m. Examination of the borings suggests that much of the fill is sludge from the holding ponds and also contains broken concrete, clay bricks, glass, and rocks, and is covered by a sandy soil. Below a depth of 1 m, a layer of liquid hydrocarbon as thick as 1 m is commonly found. After rain storms, the dense liquid hydrocarbon frequently is observed to flow into the drainage ditch shown in figure A-13. Additionally, one of the observation wells drilled before 1981, designated well 12 and adjacent to site 4, shows a much higher level of contamination than the shallow well at site 4 (table A-7). Well 12 is screened through the water table, which is about 2 m below land surface at that site, whereas the sample from site 4 was taken at the 6-m level. The higher levels of contamination at well 12 give further evidence of overland transport of oily wood treating fluid.

Table A-7. — Concentrations of polynuclear aromatic hydrocarbon compounds, phenolic compounds, and nitrogen compounds in samples taken at the water table and 6 m below the water table

[Site locations shown in figure A-14. Concentrations in milligrams per liter]

Compound	Concentration	
	Site 4 ¹	Well 12 ²
Polynuclear aromatic hydrocarbon compounds		
Indene	0	0.059
Naphthalene	2.070	4.520
Benzothiophene	.157	.376
2-methylnaphthalene	.101	.594
1-methylnaphthalene	.060	.295
Biphenyl	0	.087
Acenaphthalene	0	0
1,2-dihydroacenaphthalene	.052	.300
Dibenzofuran	0	.163
Fluorene	.036	.173
Phenanthrene	0	.058
2-phenylnaphthalene	0	0
Pyrene	0	0
Benz(a)pyrene	0	0
Total	2.476	6.625

¹Sample collected on March 26, 1985, at a depth of 6 m.

²Sample collected on March 25, 1985, at a depth of 1 to 3 m.

Table A-7. — Concentrations of polynuclear aromatic hydrocarbon compounds, phenolic compounds, and nitrogen compounds in samples taken at the water table and 6 m below the water table — Continued

Compound	Concentration	
	Site 4 ¹	Well 12 ²
Phenolic compounds		
Phenol	0.081	0
2-methylphenol	.029	1.080
3-methylphenol	.076	.172
4-methylphenol	.030	.080
2,6-dimethylphenol	.102	.235
2-ethylphenol	0	.057
2,4-dimethylphenol	.154	1.040
2,5-dimethylphenol	.070	.510
3,5-dimethylphenol	.038	1.310
2,3-dimethylphenol	0	.180
3,4-dimethylphenol	.029	.368
2,4,6-trimethylphenol	.025	.054
2,3,6-trimethylphenol	.038	.152
ethylmethylphenol	0	0
2,3,5-trimethylphenol	.017	.117
2,3,5,6-tetramethylphenol	0.015	0.016
1-naphthol	0	.061
2-naphthol	0	.064
PCP	.083	.200
Total	.787	5.696
Nitrogen compounds		
Pyridine	0	0
2-methylpyridine	0	.156
4-methylpyridine	0	.052
3-methylpyridine	0	.105
2,6-dimethylpyridine	0	.174
2,5-dimethylpyridine	0	.193
2,4-dimethylpyridine	0	.815
2,3-dimethylpyridine	0	.183
2,4,6-trimethylpyridine	0	.454
2,3,6-trimethylpyridine	0	.340
Quinoline	0	.015
Isoquinoline	0	.017
2-methylquinoline	0	.744
6-methylquinoline	0	.010
2,6-dimethylquinoline	0	.020

¹Sample collected on March 26, 1985, at a depth of 6 m.

²Sample collected on March 25, 1985, at a depth of 1 to 3 m.

Table A-7.—Concentrations of polynuclear aromatic hydrocarbon compounds, phenolic compounds, and nitrogen compounds in samples taken at the water table and 6 m below the water table—Continued

Compound	Concentration	
	Site 4 ¹	Well12 ²
Nitrogen compounds—Continued		
4-methylquinoline	0	.080
2,4-dimethylquinoline	0	.097
2-quinolinone	3.760	1.760
1-isoquinolinone	.558	3.580
Acridine	0	.024
Carbazole	0	.247
Total	4.318	9.066

¹Sample collected on March 26, 1985, at a depth of 6 m.

²Sample collected on March 25, 1985, at a depth of 1 to 3 m.

Results of the sampling may be summarized as follows:

Specific chemical determinations are needed to adequately delineate the contaminated parts of an aquifer because hydrologic and nonspecific chemical tests may fail to provide adequate information. Field analyses or onsite determinations of individual solutes are most useful for evaluation of the extent and nature of the contamination, and during test well drilling, permit immediate adjustment of the sampling scheme, and reduce possible sample degradation.

Soluble nitrogen heterocycles are abundant in ground water near the former ponds, but are transformed or degraded in the aquifer. Nitrogen heterocycles in water samples taken from the 6-m depth were not detected more than 150 m downgradient from the original ponds.

The nitrogen heterocycles in ground water appear to undergo transformation or degradation, not only in the aerobic but also the anaerobic part of the aquifer. Quinoline, isoquinoline, 2-quinolinone, and 1-isoquinolinone, the most abundant compounds in ground water near the

site, all appear to readily degrade in the deeper parts of the aquifer.

At this site, overland flow and land-surface features have substantially influenced the upper 6 to 10 m of the ground water. Factors such as the changes in surface-drainage patterns, overland flow of liquid hydrocarbon, and subsequent burial of the pooled hydrocarbon, all together have complicated the near-surface system.

REFERENCES

- Goerlitz, D.F., 1982, Determination of pentachlorophenol in water and aquifer sediments by high-performance liquid chromatography: U.S. Geological Survey Open-File Report 82-124, 12 p.
- Goerlitz, D.F., Troutman, D.E., Godsy, E.M., and Franks, B.J., 1985, Migration of wood-preserving chemicals in contaminated ground water in a sand aquifer at Pensacola, Florida: Environmental Science and Technology, v. 19, no. 10, p. 955-961.
- Matraw, H.C., Jr., and Franks, B.J., eds., 1986, Movement and fate of creosote waste in ground water, Pensacola, Florida: U.S. Geological Survey Toxic Waste—Ground-Water Contamination Program: U.S. Geological Survey Water-Supply Paper 2285, 63 p.
- Pereira, W.E., and Rostad, C.E., 1986, Geochemical investigations of organic contaminants in the subsurface at a creosote works, Pensacola, Florida, MU in Matraw, H.C., Jr., and Franks, B.J., eds., Movement and fate of creosote waste in ground water, Pensacola, Florida: U.S. Geological Survey Toxic Waste—Ground-Water Contamination Program: U.S. Geological Survey Water-Supply Paper 2285, p. 33-40.
- Troutman, D.E., Godsy, E.M., Goerlitz, D.F., and Ehrlich, G.G., 1984, Phenolic contamination in the sand-and-gravel aquifer from a surface impoundment of wood treatment wastes, Pensacola, Florida: U.S. Geological Survey Water-Resources Investigations Report 84-4230, 36 p.

DETERMINATION OF THE RATES OF ANAEROBIC DEGRADATION OF THE WATER-SOLUBLE FRACTION OF CREOSOTE

By Edward M. Godsy¹ and Donald F. Goerlitz¹

INTRODUCTION

Creosote is the most extensively used insecticide and industrial wood preservative in use today. It is estimated that there are more than 600 wood-preserving plants in the United States today, and their collective use of creosote exceeds over 4.5×10^6 kg/yr (kilograms per year) (von Rumker and others, 1975). Creosote is a complex mixture of more than 200 major individual organic compounds with differing molecular weights, polarities, and functionalities, along with dispersed solids and products of polymerization (Novotny and others, 1981). The major classes of compounds previously identified in creosote show that it consists of ~85 percent by weight polynuclear aromatic compounds, ~12 percent phenolic compounds, and ~3 percent heterocyclic nitrogen, sulfur, and oxygen containing compounds.

Large but unknown quantities of the waste from the wood-preserving plant at Pensacola, Fla. (fig. A-1), infiltrated the soil and moved downward to the water table. Upon reaching the water table, the creosote mixed with the ground water, and two distinct phases resulted — a denser than water hydrocarbon phase that moved vertically downward somewhat perpendicular to the direction of ground-water flow, and an aqueous phase. The aqueous phase, or water-soluble fraction, has been enriched in phenolic compounds, single- and double-ring aromatic compounds, and single- and double-ring aromatic compounds with nitrogen, sulfur, and oxygen incorporated into the ring structure.

ANAEROBIC DEGRADATION

Aquifer materials typically have a large surface area to which bacteria can attach, which results in high concentrations of attached bacteria relative to the concentration of free cells in the surrounding pore water. In the contaminated aquifer at the wood-preserving plant, ~91.5 percent per unit volume of the total bacteria, or $\sim 5.0 \times 10^5$ bacteria

per gram dry weight, are attached to the sediment. The thickness of the biofilm is a function of the substrate available to support the growth of the bacteria. Because the plant was in operation for nearly 80 years, the biofilm surrounding the aquifer material probably has reached equilibrium and can, therefore, be described by a steady-state approach, whereby microbial growth in the biofilm equals the death rate of the microorganisms (Rittman and McCarty, 1980).

As the contaminated water moves along with the ground-water flow, the anaerobically biodegradable compounds will be used by those bacteria residing in the aquifer. In previous laboratory studies, Godsy and Goerlitz (1986) demonstrated that phenol, 2-methyl phenol, 3-methyl phenol, 4-methyl phenol, benzoic acid, and volatile fatty acids were anaerobically biodegradable to CO_2 and CH_4 by a consortium of bacteria isolated from the contaminated aquifer. The volatile fatty acids are rapidly converted to CO_2 and CH_4 by the bacteria. A relatively low concentration of acetic acid, which is the major intermediate compound in anaerobic environments and a major intermediate product in the degradation of the phenolic compounds, persisted throughout the experiment. Once all of the organic material is degraded, the acetic acid is also degraded.

By contrast, none of the unsubstituted aromatic hydrocarbons were observed to degrade under the same anaerobic conditions, either in this study or in previous laboratory experiments, and no examples of anaerobic degradation of these compounds have been reported in the literature.

No information on the anaerobic degradation of nitrogen substituted heterocycles that are found in the water-soluble fraction of creosote could be found in the literature, except indole (Wang and others, 1984); but detailed laboratory analysis of contaminated ground water suggested that the nitrogen compounds in solution were being unaccountably attenuated, as mentioned by Goerlitz (chapter A, this report).

¹U.S. Geological Survey, Menlo Park, Calif.

Anaerobic-degradation experiments were conducted with laboratory scale digestors in which only the water-soluble fraction and the aquifer material were used to determine the biodegradability of the nitrogen heterocyclic compounds and the phenolic compounds under anaerobic conditions. Aquifer material from site 3 (see fig. A-14) at a depth of 6.1 m (meters) was collected in 5-L (liter) bottles using anaerobic techniques after augering to depth with a hand-operated power auger. The anaerobic digestors contained approximately 4 kg (kilograms) of aquifer material and approximately 2.5 L of contaminated ground water from the same site. All operations were performed under an O₂-free argon atmosphere. The digestors were fitted with both gas- and liquid-sampling ports. Samples for organic analysis were analyzed by gas chromatography (GC), high pressure liquid chromatography (HPLC), and computer-assisted gas chromatography-mass spectrometry (GC/MS/DS) at approximately 7-day intervals. At the same time, the increase in gas volume was recorded and the gas composition determined by GC. Microbial biomass was determined by dry weight and by acridine-orange direct microscopic counts.

Results indicate that, along with the phenolic compounds and organic acids previously reported to be anaerobically biodegradable (fig. A-15), the nitrogen containing compounds, quinoline, isoquinoline, 2-quinolinone, 1-isoquinolinone, also are anaerobically biodegradable (fig. A-15). The degradation times shown in figure A-15 indicate a sequential three part degradation of these compounds in the following order:

1. 50 days: quinoline, isoquinoline, benzoic acid, formic acid, and propionic acid.
2. 100 days: phenol.
3. more than 100 days: 2-, 3-, 4-methyl phenol, 2-quinolinone; and 1-isoquinolinone.

A mass balance was performed on the anaerobic digestors by first converting all identified components in the water to millimoles of carbon and comparing this value with the amount of CO₂ and CH₄ produced during the degradation. As shown in figure A-16, more total gas was produced than can be accounted for by the identified carbon compounds. Wet-oxidation dissolved organic carbon analysis of substrate disappearance with time is plotted in figure A-17. Both methods (DOC and

calculated millimoles of carbon) give comparable results during the first 90 days (fig. A-17), but after this period, the amount of carbon indicated by the DOC analysis is higher than the calculated value. The additional carbon apparently comes from the microbial degradation of organic material on the sediments. This observation was corroborated by volatile solids analysis of aquifer material from site 3. This determination showed that the concentration of organic material on the sediment (6.6 mg/g (milligram per gram) dry weight) was several orders of magnitude higher than can be accounted for by only the bacterial biomass. Further, this organic material was not found on sediments from areas that are not contaminated with creosote compounds. The nature of this organic compound is unknown at this time.

MODELING SUBSTRATE UTILIZATION

Several types of curves are shown as plots of the depletion of organic molecules added to samples from natural environments. On arithmetic axes, substrate-depletion curves may be concave-up (first-order and Monod—no growth), concave down (logarithmic), or linear (zero-order) with time. In a natural system, the shape of the biodegradation curve is probably influenced by such factors as temperature, pH, dissolved oxygen, Eh, salinity, nutrients, toxicity, and the concentrations of microorganisms and compounds. The effects or interactions of such potentially important factors make it difficult to predict the biodegradation kinetics of a particular substrate.

Substrate utilization by microorganisms in laboratory digestors filled with the contaminated aquifer material generally can be treated in the same manner as for dispersed growth. In this low nutrient, static anaerobic digester environment, fully penetrated biofilms develop in which all bacteria are exposed to the same concentrations of organic compounds that are present in the bulk liquid. This can be done with only the variables of substrate concentration and bacterial biomass in one of the following expressions:

- | | |
|--|---|
| 1. <u>Monod kinetics</u> | 4. <u>First order in S</u> |
| - $\frac{dS}{dt} = \frac{\mu_{max} X S}{Y(K_s + S)}$ | - $\frac{dS}{dt} = \frac{\mu_{max} X_0}{K_s} S$ |
| 2. <u>Monod—no growth</u> | 5. <u>Second order in S</u> |
| - $\frac{dS}{dt} = \frac{\mu_{max} X_0 S}{K_s + S}$ | - $\frac{dS}{dt} = \frac{\mu_{max}}{K_s} S X$ |

Figure A-15.—Degradation of organic acids (top), phenolic compounds (middle), and heterocyclic compounds (bottom) in anaerobic digestors.

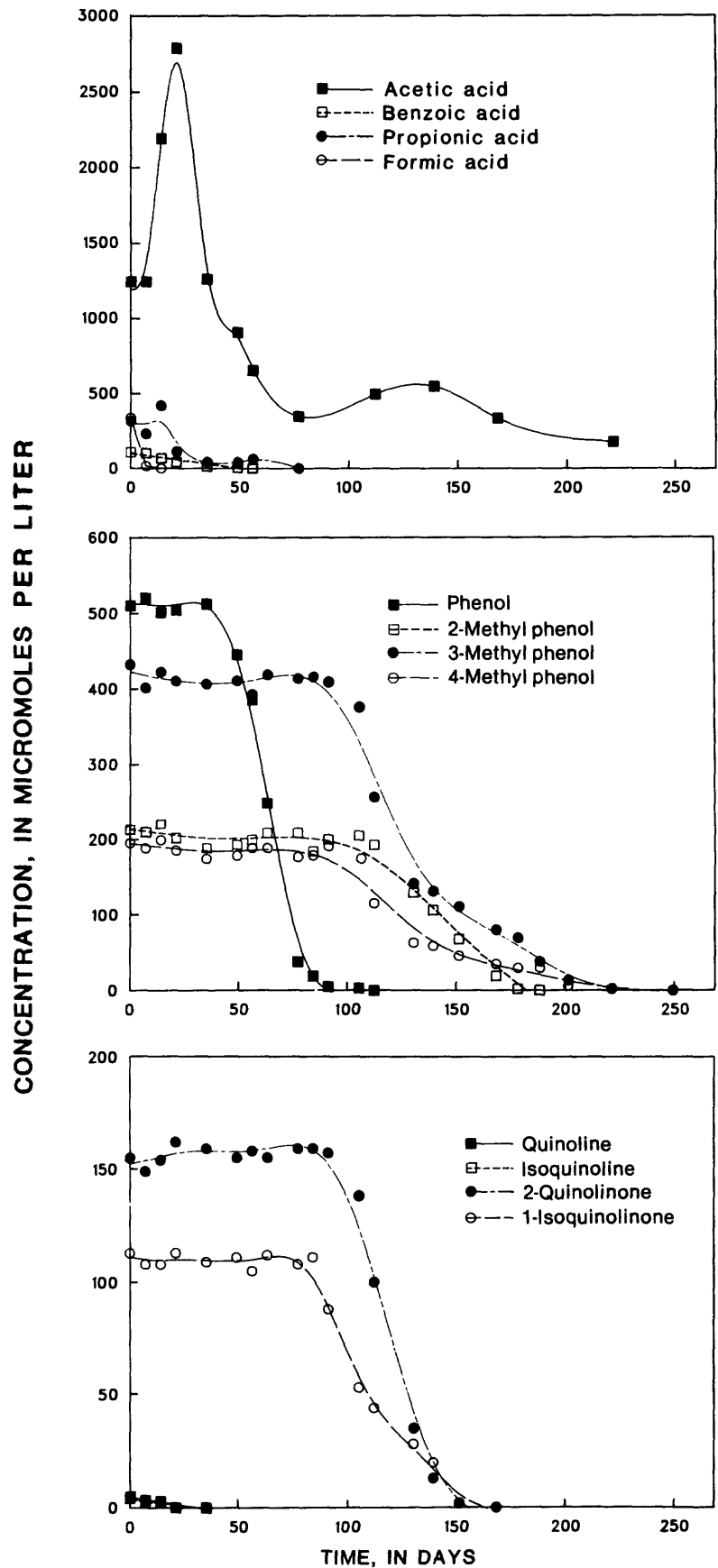


Figure A-16.—Calculated carbon balance for identified compounds in water-soluble fraction in anaerobic digester.

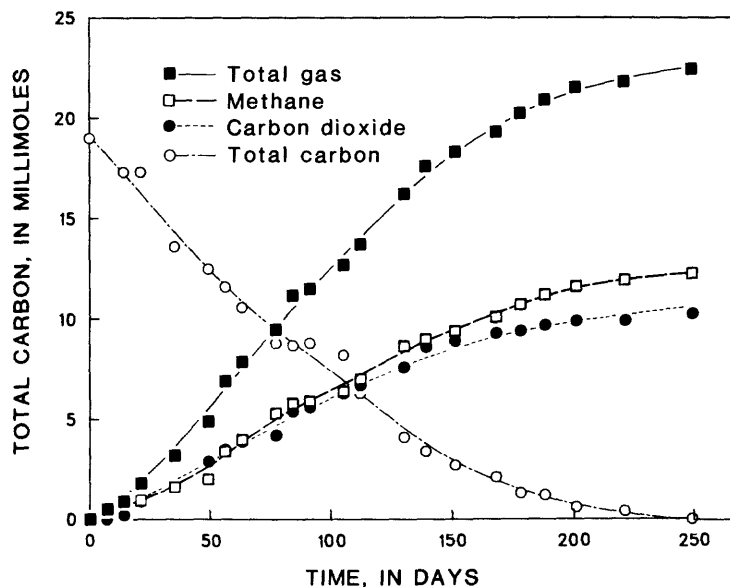
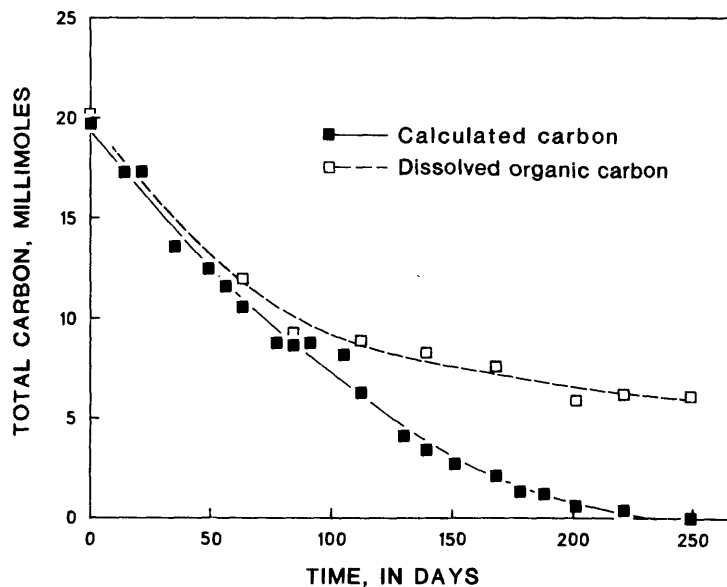


Figure A-17.—Total carbon values obtained by mass-balance computation (fig. A-16) and by dissolved organic carbon analysis.



3. Zero order in S

$$-\frac{dS}{dt} = \mu_{\max} X_0$$

where

S = substrate concentration at time t (mass/unit volume);

t = time;

μ_{\max} = maximum specific growth rate (time^{-1});

X = biomass [$Y(S_0 - S) + X_0$] at time t (mass/unit volume), where

6. Logarithmic

$$-\frac{dS}{dt} = \mu_{\max} X$$

S_0 = initial substrate concentration (mass/unit volume), and

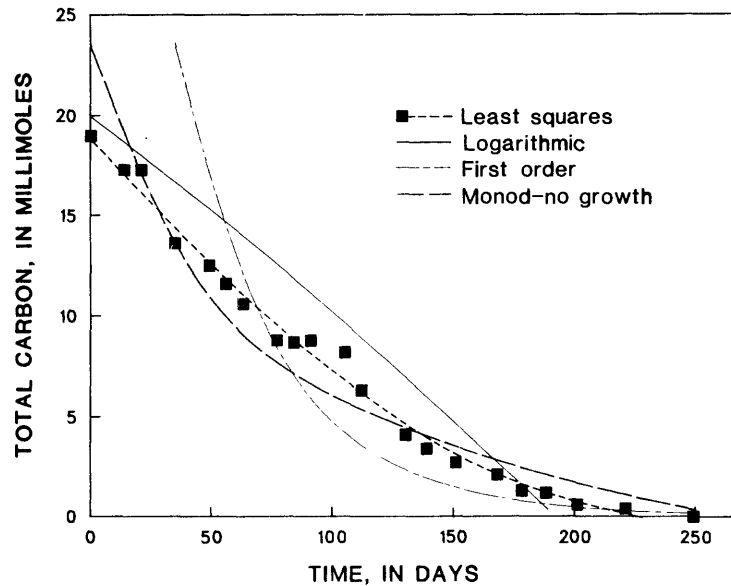
Y = yield coefficient (mass/mass);

X_0 = initial biomass (mass/unit volume); and

K_s = half-velocity coefficient (mass/unit volume).

The preceding mathematical expressions generally concern a single population of microorganisms growing on a readily degradable substrate. Under these conditions, the Monod

Figure A-18.— Comparison of best-fit mathematical models to calculated carbon substrate-disappearance curve.



equation (eq. 1) generally can describe substrate utilization by bacteria. These equations also can apply to such complex mixtures of microorganisms and substrates as domestic sewage but commonly do not apply to complex mixtures of difficult-to-degrade, slightly to highly toxic compounds such as those in the water-soluble fraction of creosote.

The other equations presented are simplifications of the Monod equation that can be used under certain specified conditions. Because the relationships of K_s to S_0 and of X_0 to S_0 are not known, the other equations were fit to the data. The zero-order equation (eq. 3) can be used when $X_0 \gg S_0$ and $S_0 \gg K_s$; the first-order approximation (eq. 4) can be used when $X_0 \gg S_0$ and $S_0 \ll K_s$; the second-order equation (eq. 5) can be used when $S_0 \ll K_s$; the logarithmic equation (eq. 6) can be used when $S_0 \gg K_s$; and the Monod-no growth equation (eq. 2) can be used when $X_0 \gg S_0$.

Figure A-18 shows the best mathematical fits to the experimental data for the degradation of the water-soluble fraction. Not shown are the linear zero-order equation (eq. 3) and the Monod equation (eq. 1), which could not be fit to this data. The second-order curve (not shown) coincided closely with the logarithmic curve and is omitted for clarity. The disparity among these curves indicate

that these equations do not adequately describe the anaerobic microbial utilization of this complex multi-component substrate. In light of this finding, transport models that incorporate bacterial degradation will require specific data for each compound or, at least, for groups of compounds. These considerations are under study, and, because of the nature of the water-soluble fraction, models that contain inhibition terms are also being considered.

REFERENCES

- Godsy, E.M., and Goerlitz, D.F., 1986, Anaerobic microbial transformations of phenolic and other selected compounds in contaminated ground water at a creosote works, Pensacola, Florida, in Matraw, H.C., Jr., and Franks, B.J., eds., Movement and fate of creosote waste in ground water, Pensacola, Florida: U.S. Geological Survey Toxic Waste—Ground-Water Contamination Program: U.S. Geological Survey Water-Supply Paper 2285, p. 55-58.
- Novotny, M., Strand, J.W., Smith, S.L., Wiesler, D., and Schwende, F.J., 1981, Compositional studies of coal tar by capillary gas chromatography-mass spectrometry: Fuel, v. 60, p. 213-220.

Rittman, B.E., and McCarty, P.L., 1980, Model of steady-state-biofilm kinetics: *Biotechnology and Bioengineering*, v. 22, p. 2343-2357.

von Rumker, R., Lawless, E.W., and Meiners, A.F, 1975, Production, distribution, use and environmental impact potential of selected pesticides: U.S. Environmental Protection

Agency, EPA 540/1-74-001, 439 p.

Wang, Y., Suidan, M.T., and Peffer, J.T., 1984, Anaerobic biodegradation of indole to methane: *Applied and Environmental Microbiology*, v. 48, p. 1058-1060.

CONTAMINATION, BIOACCUMULATION, AND ECOLOGICAL EFFECTS OF CREOSOTE-DERIVED COMPOUNDS IN THE NEARSHORE ESTUARINE ENVIRONMENT OF PENSACOLA BAY, FLORIDA

By Paul V. Dresler¹ and John F. Elder²

Seven sites in Pensacola Bay near an abandoned creosote plant (fig. A-19) were examined seasonally from June 1983 through June 1984 for possible contamination by creosote-constituent compounds and for the effects such contaminants may have on the distribution and abundance of benthic invertebrates (fig. A-20). A similar site on the opposite side of the bay was used as a control. Additional samples were taken from the bed of a drainage stream that flows from the area of the creosote works directly to the bay.

Analyses of streamflow and bay waters showed no trace of contamination at any of the sites, but streambed sediments were heavily contaminated. Compounds detected at the drainage stream site 2 and their concentrations in micrograms per kilogram ($\mu\text{g}/\text{kg}$) of sediment, included anthracene (3,200), chrysene (7,100), fluoranthene (17,000), fluorene (3,100), phenanthrene (12,000), and pyrene (11,000). Some of these compounds also were found in estuarine sediments. The data suggest that most compounds near the sediment surface are rapidly diluted and degraded in the estuarine environment. Analyses of sediment core segments, however, showed that some compounds have accumulated just below the surface, at depths of 8 to 13 cm (centimeters) and that below 13 cm, concentrations rapidly diminished (fig. A-20). Compounds that commonly occurred in estuarine sediments included anthracene, pyrene, phenanthrene, fluoranthene, and benzo(k)fluoranthene.

Bioaccumulation of creosote-constituent compounds was investigated in two ways. Native snails (*Thais haemastoma*) were collected, shelled, and analysed for bioaccumulation in whole-body tissue. Oysters (*Crassostrea virginica*) that had been collected in another part of the bay, were placed in cages at some of the test sites and at the control site to determine bioaccumulation over a 6-week period. Some evidence of bioaccumulation was

found, but at very low levels (less than 100 mg/kg). The compounds that most frequently occurred in the sediments include pyrene, phenanthrene, and fluoranthene (fig. A-20), which were also among the commonly bioaccumulated compounds.

Four times during the study, 10 sediment cores were collected at each site to assess the benthic microinvertebrate community. The benthic communities of the nearshore environment of Pensacola Bay consist of 72 species distributed over 10 phyla (table A-8). Over 60 percent of the fauna collected over the entire study period consists of polychaetes; the polychaete *Paraonis fulgens* forms 31 percent of the total faunal collection. Rankings of total abundance and total numbers of species collected by season for each of the sites indicated no statistically significant difference between the nearshore sites proximal to the creosote plant and the controls. Site 7, located in Bayou Chico, and all drainage stream sites consistently had lower abundance and numbers of species than all other sites, including the control.

Studies of recolonization of fresh bottom substrate (recruitment) were performed at site 1 and the control site. No significant differences between invertebrate recruitment patterns were found at either site, but the results indicated that the nearshore sediments are alternately scoured and redeposited. The resultant instability of bottom sediments may account for the observed paucity of mollusks and the observed failure by the majority of the infaunal community at any of the sites to mature past the juvenile stage. Larval recruitment was high and was observed to exceed 20,000 individuals per m^2 (square meter) over one tidal cycle.

Normal cluster analyses performed on a seasonal basis indicated that at the 0.60 similarity level four site clusters exist (drainage stream sites,

¹U.S. Geological Survey, Reston, Va.

²U.S. Geological Survey, Madison, Wisc.

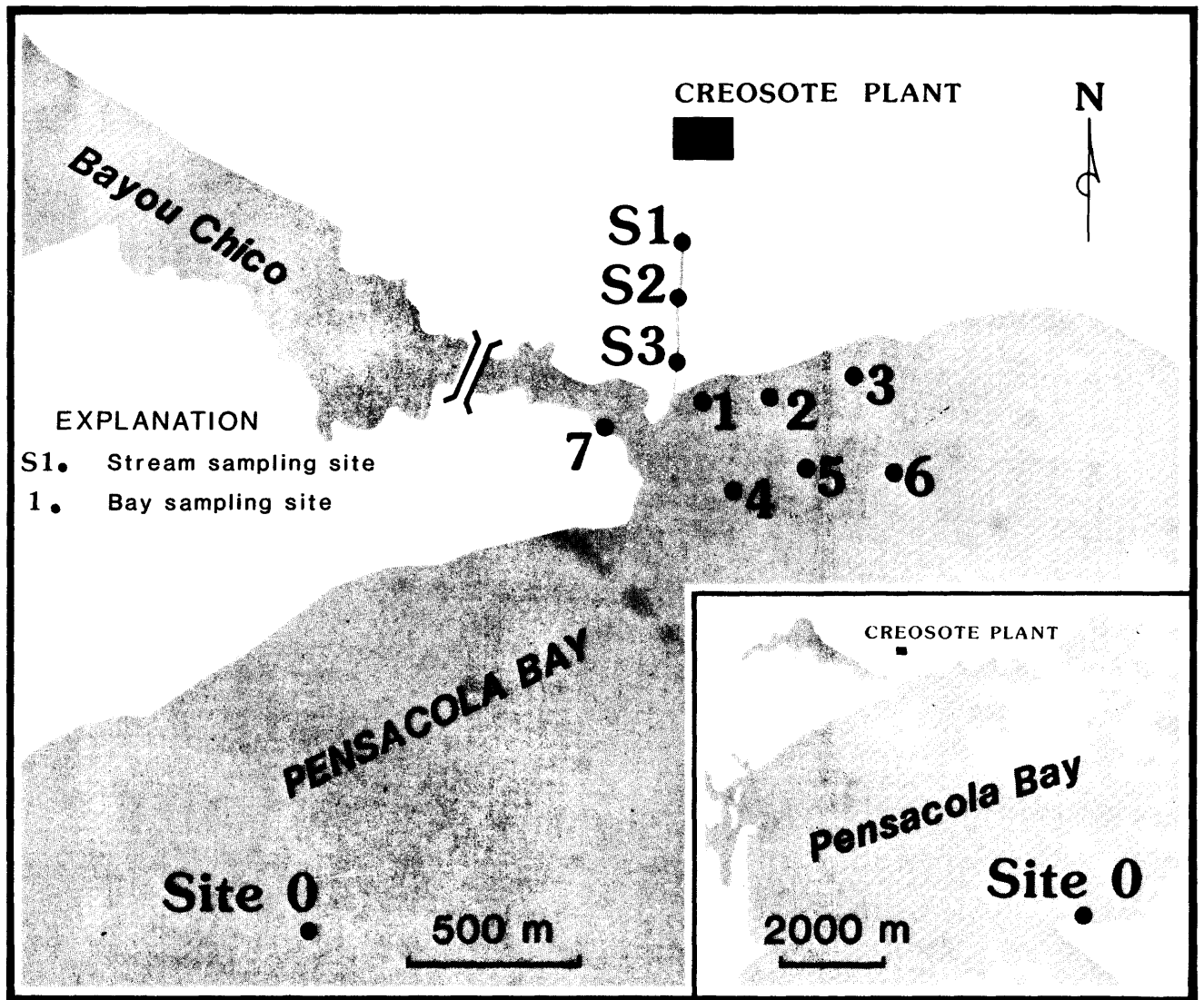


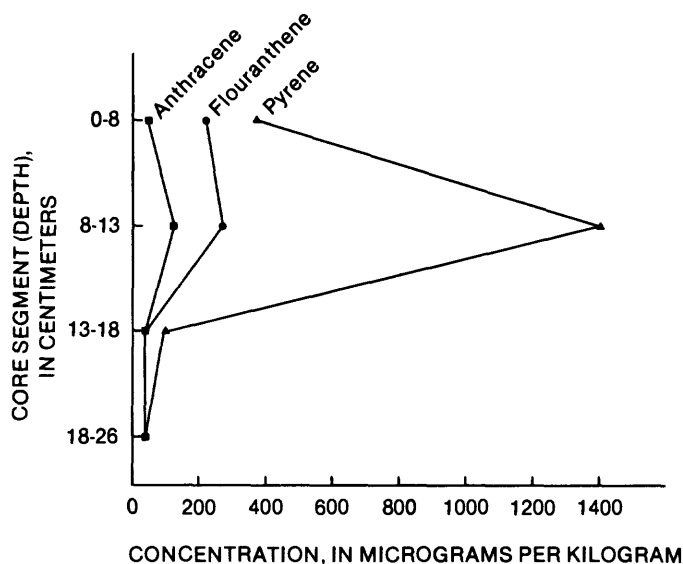
Figure A-19. — Location of sampling sites in Pensacola Bay, Bayou Chico, and along drainage channel near abandoned creosote works, Pensacola, Florida.

site 7, the control site, and the six nearshore sites). Drainage stream sites varied in their degree of similarity to each other. Species composition in the stream is controlled by the extent of saltwater intrusion. High tides deliver organisms originating from the bay, whereas low tides allow organisms of freshwater origin to be washed toward the mouth of the drainage stream. Organisms fail to penetrate sediments below 4 cm in the drainage stream environment; the polychaetes are isolated to the top 2 cm. Site 7, located in Bayou Chico,

consistently was found to have a very low diversity and abundance of invertebrates. Several industrial point sources in Bayou Chico are likely to account for these sparse populations.

Inverse cluster analysis and subsequent nodal analysis were performed in order to calculate a fidelity value (the preference or avoidance of a species group to a site group). Dominant species such as *Paraonis fulgens*, *Capitella capitata*, and *Aricidea (acmira) philbinae* were found at all near-

Figure A-20.—Vertical profiles for three creosote-compound concentrations in drainage-channel sediments at site 1, August 30, 1984. (Site location is shown in fig. A-19.)



shore sites but displayed no particular preference for any site group. Other species groups that included *Acanthohaustorius shoemakeri* and *Nephtys bucera* were found to highly prefer the control site while avoiding all other sites. Composition of the communities at the various sites suggests that species residing in nearshore habitats are primarily controlled by physical events such as sediment resuspension, deposition, and seasonal influences. Cluster analysis of combined seasonal collections showed that the majority of nearshore sites proximal to the creosote plant, regardless of

season, clustered together; although, higher similarity was noted between sites within a given season than among collections from the same site over all seasons. The control site consistently formed a single site cluster for any given season. These results, together with the results of bioaccumulation studies, suggest that benthic communities proximal to the creosote plant are influenced by the presence of contaminants. The major factor, however, controlling the distribution of species, appears to be seasonal variations in association with invertebrate recruitment patterns.

Table A-8.—Species list including seasonally averaged benthic invertebrate distributions and abundances by sampling site, Pensacola, Florida, 1983-84

[Values indicate number of individuals per meter squared; site locations shown in fig. A-19]

	Sites							Drainage stream	
	0	1	2	3	4	5	6		7
Polychaetes									
Aricidea (Acmira) philbinae	≤100	≤100	100-500	100-500	100-500	100-500	>500	≤100	
Aricidea (Acmira) taylori							≤100		
Armandia maculata							≤100		
Cabira incerta	≤100								
Capitella capitata	≤100	100-500	100-500	≤100	100-500	100-500	≤100	≤100	≤100
Chone americana				≤100			≤100		
Eteone heteropoda	≤100	≤100	≤100	≤100	≤100	≤100	≤100	≤100	
Eteone lactea		≤100	≤100	≤100		≤100	≤100		
Gyptis sp.	≤100								
Gyptis brevipalpa	≤100			≤100		≤100			
Heteromastus filiformis	≤100	100-500	≤100	≤100	≤100	≤100	≤100	≤100	
Laoneresis culveri	100-500	100-500	100-500	100-500	100-500	100-500	>500	≤100	

Table A-8.—Species list including seasonally averaged benthic invertebrate distributions and abundances by sampling site, Pensacola, Florida, 1983-84—Continued

	Sites							Drainage stream	
	0	1	2	3	4	5	6		7
Polychaetes--Continued									
Leitoscoloplos foliosus	≤100	≤100	≤100		≤100			≤100	
Linopherus ambigua					≤100		≤100		
Magelona pettiboneae	100-500		≤100	≤100	≤100	≤100	≤100	≤100	≤100
Neanthes succinea		≤100							
Nephtyidae	≤100								
Nephtys bucera	≤100								
Nereidae									≤100
Parandalia americana	≤100	≤100	≤100	≤100	≤100	≤100	≤100	≤100	
Paraonis fulgens	100-500	100-500	>500	>500	>500	>500	>500	≤100	
Phyllodoce cf. longipes					≤100			≤100	
Poecilochaetus johnsoni		≤100							
Polydora ligni		≤100		≤100	≤100		≤100		≤100
Polydora socialis					≤100				
Polygordius sp.	≤100				≤100		≤100		
Prionospio (Prionospio) heterobranchia	≤100		≤100	≤100	≤100	≤100	≤100	≤100	
Protodrilus sp.			≤100	≤100	≤100		≤100		
Scoleopsis texana	≤100	≤100	≤100	≤100	≤100	≤100	≤100		
Sigambra bassi	≤100	≤100	≤100	≤100	≤100	≤100	≤100		
Sphaerosyllis sp.	≤100								
Spio pettiboneae	≤100		≤100				≤100		
Spiochaetopterus costarum					≤100				
Spiophanes bombyx	≤100	≤100		≤100	≤100	100-500	100-500	≤100	
Streblospio benedicti	≤100	≤100	≤100	≤100					
Syllis sp.		≤100	≤100	≤100	≤100		≤100		
Amphipoda									
Acanthohaustorius shoemakeri	>500								
Ampelisca verrilli	≤100			≤100	≤100	≤100	≤100		
Amphilocheidae								≤100	
Atylus urocarinatus								≤100	
Corophium simile	≤100	≤100	≤100	≤100	≤100		≤100	≤100	
Gammarus sp.				≤100					
Hyperiidea amphipoda		≤100							
Lepidactylus dytiscus		≤100	≤100		≤100				100-500
Listriella sp.								≤100	
Melita sp.			≤100						
Monoculodes edwardsi	≤100	≤100	≤100	≤100	100-500	100-500	≤100		
Mollusks									
Corbula sp.				≤100	≤100		≤100		
Solenidae					≤100		≤100		
Tagelus sp.	≤100	≤100	≤100	≤100					
Tellina sp.					≤100				
Cumaceans		≤100	≤100		≤100	≤100			
Cumacea		≤100	≤100		≤100	≤100			
Oxyurostylis smithi		≤100		≤100	≤100	≤100	≤100		

Table A-8. — Species list including seasonally averaged benthic invertebrate distributions and abundances by sampling site, Pensacola, Florida, 1983-84 — Continued

	Sites							Drainage stream	
	0	1	2	3	4	5	6		7
Isopods									
Xenanthura brevitelson	≤100		≤100	≤100	≤100	100-500	100-500		
Mysids	≤100	≤100	≤100	≤100	≤100	≤100		≤100	
Tanaidaceans		≤100	≤100	≤100	≤100				
Decapods									
Megalopa decapoda			≤100						
Pinnotheridae							≤100		
Upogebia affinis			≤100						
Miscellaneous Taxa									
Anemone	≤100		≤100		≤100	≤100			
Cephalochordata	100-500	≤100	≤100	≤100	≤100		≤100	≤100	>500
Chironomidae					≤100		≤100		>500
Hemichordata	≤100						≤100		
Holothuridea	≤100	≤100	≤100	100-500	≤100	≤100	≤100	≤100	
Nematoda	100-500	100-500	100-500	100-500	>500	100-500	>500	>500	100-500
Nemertinea	100-500	100-500	100-500	100-500	100-500	100-500	100-500	≤100	
Oligochaeta	100-500	100-500	100-500	100-500	100-500	100-500	100-500	≤100	>500
Turbellaria	≤100					≤100	≤100		

CHAPTER B – FATE AND TRANSPORT OF CONTAMINANTS IN SEWAGE-CONTAMINATED GROUND WATER ON CAPE COD, MASSACHUSETTS

	Page
Introduction	B-3
Hydrogeologic controls on solute transport in a plume of sewage-contaminated ground water, by D.R. LeBlanc, S.P. Garabedian, R.D. Quadri, R.H. Morin, W.E. Teasdale, and F.L. Paillet	B-7
Design and implementation of a large-scale natural-gradient tracer test, by S.P. Garabedian, D.R. Leblanc, R.D. Quadri, K.M. Hess, K.G. Stollenwerk, and W.W. Wood	B-13
Identification of trace organic substances in sewage-contaminated ground water, by L.B. Barber, II, E.M. Thurman, and M.P. Schroeder	B-19
Sampling and analysis of volatile organic compounds in a plume of sewage-contaminated ground water, by E.M. Thurman, M.G. Brooks, and L.B. Barber, II	B-21
Movement and fate of detergents in sewage-contaminated ground water, by E.M. Thurman and L.B. Barber, II	B-23
Bacterial distribution and transport in a plume of sewage-contaminated ground water, by R.W. Harvey and Leah George	B-25
Nitrate reduction in a sewage-contaminated aquifer, by R.L. Smith and J.H. Duff.....	B-27
Fate of ammonium in a sewage-contaminated ground water, by M.L. Ceazan, R.L. Smith, and E.M. Thurman	B-29

ILLUSTRATIONS

	Page
Figure	
B-1. Map showing location of study area at Otis Air Base on Cape Cod, Massachusetts	B-4
B-2. Map showing path of sewage-contaminated ground-water plume and water-table altitude downgradient from sewage-infiltration beds.....	B-8
B-3. Geologic section along axis of sewage plume and vertical profiles of specific conductance at four sites along plume, 1983-85.....	B-9
B-4. Plot of observed drawdown in observation wells 20 feet from pumping well and screened above, opposite, and below pumping interval, July 7-14, 1984	B-10
B-5. Plot of bromide-tracer concentration during pumping test at pumping well 20 feet from injection point, July 1984	B-10
B-6. Plot of bromide-tracer concentration at top, middle, and bottom of injection zone in divergent-flow tracer test, September 1984, at points 5 and 10 feet from injection well	B-11
B-7. Map showing water-table altitude, location of injection and monitoring wells, and projected path of tracer cloud at abandoned gravel pit used for solute-dispersion test, Cape Cod, Massachusetts.....	B-14
B-8. Map showing vertically averaged bromide concentrations in aquifer 13 days after injection of tracer	B-15
B-9. Map showing vertically averaged bromide concentrations in aquifer 32 days after injection of tracer	B-16
B-10. Plot of vertical distribution of bromide cloud along section A-A' 32 days after injection of tracer	B-17

CHAPTER B – FATE AND TRANSPORT OF CONTAMINANTS IN SEWAGE-CONTAMINATED GROUND WATER ON CAPE COD, MASSACHUSETTS

INTRODUCTION

Treated sewage, discharged since 1936 to infiltration beds above a sand and gravel aquifer at Otis Air Base, on Cape Cod, Mass. (fig. B-1), has formed a plume of sewage-contaminated ground water about 25 m thick, 800 m wide, and more than 3,400 m long. The plume was originally described by the U.S. Geological Survey during a cooperative study with the Massachusetts Department of Environmental Quality Engineering, Division of Water Pollution Control (LeBlanc, 1984c).

Sewage from Otis Air Base receives secondary treatment before discharge to the infiltration beds. Present sewage flow at the treatment plant is 1,100 m³/d, although flow rates were as high as 6,800 m³/d in 1941–43. The treated sewage, which has a total dissolved solids concentration of about 170 mg/L, recharges a stratified sand and gravel aquifer 30 to 40 m thick that is underlain by fine-grained sediments. Uncontaminated ground water in the aquifer has a total dissolved solids concentration of about 40 mg/L. Ground water in the sand and gravel is moving downgradient toward Nantucket Sound at an estimated velocity of 0.3 to 0.6 m/d.

The original description of the sewage plume (LeBlanc, 1984c) provided evidence of a variety of transport processes that are the focus of the current investigations. Chloride, sodium, and boron seem to move conservatively, whereas phosphorus, ammonia, and nitrate are retarded or are undergoing chemical and microbiological transformations. Detergent concentrations reflect the change from nonbiodegradable to biodegradable detergents in 1964, and are highest about 3,000 m from the disposal site.

Reports published since the inception of the U.S. Geological Survey's interdisciplinary research effort in 1983 describe:

- Simulation of ground-water flow and solute transport in the sewage plume with a two-dimensional numerical model (LeBlanc, 1984a);
- Distribution of inorganic and organic contaminants in the plume, including volatile organic compounds (Thurman and others, 1984);
- The fate of detergents in the plume and the relation between the distribution of detergents in the aquifer and the history of detergent use (Thurman and others, 1986);
- A closed-loop stripping procedure for determination of trace-level concentrations of organic contaminants that was used to identify zones in the plume on the basis of predominant organic compounds (Barber and others, 1984);
- The distribution and activity of bacteria in the aquifer and their relation to contaminant concentrations and distance from the disposal site (Harvey and others, 1984a; 1984b; 1984c);
- Delineation of zones of nitrogen transformations, including denitrification near the infiltration beds (Smith and Duff, 1984a; 1984b) and nitrification at a distance of 2,400 m downgradient of the beds (Ceazan and others, 1984).

The eight abstracts in this chapter present additional information on the fate of contaminants in the sewage plume including physical transport of solutes in ground water, the distribution of organic contaminants, and microbial processes in the subsurface. Initial results of a major field experiment to study dispersion of conservative and nonconservative solutes in ground water at the Cape Cod site are also presented.

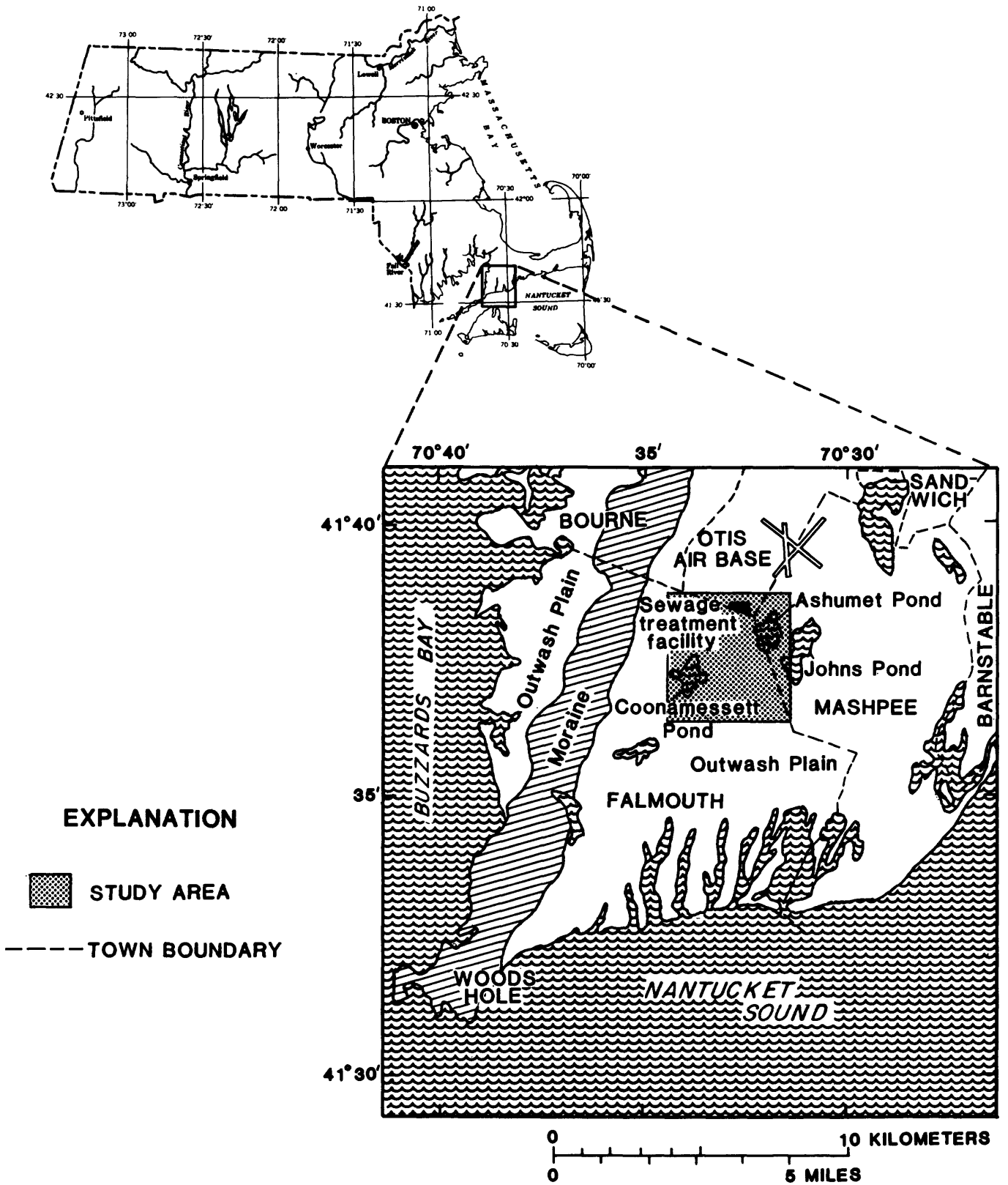


Figure B-1. - Location of study area at Otis Air Base on Cape Cod, Massachusetts.

SELECTED REFERENCES

- Barber, L.B., II, Thurman, E.M., and Schroeder, M.P., 1984, Closed-loop stripping, combined with capillary gas chromatography/mass spectrometry analysis, to define a semi-volatile organic-contaminant plume, *in* LeBlanc, D.R., ed., 1984, Movement and fate of solutes in a plume of sewage-contaminated ground water, Cape Cod, Massachusetts: U.S. Geological Survey Toxic Waste Ground-Water Contamination Program: U.S. Geological Survey Open-File Report 84-475, p. 89-113.
- Ceazan, M.L., Updegraff, D.M., and Thurman, E.M., 1984, Evidence of microbial processes in sewage-contaminated ground water, *in* LeBlanc, D.R., ed., 1984, Movement and fate of solutes in a plume of sewage-contaminated ground water, Cape Cod, Massachusetts: U.S. Geological Survey Toxic Waste Ground-Water Contamination Program: U.S. Geological Survey Open-File Report 84-475, p. 115-138.
- Harvey, R.W., Smith, R.L., and George, L.H., 1984a, Bacterial distribution and heterotrophic uptake in a sewage-contaminated ground water: EOS, Transactions of the American Geophysical Union, v. 65, no. 45, p. 880.
- 1984b, Effect of organic contamination upon microbial distributions and heterotrophic uptake in a Cape Cod, Massachusetts, aquifer: Applied and Environmental Microbiology, v. 48, p. 1197-1202.
- 1984c, Microbial distribution and heterotrophic uptake in a sewage plume, *in* LeBlanc, D.R., ed., 1984, Movement and fate of solutes in a plume of sewage-contaminated ground water, Cape Cod, Massachusetts: U.S. Geological Survey Toxic Waste Ground-Water Contamination Program: U.S. Geological Survey Open-File Report 84-475, p. 141-152.
- LeBlanc, D.R., 1984a, Digital modeling of solute transport in a plume of sewage-contaminated ground water, *in* LeBlanc, D.R., ed., 1984, Movement and fate of solutes in a plume of sewage-contaminated ground water, Cape Cod, Massachusetts: U.S. Geological Survey Toxic Waste Ground-Water Contamination Program: U.S. Geological Survey Open-File Report 84-475, p. 11-45.
- ed., 1984b, Movement and fate of solutes in a plume of sewage-contaminated ground water, Cape Cod, Massachusetts: U.S. Geological Survey Toxic Waste Ground-Water Contamination Program: U.S. Geological Survey Open-File Report 84-475, 175 p.
- 1984c, Sewage plume in a sand and gravel aquifer, Cape Cod, Massachusetts: U.S. Geological Survey Water-Supply Paper 2218, 28 p.
- Smith, R.L., and Duff, J.H., 1984a, Preliminary study of denitrification in a plume of sewage-contaminated ground water, *in* LeBlanc, D.R., ed., 1984, Movement and fate of solutes in a plume of sewage-contaminated ground water, Cape Cod, Massachusetts: U.S. Geological Survey Toxic Waste Ground-Water Contamination Program: U.S. Geological Survey Open-File Report 84-475, p. 153-175.
- 1984b, Denitrification in a sewage-contaminated aquifer at Cape Cod, Massachusetts: EOS, Transactions of the American Geophysical Union, v. 65, no. 45, p. 879-880.
- Thurman, E.M., Barber, L.B., II, Ceazan, M.L., Smith, R.L., Brooks, M.G., Schroeder, M.P., Keck, R.J., Driscoll, A.J., LeBlanc, D.R., and Nichols, W.J., Jr., 1984, Sewage contaminants in ground water, *in* LeBlanc, D.R., ed., 1984, Movement and fate of solutes in a plume of sewage-contaminated ground water, Cape Cod, Massachusetts: U.S. Geological Survey Toxic Waste Ground-Water Contamination Program: U.S. Geological Survey Open-File Report 84-475, p. 47-87.
- Thurman, E.M., Barber, L.B., II, and LeBlanc, D.R., 1986, Movement and fate of detergents in ground water: A field study: Contaminant Hydrology, v. 1, no. 1, p. 143-161.

HYDROGEOLOGIC CONTROLS ON SOLUTE TRANSPORT IN A PLUME OF SEWAGE-CONTAMINATED GROUND WATER

By Denis R. LeBlanc¹, Stephen P. Garabedian¹, Richard D. Quadri¹, Roger H. Morin², Warren E. Teasdale², and Frederick L. Paillet²

Treated sewage has been discharged to a sand and gravel outwash aquifer at Otis Air Base on Cape Cod, Mass., since 1936, and has formed an extensive contaminant plume (LeBlanc, 1984b). The longitudinal axis of the plume (fig. B-2) is aligned with the direction of ground-water flow as interpreted from the observed water-table gradient. Vertical profiles of specific conductance through the plume (fig. B-3) show that contaminants are not mixed through the entire thickness of the aquifer and that, near the toe of the plume, contaminants enter the fine-grained sediment underlying the outwash.

Accurate simulation of the rate and three-dimensional direction of contaminant movement is needed to predict the fate of contaminants in the sewage plume. A two-dimensional areal flow and solute-transport model that was used earlier to simulate the plume (LeBlanc, 1984a) reproduced the path accurately but could not simulate the observed vertical movement and distribution of contaminants in the outwash nor their movement into the fine-grained sediments underlying the outwash. The path of the plume was simulated accurately because hydraulic heads calculated by the flow model matched the observed head distribution. However, the computed heads were relatively insensitive to aquifer hydraulic properties during flow-model calibration. Therefore, hydraulic conductivity, which directly affects the rate of contaminant movement, was not well quantified during calibration.

Simulation of the rate of contaminant movement and dispersion requires correct values of aquifer properties. These values cannot be obtained solely by model calibration because the calculated hydraulic heads are insensitive to aquifer properties. Therefore, several field methods, including aquifer-pumping tests, small-scale tracer tests, sediment-core collection, and borehole geo-

physical logging, have been applied to obtain independent estimates of aquifer properties at the site.

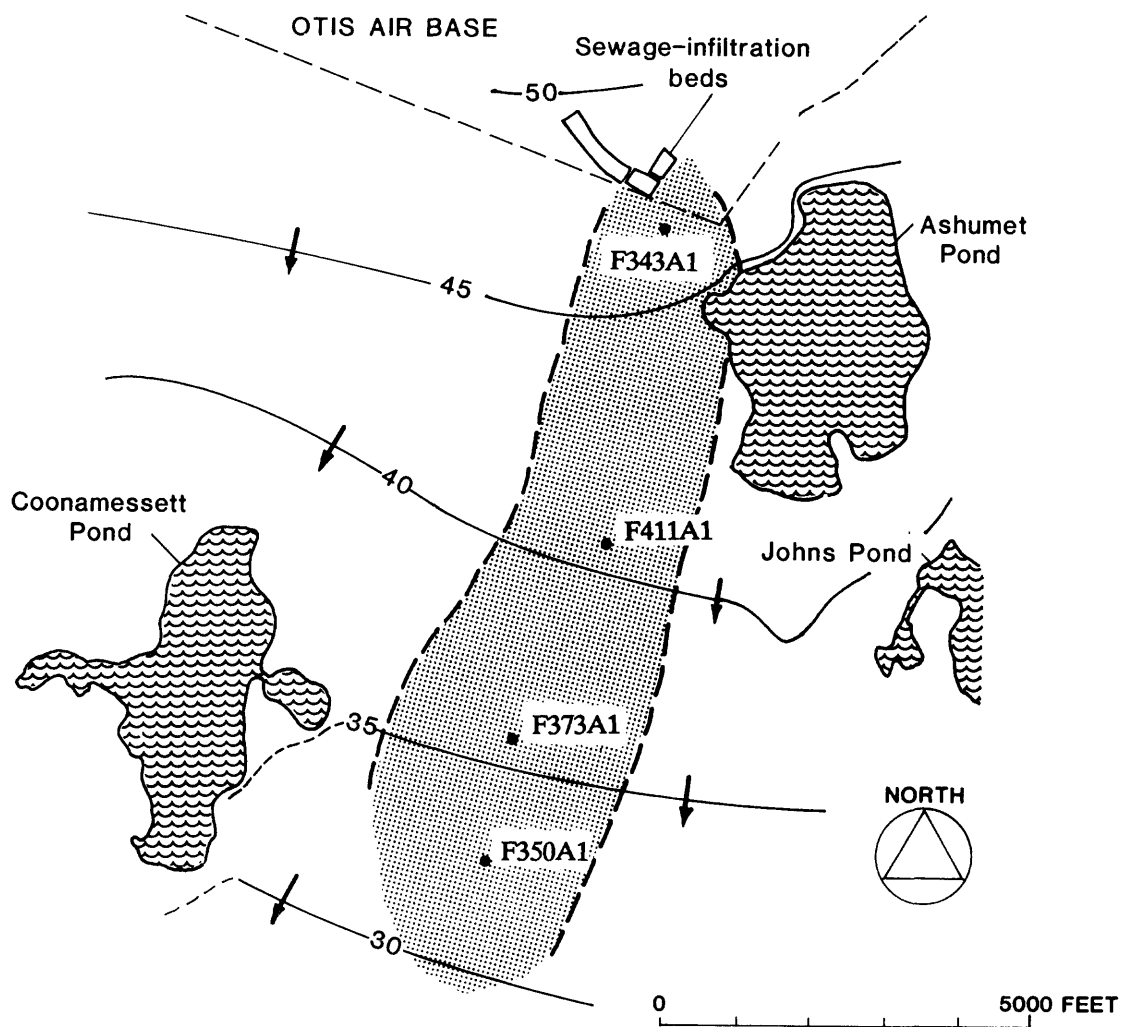
An aquifer test at a partially penetrating well pumped at a rate of 475 gal/min was used to measure hydraulic properties of the sand and gravel. The observed drawdowns (fig. B-4) match the unconfined drawdown response described by Neuman (1975). Analysis of the drawdowns with Neuman's analytical solutions and with a three-dimensional finite-difference model yielded an average hydraulic conductivity of 380 ft/d and a ratio of horizontal to vertical hydraulic conductivity ranging from 2:1 to 5:1.

During the aquifer test, a conservative tracer (bromide) was injected as a pulse into an observation well 20 feet from the pumping well. The arrival time of the peak breakthrough (fig. B-5) was 200 minutes. On the assumption that flow to the pumping well was spherically symmetric, the estimated effective porosity is 0.38. Given the average hydraulic conductivity of 380 ft/d from the aquifer test and a hydraulic gradient of 0.0015 from a regional water-table map, the estimated average ground-water velocity in the outwash is 1.5 ft/d. The two-dimensional model of the sewage plume had predicted an average velocity of 0.9 ft/d; this difference between modeled and field-estimated velocities reflects the inability of the model to predict hydraulic conductivity accurately by calibration.

The aquifer test was used to measure average hydraulic conductivity of the outwash. Six small-scale tracer tests were conducted to determine the effect of small-scale, local variations in hydraulic conductivity, which probably cause field-scale macrodispersion, on solute transport. As one example, a divergent test was conducted in which a bromide solution was injected as a pulse into a radially divergent flow field and monitored as it moved past multilevel samplers set at 5 and 100 feet from the injection well. The observed breakthrough curves (fig. B-6) for 5 and 10 feet from

¹U.S. Geological Survey, Boston, Mass.

²U.S. Geological Survey, Denver, Colo.



EXPLANATION



GENERAL AREA OF PLUME OF SEWAGE-CONTAMINATED GROUND WATER, AUGUST 1985--Area delineated by field observations of elevated specific conductance and foaming caused by detergents



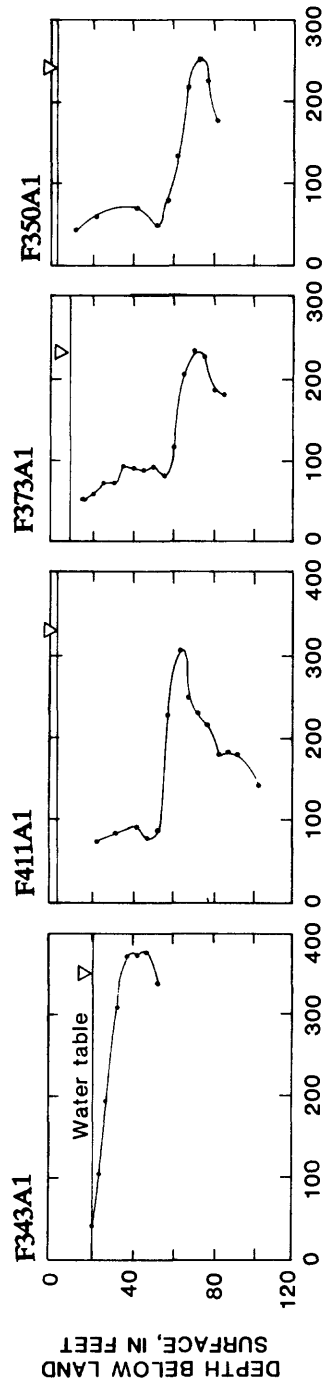
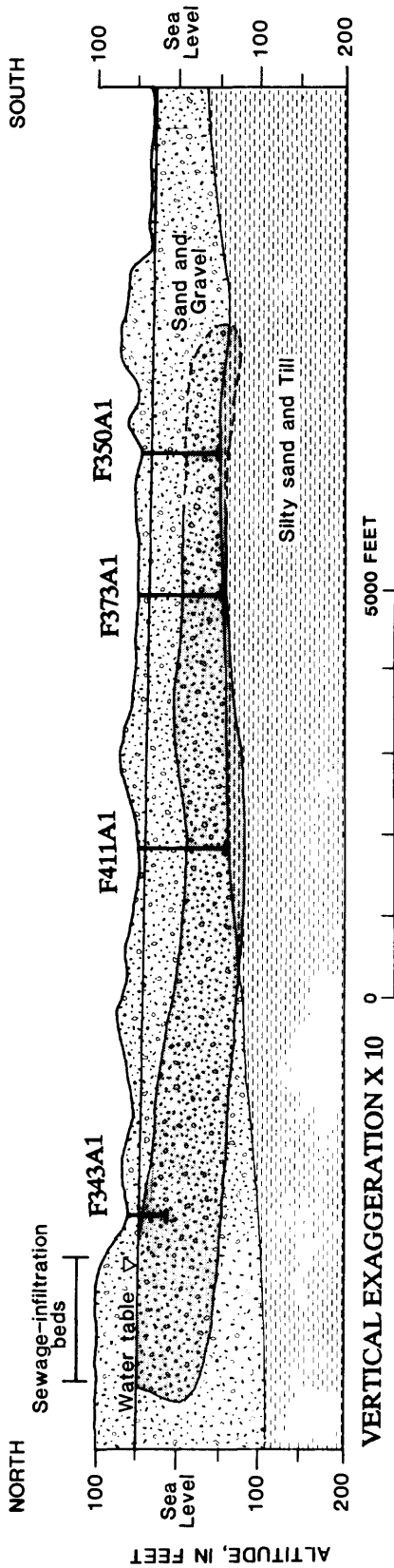
WATER-TABLE CONTOUR, NOVEMBER 1979--Shows altitude of water table in feet. Contour interval 5 feet. Datum is sea level. Arrows indicate direction of ground-water movement

F343A1



SITE OF SPECIFIC-CONDUCTANCE MEASUREMENT--Profiles shown in figure B-3

Figure B-2. — Path of sewage-contaminated ground-water plume and water-table altitude downgradient from sewage-infiltration beds. (Location is shown in fig. B-1.) (Modified from LeBlanc, 1984a, p. 23.)



SPECIFIC CONDUCTIVITY, IN
MICROSIEMENS PER CENTIMETER

EXPLANATION

- GENERAL ZONE OF PLUME OF SEWAGE-CONTAMINATED GROUND WATER, AUGUST 1985--Zone delineated by field observations of elevated specific conductivity and foaming caused by detergents.
- SCREENED AUGER PROFILES-- Locations shown in figure B-2

Figure B-3.—Geologic section along axis of sewage plume and vertical profiles of specific conductance at four sites along plume, 1983-85. (Location of sites is shown in fig. B-2.) (Modified from LeBlanc, 1984a, p. 24.)

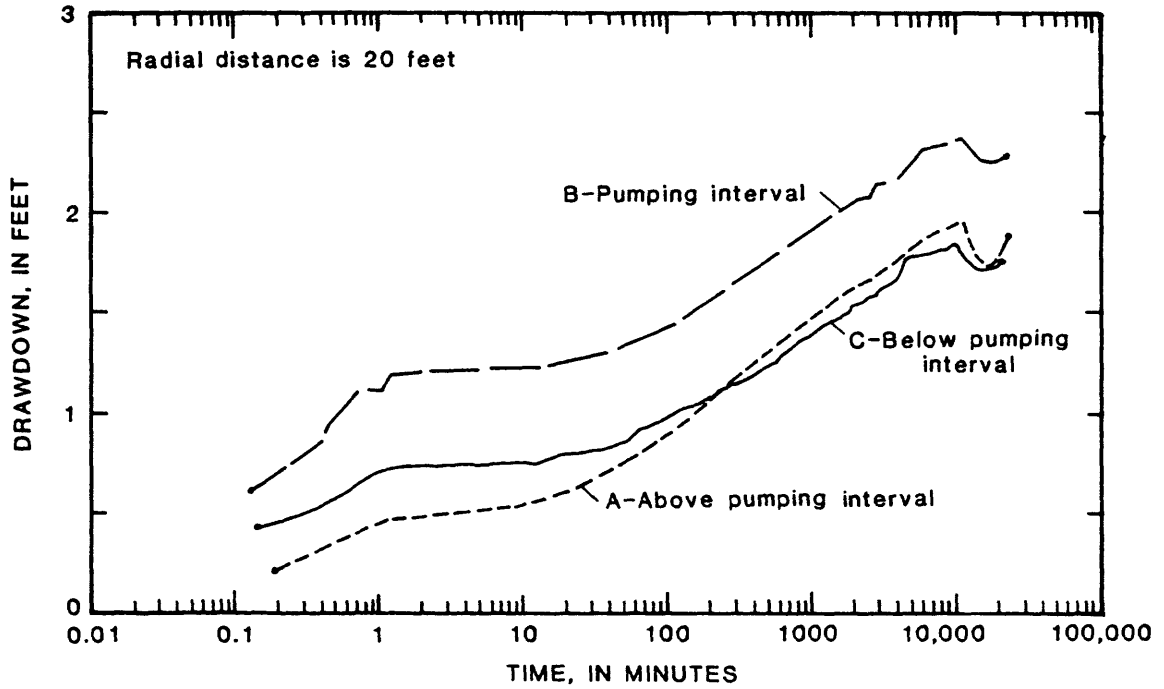


Figure B-4.— Observed drawdown in observation wells 20 feet from pumping well and screened above, opposite, and below pumping interval, July 7-14, 1984. Pumping-well screen is 10 feet long.

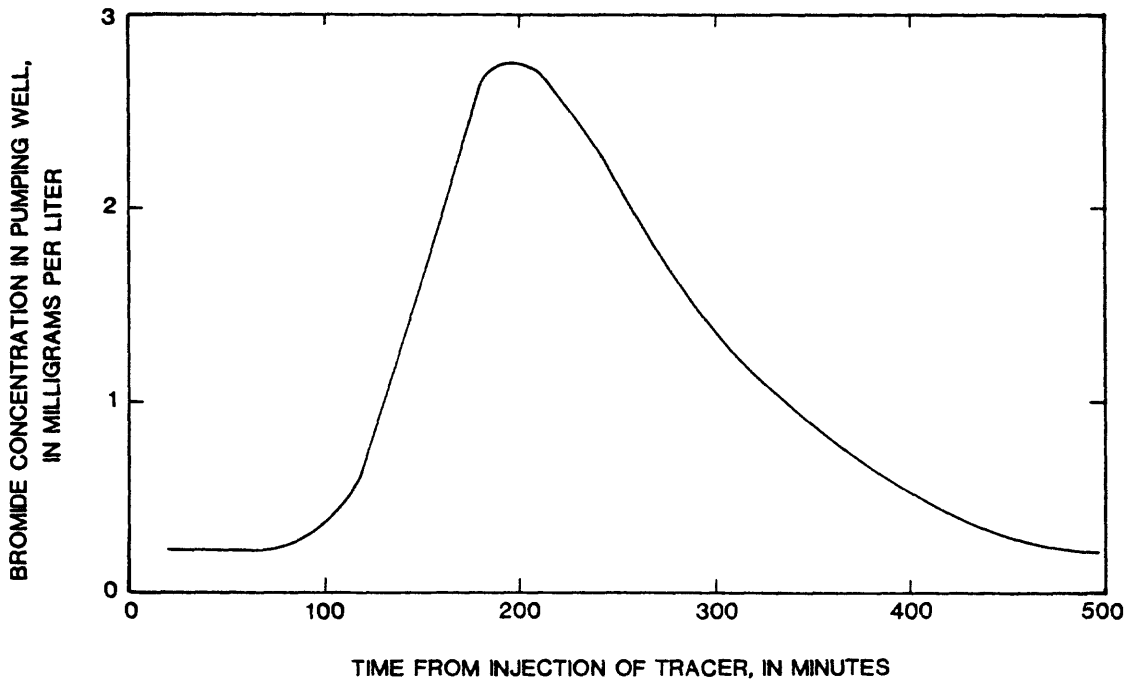


Figure B-5.— Bromide-tracer concentration during pumping test at pumping well 20 feet from injection point, July 1984.

the injection well at three depths opposite the injection zone show widely differing breakthrough times. These curves clearly demonstrate the presence of "fast" and "slow" zones in the aquifer that correspond to vertical differences in hydraulic conductivity in zones less than 2 feet thick.

Methods to collect undisturbed cores of sand and gravel from different zones in the aquifer for hydraulic analysis were tested extensively. Attempts to use split-spoon samplers, rotary core barrels, and a continuous auger-coring system were unsuccessful because the silt-free sand

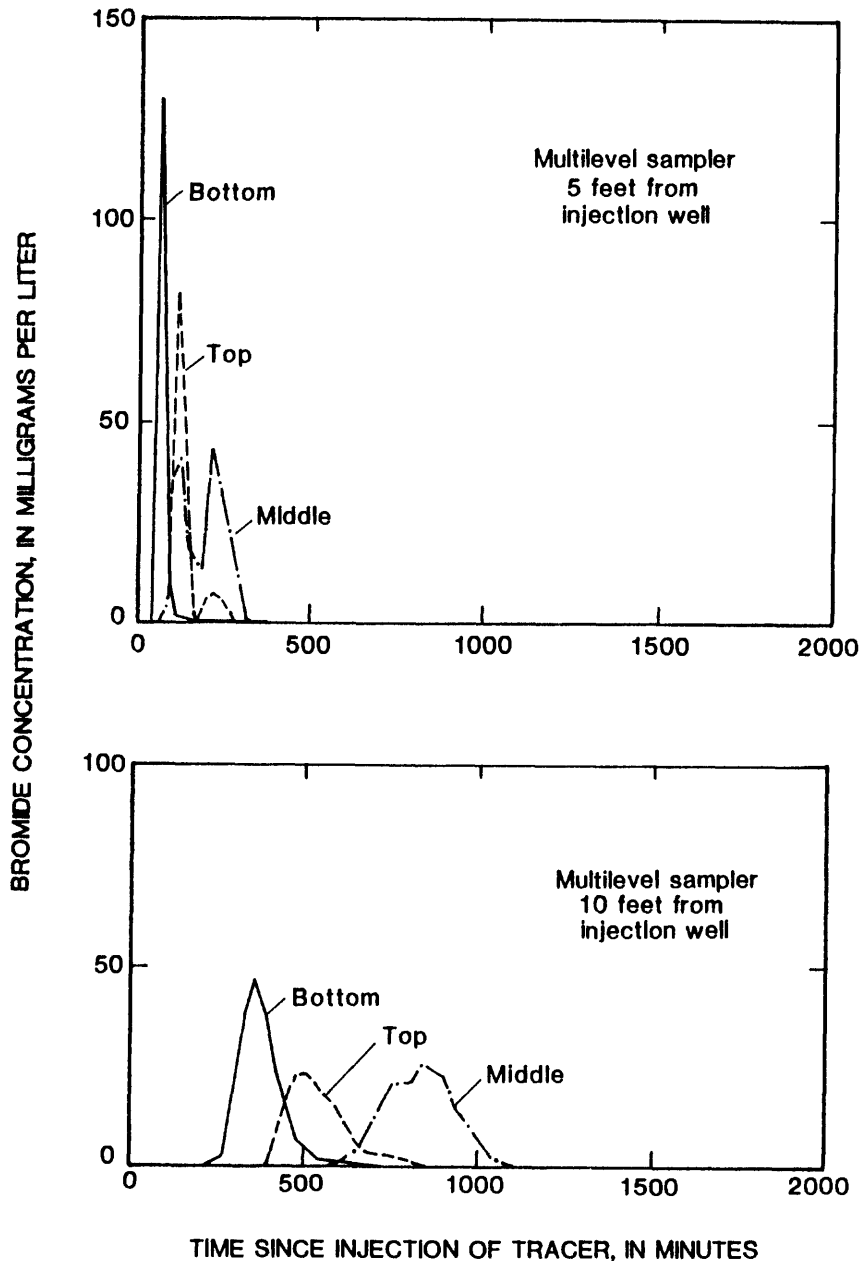


Figure B-6. — Bromide-tracer concentration at top, middle, and bottom of injection zone in divergent-flow tracer test, September 1984, at points 5 and 10 feet from injection well. Injection-well screen is 4 feet long.

tended to fall from the barrels during retrieval. A piston-type core barrel, developed by Michael Zapico of the University of Waterloo, which maintains a vacuum on the core during retrieval, was used successfully to obtain 5-foot-long cores of the sand and gravel. These cores seem to preserve the structure of the outwash seen in the shallow pits and to retain the ambient pore fluids. A coring program planned for 1986 should obtain detailed data on hydraulic conductivity and porosity.

Borehole geophysical logs also may yield detailed information on physical characteristics of the outwash. Natural-gamma logs may correlate with hydraulic conductivity. Spacing of peaks on the logs is roughly equal to thickness of layers observed in test pits. Preliminary uncalibrated neutron logs suggest that the outwash porosity may vary only 3 to 5 percent. These logs, when calibrated against data from hydraulic tests of cores, should provide an indirect method of determining hydraulic conductivity and porosity. These data can then be applied to a three-dimensional flow model that will be the basis for simulations of the three-dimensional features of the plume. The detailed information on variability of

hydraulic conductivity and porosity of the outwash also will be used to predict in macroscale dispersion by stochastic methods. (See Garabedian and others, Chapter B, this report.)

REFERENCES

- LeBlanc, D.R., 1984a, Digital modeling of solute transport in a plume of sewage-contaminated ground water, *in* LeBlanc, D.R., ed., 1984, Movement and fate of solutes in a plume of sewage-contaminated ground water, Cape Cod, Massachusetts: U.S. Geological Survey Toxic Waste Ground-Water Contamination Program: U.S. Geological Survey Open-File Report 84-475, p. 11-45.
- — — 1984b, Sewage plume in a sand and gravel aquifer, Cape Cod, Massachusetts: U.S. Geological Survey Water-Supply Paper 2218, 28 p.
- Neuman, S.P., 1975, Analysis of pumping data from anisotropic unconfined aquifers considering delayed gravity response: *Water Resources Research*, v. 11, p. 329-342.

DESIGN AND IMPLEMENTATION OF A LARGE-SCALE NATURAL-GRADIENT TRACER TEST

By Stephen P. Garabedian¹, Denis R. LeBlanc¹, Richard D. Quadri¹, Kathryn M. Hess¹, Kenneth G. Stollenwerk², and Warren W. Wood³

A large-scale natural-gradient tracer test that is in progress at a sewage-contaminated site near Otis Air Base on Cape Cod, Mass. (fig. B-1), was designed to examine solute dispersion in a sand and gravel aquifer. Dispersion of solutes transported in aquifers has been found to differ from dispersion in laboratory column tests. Dispersive solute flux in laboratory column tests generally follows an analogy to Fick's law, where flux is equal to the product of the solute-concentration gradient, fluid velocity, and a constant length (dispersivity). Longitudinal dispersivity values from laboratory tests are typically 10^{-1} feet or less, but dispersivity values from field tracer tests are typically orders of magnitude greater (Anderson, 1979). Field studies have also indicated that dispersion is scale dependent; dispersivity increases with time or travel distance (Sudicky and others, 1983). Therefore, the analogy to Fick's law represents the field-scale dispersion process poorly, particularly over small travel distances. Proper modeling of the dispersion process is important for predicting concentrations of conservative solutes and of solutes affected by concentration-dependent chemical and microbiological reactions.

Recent research into dispersion of ground-water solutes by Gelhar and others (1979) and Gelhar and Axness (1983) has focused on variations in ground-water velocity resulting from local differences in hydraulic conductivity to explain the differences between values of dispersivity measured in laboratory and field tracer tests. These investigations have shown that (1) the early dispersive process is significantly non-Fickian; (2) the mean transport process approaches Fickian conditions after an extended time; and (3) the asymptotic value of dispersivity is related to the statistical properties of the porous medium. An example of the last relation is:

$$A = \frac{r^2 L}{g^2} \quad (1)$$

¹U.S. Geological Survey, Boston, Mass.

²U.S. Geological Survey, Denver, Colo.

³U.S. Geological Survey, Reston, Va.

where:

A = asymptotic dispersivity (L),

r^2 = variance of log hydraulic conductivity (dimensionless),

L = correlation scale of hydraulic conductivity (L), and

g = part of specific discharge in the direction of variations in hydraulic conductivity (dimensionless).

These and other theoretical results are being tested for validity and applicability to field-scale problems.

The natural-gradient tracer test was started in July 1985 with the pulse injection of four tracers into the outwash sand and gravel aquifer at an abandoned gravel pit near the site. The tracers include a conservative solute (bromide) and three nonconservative solutes (lithium, molybdenum as molybdate, and fluoride). The injected volume was about 2,000 gallons, and concentrations of tracers in the injected solution were about 630 mg/L bromide, 80 mg/L molybdenum, 50 mg/L fluoride, and 80 mg/L lithium.

A network of observation wells was installed to define the water-table altitude in the area of the tracer test. Water-table contours, locations of tracer-injection wells, and projected flow path of the solute cloud are shown in figure B-7. Test instrumentation includes several hundred multi-level sampling devices, each with 15 ports arranged vertically, that are used to observe the solute distribution as the tracers move downgradient. The tracer cloud is expected to be monitored for about 700 feet before it moves out of the test area.

To date (October 1985), four rounds of sampling have been done to identify the spatial distribution of solutes in the tracer cloud. A sampling round is performed over 2 days and involves pumping more than 2,000 sampling ports and filling more than

6,000 sample bottles. From 8 to 12 monthly sampling rounds are expected to be made before the tracer cloud leaves the test area. More frequent sampling also is being done to define variations in

concentrations over time along the projected axis of the cloud.

Vertically averaged bromide concentrations 13 and 32 days after injection are shown in figures

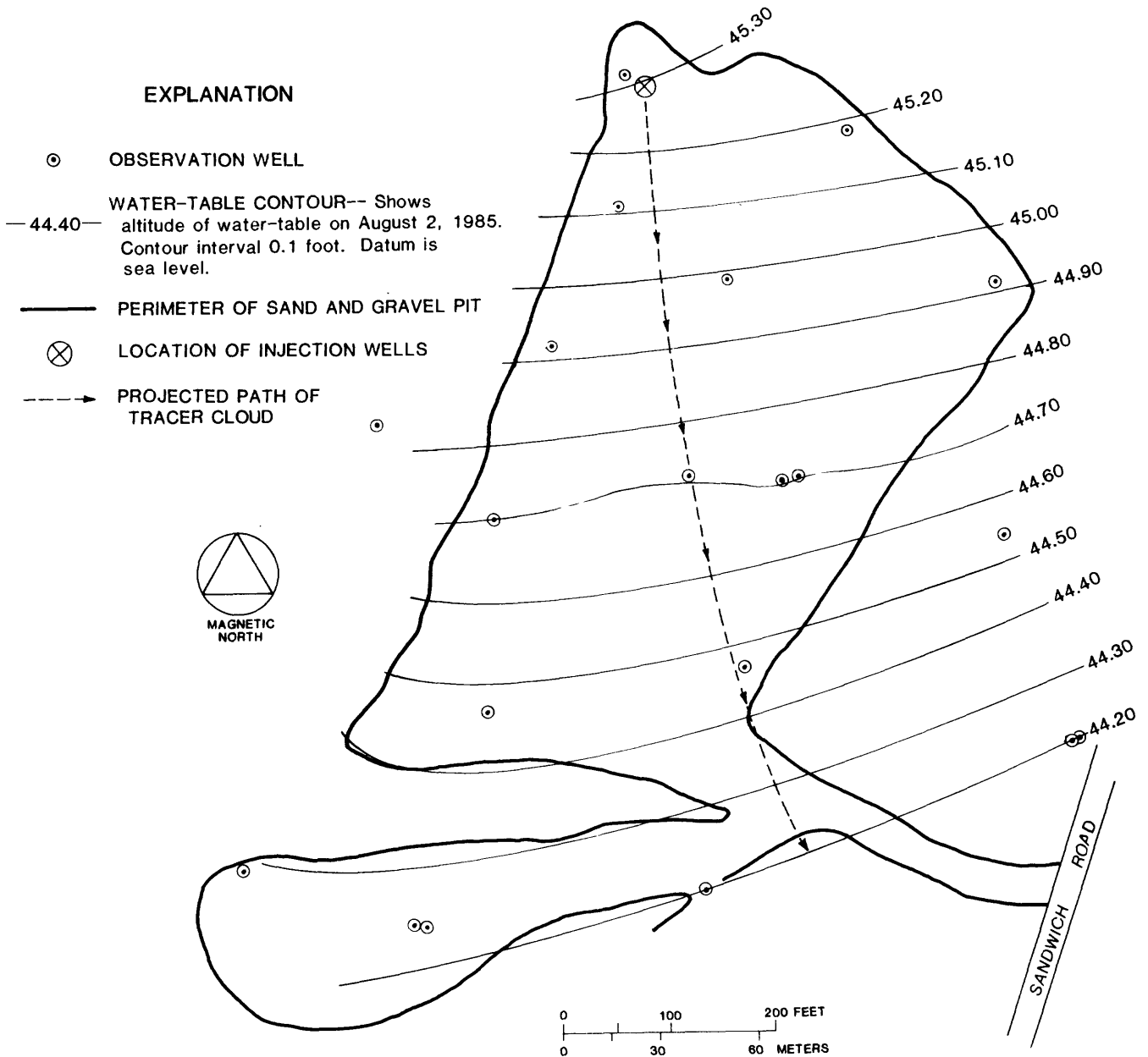


Figure B-7. — Water-table altitude, location of injection and monitoring wells, and projected path of tracer cloud at abandoned gravel pit used for solute-dispersion test, Cape Cod, Massachusetts.

B-8 and B-9, respectively. The average velocity of the bromide cloud, as indicated by peak concentration, is about 1.6 ft/d. This velocity is similar to a prediction of 1.5 ft/d based on estimates of hydraulic conductivity (380 ft/d), porosity (0.35), and water-table gradient (0.0014) at the test site. The average direction of bromide movement also closely follows the projected flow path based on the water-table configuration. These results indicate that the average rate and direction of bromide transport can be predicted from average aquifer

properties. A comparison of figures B-8 and B-9 also shows a decrease over time in peak concentration and a rapid longitudinal spreading of the bromide cloud caused by the velocity differences between the leading (3 ft/d) and trailing (0.4 ft/d) edges. This range in velocity is likely related to local variations in hydraulic conductivity.

A longitudinal section of the bromide cloud at 32 days after injection is shown in figure B-10. The bromide cloud has moved vertically down-

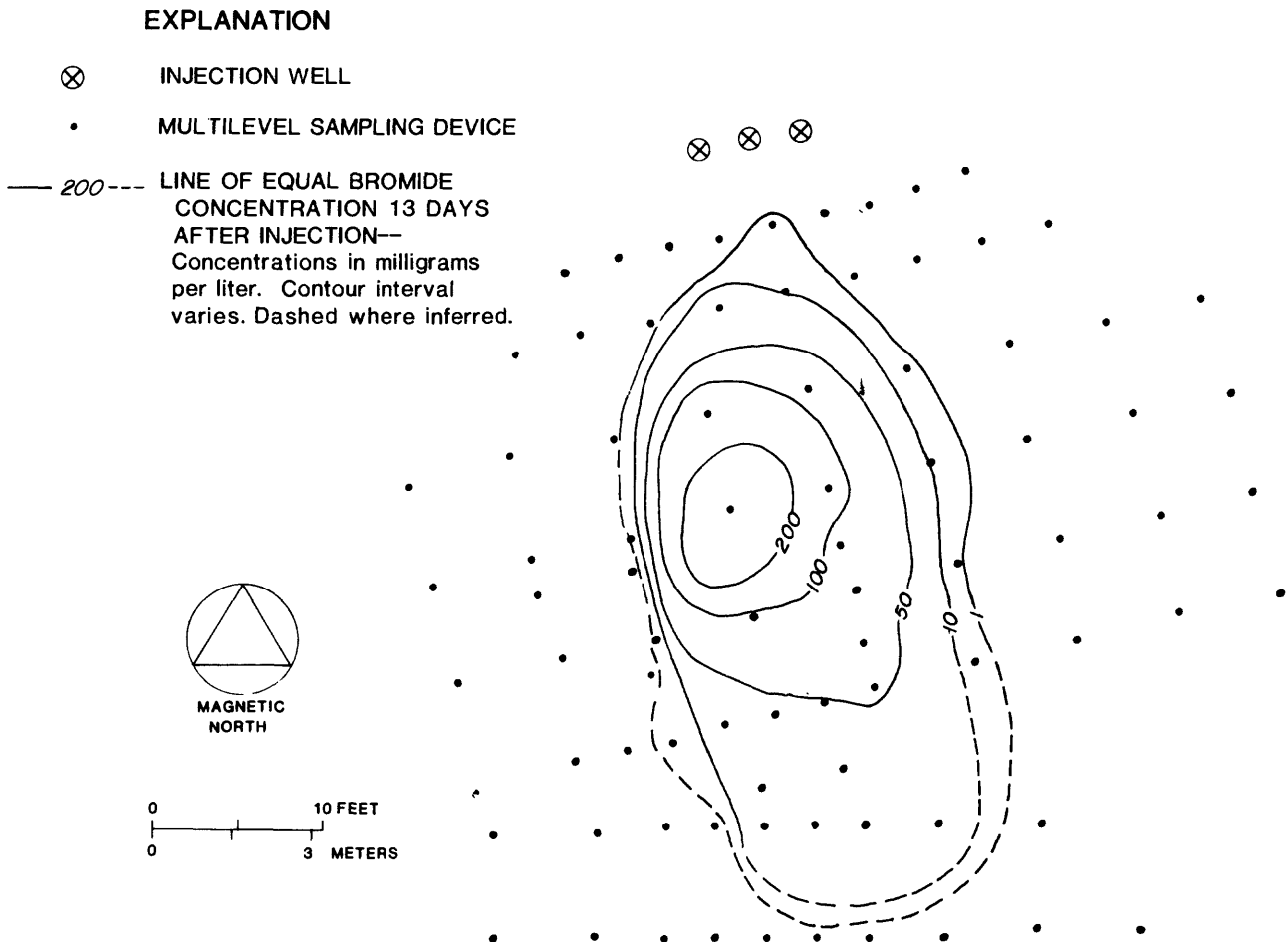


Figure B-8.—Vertically averaged bromide concentrations in aquifer 13 days after injection of tracer.

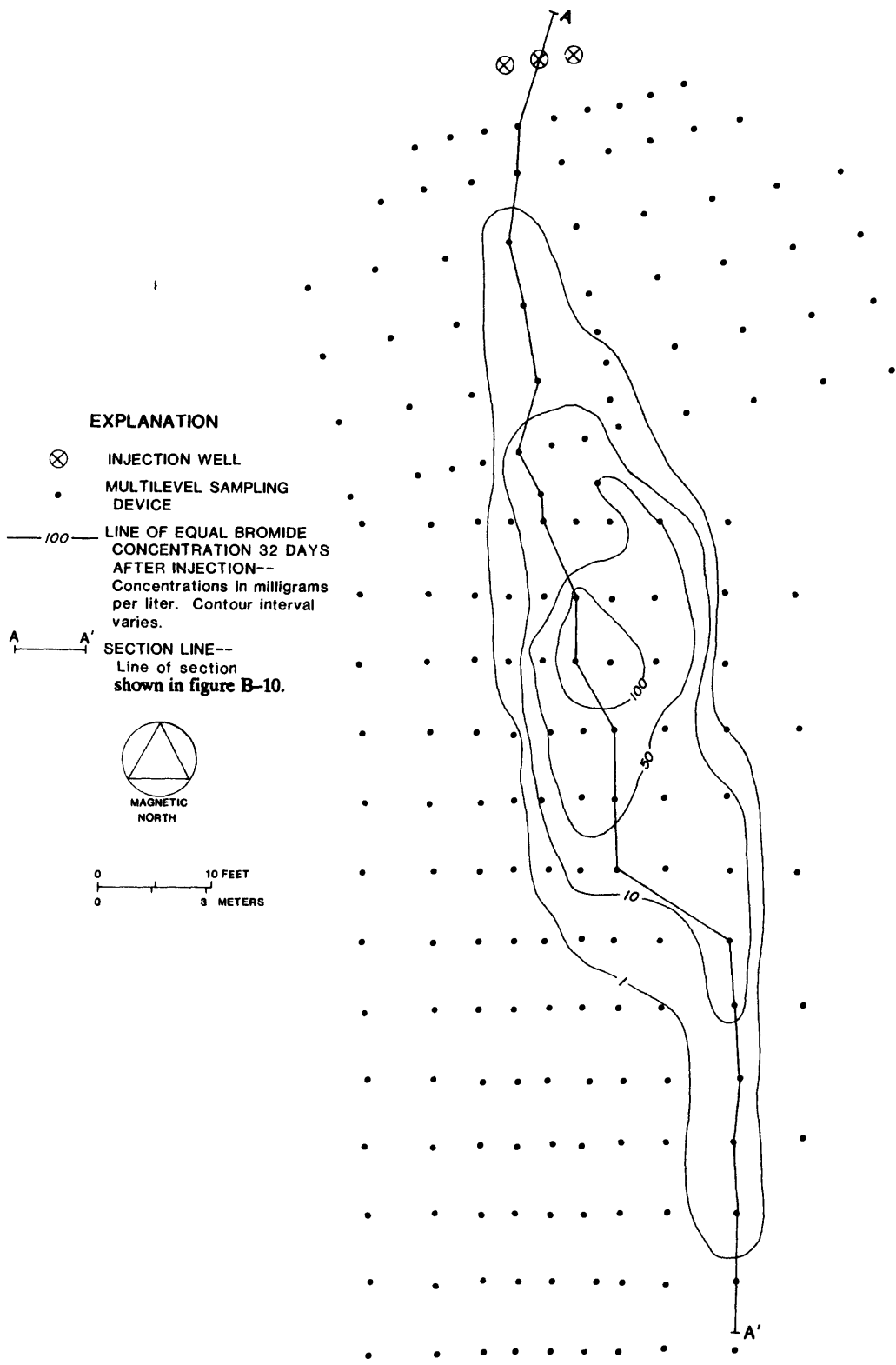


Figure B-9. — Vertically averaged bromide concentrations in aquifer 32 days after injection of tracer. Vertical section shown in figure B-10.

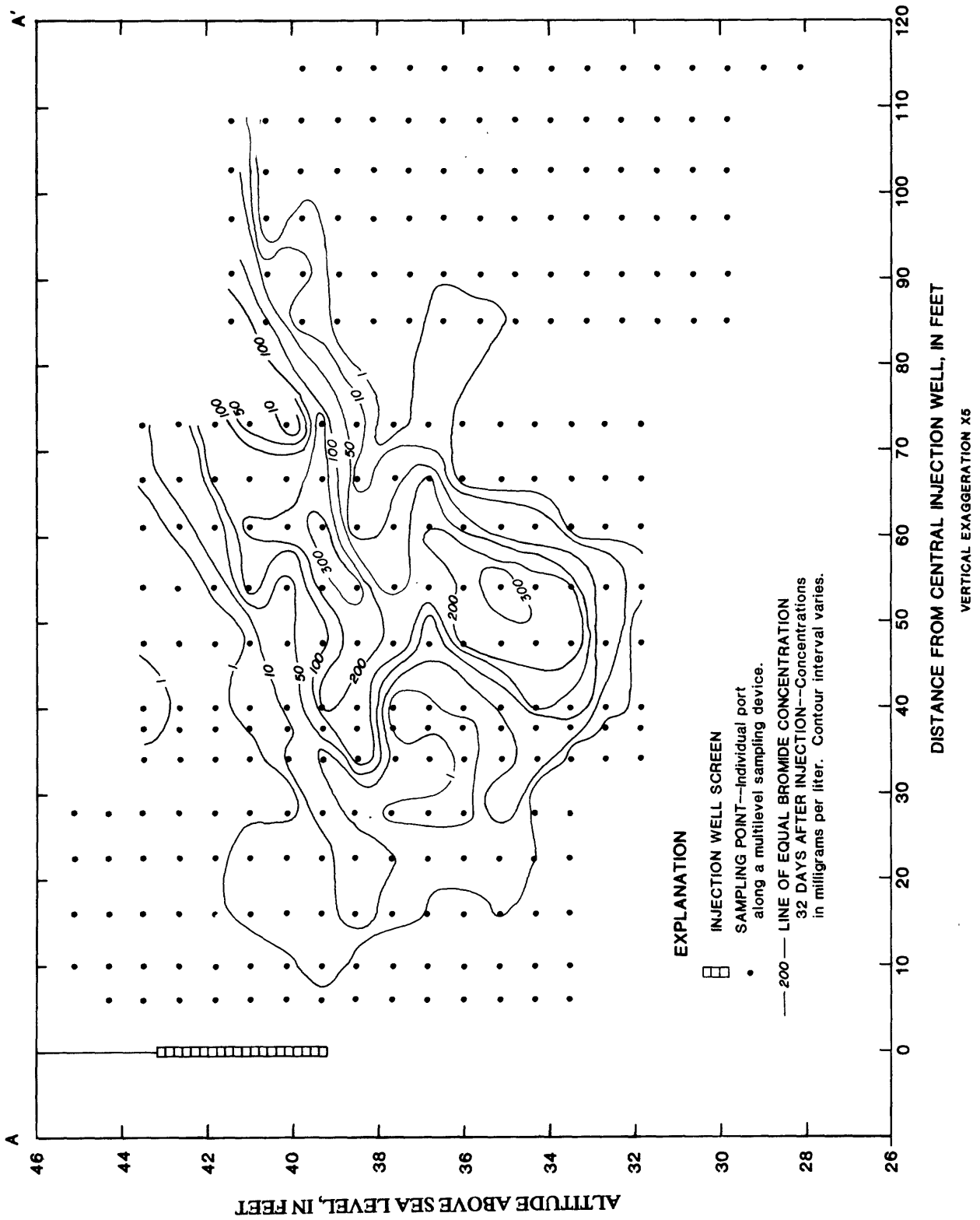


Figure B-10.— Vertical distribution of bromide cloud along section A-A' 32 days after injection of tracer. Location of section is shown in figure B-9.

ward, either in response to ambient ground-water movement or to a density contrast between the solute cloud and native ground water. Bromide concentrations are more dilute in fast-moving zones at the leading edge of the tracer cloud than near the center of mass because of the effects of local longitudinal and transverse dispersion. At this early stage of the test, the concentration distribution is highly variable, both vertically and longitudinally. This variability is related to velocity differences caused by nonuniform hydraulic conductivity. The vertically averaged values plotted in figures B-8 and B-9 are useful in approximating the solute-cloud location; the actual distribution, as indicated by figure B-10, is much more complex.

Planned analyses include calculations of dispersivity from the change in variance of the solute distribution with travel distance. These observed dispersivity values will be compared to those calculated from the statistical properties of the porous media. Statistical properties of aquifer hydraulic conductivity will be obtained from permeameter analysis of sediment cores and from borehole geophysical logs. The distribution of nonconservative solutes will be used to evaluate

various models of reactive transport, including ion exchange, complexation, desorption, and effective distribution coefficients.

REFERENCES

- Anderson, M.P., 1979, Using models to simulate the movement of contaminants through groundwater flow systems: *CRC Critical Reviews in Environmental Control*, v. 9, p. 97-156.
- Gelhar, L.W., and Axness, C.L., 1983, Three-dimensional stochastic analysis of macrodispersion in aquifers: *Water Resources Research*, v. 19, no. 6, p. 161-180.
- Gelhar, L.W., Gutjahr, A.L., and Naff, R.L., 1979, Stochastic analysis of macrodispersion in a stratified aquifer: *Water Resources Research*, v. 15, no. 6, p. 1387-1397.
- Sudicky, E.A., Cherry, J.A., and Frind, E.O., 1983, Migration of contaminants in groundwater at a landfill - a case study. 4. A natural gradient dispersion test: *Journal of Hydrology*, v. 63, p. 81-108.

IDENTIFICATION OF TRACE ORGANIC SUBSTANCES IN SEWAGE-CONTAMINATED GROUND WATER

By Larry B. Barber, II¹, E. Michael Thurman¹, and Michael P. Schroeder¹

The distribution of dissolved organic compounds in a sand and gravel aquifer on Cape Cod, Mass (fig. B-1), was studied in a plume of sewage-contaminated ground water. The plume resulted from disposal of secondary-treated sewage by rapid infiltration at Otis Air Base (LeBlanc, 1984). Maximum DOC (dissolved organic carbon) concentrations in the plume were 5 mg/L, whereas those in uncontaminated ground water at the site were 0.7 mg/L. Although these data suggest that the ground water is not heavily contaminated by organic compounds, water with very low DOC concentrations can contain undesirable levels of toxic organic substances. Therefore, methods to identify trace organic compounds were tested at the site.

Three methods were used to isolate trace organic compounds from ground-water samples—closed-loop stripping, purge and trap, and liquid extraction. Identification and quantification of compounds were performed by gas chromatography/mass spectrometry (GC/MS).

The closed-loop stripping GC/MS method of Grob and Zurcher (1976) was used to determine nanogram per liter (ng/L) concentrations of semi-volatile organic compounds (Barber and others, 1984; Barber, 1985). More than 100 compounds were detected within the contaminant plume, including trichloroethene, tetrachloroethene, dichlorobenzene isomers, alkyl benzenes, di-*t*-butyl-benzoquinone, and nonylphenol isomers. Other compounds detected included: *n*-aldehydes, phthalate esters, and saturated and unsaturated hydrocarbons. Concentrations of individual compounds ranged from less than 10 ng/L to more than 10,000 ng/L. These persistent compounds are common components of secondary sewage effluents.

The purge and trap GC/MS method (Longbottom and Lichtenberg, 1981, Method 624; Wershaw and others, 1983) was used to determine $\mu\text{g/L}$ concentrations of volatile organic compounds. Results showed a plume of ground water contaminated by dichloroethene, trichloroethene (TCE), and tetrachloroethene (PCE) at concentrations ranging from 1 $\mu\text{g/L}$ to more than 1,000 $\mu\text{g/L}$.

¹U.S. Geological Survey, Denver, Colo.

The liquid extraction GC/MS method (Wershaw and others, 1983) has a relatively high detection limit and detected only TCE and PCE in water from the most contaminated wells.

A comparison of data from these three isolation procedures illustrates the importance of analytical sensitivity and selectivity of a method as criteria in choosing a method to measure organic compounds in natural waters, particularly in screening for trace-level contamination. The liquid extraction method has a detection limit of 5 to 10 $\mu\text{g/L}$ and is best suited for compounds of intermediate molecular weight. Because the sewage plume contains primarily low molecular-weight compounds at sub- $\mu\text{g/L}$ concentrations, the liquid extraction data indicated that ground water in the plume was essentially unaffected by organic contaminants. The purge and trap method has the same general detection limit as the liquid extraction method but is most selective for low molecular-weight organic substances, the class of organic compounds most likely to be major contaminants in ground water. As a result, the purge and trap method indicated high levels of TCE and PCE in the plume.

The closed-loop stripping method, in contrast, has a detection limit that is 2 orders of magnitude lower than that for purge and trap and liquid extraction. It also isolates a broad range of compounds, including low and intermediate molecular-weight substances. As a result, the closed-loop stripping method showed a complex distribution of more than 100 compounds in the sewage plume; it also provided more information about trace organic compounds from a single water sample than did the other two methods.

Concentrations of volatile organic compounds determined by closed-loop stripping and purge and trap were generally comparable, with two major differences: (1) the closed-loop stripping indicated a greater extent of TCE and PCE contamination than did purge and trap because closed-loop stripping has a lower detection limit, and (2) in samples where TCE and PCE concentrations exceeded 10 $\mu\text{g/L}$, concentrations deter-

mined by closed-loop stripping were considerably lower than concentrations determined by purge and trap. At the higher concentrations, the sorbent of the closed-loop stripping device became overloaded and failed to trap all the volatile organic compounds in the sample.

The primary control on the distribution of organic compounds in the plume seems to be variation in sewage-effluent composition over time; however, no data on concentrations of trace organic compounds in the treated sewage before 1983 are available to test this hypothesis. Concentrations of trace organic compounds in some wells changed by several orders of magnitude over a 1-year period, as indicated from three rounds of sampling. A general trend of increasing concentrations in the downgradient part of the plume and decreasing concentrations near the infiltration beds suggests that volatile organic compounds were introduced as a pulse and are moving downgradient with the ground-water flow.

The limited distribution of hydrophobic compounds such as nonylphenol suggests that retardation by sorption also may limit the distribution of organic substances in the plume. The apparent retardation of selected trace organic compounds was noted through comparison with the distribution of boron, which is presumed to move conservatively in this system (Barber, 1985). Calculation of apparent retardation factors assumes that the trace organic compounds and boron have similar disposal histories. Most trace organic compounds had relative retardation factors that were consistent with those predicted by the relation between octanol/water partition coefficient (K_{ow}) and organic carbon content of the aquifer material (Schwarzenbach and others, 1983; Schwarzenbach and Westall, 1981). However, some compounds had retardation factors that were the inverse of the predicted factors. This inconsistency between observed and predicted retardation for some compounds and not for others suggests that the effects of retardation are superimposed on the effects of variations in source composition.

In conclusion, most of the readily degradable dissolved organic carbon in the sewage is removed during treatment and infiltration at the disposal site. The remaining refractory dissolved organic carbon compounds reach the water table and were detected as far as 11,000 feet from the infiltration

beds. These compounds are common components of sewage effluents; thus, their presence in the ground water is evidence that the trace organic contamination has resulted from sewage disposal.

REFERENCES

- Barber, L.B., II, 1985, Geochemistry of organic and inorganic compounds in a sewage contaminated aquifer, Cape Cod, Massachusetts: Boulder, Colo., University of Colorado, unpublished Master's thesis, 169 p.
- Barber, L.B., II., Thurman, E.M., and Schroeder, M.P., 1984, Closed-loop stripping, combined with capillary gas chromatography/mass spectrometry analysis, to define a semi-volatile organic-contaminant plume, in LeBlanc, D.R., ed., 1984, Movement and fate of solutes in a plume of sewage-contaminated ground water, Cape Cod, Massachusetts: U.S. Geological Survey Toxic Waste Ground-Water Contamination Program: U.S. Geological Survey Open-File Report 84-475, p. 89-113.
- Grob, K., and Zurcher, F., 1976, Stripping of trace organic substances from water: Equipment and procedures: *Journal of Chromatography*, v. 117, p. 285-294.
- LeBlanc, D.R., 1984, Sewage plume in a sand and gravel aquifer, Cape Cod, Massachusetts: U.S. Geological Survey Water-Supply Paper 2218, 28 p.
- Longbottom, J.E., and Lichtenberg, J.J., eds., 1981, Methods for organic chemical analysis of waters and wastes by GC, HPLC, and GC/MS: Cincinnati, Ohio, U.S. Environmental Protection Agency, Office of Research and Development, 345 p.
- Schwarzenbach, R.P., Giger, W., Hoehn, E., and Schneider, J.K., 1983, Behavior of organic compounds during infiltration of river water to ground water. Field studies: *Environmental Science and Technology*, v. 17, p. 472-479.
- Schwarzenbach, R.P., and Westall, J., 1981, Transport of nonpolar organic compounds from surface water to ground water. Laboratory sorption studies: *Environmental Science and Technology*, v. 15, p. 1360-1367.
- Wershaw, R.L., Fishman, M.J., Grabbe, R.R., and Lowe, L.E., eds., 1983, Methods for the determination of organic substances in water and fluvial sediments: U.S. Geological Survey Techniques of Water Resources Investigations, book 5, chapter A3, 173 p.

SAMPLING AND ANALYSIS OF VOLATILE ORGANIC COMPOUNDS IN A PLUME OF SEWAGE-CONTAMINATED GROUND WATER

By E. Michael Thurman¹, Michael G. Brocks², and Larry B. Barber, II¹

Volatile organic compounds, including tetrachloroethene, trichloroethene, trans-1,2-dichloroethene, and 1,1-dichloroethane, were found in a study of sewage-contaminated ground water on Cape Cod, Mass. The purposes of the study were: (1) to examine differences in recovery of volatile organic compounds from samples taken by two commonly used pumps—a submersible and a peristaltic pump; (2) to evaluate possible sample loss during storage; and (3) to determine reproducibility of gas-chromatographic/mass spectrometric (GC/MS) analyses. The submersible pump recovered 1.4 times the concentration of volatile organic compounds as did the peristaltic pump in two separate sampling trips; peristaltic pumps clearly have poorer recoveries, even when used in shallow wells where the depth to water is less than 10 feet. Sample loss because of storage or instrumental variation was evaluated by spiking samples with surrogate standards at the

time of collection. Storage of samples for as long as 1 month before analysis did not result in significant sample loss. In a comparison of concentrations of volatile organic compounds from 100 samples collected from one well on two sampling trips, it was possible to differentiate error due to sampling (40 percent relative deviation) from errors due to analytical analysis (10 percent) and from spiking error (1 percent).

The purge-and-trap method gave reproducible results for the organic compounds studied. Variations due to spiking and analysis were small compared with variations due to time between sampling (about 1 year) and type of pump used to collect the samples. The data clearly show that time of sampling, which reflects changes in contaminant concentrations in the aquifer, was the factor that most strongly determined the concentrations of volatile organic compounds in the samples.

¹U.S. Geological Survey, Denver, Colo.

²Rocky Mountain Analytical Labs, Arvada, Colo.

MOVEMENT AND FATE OF DETERGENTS IN SEWAGE-CONTAMINATED GROUND WATER

By E. Michael Thurman¹ and Larry B. Barber, II¹

The major cations, anions, and detergents in a plume of contaminated ground water at Otis Air Base on Cape Cod, Mass. (fig. B-1), have moved approximately 11,000 feet downgradient from the sand beds where treated sewage is discharged to a sand and gravel aquifer. The detergents form two distinct zones in the plume, based on methylene-blue active substances. Chemical analyses suggest that one zone consists of ABS (alkyl benzene sulfonates) detergents and that the other consists of LAS (linear alkyl sulfonates) and NaLS (sodium dodecyl sulfate) detergents. The

ABS detergents, which were deposited from about 1946 until 1965, seem to be transported in the aquifer at the same rate as the major cations and anions and boron, which are being used as conservative tracers of the plume and have moved about 11,000 feet downgradient from the infiltration beds. Little biological degradation of the ABS detergents is evident. In contrast, the LAS and NaLS detergents, which have been deposited since about 1965, degrade rapidly and have moved only several thousand feet downgradient from the infiltration beds.

¹U.S. Geological Survey, Denver, Colo.

BACTERIAL DISTRIBUTION AND TRANSPORT IN A PLUME OF SEWAGE-CONTAMINATED GROUND WATER

By Ronald W. Harvey¹ and Leah George¹

Bacterial abundance, particle/solution partitioning, and cell-size distribution were determined from microscopic analysis of ground water and subsurface sediment-core samples taken from a sewage-contaminated aquifer on Cape Cod, Mass. (fig. B-1). An aseptic wet-sieving preparative procedure (Harvey and others, 1984) and acridine-orange epifluorescence direct-counting (Hobbie and others, 1977), indicated the numbers of particulate-bound bacteria in the saturated subsurface to range from $1.21 \pm 0.23 \times 10^5$ per gram sediment in an uncontaminated zone to $1.19 \pm 0.14 \times 10^7$ per gram in the plume of sewage-contaminated ground water downgradient from the infiltration beds. Although more than 90 percent of the bacteria in the contaminated zone were particle-bound, fractions of particle-bound bacteria ranged from less than 65 percent 0.01 km from the point of sewage infiltration to more than 98 percent 0.4 km downgradient in the plume. Hence, the contribution of free-living bacteria (not bound to particles) in the mineralization of organic contaminants in the saturated subsurface may be more important near the sewage-disposal beds than farther away.

Abundances of particle-bound bacteria in vertical transects did not correlate with abundances of unattached bacteria, except at a highly contaminated zone immediately adjacent to the infiltration beds ($r = 0.95$, $p \leq 0.05$). Little variability (0.127 coefficient of variation) was observed in abundance of particle-bound bacteria among five replicate subsurface core samples taken 0.3 m apart. However, the relative silt content varied fourfold in these samples. Because silt particles were found to harbor more than 90 percent of the attached microbial community and provide much of the total solid-surface area in the aquifer, subsurface bacterial abundance seems to be relatively independent of the total number of suitable binding sites; thus, the number of suitable binding sites is assumed to be in excess.

Abundance of free-living (unattached) bacteria in the subsurface ranged from $1.03 \pm 0.10 \times 10^7$ per milliliter immediately adjacent to the sewage-disposal beds to $1.6 \pm 0.02 \times 10^4$ per milliliter at a control site upgradient from the zone of contamination. The latter population density was the lowest reported for a freshwater habitat by a direct-counting procedure. Numbers of unattached bacteria at most sites varied little over a 2-year span; however, bacterial abundance along a vertical transect through contaminated ground water varied up to threefold in less than 1 m. This suggests a high degree of local variation and vertical stratification within the plume's bacterial community and a need for ground-water samplers at closely spaced vertical intervals.

Field evidence suggests that unattached bacteria may be transported through a substantial length of the contaminant plume. Although bacterial abundance in a zone 0.4 km to 2.4 km downgradient from the sewage-disposal beds changed linearly with specific conductance of ground water ($r = 0.75$, $p < 0.001$), the numbers of unattached bacteria closer than 0.4 km to the infiltration beds were many times higher than would be predicted from specific conductance values. Furthermore, preliminary results from laboratory microcosm experiments using flow-through columns packed with aquifer sediments and representative flow rates (0.4–1.0 m/d) indicate that, under certain physical and chemical conditions, the mobility of some ground-water bacteria may approach that of a conservative tracer. This suggests that a fraction of the unattached microbial community in downgradient sections of the contaminant plume may have originated from nutrient-enriched ground water near the point of sewage infiltration. Such a mechanism would explain the relatively high abundance of unattached bacteria in nutrient-poor regions of the contaminant plume.

¹U.S. Geological Survey, Menlo Park, Calif.

Average size of unattached bacteria in contaminated ground water increases from 0.50 μm (average cell length) at a distance of 0.01 km from the infiltration beds to 0.90 μm at a distance of 0.64 km downgradient. This is due to corresponding decreases in the relative abundance of small (less than 0.4- μm diameter) bacteria. The observation that larger bacteria are transported more readily than smaller bacteria in moving ground water is consistent with subsurface transport studies done with nonendemic "tracer" microorganisms (Bitton and others, 1974). The relationship between specific physical, chemical, and nutrient conditions and transport of resident bacterial populations in the subsurface is a complex subject and is to be investigated in laboratory column experiments and in ground-water-injection tests at the Cape Cod site.

REFERENCES

- Bitton, G., Lahav, N., and Henis, Y., 1974, Movement and retention of *Klebsiella arogenes* in soil columns: *Plant Soil*, v. 40, no. 2, p. 373-380.
- Harvey, R.W., Smith, R.L., and George, Leah, 1984, Effect of organic contamination upon microbial distributions and heterotrophic uptake in a Cape Cod, Massachusetts, aquifer: *Applied and Environmental Microbiology*, v. 48, p. 1197-1202.
- Hobbie, J.E., Daley, R.J., and Jasper, S., 1977, Use of Nuclepore filters for counting bacteria by fluorescence microscopy: *Applied and Environmental Microbiology*, v. 33, no. 5, p. 1225-1228.

NITRATE REDUCTION IN A SEWAGE-CONTAMINATED AQUIFER

By Richard L. Smith¹ and John H. Duff²

Secondary-treated sewage from a military base on Cape Cod, Mass. (fig. B-1), is discharged to sand infiltration beds where it percolates into the ground. Continuous operation for 48 years has resulted in a plume of contaminated ground water approximately 25 m thick, 800 m wide, and 3.4 km long. High concentrations of nitrate (1 millimolar) were present in the effluent. The absence of detectable concentrations of nitrate and oxygen and high concentrations of ammonia in the center of the plume 100 m downgradient from the infiltration beds suggests that a zone of nitrate reduction had been established within the contaminated area. Depth profiles of well water and core samples were assayed for denitrification and

dissimilatory nitrate reduction by the acetylene blockage technique. Denitrification was the predominant nitrate-reducing activity; rates were highest nearest the beds and nonexistent outside the plume. The zone of maximal activity was limited to a depth interval only 1 to 2 m thick. For a given site within the plume, endogenous activity in core material was 20-fold higher than in corresponding well water from the same site. Thus, well-water samples alone do not seem to be adequate for assessing denitrification. Results of this study establish that nitrate reduction can occur in subsurface systems and, thereby, serve as a mechanism to transform nitrate in contaminated ground water.

¹U.S. Geological Survey, Denver, Colo.

²U.S. Geological Survey, Menlo Park, Calif.

FATE OF AMMONIUM IN A SEWAGE-CONTAMINATED GROUND WATER

By Marnie L. Ceazan¹, Richard L. Smith¹, and E. Michael Thurman¹

The plume of sewage-contaminated ground water at the Otis Air Base site on Cape Cod, Mass., contained ammonium (NH_4^+) in high concentrations (7 to 10.7 mg N/L) within about 1,000 feet downgradient from the infiltration beds; however, NH_4^+ was depleted (less than 2 mg N/L) from 6,000 to 8,000 feet downgradient from the beds and absent beyond 8,000 feet. Conversely, nitrate (NO_3^-) was the predominant species of inorganic nitrogen from 6,000 feet to the toe of the plume (about 11,000 feet downgradient from the beds). In the zone of depleted NH_4^+ , NO_3^- levels were elevated (greater than 2 mg N/L) and dissolved oxygen was present. These results suggest that NH_4^+ attenuation is due to nitrification or to differential rates of transport of NH_4^+ and NO_3^- caused by sorption of NH_4^+ on aquifer solids. To test these hypotheses, evidence for nitrification and sorption was obtained in laboratory studies conducted on aquifer material.

Nitrification assays were conducted on ground water and solid aquifer material obtained from two sites located 700 and 6,000 feet downgradient from the infiltration beds. Ground water was collected from screened wells located at these sites and cores of solid aquifer material were obtained at depths adjacent to the screened wells. Water from each depth was added to the respective solid material from that depth to form slurries, which were assayed for nitrifying activity and nitrifying bacteria. Nitrifying activity was assayed by modifying incubation techniques employed by Cavari (1977), Schell (1978), and Mevel and Chamroux (1981) and monitoring slurries for changes in concentrations of dissolved substrates and products of nitrification (NH_4^+ , NO_3^- , and nitrite; NO_2^-). Slurries were examined for the presence of nitrifying bacteria using most-probable-number (MPN) dilution counts for NH_4^+ oxidizing bacteria (Soriano and Walker, 1968; American Public Health Association, 1981).

Nitrification assays were conducted at four depths at the site located 6,000 feet from the infil-

tration beds. These results indicated that nitrifying bacteria were present (150 bacteria per 100 mL) at a depth of 69 feet below land surface. Furthermore, during the course of incubation, slurries obtained from the 69-foot depth showed a decrease in dissolved NH_4^+ and a production of NO_3^- , indicating that measurable nitrifying activity was occurring.

Zones of nitrification in marine sediments may be thin (2 cm) (Vanderborcht and Billen, 1975) and occur at the interface of NO_3^- and dissolved oxygen gradients; thin zones of nitrification may also occur in ground-water systems. To test this hypothesis, sediment and ground water were sampled at thin vertical intervals of 2 feet at a location where steep concentration gradients of NO_3^- , oxygen, and NH_4^+ were present (700 feet downflow from the infiltration beds). Slurries from all depths showed a linear decrease in NH_4^+ with no time lag over a 13-day incubation period. The average rate of decrease of NH_4^+ in these incubations was 48 ($\mu\text{g/L}$)/day. Initial NO_3^- concentrations in most of these incubations were high (8 to 15 mg N/L); therefore, small increments of change in NO_3^- concentration could not be measured. The control incubations, which were sterilized by autoclaving, did not show a linear decrease in NH_4^+ . Thus, loss of NH_4^+ was at least partly due to microbial processes, with nitrification or assimilation into biomass. The MPN enumerations showed that nitrifying bacteria were present in this depth profile (400 to 13,150 bacteria per 100 mL).

As a preliminary experiment to test for adsorption, NH_4^+ was extracted with 2 N KCl from the same slurries that had been incubated for microbial analyses (Bowden, 1984). Results indicated that a significant fraction of NH_4^+ is sorbed on aquifer sediments. Studies are underway with laboratory batch experiments to investigate the importance of adsorption in NH_4^+ transport in the aquifer.

The results of this study indicate that both microbiological and adsorption processes play a

¹U.S. Geological Survey, Denver, Colo.

role in the transport and fate of NH_4^+ in the aquifer. The relative importance of each and the effect of sorption upon nitrification remains to be determined.

REFERENCES

- American Public Health Association, 1981, Standard methods for the examination of water and wastewater, 15th ed.: Washington, D.C., American Public Health Association, 1134 p.
- Bowden, W.B., 1984, A nitrogen-15 isotope dilution study of ammonium production and consumption in a marsh sediment: *Limnology and Oceanography*, v. 29, p. 1004–1015.
- Cavari, B.Z., 1977, Nitrification potential and factors governing the rate of nitrification in Lake Kinneret: *Oikos*, v. 28, p. 285–290.
- Mevel, G., and Chamroux, S., 1981, An experimental study of regulation of nitrification in marine sediments: *Oceanol. Acta*, v. 4, p. 457–463.
- Schell, D., 1978, Chemical and isotopic methods in nitrification studies: *Microbiology*, v. 20, p. 292–295.
- Soriano, S., and Walker, N., 1968, Isolation of ammonia-oxidizing autotrophic bacteria: *Journal of Applied Bacteriology*, v. 31, p. 493–497.
- Venderborght, J.P., and Billen, G., 1975, Vertical distribution of nitrate concentration in interstitial water of marine sediments with nitrification and denitrification: *Limnology and Oceanography*, v. 20, p. 953–960.

CHAPTER C. – GROUND-WATER CONTAMINATION BY CRUDE OIL AT BEMIDJI, MINNESOTA

	Page
Introduction	C-3
Surficial and subsurface distribution of aquifer sediments at the Bemidji, Minnesota, research site, by D.A. Franzi	
Surficial geomorphology	C-5
Stratigraphy	C-5
Hydrologic aspects	C-9
Hydrogeology and preliminary regional flow modeling at the Bemidji, Minnesota, research site, by R.T. Miller	C-11
Inorganic geochemistry of ground water and aquifer matrix: First-year results, by D.I. Siegel, P.C. Bennett, M.J. Baedecker, M.P. Berndt, and D.A. Franzi	C-17
Distribution of gases and hydrocarbon vapors in the unsaturated zone, by M.F. Hult and R.R. Grabbe	C-21
Composition and alteration of hydrocarbons in ground water, by R.P. Eganhouse, M.J. Baedecker, Curtis Phinney, and Jessica Hopple	C-27
Mass transfer at the alkane-water interface in laboratory columns of porous media, by H.O. Pfannkuch, S.N. Nourse, and M.F. Hult	C-29
Objectives and hypotheses	C-29
Experimental apparatus and methods	C-29
Data and results	C-29
Discussion	C-31
Microbial degradation of crude oil and some model hydrocarbons, by F.H. Chang, N.N. Noben, Danny Brand, and M.F. Hult	C-33

ILLUSTRATIONS

	Page
Figure	
C-1. Map showing location of crude-oil spill near Bemidji, Minnesota	C-4
C-2. Map showing surficial geology of Bemidji crude-oil spill site and vicinity	C-6
C-3. Composite stratigraphic column of the principal lithofacies at the Bemidji crude-oil spill site	C-7
C-4. Fence diagram of ground-water flow-model area near Bemidji, Minnesota	C-8
C-5. Map showing observed steady-state water-table altitude, 1983–85, and locations of observation wells and model-area boundary	C-12
C-6. Areal view of: A. three-dimensional model area, location of section A–A', and well locations, B. two-dimensional vertical model grid	C-13
C-7. Map and vertical section showing comparison of observed and simulated steady-state water levels for 1983–85 in: A. three-dimensional flow model, and B. two-dimensional vertical-section model	C-14
C-8. Map and vertical section showing comparison of observed water levels resulting from applied 1.0-foot increase and decrease in level of unnamed lake with simulated levels in: A. three-dimensional model, and B. two-dimensional vertical-section model	C-15
C-9. Map showing comparison of observed with simulated water-table levels at end of 90-day spring recharge period, 1984	C-16

C-10. Maps showing areal distribution of selected ground-water constituents or properties at water table downgradient of crude-oil spill, August 1985: A. pH, B. silicon, and C. iron and magnesium	C-18
C-11. Scanning electron photomicrographs of feldspar: A. Unetched sample from uncontaminated zone; B. Etched sample from contaminated zone.....	C-20
C-12. Maps showing areal distribution of: A. organic carbon in upper meter of saturated zone, and B. methane in lower meter of saturated zone.....	C-22
C-13. Examples of chromatograms used to detect presence of organic compounds, carbon dioxide, oxygen, and nitrogen in gas samples from lower meter of the saturated zone.....	C-24
C-14. Vertical sections showing distribution of selected constituents within the unsaturated zone	C-25
C-15. Diagram of laboratory-column setup.....	C-30
C-16. Plot showing mass transfer of pure liquid hydrocarbons to formation water in relation to Sherwood and Peclet numbers.....	C-31
C-17. Graph showing mass-transfer rates for selected hydrocarbons obtained from published values and those obtained in this study in relation to Sherwood numbers and Peclet numbers.....	C-32
C-18. Plot of oxygen uptake by indigenous microorganisms in sediment and ground-water mixture mixed with hexadecane or crude oil and incubated at 12 °C and 2 °C.....	C-34
C-19. Graphs showing heterotrophic bacterial counts in sediment and ground-water microcosms with varied amounts of selected nutrients: A. at 2 °C, and B. 7 °C.....	C-36
C-20. Graphs showing heterotrophic bacterial counts in sediment and ground-water microcosms with varied amounts of selected nutrients: A. at 12 °C, and B. 17 °C.....	C-37
C-21. Plot of cumulative carbon mineralization of hexadecane mixed with sediment and ground water with varied amounts of selected nutrients and antibacterial or antifungal agents	C-38
C-22. Plot of bacterial and fungal counts with varied amounts of selected nutrients or antifungal agent at 17 °C.....	C-41

TABLES

	Page
Table	
C-1. Metal oxide distribution in uncontaminated drift near the water table	C-17
C-2. Peclet numbers, Sherwood numbers, and mass-transfer coefficients obtained in laboratory column experiments with alkane over aquifer sand in distilled water	C-31
C-3. Rates of oxygen uptake before and after 10 °C temperature change, and values for Q_{10} with sediment nutrients.....	C-34
C-4. Cumulative CO ₂ evolution and carbon mineralization from oil-contaminated topsoil samples.....	C-35
C-5. Cumulative CO ₂ evolution and carbon mineralization from crude oil in aquifer-sediment samples.....	C-39
C-6. Cumulative CO ₂ evolution and carbon mineralization from ¹⁴ C ₁ through C ₁₀ (hexadecane) in control sediment- and ground-water mixture by indigenous microbes.....	C-40
C-7. Degradation of model hydrocarbons by bacteria and fungi	C-42

CHAPTER C. — GROUND-WATER CONTAMINATION BY CRUDE OIL AT BEMIDJI, MINNESOTA

INTRODUCTION

On August 20, 1979, a pipeline break in a remote area near Bemidji, Minnesota (fig. C-1), resulted in the release of 10,500 barrels (167 m³) of crude oil. Although about 7,800 barrels (1,200 m³) were removed from the site as part of the cleanup, some crude oil infiltrated the ground and percolated to the water table. The spill occurred in the recharge area of a local flow system that discharges to a small lake 300 m feet downgradient. The aquifer is a pitted and dissected outwash plain underlain at a depth of about 20 m by low-permeability till. Crude oil is floating on the water table about 6 m below land surface and has migrated about 12 m as a separate fluid phase. Soluble petroleum derivatives have dissolved in and are moving with ground water. Volatile constituents are migrating through the unsaturated zone by diffusion.

Little information concerning the hydrogeology and natural geochemistry of the site was available at the time of the pipeline break, but the nature and extent of contaminant introduction are well known because initial remedial measures were prompt. A major early effort of the Geological Survey was to define the hydrogeologic framework and establish field facilities needed for the proposed investigations. This phase of the project has been completed, enabling productive research. Reports that have been published and papers that have been presented at scientific meetings describe:

- Changes in the physical and chemical characteristics of the oil due to preferential volatilization and dissolution,

- Dependence of the rate of hydrocarbon dissolution by the ground water on ground-water velocity and other physical factors,
- Dependence of the rate of hydrocarbon degradation by indigenous microbes on ambient temperature and nutrient availability,
- Volatilization, diffusion, and degradation of toxic and(or) explosive petroleum vapors in the unsaturated zone, to carbon dioxide and water.
- Dissolution, movement with ground water, and subsequent reprecipitation of inorganic components of the aquifer matrix by organic acids produced from the partial microbial breakdown of the oil,
- The use of molecular markers to distinguish between naturally occurring hydrocarbons and those derived from the oil spill,
- The emergence of biorefractory compounds, present in minor amounts in the original oil, from the zone of highest concentrations of dissolved contaminants. This is significant because the constituents that have migrated the greatest distances are generally also those that are considered the most toxic.

The abstracts in this chapter present additional information on the physical, chemical, and biologic processes at the site. Results of the interdisciplinary studies will be combined and used to develop predictive models of contaminant mobilization, transport, and fate.

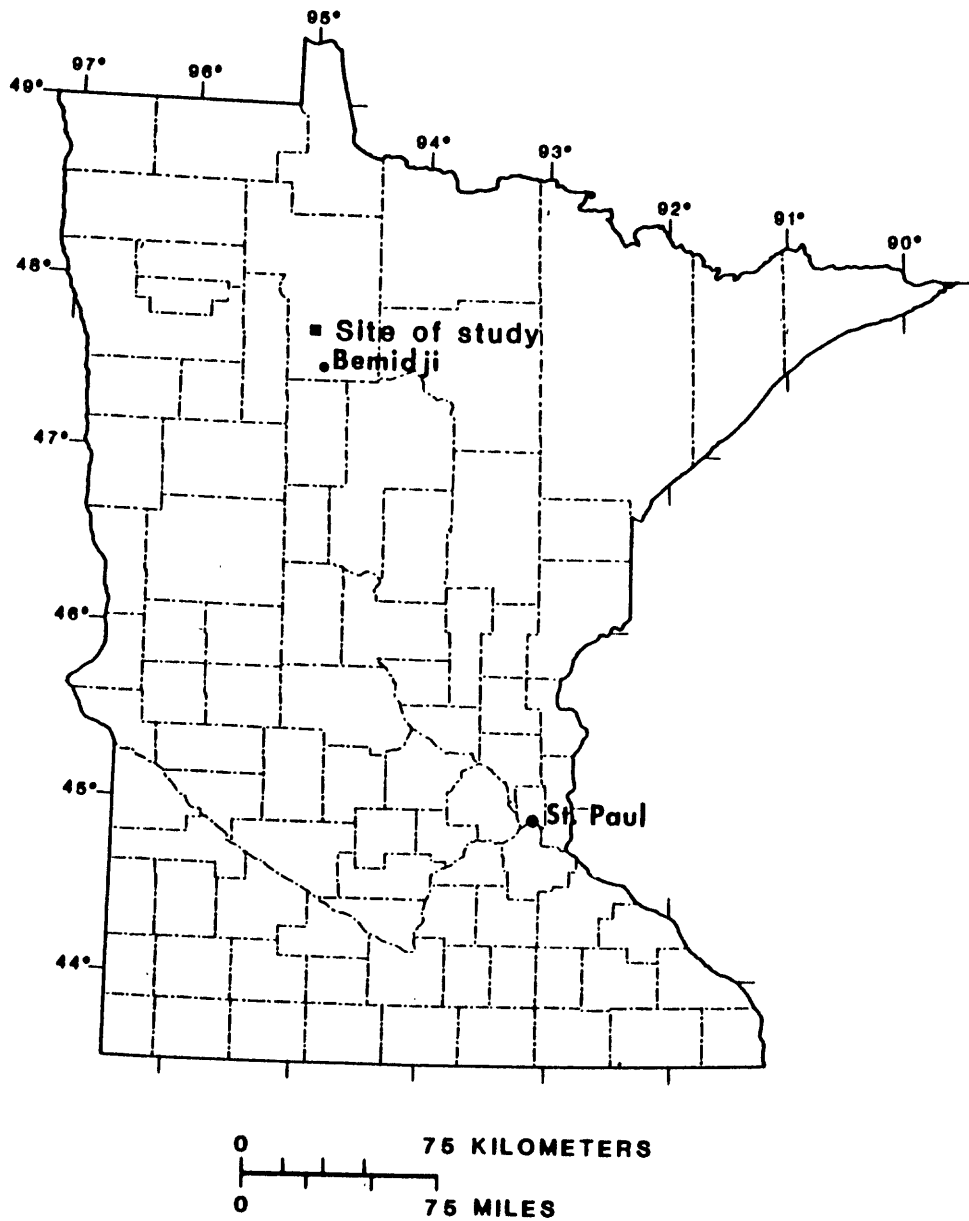


Figure C-1.— Map showing location of crude-oil spill near Bemidji, Minnesota.

SURFICIAL AND SUBSURFACE DISTRIBUTION OF AQUIFER SEDIMENTS AT THE BEMIDJI, MINNESOTA, RESEARCH SITE

By David A. Franzi¹

SURFICIAL GEOMORPHOLOGY

The Bemidji research site (fig. C-1) lies within a pitted and dissected outwash plain that is bordered on the southwest by a low-relief till upland and on the north by an end moraine complex. Older ice-contact deposits of a partly buried esker system are exposed locally where the outwash is thin or absent. The trend of the esker system is indicated by areas of intense kettle development and linear surface morphology within the outwash plain (fig. C-2).

The upland south of the research site is underlain by a silty to clayey, light olive-gray diamicton. Textural and petrographic analyses indicate a northwestern or Red River valley origin. The surface of the upland forms a low-relief, gently undulating plain, upon which are strewn boulders of igneous and metamorphic rock.

The morainal sediments north of the site consist of complexly interbedded diamictons, gravels, and sands. The diamictons are massive to medium bedded, light olive brown, with sandy to silty texture. The lithofacies associations and the presence of flow structures within the sedimentary sequence indicate deposition in an ice-proximal, subaerial environment. The northern margin of the moraine is overlain by a massive, silty to clayey, dark-brown diamicton. This unit has only limited surficial exposure within the study area.

The outwash sediments consist of moderately calcareous, yellowish brown to very pale brown, moderately to poorly sorted sandy gravel, gravelly sand, and sand. The outwash surface is extensively pitted and is transected by numerous meltwater channels. The largest concentration of kettles is associated with the buried esker complex, indicating that remnants of stagnant ice must have survived between glacial phases. Two major sequences of outwash sand and gravel were built by southeastward flowing meltwater streams during the final deglaciation of the region. Lower outwash terraces in the Clearwater River valley to the west probably are graded to base levels that were controlled by ice dams north of the study area.

¹State University of New York, Plattsburgh, New York

STRATIGRAPHY

The composite stratigraphic column for the study area (fig. C-3) depicts a sequence of four glacial lithofacies associations that are discontinuously overlain by postglacial lacustrine sediments. Each of the glaciogenic associations represents a distinct phase of glacial advance and retreat. The subsurface distribution of the units within the area delineated for ground-water-flow modeling (Miller, this report) is shown in figure C-4.

The basal unit is a sandy, dark olive-gray diamicton (D1, fig. C-3) that forms a continuous layer at least 1-m thick throughout the study area. At one locality this unit is overlain by lacustrine sand and silt, some of which is oxidized. Throughout most of the study area, however, the basal diamicton is overlain by a 0- to 10-m-thick sequence of olive, medium- to coarse-grained sand and gravelly sand that is correlated with the second lithofacies association (SD2, fig. C-3).

The stratified drift sequence is overlain by a thin to discontinuous (0- to 1-m thick), silty to clayey, dark gray, diamicton (D2, fig. C-3). The discontinuous occurrence of the unit in the subsurface makes its correlation problematic. From textural and compositional similarities, however, the unit is correlated with the diamicton that caps the upland south of the research site. Its position within the stratigraphic column was inferred from well-log data and surficial morphostratigraphic relationships.

The next younger lithofacies association consists of silty to sandy, light olive brown diamicton (D3, fig. C-3) interbedded with fine silty sand to medium gravel. The subcrop extent of the stratified diamicton lithofacies is restricted to the northeastern part of the ground-water-flow-model area (fig. C-4). This lithofacies association is inferred to represent the buried, distal margin of the moraine complex from its subsurface distribution and sediment characteristics.

95°07' 30"

95°02' 30"

47° 37' 30"

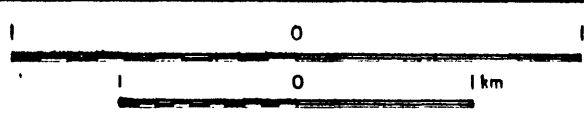
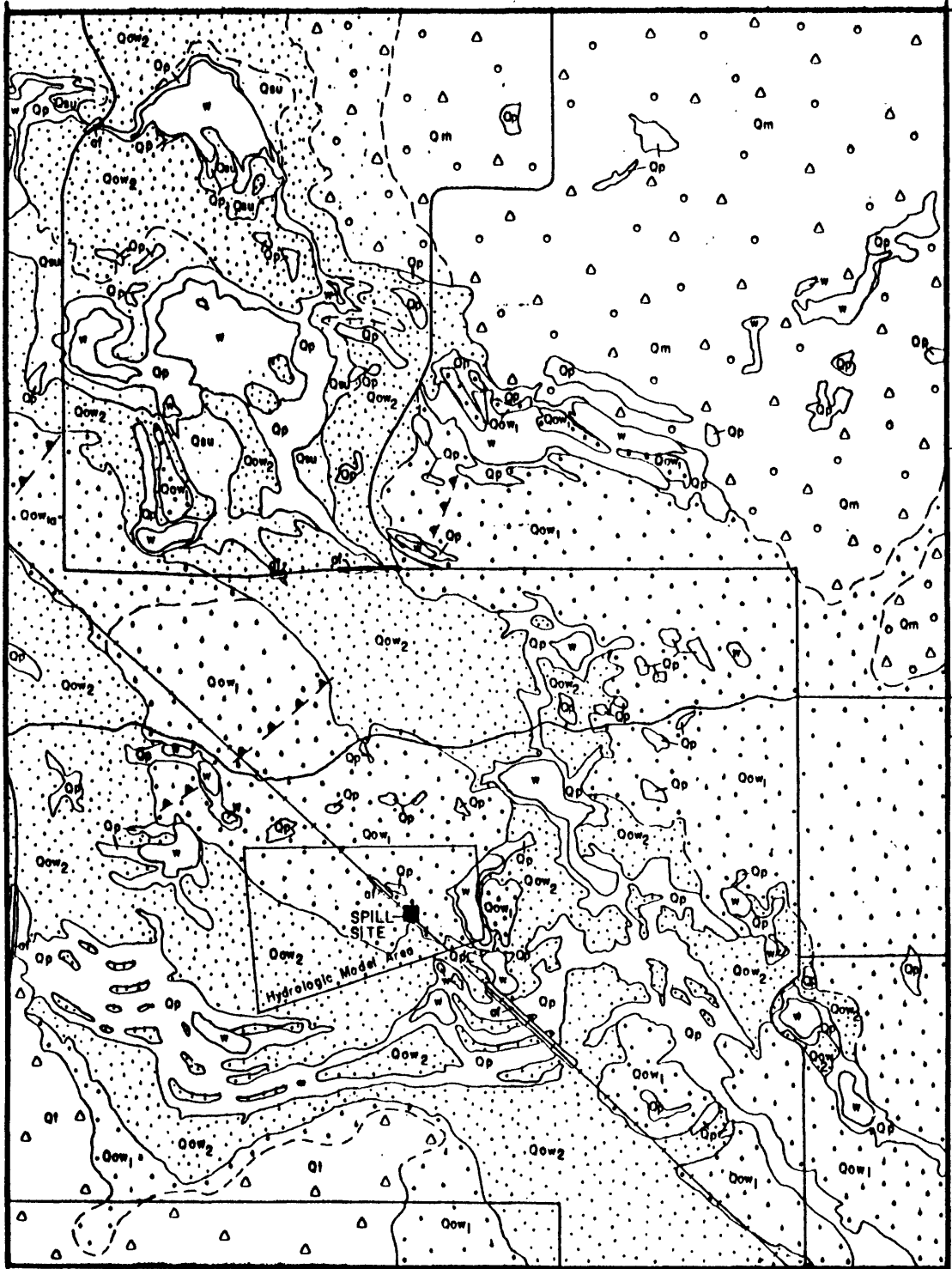
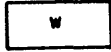
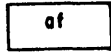


Figure C-2. Surficial geology of Bemidji crude-oil spill site and vicinity.

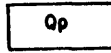
EXPLANATION



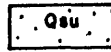
Surface Water



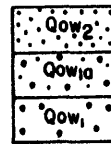
Artificial Fill



Paludal Deposits

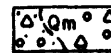


Stratified Deposits
(Undifferentiated)



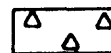
Outwash

Sand and gravel deposited at and beyond the ice margin by meltwater streams. Subscripts denote relative age.



Morainal Deposits

Diamicton, gravel, and sand deposited at the ice margin (lithofacies D3, fig. C-3). Stippled pattern denotes area overlain by younger diamicton (D4, fig. C-3).



Till

(lithofacies D2, fig. C-3)



Ice Margin

The stratified diamicton and its associated lithofacies are separated from the overlying outwash sand and gravel by an unconformity that is marked by a discontinuous layer (0 to 5 m) of thinly bedded to laminated, gray, fine sand, silt, and clay. These sediments probably were deposited in local kettle lakes formed after the retreat of ice from the moraine position. Where the lacustrine sediments are absent, the unconformity may be marked by a thin oxidized horizon.

Two sequences of outwash sand and gravel are represented by pitted terraces at elevations of 434.6 and 425.9 m in the vicinity of the research site (Qow1 and Qow2, fig. C-2). The terraces were built by southeastward flowing meltwater streams during the final deglaciation of the region. A lower surface at about 425.5 m is shown as a third outwash terrace (Qow3, fig. C-2) on the preliminary map. However, recent reinterpretation of drill-hole and other field data suggests that this surface probably represents the combined effects of late-glacial lacustrine sedimentation and meltwater erosion and deposition. Outwash terraces in the Clearwater River valley to the west are graded to base levels that were probably controlled by ice dams north of the study area.

The outwash sand and gravel may be genetically related to the diamicton that overlies the morainal sediments north of the study area (fig. C-2; D4, fig. C-3). The nature of this association, however, has not been sufficiently investigated.

HYDROLOGIC ASPECTS

Estimates of the intrinsic permeability of the aquifer sediments from granulometric analyses range from 0.5 to 2.7×10^{-4} m/s for the stratified drift units to 0.002 to 9.9×10^{-9} m/s for the lacustrine sediments and diamictons. The base of the local ground-water-flow system is most clearly defined by the basal diamicton (D1 in fig. C-3) that forms a continuous confining layer at depths of 18 to 27 m in the area of the ground-water-flow model (fig. C-4). Stratigraphically higher confining layers occur throughout the model area but none are continuous, and their distribution is generally difficult to predict. Delineation of these upper confining layers will be an important aspect of future field studies at the research site.

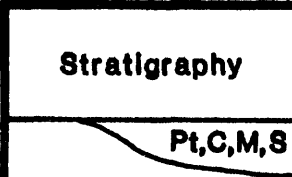
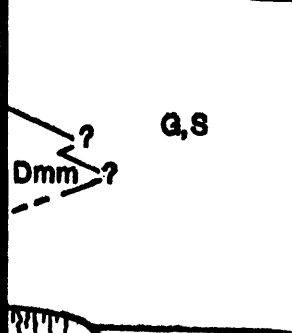
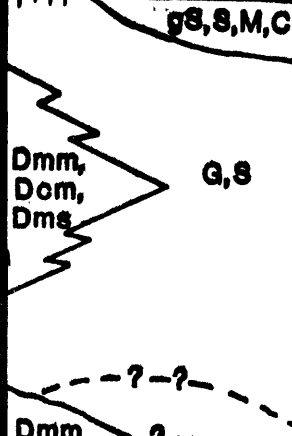
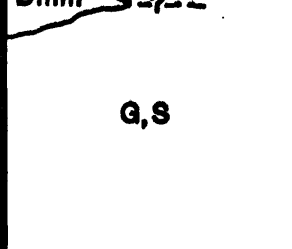
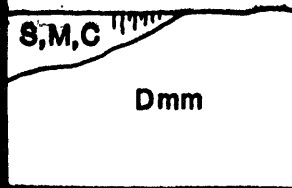
Stratigraphy	Lithofacies Symbols	Genetic Symbols	Genetic Interpretation
 Pt,C,M,S	Pt,C,M,S	L5	Post-glacial lacustrine sed.
 G,S Dmm?	G,S Dmm	Ow4 D4	Outwash Till
 gS,S,M,C Dmm, Dcm, Dms	gS,S,M,C G,S Dmm,Dcm, Dms	L3 Sd3 D3	Lacustrine sediment Stratified drift Morainal sediment: sediment-flow deposits, ice-proximal outwash, and till(?)
 Dmm G,S	G,S Dmm	Sd2 D2	Stratified drift Till
 S,M,C Dmm	S,M,C Dmm	L1 D1	Lacustrine sediments Till

Figure C-3. — Composite stratigraphic column of the principal lithofacies at the Bemidji crude-oil spill site. Location is shown in figure C-2.

Explanation

Lithofacies Symbols

Diamictons

Dmm	matrix-supported, massive
Dms	matrix-supported, stratified
Dcm	clast-supported, massive

Stratified Facies

		Prefixes
G	gravel	g gravelly
S	sand	s sandy
M	silt	m silty
C	clay	c clayey
Pt	peat	

Genetic Symbols

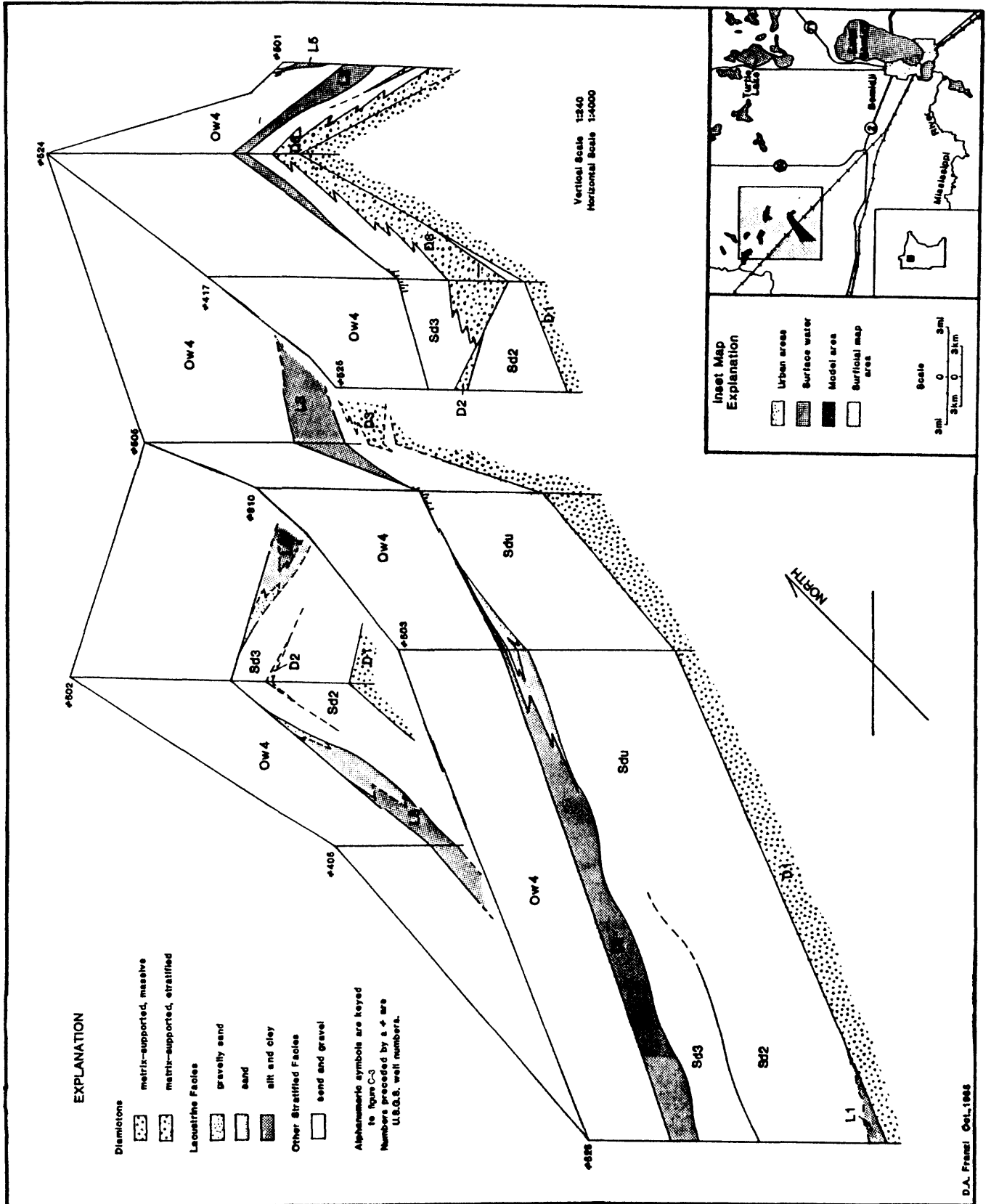
D	diamictons: sediment-flow deposits, ice-proximal outwash, and till
Ow	outwash
Sd	stratified drift
L	lacustrine sediments

Numbers following the genetic symbols indicate the relative age of the lithofacies associations

The postscript **u**, used on figure C-4, indicates uncorrelated units

Miscellaneous Symbols

 oxidized horizons



C-10...Bemidji, Minnesota

Figure C-4. -- Fence diagram of ground-water-flow model area near Bemidji, Minnesota.

D.A. Frame! Oct., 1985

HYDROGEOLOGY AND PRELIMINARY REGIONAL FLOW MODELING AT THE BEMIDJI, MINNESOTA, RESEARCH SITE

By Robert T. Miller¹

The Bemidji research site (fig. C-1) is located on an outwash plain, (fig. C-5) that is pitted and dissected regionally by gravel-filled channels that are now partly occupied by kettle lakes. Approximately 35 water-table wells and 10 piezometer nests have been installed to determine the direction and velocity of ground-water flow through the site. A steady-state approximation of regional ground-water flow indicates that flow generally is northeastward through the site toward an unnamed lake (fig. C-5). Locally, flow is seasonally influenced by a small kettle wetland approximately 500 feet north of the main spill site. Water levels upgradient of the spill site fluctuate as much as 1.0 foot in response to recharge, whereas water levels downgradient fluctuate only 0.3 foot and are influenced by water levels in the unnamed lake. Ground-water recharge during the 1984 water year ranged from 2.0 to 4.0 inches and was greatest near the kettle wetland north of the spill site.

The horizontal hydraulic gradient ranges from 0.002 to 0.003. Vertical gradients beneath the unnamed lake indicate upward flow into the lake and downward flow at depth. These differences in vertical gradient direction may be due to a discontinuous clay lens in the sand and gravel outwash that underlies the lake.

Two finite-difference ground-water-flow models were constructed to simulate the flow system at the site. One is a fully three-dimensional model with 19 x-axis nodes, 16 y-axis nodes, and 6 z-axis nodes; the other is a two-dimensional vertical-section flow model that corresponds to the 11th row (section A-A', fig. C-6) of the three-dimensional model. It has the identical nodal discretization in the x direction, and is divided vertically into 16 nodes of approximately equal spacing (fig. C-6). The x and y boundaries of the three-dimensional model represent 3,500 and 1,700 feet, respectively; and the z dimension (depth) is approximately 60 feet. The model discretization is variably spaced to accommodate two local flow models that are to be used in a detailed study of crude-oil transport.

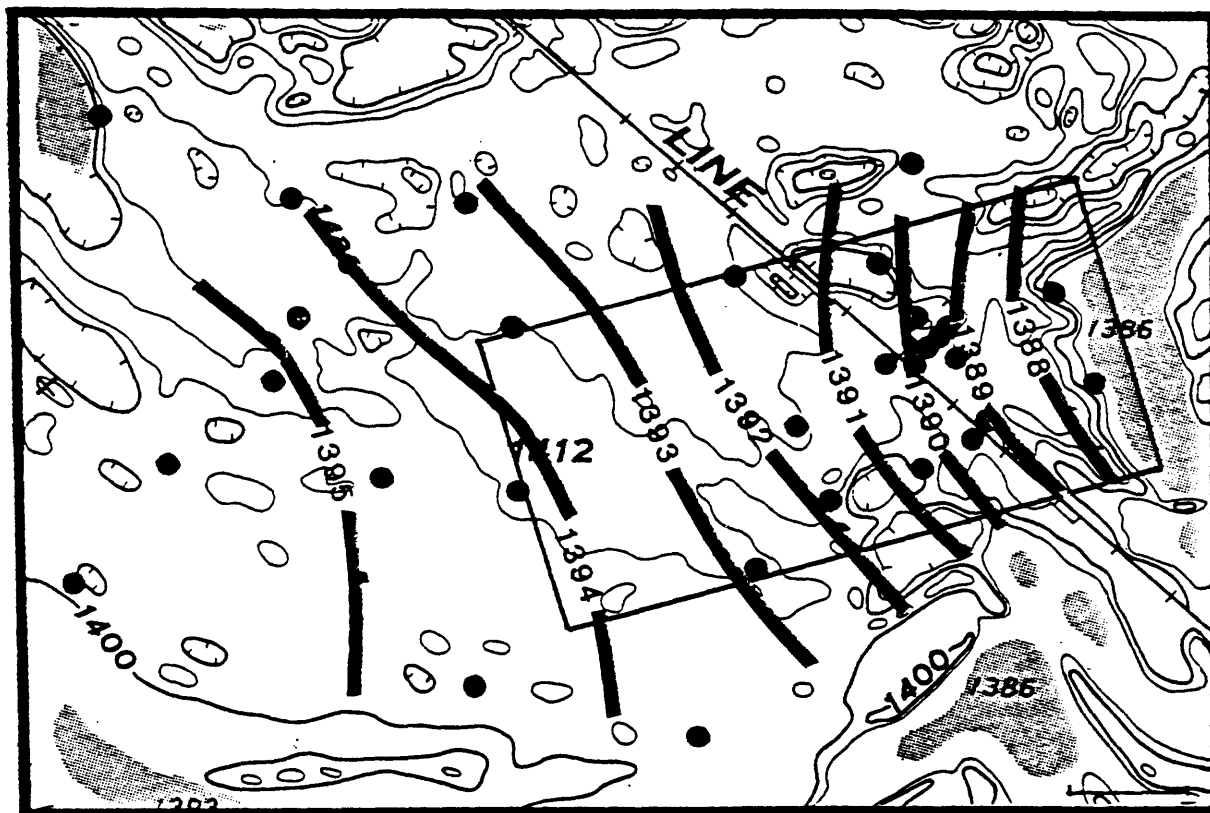
Model boundaries are simulated as free surface for the upper boundary, no flow for the lower boundary, and specified head-dependent leakage for all lateral boundaries. The head-dependent-leakage boundary is further divided into a general-leakage and a lake-leakage boundary. The use of the head-dependent-leakage boundary enables a more realistic representation of ground-water flux by allowing heads at the boundary to reflect changes outside the modeled area, a condition that is not simulated with specified-head or no-flow boundaries.

The three-dimensional flow model has five defined goals: (1) to aid in the description of the general ground-water flow field through the site in three dimensions, (2) to determine the sensitivity of various proposed flow models to boundary types, (3) to determine the sensitivity of inflow through the site to changes in water level in the unnamed lake, (4) to define the potential direction and distance of flow of the crude-oil residuals to aid in future data collection, and (5) to determine the thermal effects of ground-water temperature on the direction of ground-water flow. This article describes some results of the first four of these objectives.

Calibration of the steady-state ground-water-flow model was accomplished concurrently between the fully three-dimensional model for water-table contours and the two-dimensional cross-section model for refining the vertical component of flow. Figure C-7 illustrates final computed water levels for both models compared to approximate steady-state field conditions.

The calibrated steady-state model was used to examine the sensitivity of the level of the unnamed lake on the regional flow system (fig. C-8). Lake levels were simulated as being 1.0 foot above and 1.0 foot below the steady-state model-calibrated value. These lake-level changes are approximately twice those recorded on a staff gage located in the unnamed lake during the 1984 water year. Figure C-8 shows that, although a change in lake level

¹U.S. Geological Survey, St. Paul, Minnesota.



EXPLANATION

-  LINE OF EQUAL WATER-TABLE ALTITUDE, IN FEET--Contour interval 1 foot.
Datum is sea level
-  OBSERVATION WELL
-  BOUNDARY OF MODELED AREA

Figure C-5.—Observed steady-state water-table altitude, 1983–85, and locations of observation wells and model-area boundary.

causes only a small change in the horizontal hydraulic gradient, it causes a relatively large change in the vertical hydraulic gradient, suggesting that lake stage is a major factor in controlling three-dimensional flow northeastward from the spill site.

Model lateral boundaries were further examined in simulations of the 90-day spring-recharge period of 1984. Model results in figure C-9) show the effect of the the lateral boundaries on computed heads by predicting head values less than field-approximated values at the boundaries in areas with large water-table fluctuations. This is because the values for specified head outside the model area were held constant at the steady-state

calibrated value throughout the simulation period. The boundary effects are less obvious in the 1/2-mi area between the spill site and the unnamed lake because the head decrease in this area is considerably less than that upgradient of the spill.

Finally, the components of ground-water velocity that were computed by the model were examined in a scaled-mass fraction contaminant-transport simulation of a 6 year period using the steady-state water-level configuration. Three-dimensional model results indicate that the general shape of the contaminant plume is similar to that delineated from dissolved organic carbon data collected August 20, 1985. The model also indicates

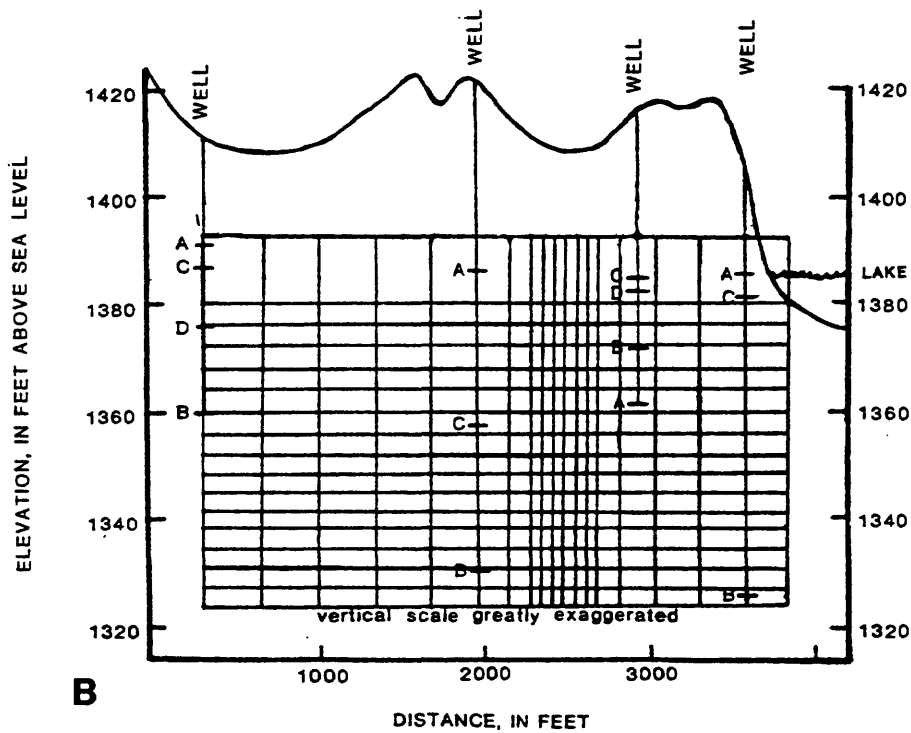
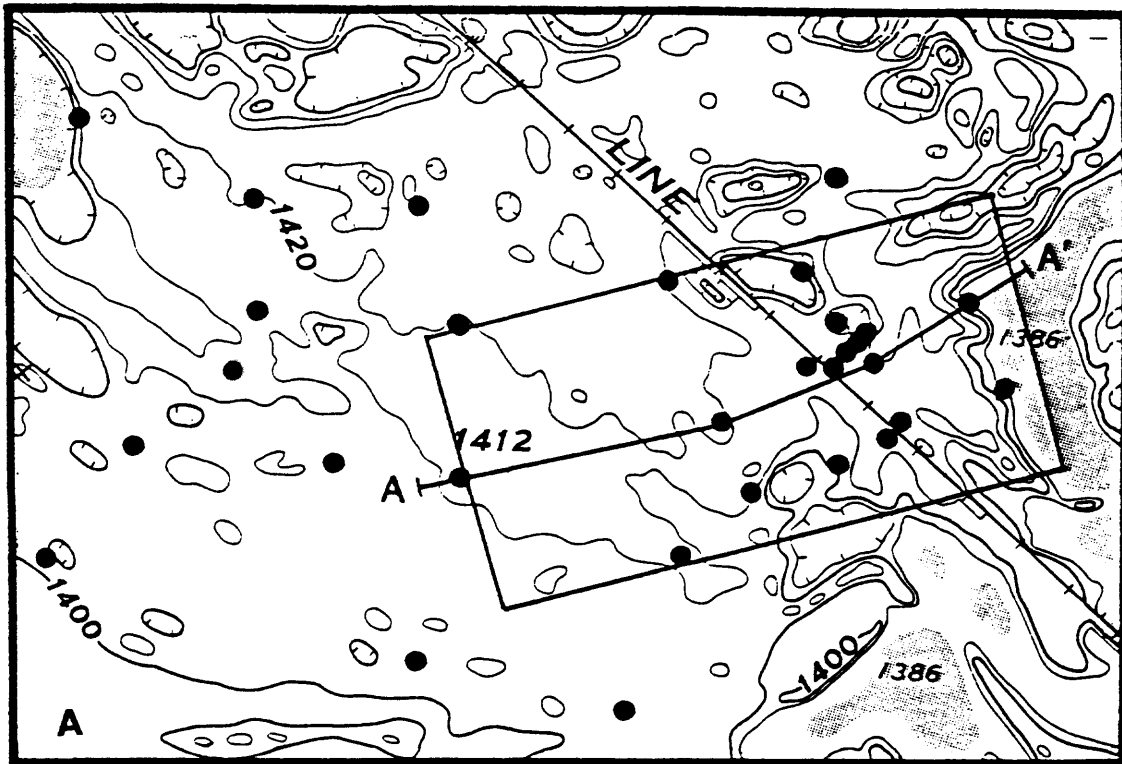


Figure C-6.—Areal view of: A. three-dimensional model area, location of section A-A', and well locations, B. two-dimensional vertical model grid.

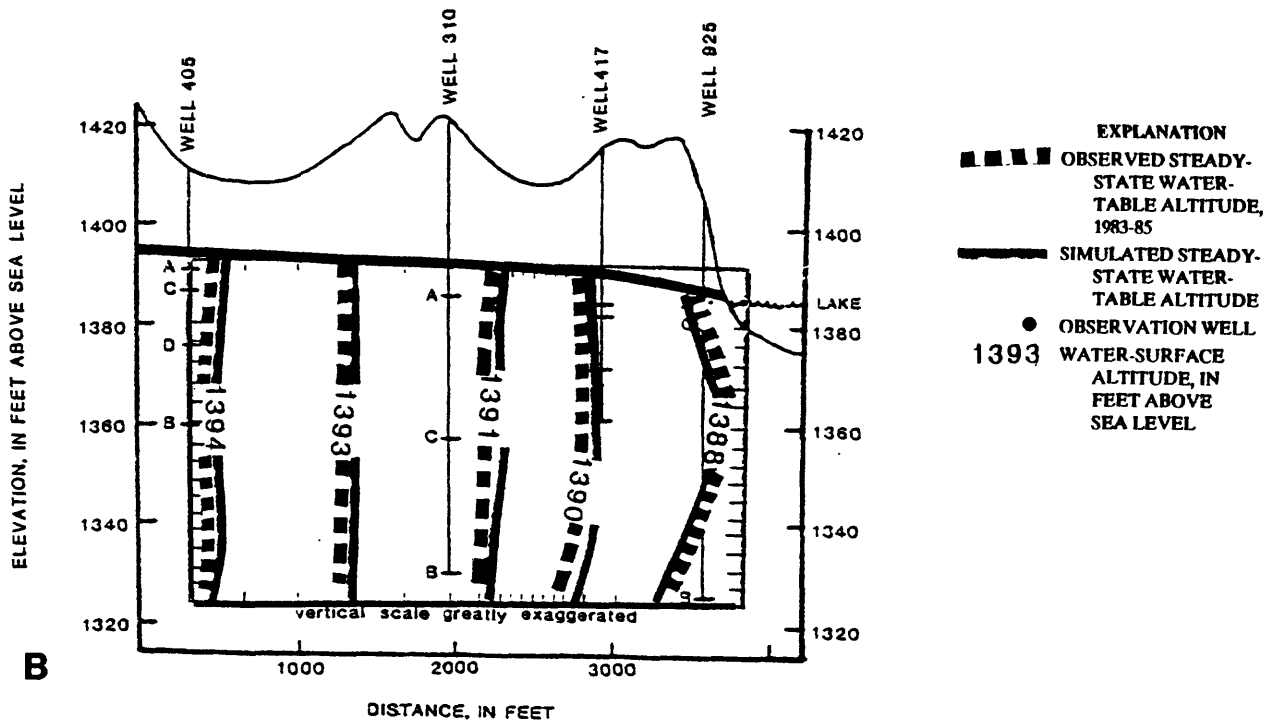
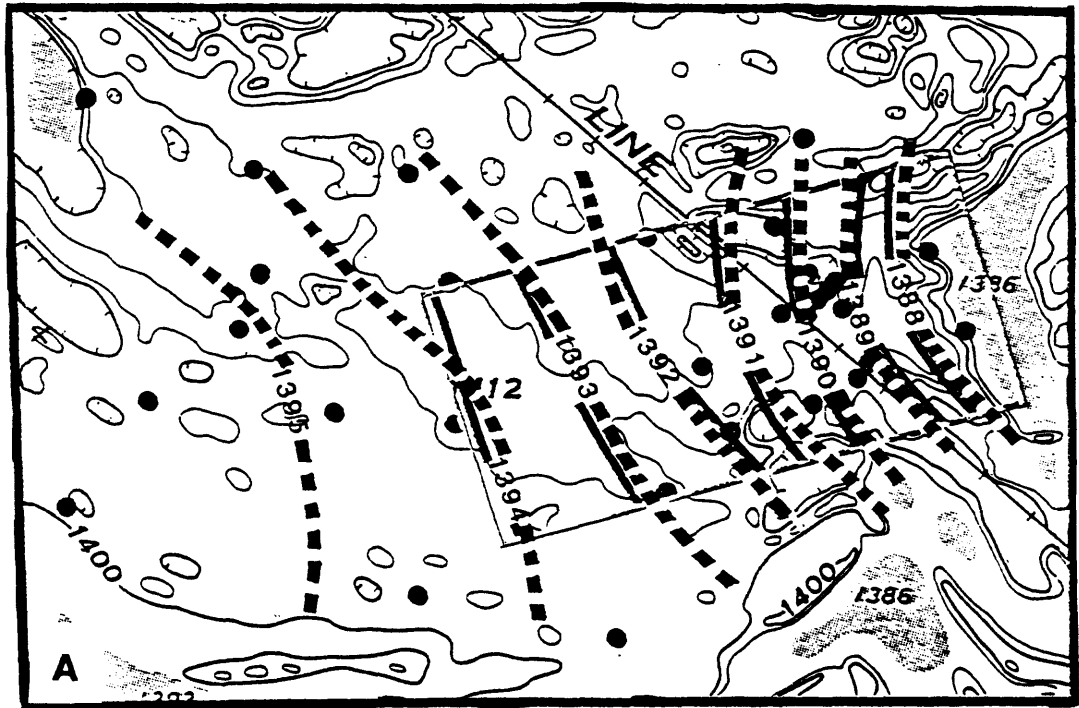
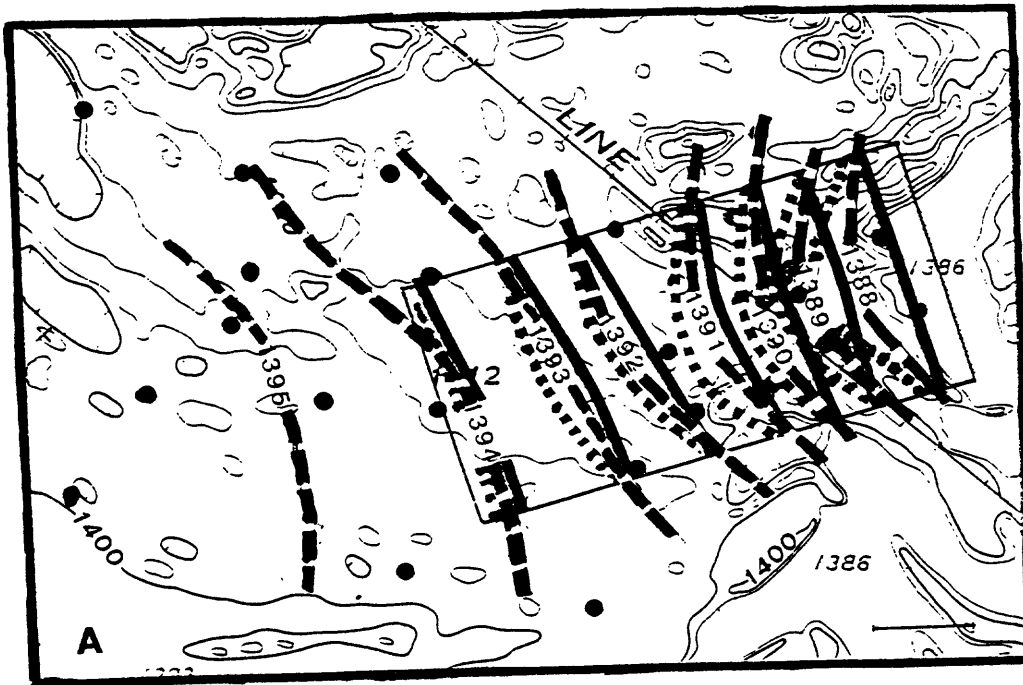


Figure C-7. — Comparison of observed and simulated steady-state water levels for 1983–85 in: A. three-dimensional flow model, and B. two-dimensional vertical-section model.



- EXPLANATION**
- OBSERVATION WELL
 - - - OBSERVED STEADY-STATE WATER-TABLE ALTITUDE, 1983-85
 - SIMULATED LINE OF EQUAL WATER TABLE ALTITUDE RESULTING FROM 1.0-FOOT INCREASE IN UNNAMED LAKE LEVEL
 - SIMULATED LINE OF EQUAL WATER-TABLE ALTITUDE RESULTING FROM 1.0-FOOT DECREASE IN UNNAMED LAKE LEVEL

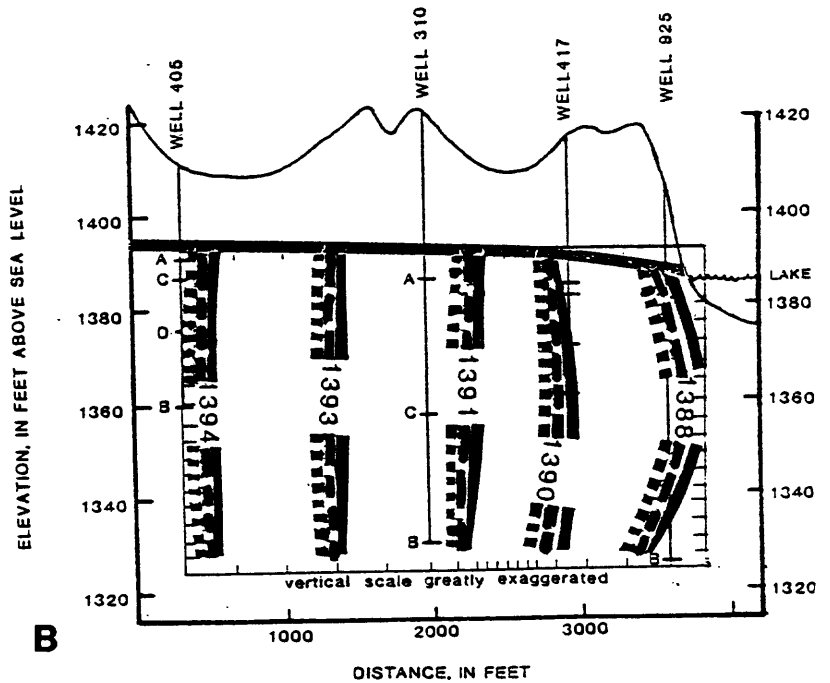
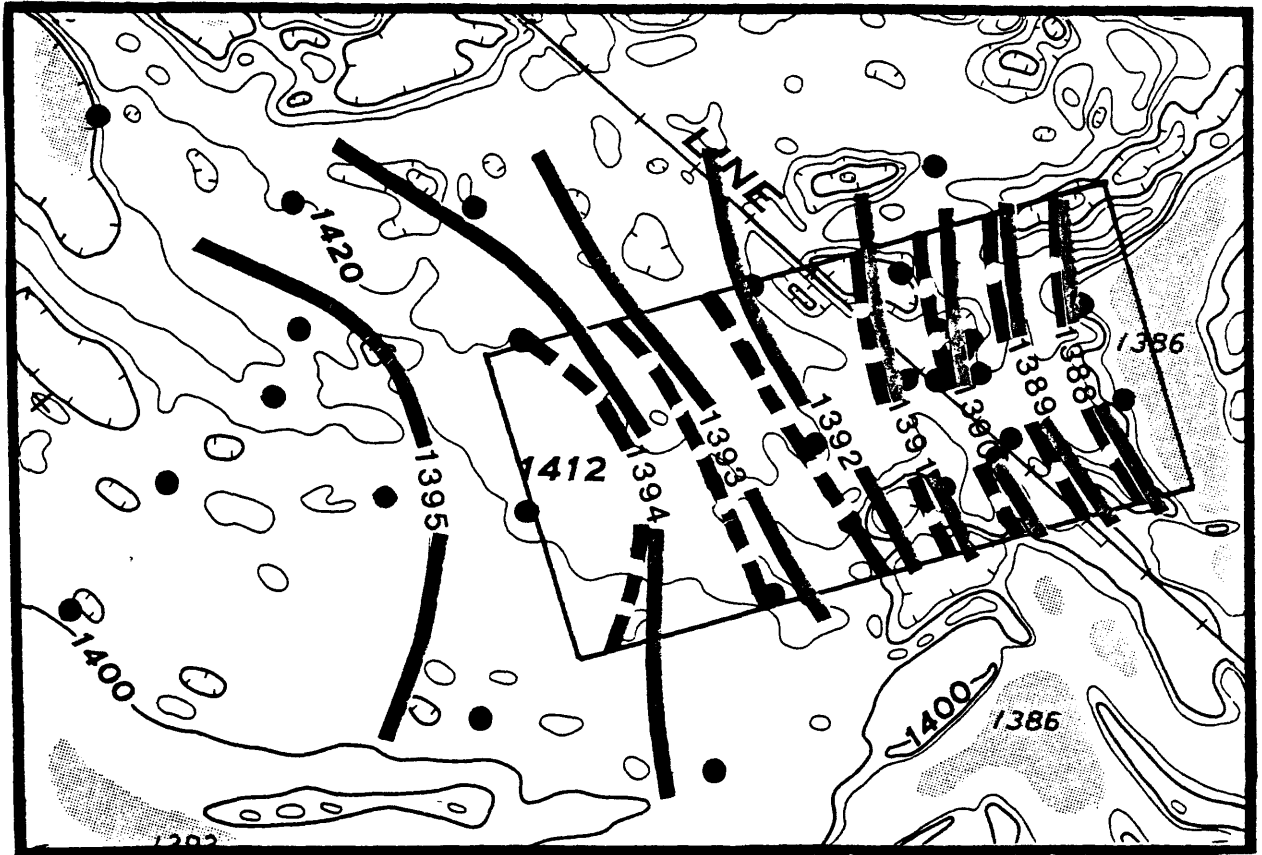


Figure C-8.— Comparison of observed water levels resulting from applied 1.0-foot increase and decrease in level of unnamed lake with simulated levels in: A. three-dimensional model, and B. two-dimensional vertical-section model.

that a low concentration of contaminant has probably reached the unnamed lake. The two-dimensional cross-section model suggests that contaminants have the potential to reach a depth of 4 feet below the water table. Although both simulations assume the viscosity and density of the oil

residuals to be equal to those of the ambient ground water and do not simulate the decay or chemical/biological changes in the oil residuals, the models indicate that the predicted ground-water velocities are reasonable for the simulation area.



EXPLANATION

- OBSERVATION WELL
- WATER-TABLE ALTITUDES
AT END OF 90-DAY
SPRING RECHARGE PERIOD,
1984, IN FEET--Contour interval
1 foot. Datum is sea level
- OBSERVED LEVEL
- - - - - SIMULATED LEVEL

Figure C-9. — Comparison of observed with simulated water-table levels at end of 90-day spring recharge period, 1984.

INORGANIC GEOCHEMISTRY OF GROUND WATER AND AQUIFER MATRIX: FIRST-YEAR RESULTS

By Donald I. Siegel¹, Philip C. Bennett¹, Mary Jo Baedecker², Marian P. Berndt¹,
and David A. Franzi³

The effects of oil contamination on the inorganic geochemistry of the surficial aquifer at Bemidji, Minn. (fig. C-1), were investigated in studies of both the aqueous and solid phases. Ninety-six samples of ground water were collected from October 1984 to September 1985 and analyzed for dissolved Ca, Mg, Na, K, Si, Fe, Mn, Al, and Sr. Some samples were analyzed for unstable field properties (pH, alkalinity, S²⁻, NH₄, Eh, and dissolved oxygen), anions (Cl and SO₄), trace metals (Ni, V, Cr, and Zn) and stable isotopes of carbon and water, depending on the objective of the particular sampling. Samples from an aquifer core collected upgradient of the oil-spill site were analyzed by petrographic, x-ray diffraction, plasma-emission spectrometric, and scanning electron-microscopic/x-ray-energy spectroscopic (SEM/XES) methods. SEM/XES studies were made on fine sand-sized fractions of the surficial materials in the contaminated zone.

Initial ground-water sampling was done in 1984 from piezometer nests installed along an east-west transect from the contamination zone. These analyses showed that oil degradation has significantly enhanced the dissolution of aquifer minerals. Concentrations of Ca, Mg, Sr, and HCO₃ are 2 to 3 times greater in the contaminated area than in background wells. Concentrations decrease with depth, showing that dissolution is greatest at or just below the water table. For example, Ca concentrations at a piezometer nest about 30 feet downgradient of the oil body decreased from 3.4 mmol/L at the water table to a background concentration of 1.4 mmol/L 10 feet deeper in an October 1984 sampling.

The areal distributions of major cations, Mn, Si, field pH, and alkalinity, as measured at several water-table wells in 1985, form distinct narrow plumes that trend northeastward from the spill site. Figure C-10, for example, shows distribu-

tions of pH, Si, and Fe and Mn. The plumes coincide approximately with a plume of elevated concentrations of dissolved organic carbon (Hult and Grabbe, chapter C, this report), indicating that the extent of organic contamination can be identified by increased concentrations of inorganic constituents dissolved from the aquifer matrix. Increased mass transfer of solutes from matrix to water probably is caused by elevated partial pressures of CO₂ and concentrations of organic acids generated from the degrading oil.

Preliminary background data on the chemical composition of the silt- and clay-size fractions (table C-1) is consistent with the mineralogical composition determined by petrography, XES, and x-ray diffractometry. Major minerals of the aquifer are quartz, plagioclase and microcline, and dolomite, which form about 80, 11, and 7 percent of the drift, respectively. The clay minerals in the drift are montmorillonite and chlorite + kaolinite.

Table C-1.—*Metal oxide distribution in uncontaminated drift near the water table, as percentage of bulk sediment*

[Sample B 310-9, less than 200-mm mesh]

Oxide	Percent
SiO ₂	57.20
Al ₂ O ₃	10.70
Fe ₂ O ₃	3.25
CaO	7.27
MgO	2.13
Na ₂ O	2.68
K ₂ O	1.95
MnO	.06
Sr	447 (ppm)

¹Syracuse University, Syracuse, N.Y.

²U.S. Geological Survey, Reston, Va.

³State University New York, Plattsburg, N.Y.

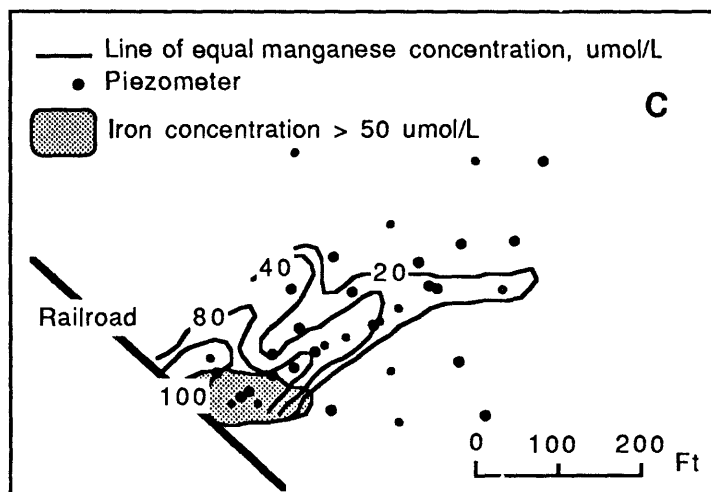
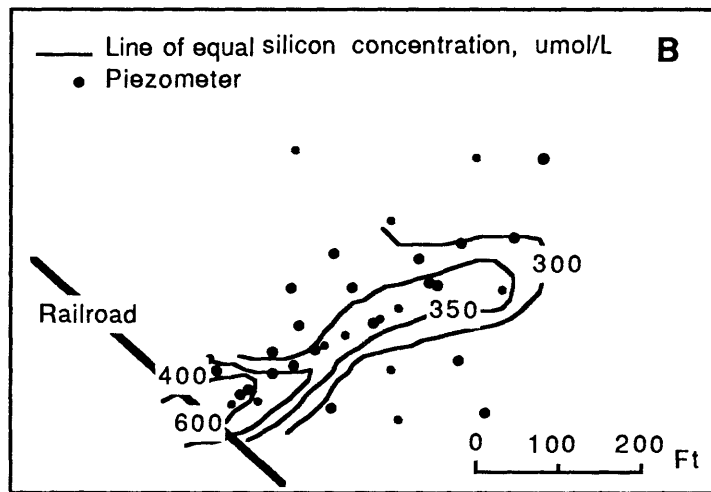
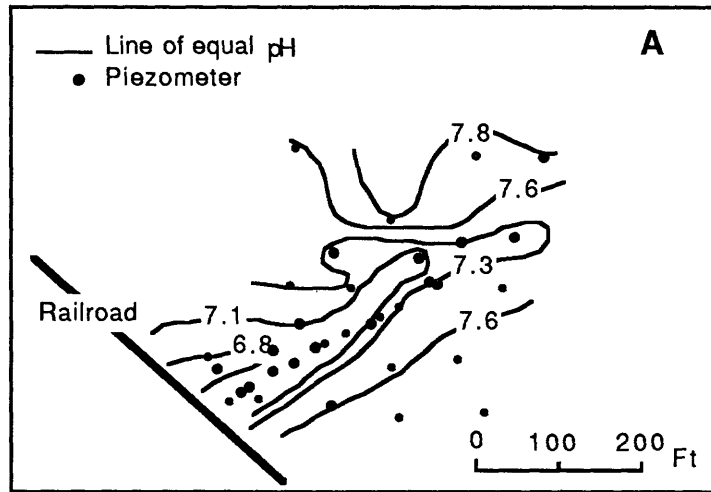


Figure C-10. — Areal distributions of selected ground-water constituents at water table downgradient of crude-oil spill, August 1985: A. pH, B. silicon, and C. iron and manganese.

SiO₂, Al₂O₃, and CaO constitute about 70 percent of the bulk sediment. Fe₂O₃ content of the drift is hundreds of times greater than that of MnO, but, the areal distribution of Fe in ground water shows no distinct plume, whereas Mn forms a plume with concentrations hundreds of times greater than concentrations of Fe (fig. C-10c). The crude oil contains no detectable Mn; therefore, the degradation of the oil is preferentially enhancing solubilization and mobility of Mn relative to Fe and other trace metals. No plumes of V, Cr, or Ni have been recognized in the contaminated zone.

SEM and XES studies of the fine, sand-sized part of the drift suggest three distinct geochemical zones at the site. Downgradient from the major part of the contaminant plume, the surfaces of mineral grains show little or no evidence of active dissolution (fig. C-11). Within the contaminant plume area, however, coatings of aluminum and iron sesquioxides are found on quartz along with extensive dissolution pits on feldspar, carbonate, and quartz surfaces (fig. C-11). Quartz precipitates also are found in this zone, suggesting complex local controls on chemical equilibrium.

Quartz is relatively insoluble at a pH between 4 and 8. Therefore, the dissolution pits on quartz surfaces suggest that organic acids or microbes may be enhancing the dissolution process in the contaminated zone. In the area directly under the oil spill, minor precipitates were identified, but evidence for dissolution was identified only on feldspar grains.

Microbial degradation of the oil at the water table has created a reducing geochemical environment. Dissolved oxygen and Eh decrease from

about 9.0 mg/L and 250 mv (millivolts) in the uncontaminated region to nondetectable dissolved oxygen and -80 mv, respectively, in the major part of the plume. Concentrations of sulfate in the contaminated zone near the water table are generally less than 100 mmol/L but exceed 100 mmol/L in background wells and wells completed deeper in the aquifer. Although sulfide was not detected in the contaminated water, the decrease in sulfate concentrations was probably caused by reduction.

Preliminary data on the stable isotopes of carbon in inorganic dissolved carbonate (mostly HCO₂) suggest that degradation of the hydrocarbons may be quite complicated. $\delta^{13}\text{C}$ of dissolved inorganic carbon in the uncontaminated part of the aquifer ranges from -15 to -12 ‰, typical of $\delta^{13}\text{C}$ of HCO₃ resulting from the dissolution of carbonate minerals ($\delta^{13}\text{C}$ about 0 ‰) by soil carbon dioxide ($\delta^{13}\text{C}$ about -25 ‰). However, the $\delta^{13}\text{C}$ of HCO₃ in the contaminated plume ranges from -21 to -19 ‰. This is significantly lighter than expected because the $\delta^{13}\text{C}$ of the crude oil should be similar to that of the natural soil organic material – about -25 ‰. Although the cause of the light isotopic content is still unknown, preliminary mass-balance calculations on carbon suggest that the depleted ¹³C probably is related to aerobic oxidation of the oil. Future studies will focus on (1) vertical chemical changes at near the water table along the center of the plumes, (2) sources and sinks for major and minor metals in the different hypothesized geochemical environments, (3) sources of acidity in the water, and (4) rates of dissolution and precipitation of major solid phases.



Figure C-11.—Scanning electron photomicrographs of feldspar: A. Unetched sample from uncontaminated zone; B. Etched sample from contaminated zone.

DISTRIBUTION OF GASES AND HYDROCARBON VAPORS IN THE UNSATURATED ZONE

By Marc F. Hult¹ and Rolland R. Grabbe²

A spill of crude oil in August 1979 near Bemidji, Minn. (fig C-1), contaminated a glacial-outwash aquifer. Crude oil is present as (1) a separate fluid phase floating on the water table, (2) constituents dissolved in ground water, and (3) vapors in the unsaturated zone. This paper describes initial research to determine the distribution and geochemistry of the hydrocarbon vapors and inorganic gases in the unsaturated zone.

The general configuration of the plume of contaminated ground water is shown by the distribution of dissolved organic carbon (DOC) in water samples bailed from wells completed in about the upper meter of the saturated zone (fig. C-12a). The DOC data were collected in conjunction with aqueous-phase research conducted by Siegel and others (chapter C, this report) and by Eganhouse and others (chapter C, this report). The contaminant distribution is reflected in the distribution of methane in about the lower meter of the unsaturated zone, as shown in figure C-12b. Portable instruments for analysis of methane and other hydrocarbon gases are widely available, and the data show that such measurements can be used to delineate plume geometry rapidly if suitable sampling points are available.

Field samples were collected during June-July 1984 and September-October 1985. The purpose of the first sampling was to qualitatively delineate the plume of contaminated ground water by measuring the concentration of hydrocarbon vapors in the unsaturated zone. The second sampling provided quantitative data on individual organic compounds, oxygen, and carbon dioxide needed to determine chemical and microbial processes that affect contaminant movement and fate.

Samples analyzed during the first sampling period were obtained from the headspace of soil samples collected at a depth of 60 cm, from 5-cm-

diameter wells with screens 1.5 m long in which the water level was at the approximate midpoint of the screen, and from a 2.9-cm O.D. probe constructed of a 30-cm long, stainless-steel screen welded to AW specification drilling rod. The probe was driven into the ground using a 64-kg hammer, and samples were collected at 1.5-m intervals from land surface to the water table. Gas was withdrawn from the wells and probe through a 6.4-mm-OD stainless-steel tubing by a peristaltic pump. A packer was inflated 30 cm above the top of the screen to minimize the "dead" volume during sampling. After 5 L of gas had been pumped, a sample was collected and stored in a 10-mL₃ gas-tight syringe with a glass barrel and Teflon³ plunger and tip, and (or) a 1-L blown-glass bulb fitted with Teflon stopcocks at each end and a septum for subsample removal. Samples were brought to the laboratory and analyzed qualitatively for C1-C7 hydrocarbons by gas chromatography with flame ionization detection (FID) within 24 hours after collection. A gas-tight syringe was used to inject 50 or 500 μ L of sample into a 60-mx0.75-mm ID glass capillary column coated with a 1- μ m-thick Supelco SPB-1 stationary phase maintained at 30 °C. Inconsistent results were obtained if samples were stored for more than a few hours.

During the second sampling period, samples were collected both from wells and through 10-cm-long and 6.4 mm-O.D. stainless-steel screens attached to 3.2-mm I.D. stainless-steel tubing permanently installed 0.6, 1.5, 2.4 and 4 m below land surface and 0.6, 2.1, and 3.7 m above the top of the capillary fringe. The sampling tubes were placed in 10-cm-diameter auger holes, and the holes were backfilled with native sand and bentonite. The tubes were clamped to 19-mm I.D. PVC pipe to facilitate installation, to provide access for

¹U.S. Geological Survey, St. Paul, Minnesota

²U.S. Environmental Protection Agency, Environmental Services Division, Lakewood, Colorado (formerly U.S. Geological Survey, Lakewood, Colorado)

³The use of brand/company/trade names is for identification purposes only and does not constitute endorsement by the U.S. Geological Survey.

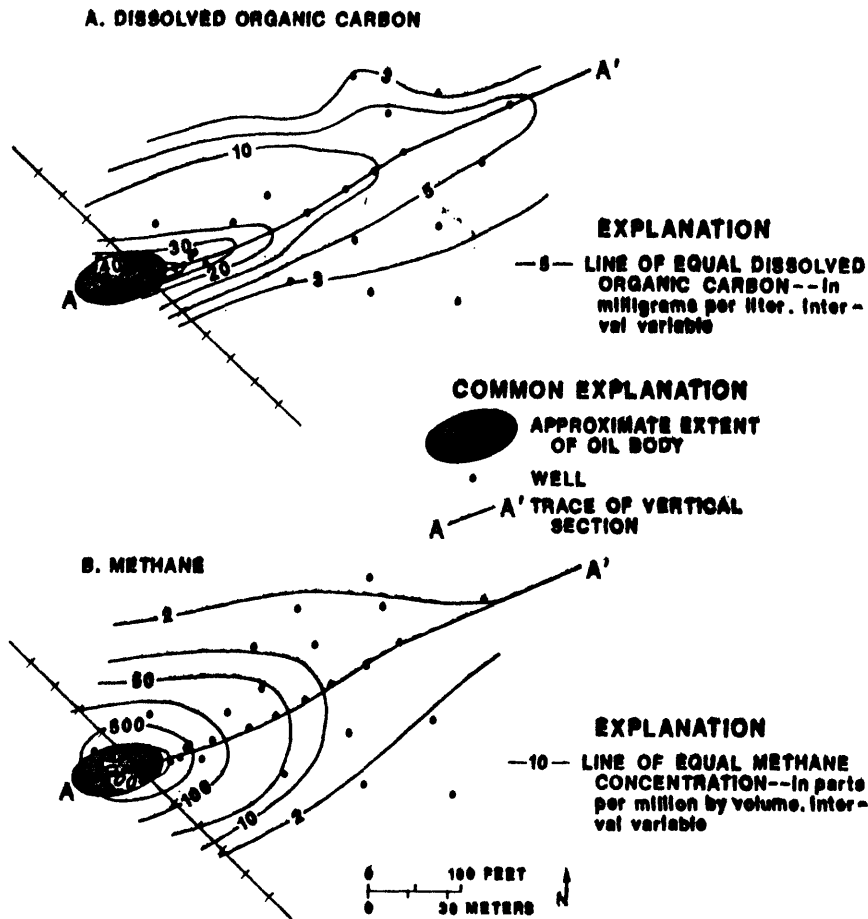


Figure C-12. Areal distribution of: A. organic carbon in upper meter of saturated zone, and B. methane in lower meter of saturated zone.

ambient-temperature measurements, and to permit flushing of the hole with high-purity nitrogen. Analyses were made in a mobile laboratory at the site. Samples were collected in unlubricated glass syringes and immediately analyzed quantitatively for individual hydrocarbons, oxygen, carbon dioxide, and nitrogen. A microcomputer was programmed to control the integrator/plotters, chromatographs, and valves, and to record the data and methods. Two sample loops (500 μ L at 60 $^{\circ}$ C) were filled simultaneously, and the samples were injected by valves into a helium carrier stream. Hydrocarbons were analyzed in the same column as before, but the oven temperature was programmed for 5 minutes at 35 $^{\circ}$ C, then increasing 15 $^{\circ}$ C per minute to 115 $^{\circ}$ C and held for 2 minutes. After passing through the column, the sample was

split; half of the effluent was analyzed with a FID, the other half with a photo-ionization detector (PID). Individual hydrocarbons were identified by matching retention times with standards, by determining analyzing FID-to-PID response ratios, and by comparing prior analyses of the gases in the headspace of a representative oil sample using gas chromatography with mass spectrometry. Chromatographic conditions selected for routine analysis did not separate methane from ethane and other C₂ hydrocarbons. To determine the contribution of C₂ compounds to the C₁ + C₂ peak, selected samples were analyzed with an initial column temperature of 5 $^{\circ}$ C at which baseline separation of methane and ethane is almost obtained. Virtually all of the C₁ + C₂ peak was methane.

Quantitation of C₁-C₇ normal alkanes and C₂-C₅ branched alkanes was based on commercial gas standards obtained from Scott Specialty Gases. Quantitation of other compounds was based on reference gases prepared from liquid standards obtained from Polyscience Corporation. Because the FID response factors for normal alkanes are nearly identical, the concentration of total volatile hydrocarbons, in g/m³, was calculated from the response factor for pentane because both the gas and liquid standards were those of pentane. The concentration of methane was calculated on a volumetric basis (parts per million by volume) to be consistent with the data on the inorganic gases that also are reported on a volumetric basis (as partial pressures). The ratio of methane to total volatile hydrocarbons was determined by the ratio of peak areas.

Inorganic gases were analyzed with a thermal conductivity detector (TCD) and separate 2-m x 2.1-mm-ID stainless-steel columns packed with 60/80-mesh Chromosorb 102 and molecular sieve

5A held at 50 °C. First, carbon dioxide was separated from the sample with the Chromosorb 102 column. Then, by switching columns, nitrogen and oxygen were separated by the molecular sieve column.

Analysis of a field sample required less than 15 minutes. Chromatograms of a typical sample close to the oil body are shown in figure C-13. The upper chromatogram is the output of the FID. The first three peaks are from samples manually injected by syringe into the carrier gas downstream from the column. The area beneath each of these peaks is a measure of the total hydrocarbons in the sample and is in close agreement with the sum of the individual peaks. The subsequent peaks represent individual hydrocarbons separated by the analytical column for identification and quantitation.

The lower chromatogram shows the output of the TCD (left) and the PID (right). Because one plotter/integrator was shared by these two detec-

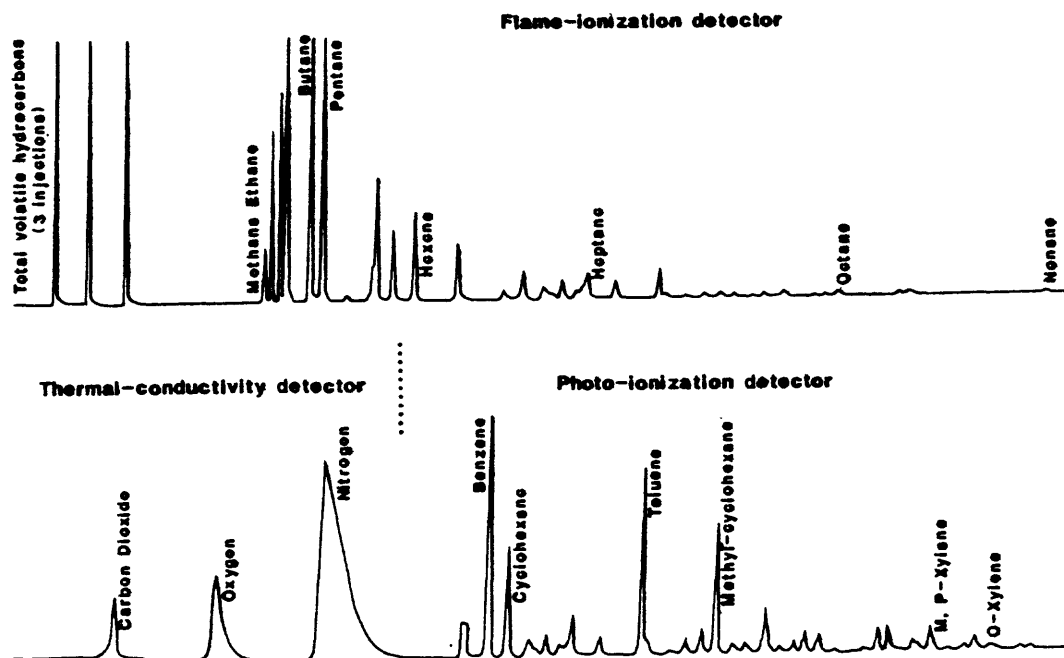


Figure C-13. Examples of chromatograms used to detect presence of organic compounds, carbon dioxide, oxygen, and nitrogen in gas samples from lower meter of the saturated zone.

tors, chromatographic conditions were optimized for highest sensitivity to carbon dioxide, consistent with the need to complete analyses on the TCD before arrival of the first compound of interest to the PID. After complete emergence of the nitrogen peak, the input to the integrator was switched from the TCD to the PID. The PID is 10 to 1,000 times more sensitive to cyclic compounds than to aliphatic compounds, and the ratio of the FID response to the PID response was used to identify cyclic compounds. For example, benzene is the most prominent peak in the PID chromatogram but is a minor peak on the FID chromatogram.

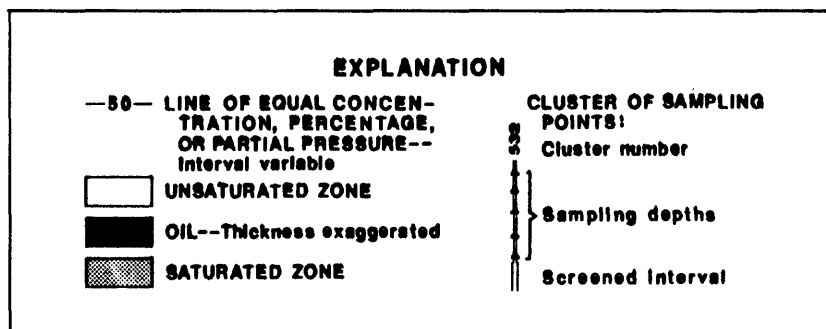
A major result of the first sampling was the indication that reliance on the total volatile hydrocarbon concentrations measured in near-surface samples for plume delineation may be inappropriate because concentrations change greatly with depth. Figure C-14, compiled from quantitative data obtained during the second sampling, illustrates this conclusion. Sampling point 533G, for example, shows a 10,000-fold increase in the concentration of total volatile hydrocarbons between land surface and a depth of about 15 feet (approximately half the thickness of the unsaturated zone). Below that depth, the concentration increases by only about 50 percent, as indicated by the measured concentrations of 200, 300, 310, and 310 g/m³ at the lower four sampling points.

The concentration of methane (fig. C-14) reaches a maximum near the main oil body. The percentage of total volatile hydrocarbons consisting of methane of the oil body but is at a minimum

above the oil body on the downgradient side. The methane is produced from the biological degradation of crude oil derivatives by microorganisms under anaerobic conditions in the unsaturated and(or) saturated zone. Although the petroleum may have originally contained some dissolved methane, no methane was found in the headspace of eight oil samples bailed from wells. Laboratory-aging experiments on the samples showed that about 15 percent of the petroleum evaporates within 24 hours under laboratory conditions. The major loss is in C₃-C₅ hydrocarbons.

The distribution of oxygen and carbon dioxide (fig. C-14) indicates that the hydrocarbons are being oxidized to carbon dioxide. The severe depletion of oxygen above the oil body is reflected by an increase in the partial pressure of carbon dioxide. The total oxygen calculated from the CO₂ and O₂ partial pressures decreases with increasing partial pressure of CO₂, presumably because the microbial processes produce both CO₂ and water.

Results of this study show that large quantities of volatile hydrocarbons move through the unsaturated zone by diffusion and are oxidized to CO₂ and (or) converted to methane. Alkanes predominate in the unsaturated zone, whereas aromatic compounds dominate the volatile fraction dissolved in the ground water (Eganhouse and others, chapter C, this report). The results provide data needed for quantitative simulations of the mass transport through the unsaturated zone and the upper part of the saturated zone.



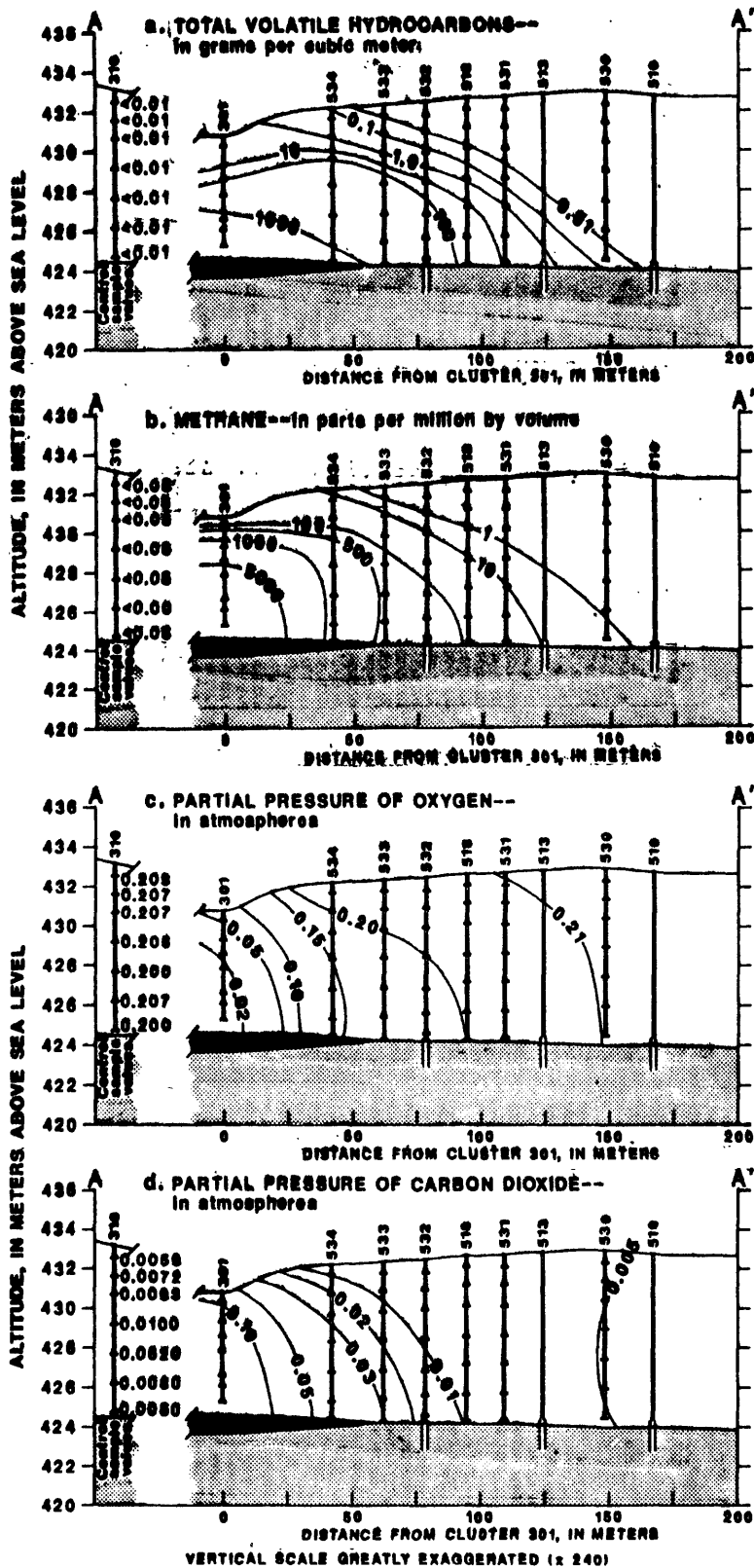


Figure C-14. Vertical sections showing distribution of selected constituents within the unsaturated zone.

COMPOSITION AND ALTERATION OF HYDROCARBONS IN GROUND WATER

By Robert P. Eganhouse¹, Mary Jo Baedecker², Curtis Phinney¹, and Jessica Hopple²

The abundance and movement of organic compounds in ground water at the Bemidji, Minn., oil spill (fig. C-1) were investigated as part of a larger study of the fate of crude-oil constituents in the subsurface. Ground-water samples were collected with a point-source bailer from 11 wells on a transect originating at the highly contaminated region (characterized by a discrete oil phase at the water table) and terminating 240 m downgradient. The samples were analyzed by direct volatile organic analysis (VOA) with a purge and trap device interfaced with a high-resolution gas chromatograph (HRGC) and a gas chromatograph/mass spectrometer (GC/MS). In addition, separate aliquots were examined for nonvolatile constituents and components of intermediate volatility with a hexane microextraction procedure followed by HRGC and GC/MS analysis. Compounds having between 5 and 35 carbon atoms per molecule (C₅ through C₃₅) were detected by these procedures. The results of this work provide direct evidence that the plume extends at least 192 m from the spill site and that biodegradation of dissolved constituents occurs close to the source.

The concentration of total volatiles in the ground water ranged from 10 mg/L to nondetectable levels with an order of magnitude decrease within about 130 m of the highly contaminated zone. The volatiles are dominated by aromatic

hydrocarbons; benzene forms 55 to 95 percent of the total. Other components include, in order of more abundant to least abundant: C₁-C₅ alkylated benzenes; alkanes (C₄-C₇); cycloalkanes (C₀-C₃-alkylated cyclohexanes and cyclopentanes); and C₀-C₂ alkylated indanes and C₀-C₃ alkylated tetrahydrothiophenes. Normal alkanes (C₈ to C₃₃) are found only in water that is in contact with oil-contaminated sediment.

Changes in the composition and concentration of individual hydrocarbons downgradient from the spill reflect the influence of processes such as dispersion, volatilization, adsorption, and biodegradation. The alkanes, cycloalkanes, and most of the alkylated benzenes decrease in abundance more rapidly than benzene with distance downgradient. The initial rapid decrease is probably a result of losses due to volatilization and microbial degradation. Naphthalene and C₃-, C₄-alkylated benzenes tentatively identified as having tertiary or quaternary benzylic carbons are removed much less rapidly and exhibit nearly conservative behavior within 60 m of the contaminated zone. Because other C₃-, C₄-alkylated benzenes decrease rapidly over the same distance, biological, not physico-chemical, removal processes are implicated. These molecules that are resistant to biodegradation may be useful as organic tracers of the plume.

¹Environmental Sciences Program, University of Massachusetts, Boston, Mass.

²U.S. Geological Survey, Reston, Va.

MASS TRANSFER AT THE ALKANE WATER INTERFACE IN LABORATORY COLUMNS OF POROUS MEDIA

By Hans-Olaf Pfannkuch¹, Susan M. Nourse¹, and Marc F. Hult²

Preliminary results of laboratory column experiments simulating mass transfer of liquid hydrocarbons to ground water indicate that the transfer coefficient may be velocity dependent at typical ground-water flow velocities. The transfer coefficient and the coefficient's dependence is strongly controlled by the aqueous solubility of the hydrocarbon. Measured coefficients are lower than values reported in the literature for dispersed, fixed-bed reactors.

Objectives and Hypotheses

The initial objective of this study is to explore systematically the relationship between mass-transfer rates, aqueous solubility, and ground-water flow velocities for a series of pure, homologous hydrocarbons. From literature research, it was postulated that, at high flow rates or large Peclet numbers, the rate of mass transfer ("dissolution") depends on the velocity at which water moves past the hydrocarbon water interface, but that ground-water velocities and Peclet numbers are typically low enough that the mass transfer is unaffected by flow rate (Pfannkuch, 1984). The literature data are sparse, and the experiments reported were conducted with multi-component fluids; thus additional phenomena might have complicated the transfer process. The use of pure compounds eliminates interferences and interactions that occur with multicomponent fluids such as crude oil and gasoline. No experiments with single compounds or mixtures of pure compounds have been reported in the literature to date.

Future research is to include experiments with representative substances such as field samples from the Bemidji site when appropriate experimental and analytical procedures have been developed. Mixtures of pure compounds and field samples will be studied for differential leaching and aging effects.

Experimental Apparatus and Methods

A diagram of the laboratory column is shown in figure C-15. The column was packed with Ottawa sand of uniform grain size (0.5 mm mean grain diameter). A valve and relief-hole system was used to establish an initially horizontal water table and to introduce the test compounds. The inlet and outlet ends were constructed to prevent horizontal fluid movement in the upper half of the column section to retain the supernatant hydrocarbon while permitting water to flow through the lower half.

The upper part of the horizontal column was filled with pentane or heptane to simulate a spill on the water table. The interface between the water and the hydrocarbon fluid was always slightly jagged or irregular owing to capillary effects. Distilled water was circulated through the lower part with a positive-displacement pump or by maintaining a positive head with an elevated reservoir. Water samples were collected at the outlet and analyzed by gas chromatography with flame-ionization detection. Measurements were made at each flow rate until conditions stabilized and consistent results obtained. Early attempts to concentrate the samples by liquid extraction methods yielded inconsistent results because of the high volatility of the substances used. Measurements reported herein were made by direct injection of the aqueous sample into the chromatograph without extraction.

Data and Results

One way to present the mass-transfer rate is to plot the Sherwood number against the Peclet number, as illustrated in figure C-16. The Peclet number is a dimensionless velocity:

$$Pe = \frac{(vd)}{D}$$

¹ Department of Geology and Geophysics, University of Minnesota, Minneapolis, Minn.

² U.S. Geological Survey, WRD, St. Paul, Minn.

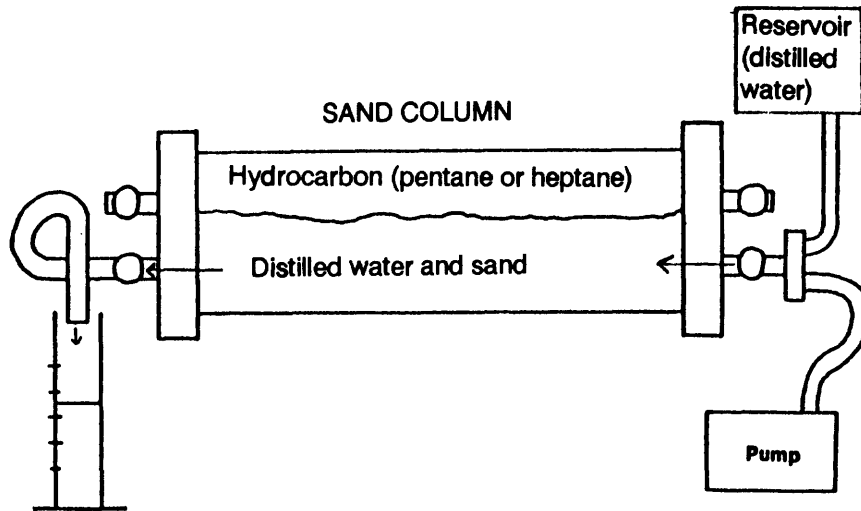


Figure C-15. — Laboratory column setup. Column is packed with aquifer sand of uniform grain size (0.5 mm mean diameter). Distilled water flows through lower layer; horizontal movement is prevented in supernatant pentane or heptane layer.

where

v = the average flow velocity of the water in the column, [L/T]

d = a characteristic length, such as the diameter of the grains that constitute the porous medium, [L],

D = the coefficient of molecular diffusion, [L²/T].

The Sherwood number (Linton and Sutherland, 1960) is a dimensionless mass-transfer rate:

$$Sh = \frac{(Ed)}{[(C_s - C_e)D]}$$

where

E = a mass-transfer coefficient that relates solute production, in mass per unit time, to unit area of contact, [M/TL²]

C_s = the equilibrium concentration of the hydrocarbon in water, [M/L³]

C_e = the concentration of hydrocarbon in the effluent, [M/L³].

The mass-transfer coefficient between the floating hydrocarbon and the water flowing beneath was calculated from:

$$E = \frac{(C_e Q)}{A}$$

where

C_e = the effluent concentration when stabilized, [M/L³]

A = the area of the interface between the hydrocarbon and the water, [L²]

Q = the flow rate through the column, [L³/T].

Results are listed in table C-2 and plotted in figure C-16.

Results from the two hydrocarbons tested indicate a strong velocity dependence of the mass transfer process and also an apparent dependence on aqueous solubility. The more soluble pentane has mass-transfer coefficients about an order of magnitude greater than those of the less soluble heptane. This is of the same order of magnitude as the solubility ratio between pentane and heptane (about 13:1). Even though the flow velocities were extended into the low Peclet number regime characteristic of ground-water-flow velocities, the velocity-independent regime was not reached. In a set of preliminary experiments using heptane, water-table fluctuations were simulated by lowering and raising the interface by 2 cm. The resulting transfer coefficients for the disturbed system were about an order of magnitude greater than those for the undisturbed system.

Figure C-16. — Mass-transfer of pure liquid hydrocarbons to formation water in relation to Sherwood and Peclet number

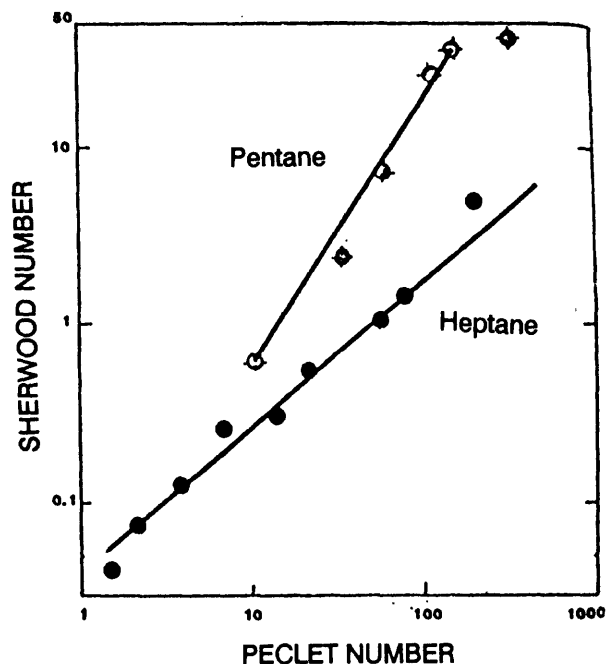


Table C-2. — Peclet and Sherwood numbers and mass-transfer coefficients obtained in laboratory column experiments with heptane or pentane over aquifer sand in distilled water

Flow velocity, v (10^{-6} m/s)	Mass-transfer coefficient, E (10^{-6} mg/m ² s)	Peclet ¹ number	Sherwood ¹ number
HEPTANE			
6.1	0.395	1.5	0.042
8.3	.649	2.1	.073
15.7	1.145	3.9	.126
27.0	2.296	6.7	.266
55.7	2.955	13.9	.302
90.5	5.291	22.6	.551
226.2	10.775	57.4	1.076
300.7	14.256	77.4	1.419
771.7	47.503	193.0	5.009
PENTANE			
40.9	45.0	10.2	0.633
87.0	148.0	21.7	2.543
131.1	121.0	32.8	2.4
225.6	335.0	56.4	7.76
449.8	758.0	112.4	26.0
596.4	1,000.0	149.1	34.6
1,285.0	1,889.0	321.1	42.7

¹For this set of experiments, the grain diameter (d) was $0.5 \cdot 10^{-3}$ m, and the molecular diffusion coefficient (D) was $2.0 \cdot 10^{-9}$ m²/s.

²No explanation is apparent for this anomalous result.

DISCUSSION

Results of the work are plotted with data from the literature in figure C-19. Experiments from Zilliox and others (1973) and Hoffman (as reported by Zilliox, 1970) had been carried out with fuel oils and gas-oil, respectively. This plot differs from a similar one in Pfannkuch (1984) which is in error by a factor of 10^{-3} . Correction of the data does not change the relative values nor the shape of the curves but does indicate extremely low transfer coefficients. Interpretation of the literature data required use of several assumptions because some information about experimental conditions was lacking. This could explain the low absolute values.

In addition to the experimental and literature curves, figure C-17 also contains a curve for mass-transfer from a sphere in an infinite medium (Bowman and others, 1961) which tends to produce a lower and constant value of $Sh = 2$ when Pe is less than 1. The velocity-dependent and the velocity-independent regions can be seen as the two straight line segments of the curve as indicated on figure C-17. Also shown is a curve for mass-transfer in packed beds, which lies above the Bowman curve (Ranz, 1952), but generally has the same aspect as the curve for a single sphere. Transfer coefficients for the packed beds are for particles that react with the flowing fluid. With our column, where the hydrocarbon is contained as droplets within a pore, reaction rates would be expected to

be lower, as shown. Moreover, the experimental setup simulated the exchange across an idealized interface between the water table and the capillary-fringe interface. The contact area was small compared to an actual spill, where a large internal surface area may develop owing to migration of the oil. A system consisting of hydrocarbon fully dispersed throughout the column might produce curves more similar to that given by Ranz (fig. C-17).

Additional experiments with other fluids and over a much wider velocity range need to be conducted to determine whether more volatile and soluble hydrocarbons reach the velocity-independent regime at very low Peclet numbers. Peclet numbers calculated from data on ground-water-flow velocities and particle sizes from the Bemidji site range between 0.1 and 10. These experiments indicate this to be within the velocity-dependent regime, suggesting that appropriate modeling of the lens of oil on the water table as the source of dissolved constituents may require a velocity-dependent source term. The preliminary experiments conducted by moving the interface in the column suggest that future simulations will also need to account for changes in source strength owing to water-table fluctuations.

REFERENCES CITED

- Bowman, C.W., Ward, D.M., Johnson, A.I., and Trass, O., 1961, Mass transfer from fluid and solid spheres at low Reynolds numbers: *Canadian Journal of Chemical Engineering*, v. 39, p. 9-13.
- Hoffman, Bernhard, 1970, Dispersion of soluble hydrocarbons in groundwater stream, in *Advances in Water Pollution Research: International Association on Water Pollution Research*, v. 2, p. HA 1-7.
- Linton, M., and Sutherland, K.L., 1960, Transfer from a sphere into a fluid in laminar flow: *Chemical Engineering Science*, v. 12, p. 214-229.
- Pfannkuch, H.O., 1984, Mass exchange processes at the petroleum water interface, Chapter C,

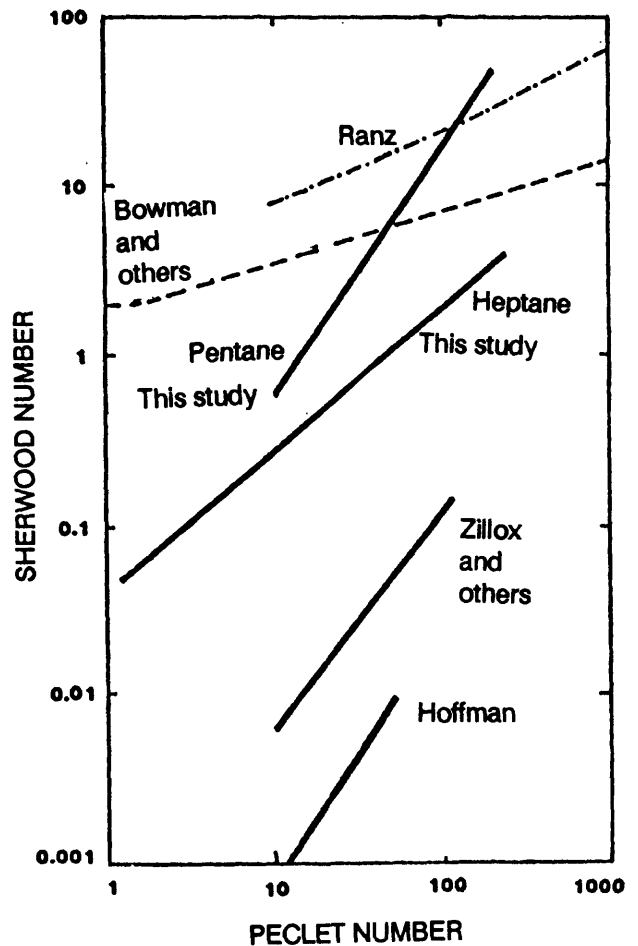


Figure C-17.—Mass-transfer rates for selected hydrocarbons obtained from published values and those obtained in this study in relation to Sherwood and Peclet number.

in Hult, M.F., ed., *Ground-water contamination by crude oil at the Bemidji, Minnesota Research Site, U.S. Geological Survey Toxic Waste—Ground-Water Contamination Study: U.S. Geological Survey Water-Resources Investigations Report 84-4188*, p. 23-48.

Ranz, W.E., 1952, Friction and transfer coefficients for single particles and packed beds: *Chemical Engineering Progress*, v. 48, p. 247-253.

Zillox, Lothaire, Muntzer, Paul, and Menanteau, J.J., 1973, Problème de l'échange entre un produit pétrolier immobile et l'eau en mouvement dans un milieu poreux: *Revue de l'Institut Français du Pétrole*, v. 28, no. 2, p. 185-200.

MICROBIAL DEGRADATION OF CRUDE OIL AND SOME MODEL HYDROCARBONS

By Fu-Hsian Chang¹, Nancy N. Noben¹, Danny Brand¹, and Marc F. Hult²

Research on microbial degradation of crude oil in the shallow subsurface at a spill site near Bemidji, Minn. (fig. C-1), began in 1983 (Hult, 1984; Chang and Ehrlich, 1984). The rate and extent of crude oil and model hydrocarbon biodegradation by the indigenous microbial community was measured in the laboratory at several concentrations of inorganic nutrients, conditions of oxygen availability, incubation temperatures, and incubation time.

Cylinders (10 cm I.D. x 35 cm) in microcosms (60 cm x 30 cm x 42 cm) and wide-mouth jars (450 mL) were filled with sediment and ground water contaminated by crude oil or by uncontaminated sediment and ground water mixed with cyclohexane, hexadecane, naphthalene, phenanthrene, or crude oil obtained from the spill site. The mixtures were inoculated with mixed microbial cultures that had been isolated from the site and were known to degrade crude oil (Chang and Ehrlich, 1984) and (or) were amended with varying amounts of MgSO₄ (10 to 500 mg/L), NH₄NO₃ (2 to 20 mg/L), or KH₂PO₄ + K₂HPO₄ (0.5 to 20 mg/L). The microcosms were incubated at 2 °C, 7 °C, 12 °C, or 17 °C for 3 to 5 months. Subsamples for chemical and biological analysis were initially collected at intervals of 3 to 10 days, increasing to triweekly. In some experiments, fungicides (Iotrimin or nystatin) or bactericides (terramycin or chloramphenicol) were added to distinguish between degradation by bacteria and fungi, respectively. All experiments were controlled with unamended and (or) uninoculated mixtures as appropriate.

Total numbers of viable heterotrophic bacteria and hydrocarbon-degrading microorganisms in each microcosm were determined at different incubation time by spread plate count and most probable number (MPN) techniques (Chang and Ehrlich, 1984).

Significant crude oil and model hydrocarbon degradative potential was observed in tests that used mixed indigenous microbial populations. The degradative potential of each hydrocarbon varied with the numbers and types of microorganisms present in incubated sediment samples. Metabolic

fate studies indicated that the aliphatic hydrocarbons cyclohexane and hexadecane, and the two-ring aromatic hydrocarbon, naphthalene, were subject to removal by microorganisms. The rate of microbial degradation was less for a three-ring aromatic compound, phenanthrene.

The rate of microbial degradation of a model hydrocarbon (¹⁴C₁-hexadecane, at 250 μCi/mmol) was measured as follows: 100 g of sediment was mixed with 20 mL ground water in 500-mL incubation bottles (BOD bottles) capped with Neoprene stoppers. The evolved CO₂ + ¹⁴CO₂ was trapped in KOH solution. Total CO₂ evolution was determined by titration and scintillation-counting techniques (Chang and Broadbent, 1981; Chang and Alexander, 1983). Biodegradation was assessed by comparing the total CO₂ and the ¹⁴CO₂ fraction in the degradation bottles to that in control bottles to which no hydrocarbon had been added or in which sterilized hydrocarbon had been added to a sterile sediment- and ground-water mixture.

Rates of biodegradation of crude oil and hexadecane in a mixture of sediment and ground water were also estimated from the oxygen uptake as described in Chang and Ehrlich (1984). A lag phase (a period before exponential growth of microbial population begins) preceded hydrocarbon oxidation. The duration of the lag phase depended on temperature and the amount of nitrogen, phosphorus, and sulfur (fig. C-18). The lag phase (2 days when incubated at 12 °C and 5 days at 2 °C) presumably represented the development of a hydrocarbon-degrading community in response to crude oil and hexadecane additions. The rates of crude oil biodegradation calculated by oxygen uptake from microcosms maintained at temperatures that differed by 10 °C (Q₁₀) were compared (table C-3). Q₁₀ values for samples kept at 12 °C and 2 °C ranged from 2.18 to 2.56; the values for those kept at 17 °C and 7 °C ranged from 2.38 to 2.73. Q₁₀ decreased with increasing nutrient concentrations and increased at higher temperatures, which suggests that enzymatic activity also increased with increasing temperature.

¹Center for Environmental Studies, Bemidji State University, Bemidji, Minnesota

²U.S. Geological Survey, St. Paul, Minnesota

Table C-3. — Rates of oxygen uptake before and after 10 °C temperature changes, and values for Q₁₀ (biodegradation rate) with selected nutrients

[Values are means of three replicates. O₂ values are in milligrams per week, temperatures are in degrees Celsius (°C)]

Bottle sets:

A, E: Ground water + sediment (30 g) + crude oil (0.1%)

B, F: A or E + P (0.5 ppm) + N (2 ppm) + MgSO₄ (10 ppm)

C, G: A or E + P (5 ppm) + N (10 ppm) + MgSO₄ (500 ppm)

D, H: A or E + P (10 ppm) + N (20 ppm) + MgSO₄ (500 ppm)

Control: no inorganic nutrient or crude oil added.

	Temperature	Bottle Set					Temperature	Bottle Set				
		A	B	C	D	Control		E	F	G	H	Control
Oxygen uptake	12 °	0.74	8.49	10.85	14.96	0.16	17 °	0.92	9.51	11.90	17.38	0.26
	2 °	0.20	3.37	4.54	6.86	0.07	7 °	0.34	3.59	4.72	7.30	0.09
Biodegradation value (Q ₁₀)		2.56	2.52	2.39	2.18	2.28		2.73	2.65	2.52	2.38	2.88

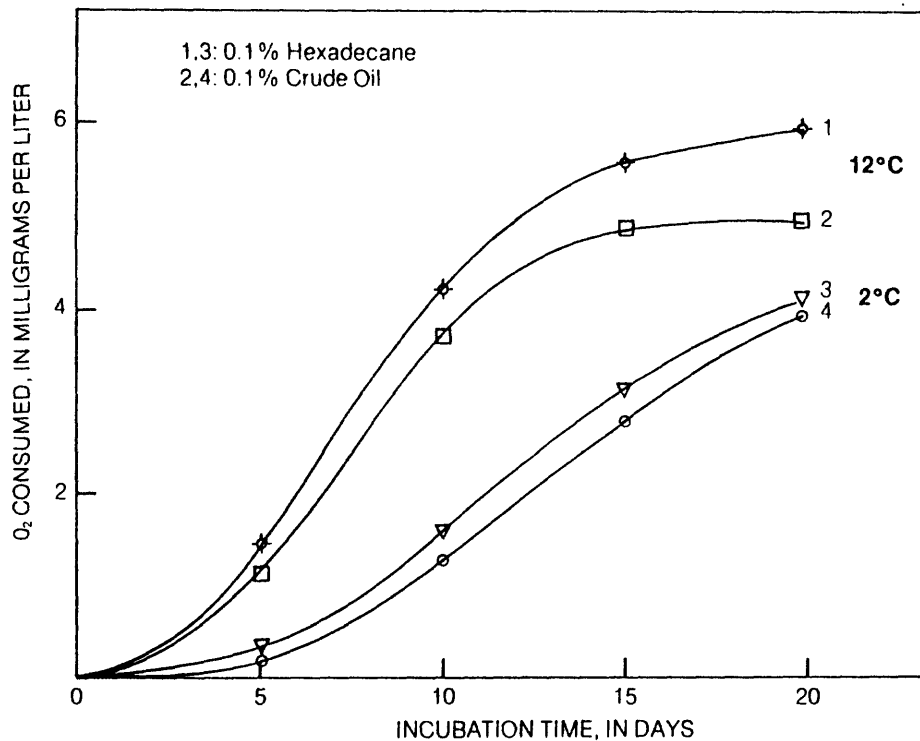


Figure C-18. — Oxygen uptake by indigenous microorganisms in sediment and ground-water mixture mixed with hexadecane or crude oil and incubated at 12 °C and 2 °C.

Heterotrophic microbial populations were affected by incubation temperature. In general, higher microbial numbers were found in samples incubated at 17 °C and 12 °C than at 7 °C or 2 °C. Microbial numbers at 12 °C and 17 °C were not significantly different ($P \leq 0.05$) from microcosms amended with nutrients. In general, the growth yield and degradation potential increased with temperature. Oil-degrading bacteria reached a stationary phase after 40 to 48 days at 2 °C, and after 35 to 40 days at 7 °C after inoculation. The

initial stationary phase for cultures incubated at 12 °C and 17 °C was reached at approximately 40 and 35 days, respectively (figs. C-19 and C-20). Additions of nutrients to aqueous sediments increased biodegradation of oil components and microbial growth about twofold (tables C-4, C-5, and C-6, and fig. C-21). Growth of yeasts and fungi in crude oil and hexadecane was insignificant at 2 °C and 7 °C, but the populations increased about 1,000-fold in similar studies at 12 °C and 17 °C (fig. C-22).

Table C-4. — Cumulative CO₂ evolution and carbon mineralization from crude-oil-contaminated topsoil samples

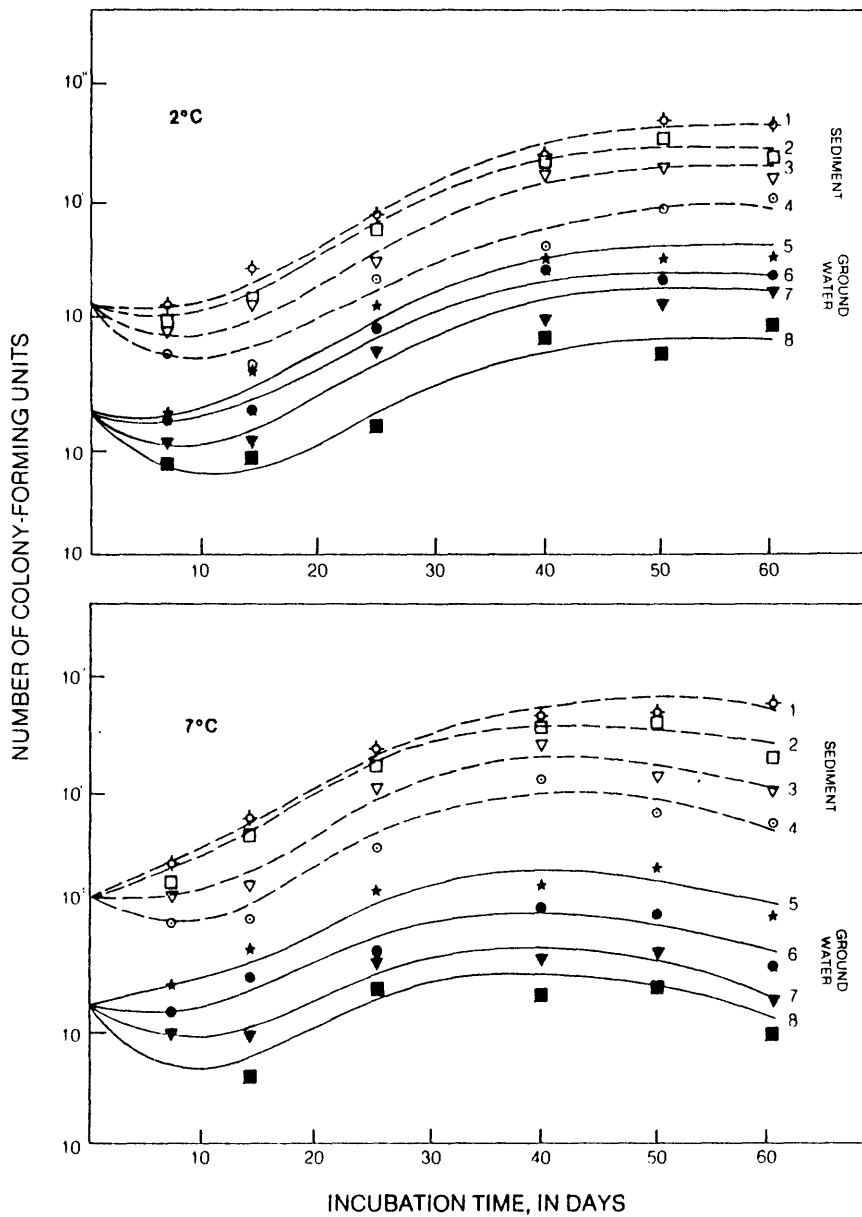
[Values are mean of three replicates, in milligrams]

Sample treatments:

- A = soil (100 g) and water (20 mL)
- B = A + N (2 mg) + P (1 mg) + SO₄ (50 mg)
- C = A + N (3 mg) + P (1.5 mg) + SO₄ (50 mg)
- D = A + N (4 mg) + P (2 mg) + SO₄ (50 mg)
- E = A + N (6 mg) + P (3 mg) + SO₄ (50 mg)
- F = A + terramycin bactericide (0.1 mL)
- G = A + lotrimin fungicide (0.2 mL)
- H = A + D + terramycin (0.1 mL)
- I = A + D + lotrimin (0.2 mL)

Sample	Incubation time(days)								
	3	11	16	21	25	32	38	46	59 ¹
Carbon dioxide									
A	9.5	18	30	37	46	62	80	100	137A
B	13	33	73	89	138	189	256	325	423D
C	14	38	79	97	153	203	269	335	429D
D	12	32	72	90	140	193	259	329	428D
E	6.8	28	67	84	136	186	258	319	409D
F	14	37	54	69	79	88	109	127	161B
G	12	19	30	37	45	48	71	94	132A
H	12	49	89	108	156	201	265	327	403D
I	13	47	86	100	136	182	235	285	356C
Carbon									
A	2.6	4.9	8.2	10.1	12.5	16.9	21.8	27.3	37.4A
B	3.6	9.0	19.9	24.3	37.6	51.5	69.8	88.6	115.4D
C	3.8	10.4	21.5	26.5	41.7	55.4	73.4	91.4	117.0D
D	3.3	8.7	19.6	24.5	38.2	52.6	70.6	89.7	116.7D
E	1.9	7.6	18.3	22.9	37.1	50.7	70.4	87.0	111.5D
F	3.8	10.1	14.7	18.8	21.5	24.0	29.7	34.6	43.9B
G	3.3	5.2	8.2	10.1	12.3	13.1	19.4	25.6	36.0A
H	3.3	13.4	24.3	29.5	42.5	54.8	72.3	89.2	109.9D
I	3.4	12.8	24.0	27.3	37.1	49.6	64.1	77.7	97.1C

¹Values followed by letter differ from specified sample value at 5 percent significance level.



EXPLANATION

- 4, 8: Water added to sediment only
- 3, 7: Water + N (200 mg/L) + P (10 mg/L) + S (0.5 g/L)
- 2, 6: Water + N (400 mg/L) + P (20 mg/L) + S (0.5 g/L)
- 1, 5: Water + N (800 mg/L) + P (40 mg/L) + S (0.5 g/L)

Figure C-19. Heterotrophic bacterial counts in sediment and ground-water microcosms with varied amounts of selected nutrients: A. at 2 °C, and B. 7 °C.

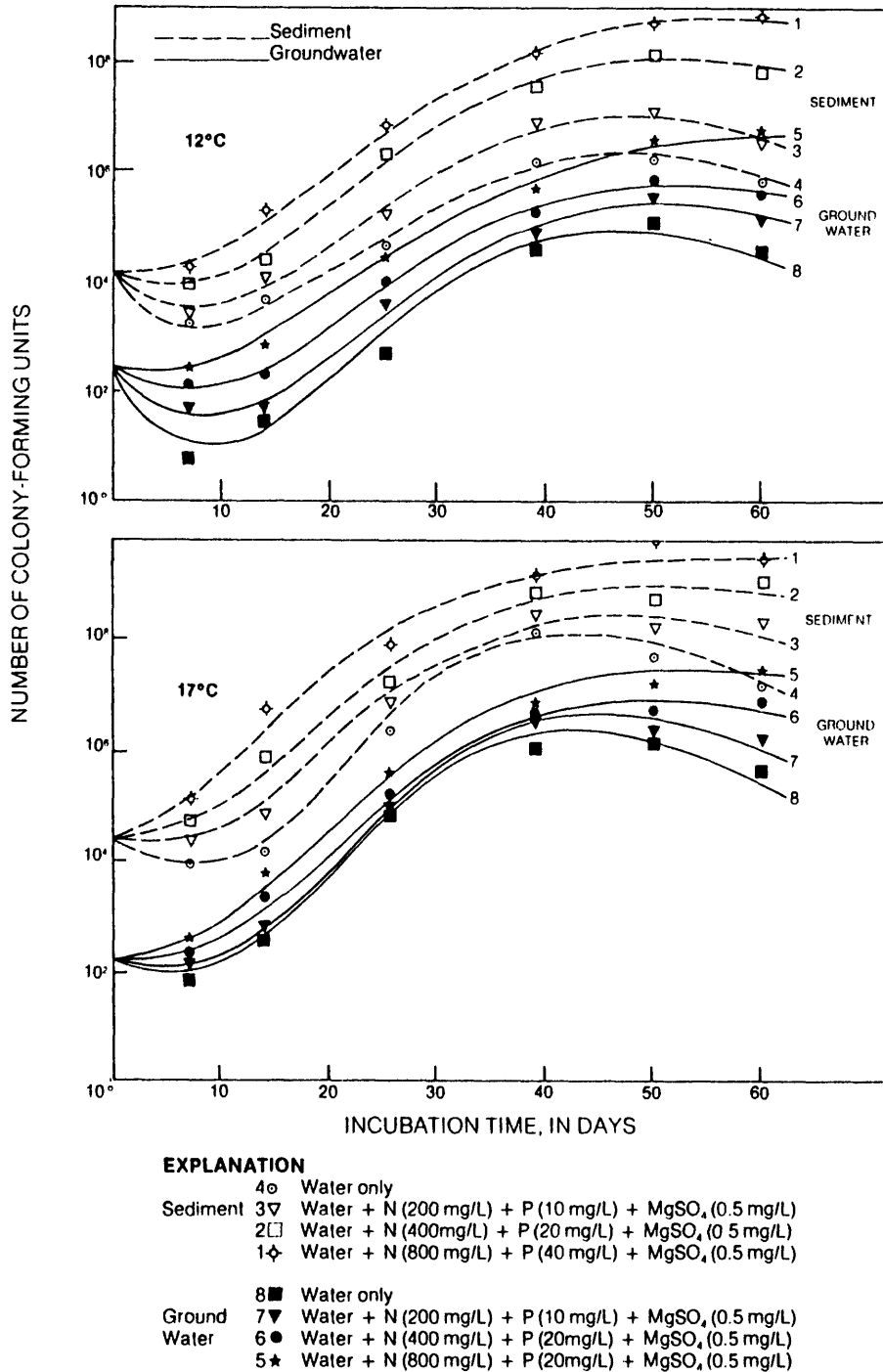
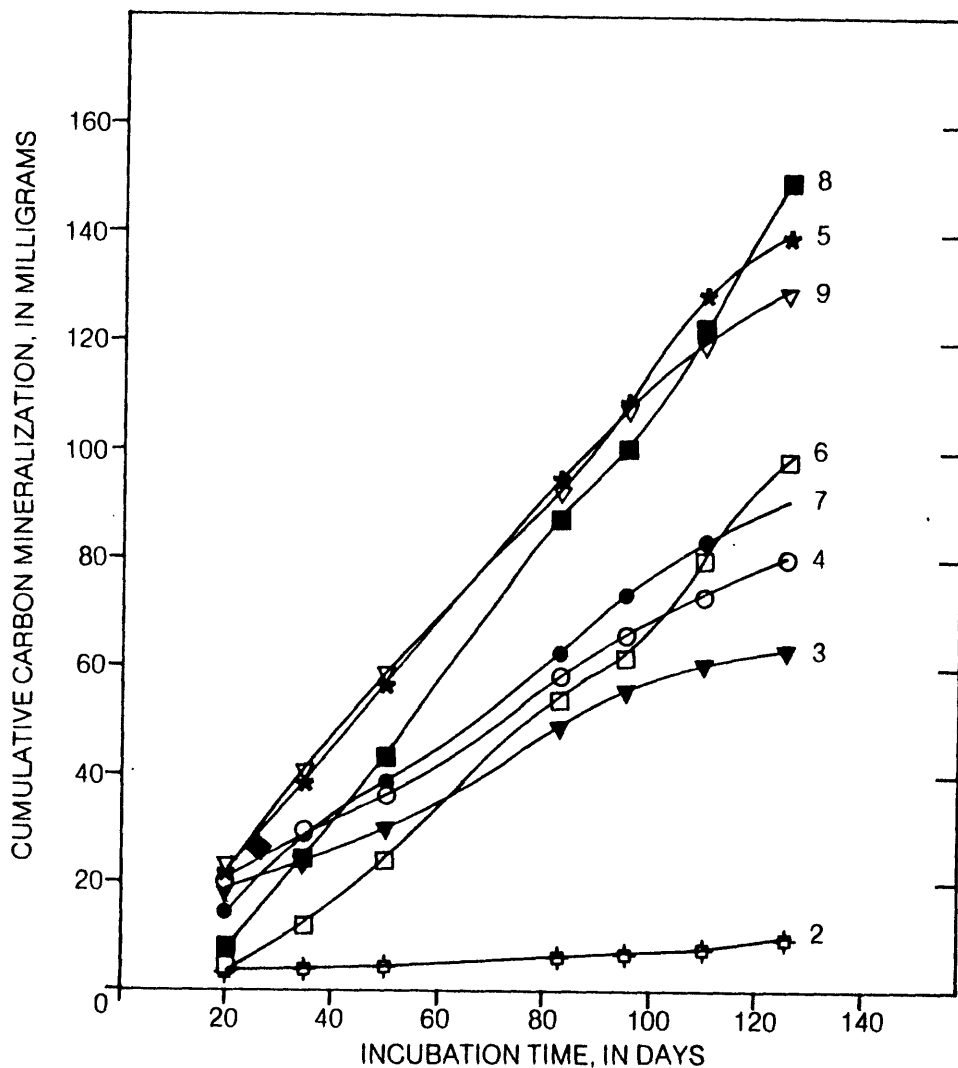


Figure C-20. Heterotrophic bacterial counts in sediment and ground-water microcosms with varied amounts of selected nutrients: A. at 12 °C, and B. 17 °C..



EXPLANATION

- 2 = Control sediment (100 g) + control ground water + $^{14}\text{C}_1$ - Hexadecane (1 μCi) + Hexadecane (1 mL)
- 3 = 2 + MgSO_4 (10 ppm) + NH_4NO_3 (2 ppm) + (K_2HPO_4 + KH_2PO_4) (0.5 ppm)
- 4 = 2 + MgSO_4 (50 ppm) + NH_4NO_3 (10 ppm) + (K_2HPO_4 + KH_2PO_4) (5 ppm)
- 6 = 4 + Chloramphenicol (10 mg)
- 7 = 4 + Nystatin (10 mg)
- 8 = 5 + Chloramphenicol (10 mg)
- 9 = 5 + Nystatin (10 mg)

Figure C-21. Cumulative carbon mineralization of hexadecane mixed with sediment and ground water with varied amounts of selected nutrients and antibacterial or antifungal agents.

Table C-5. — Cumulative CO₂ evolution and carbon mineralization from crude oil in aquifer sediment samples

[Values are mean of three replicates, in milligrams]

Sample treatment:

- D = Contaminated sediment (100 g)
- A = D + N (20 ppm) + P (10 ppm) + S (500 ppm)
- B = D + N (10 ppm) + P (5 ppm) + S (50 ppm)
- C = D + N (2 ppm) + P (1 ppm) + S (10 ppm)
- E = control sediment
- F = D + B + terramycin (0.5 mL)
- G = D + B + lotrimin (1.0 mL)
- H = D + teramycin (0.5 mL)
- I = D + lotrimin (1.0 mL)

Sample	Incubation time (days)											
	5	8	16	23	33	44	58	70	85	100	113	130 ¹
Carbon dioxide												
A	7.5	9.0	51	116	190	257	323	374	430	467	528	599 ^H
B	7.1	8.8	30	42	64	86	116	139	173	227	264	312 ^E
C	4.3	5.9	17	28	42	53	64	74	85	117	152	180 ^C
D	3.5	4.5	8.3	9.8	13.2	21	27	32	40	46	50	55 ^B
E	0.9	1.3	2.3	3.6	5.4	9	12	14	20	25	28	32 ^A
F	12.3	28.5	56	83	116	159	217	280	364	420	466	526 ^G
G	5.1	5.9	19	37	55	78	104	126	162	199	234	276 ^D
H	4.1	10.7	21	34	56	101	165	233	296	352	385	431 ^F
I	4.3	6.6	10	13	19	25	33	40	47	54	61	66 ^B
Carbon												
A	2.0	2.5	14	31	52	70	88	102	117	128	143	162 ^H
B	1.9	2.4	8.3	11.6	17	23	32	38	47	62	72	85 ^E
C	1.1	1.6	4.5	7.7	11.4	14	17	20	23	32	41	49 ^C
D	0.9	1.2	2.3	2.7	3.6	5.6	7.4	8.9	10.9	12.5	13.5	15.1 ^B
E	0.2	0.4	0.6	1.0	1.4	2.5	3.3	3.9	5.3	6.7	6.9	8.1 ^A
F	3.4	7.8	15.4	22	31	43	59	76	99	115	127	143 ^G
G	1.4	1.6	5.3	10.2	14.9	21	28	34	44	54	64	75 ^D
H	1.3	2.9	5.8	9.2	15.4	28	45	63	81	96	105	117 ^F
I	1.2	1.8	2.8	3.5	5.1	6.8	9.0	10.9	12.8	14.8	16.6	18 ^B

¹Values followed by letter differ from specified sample value at 5 percent significance level.

To test microbial growth on model hydrocarbons, triplicated 50-mL test tubes containing 20 mL Tauson broth medium and 0.2 mL model hydrocarbon were inoculated with each isolated microorganism (isolate). The inoculated tubes were incubated at 6 °C or 22 °C. Growth to turbidity after 10 to 14 days incubation confirmed the

presence of microbes capable of utilizing model hydrocarbon as a sole source of carbon. Cyclohexane was degraded by three of eight bacterial isolates and by three of four fungal isolates. Hexadecane was utilized by three of four fungal and all eight bacterial isolates. Three bacterial and one fungal isolate were capable of degrading

Table C-6.—Cumulative CO₂ evolution and carbon mineralization from ¹⁴C, through (Hexadecane) treated in control sediment-and-ground-water mixture by indigenous microbes, as total carbon

[Values are means of three replicates, in milligrams]

Sample treatment

2 = control sediment (100 g) + control ground water (20 mL) + ¹⁴C₁-hexadecane (1 μCi) + hexadecane (1 mL)

3 = 2 + MgSO₄ (10 ppm) + NH₄NO₃ (2 ppm) + (KH₂PO₄ + K₂HPO₄) (0.5 ppm)

4 = 2 + MgSO₄ (50 ppm) + NH₄NO₃ (10 ppm) + (KH₂PO₄ + K₂HPO₄) (5 ppm)

5 = 2 + MgSO₄ (500 ppm) + NH₄NO₃ (20 ppm) + (KH₂PO₄ + K₂HPO₄) (10 ppm)

6 = 4 + chloramphenicol bactericide (10 mg)

7 = 4 + nystatin fungicide (10 mg)

8 = 5 + chloramphenicol (10 mg)

9 = 5 + nystatin (10 mg)

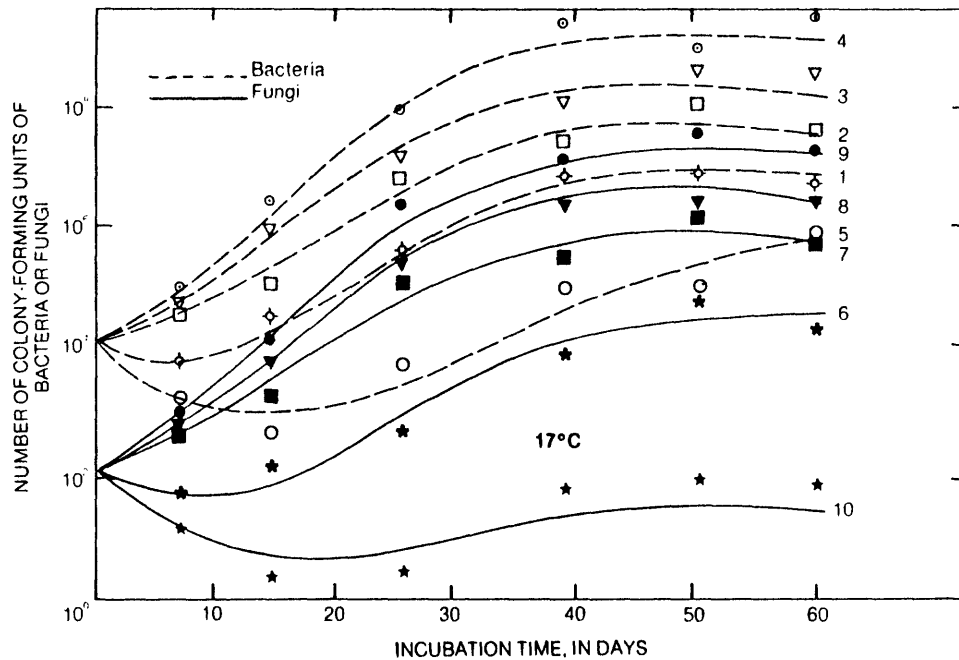
Sample	Incubation time (days)						
	20	35	49	82	95	110	124 ¹
Carbon dioxide							
2	4.96	6.54	8.07	13.51	15.65	17.0	18.0 ^A
3	65.15	91.37	108.57	181.69	210.59	222.15	231.15 ^B
4	74.23	100.55	127.46	213.30	247.12	272.68	291.98 ^C
5	78.92	148.93	201.74	337.61	391.13	482.61	509.81 ^F
6	5.28	24.64	91.00	188.55	226.98	296.94	352.44 ^D
7	69.90	110.57	139.75	233.86	270.93	301.87	326.57 ^D
8	18.46	81.24	155.16	310.70	371.97	457.62	541.52 ^G
9	82.04	141.33	204.43	342.11	396.35	441.64	472.74 ^E
Carbon							
2	1.35	1.78	2.20	3.68	4.27	4.64	4.88 ^A
3	17.77	24.92	29.61	49.55	57.40	60.58	62.98 ^B
4	20.24	27.42	34.76	58.17	67.39	74.36	79.66 ^C
5	21.52	40.62	55.02	92.08	106.68	131.63	139.03 ^F
6	1.44	6.72	24.82	51.42	61.90	80.98	96.08 ^D
7	18.52	29.61	37.57	63.24	73.55	81.78	88.48 ^D
8	5.04	22.18	42.32	84.74	101.45	124.81	147.71 ^G
9	22.37	38.55	55.75	93.30	108.09	120.44	128.94 ^E

¹Values followed by letter differ from specified sample value at 5 percent significance level.

naphthalene and phenanthrene. All of the isolated bacteria and fungi were able to grow on crude oil (table C-7).

Antibiotics were used to distinguish between the degradation of the crude oil by bacteria and by fungi and yeasts under aerobic conditions. The majority of the petroleum degradation at room temperature (22 °C) (fig. C-21 and tables C-4, C-

5, and C-6) was by fungi, but the majority of the degradation at 2 °C, 7 °C, and 12 °C was by bacteria. Bacteria also accounted for the majority of the degradative activity under facultative anaerobic conditions at all temperatures. In the latter case, only low levels of ¹⁴CO₂ were detected. Aerobic incubation of other treated samples demonstrated extensive conversion of 1-¹⁴C₁ Hexa-



EXPLANATION

- 1, 6 Water only
- 2, 7 Water + N (200 mg/L) + P (10 mg/L) + S (0.5 g/L)
- 3, 8 Water + N (500 mg/L) + P (25 mg/L) + S (0.5 g/L)
- 4, 9 Water + N (1000 mg/L) + P (50 mg/L) + S (0.5 g/L)
- 10 Water + Nystatin (20 mg/L)

Figure C-22. Bacterial and fungal counts with varied amounts of selected nutrients or antifungal agent at 17°C.

decane to ¹⁴CO₂. Interestingly, the low levels of ¹⁴CO₂ detected under facultative anaerobic conditions were also significantly ($P \leq 0.01$) increased by the addition of inorganic nutrients as electron acceptors. An isotope-recovery experiment demonstrated that less than 22 percent of the added ¹⁴C₁-Hexadecane was mineralized to ¹⁴CO₂ through various degradative pathways after 92 days of incubation under facultative anaerobic conditions, despite the presence of heterotrophic hydrocarbon-utilizing microorganisms. However, more than 75 percent of the added ¹⁴C₁-Hexadecane was converted to ¹⁴CO₂ under aerobic conditions at the end of the same incubation period.

Background concentrations of nutrients in ground water at the site are exceedingly low (M.J.

Baedecker, U.S. Geological Survey, written commun., 1985). The laboratory experiments suggest that nutrient availability is currently the major factor limiting microbial activity at the site. With time, however, the total amount of nutrients (and, therefore, the microbial biomass) will increase through nutrients that become trapped and enter the zone of active microbial degradation from the recharge area upgradient of the oil-spill site and the decomposition of the petroleum at the contaminated site.

In the laboratory experiments, degradation rates under aerobic conditions are nearly an order of magnitude greater than under anaerobic conditions. Dissolved oxygen in uncontaminated ground water upgradient from the contaminant

Table C-7.—*Degradation of model hydrocarbons by bacteria and fungi*

[+ indicates utilizations, - indicates no utilization]

Isolate number	Hydrocarbon				
	Cyclohexane	Hexadecane	Naphthalene	Phenanthrene	Crude petroleum
Bacteria					
2, 5, 6	-	+	-	-	+
1, 4	+	+	+	+	+
3	+	+	+	+	+
7, 8	-	+	-	-	+
Fungi					
1, 3	+	+	-	-	+
2	+	+	+	+	+
4	-	-	-	-	+

plume typically contains 1 to 3 mg/L, which suggests that sufficient oxygen is available, at least at the periphery of the contaminant plume, for microbial degradation.

Because the water table in the contaminated area ranges from 0 to 35 feet below land surface, the ground-water temperature locally changes seasonally. Under laboratory conditions, changes from an average ground-water temperature of 7 °C to a low of 2 °C and a high of 17 °C could account for a twofold increase or decrease in degradation rate. Therefore, the effect of temperature is relatively small compared to maximum probable ranges of dissolved oxygen and nutrient concentration, and the resulting large changes in biological activity.

Crude petroleum and model-hydrocarbon biodegradation was stimulated by an increase in temperature, inorganic nutrient concentration, and oxygen availability, as indicated by increases in CO₂ production, O₂ uptake, and heterotrophic microbial counts. The degree to which the laboratory simulations represent processes occurring in the field needs to be assessed, however, although the trends of nutrient and temperature dependence observed in laboratory would probably be applicable to the field, parallel laboratory and field experiments will be needed to assess

whether adaptation and community successions and resulting hydrocarbon mineralization in the two environments are comparable.

REFERENCES

- Chang, F.H., and Alexander, M., 1983, Effect of simulated acid precipitation on algal fixation of nitrogen and carbon dioxide in forest soils: *Environmental Science and Technology*, v. 17, p. 11-13.
- Chang, F.H., and Broadbent, F.E., 1981, Influence of trace metals on carbon dioxide evolution from a Yolo soil: *Soil Science*, v. 132, p. 416-421.
- Chang, F.H., and Ehrlich, G., 1984, Microbial reconnaissance at the site of a crude-oil spill—preliminary results and project plan, U.S. Geological Survey Program on Toxic Waste—Ground-Water Contamination: U.S. Geological Survey Water-Resources Investigations Report 84-4188, p. 97-107.
- Hult, M.F., 1984, Ground-water contamination by crude oil at the Bemidji, Minnesota research site—an introduction, U.S. Geological Survey Program on Toxic Waste—Ground-Water Contamination: U.S. Geological Survey Water-Resources Investigations Report 84-4188, p. 1-15.

CHAPTER D. – FATE OF HEAVY METALS NEAR ABANDONED LEAD AND ZINC MINES IN NORTHEASTERN OKLAHOMA AND SOUTHEASTERN KANSAS

	Page
Introduction	D-3
Mine-water discharge, metal loading, and chemical reactions, by D.L. Parkhurst	D-5
Water discharge and metal loading.....	D-5
Major chemistry of the mine water.....	D-8
Distribution of microorganisms and selected metals in mine drainage, stream water, and sediment, by K.S. Smith, L.H. Filipek, D.M. Updegraff, and C.S.E. Papp	D-11
Problems associated with analyses of plant samples in the Tar Creek study, by B.M. Erickson, T.F. Harms, and L.H. Filipek.....	D-17

ILLUSTRATIONS

	Page
Figure	
D-1. Map showing location of Tar Creek sampling sites near Picher, Oklahoma	D-4
D-2. Map showing location of mine workings of the Picher Field and selected features.....	D-6
D-3. Plots of mine discharge against: (a) water level in air shaft, and (b) mean daily discharge of Tar Creek	D-7
D-4. Histogram showing amounts of minerals and gases that must react with rainwater to evolve the chemical composition of mine water.....	D-8
D-5. Map showing location of mine-tributary sampling sites.....	D-12
D-6. Plot of total microbial counts in Tar Creek water and sediment on nutrient agar, 1984 and 1985.....	D-14
D-7. Plots of total microbial counts in 1985 water and sediment on nutrient agar and minimal yeast extract agar: (a) Tar Creek sites, and (b) mine tributary sites	D-15
D-8. Map showing Tar Creek study area and location of sampling sites	D-18
D-9. Map showing location of sampling sites near borehole discharge.....	D-19

TABLES

	Page
Table	
D-1. Analysis of two samples of vegetation and their duplicate by inductively coupled plasma-emission spectroscopy.....	D-17
D-2. Zinc analysis of three samples of grass, one sample of sumac, and their duplicates by atomic absorption spectrophotometry.....	D-20

CHAPTER D. — FATE OF HEAVY METALS NEAR ABANDONED LEAD AND ZINC MINES IN NORTHEASTERN OKLAHOMA AND SOUTHEASTERN KANSAS

INTRODUCTION

Lead and zinc ore were mined from the Picher Field in northeastern Oklahoma and southeastern Kansas from the beginning of the 20th century until the late 1960's. The ore occurs in a very transmissive aquifer of Mississippian limestones. Continuous pumping lowered the water table while the huge underground workings were being excavated. When all mining operations ended, pumping was discontinued, and the mines filled with water. In 1979, water began to discharge from the mine workings to Tar Creek, the stream draining the mining area (fig. D-1).

The mine water contains extremely large concentrations of iron and zinc and large concentrations of cadmium, lead, manganese, and nickel. The discharge of mine water causes pH values less than 3.0 in Tar Creek water during some periods. The red stains of iron precipitates are evident the entire length of Tar Creek below the mining area (14 kilometers).

The objective of the current study is to describe the mobilization of heavy metals in the mining area and determine their fate. This requires determination of metal concentrations and the associated chemical reactions; it also entails microbiological and botanical assessments. Many of the chemical transformations are mediated by microbiological activity, and microorganisms also may play an important role in concentrating metals in sediments. Concentrations of metals in plants are an indicator of the extent to which the metals are disseminated in the environment surrounding Tar Creek and the mining area.

The three abstracts presented in this chapter give preliminary results of the interdisciplinary research on the processes affecting heavy metals in the mines and in Tar Creek, and on the uptake of these metals by plants.

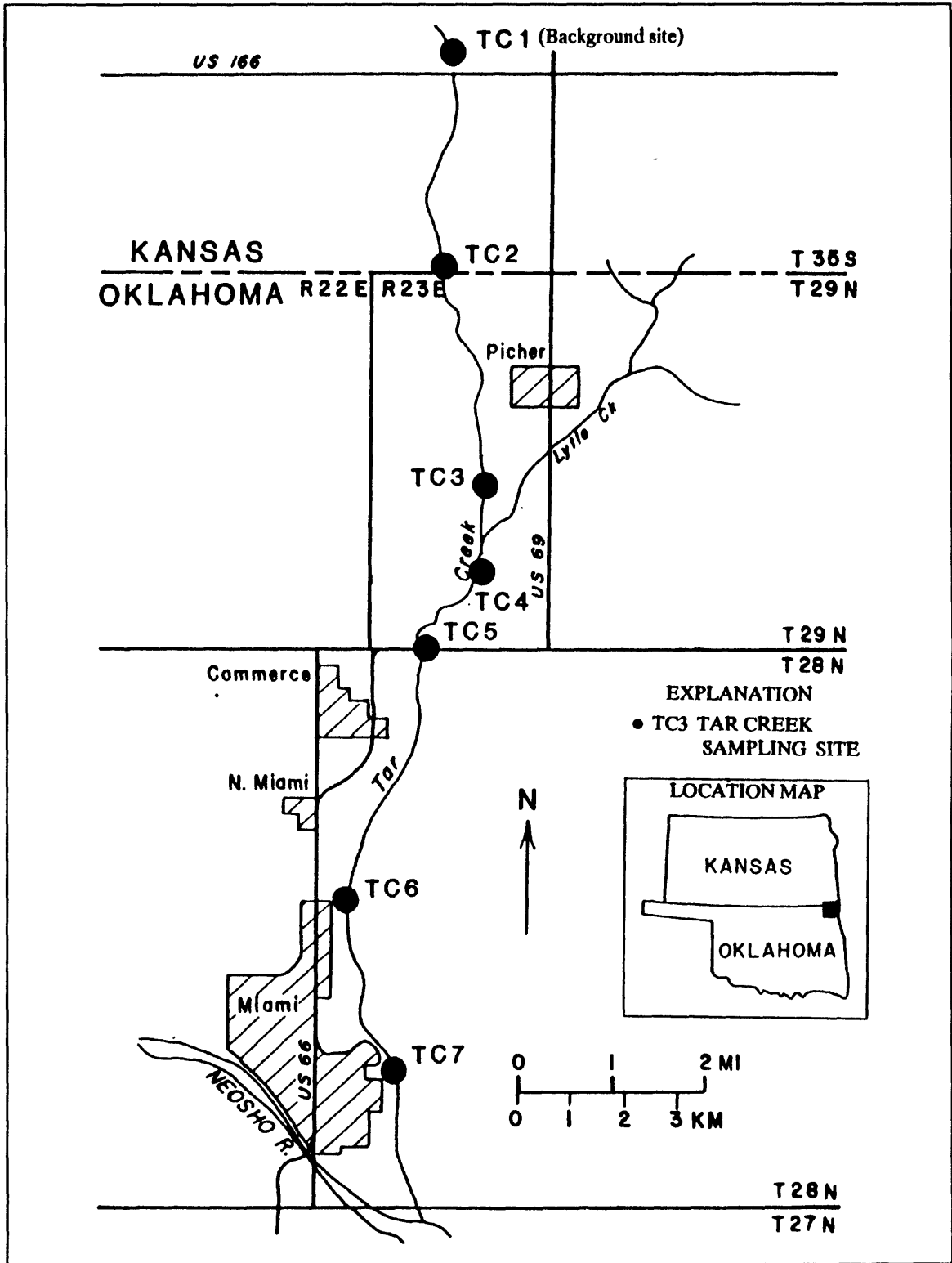


Figure D-1. — Location of Tar Creek sampling sites near Picher, Oklahoma.

MINE-WATER DISCHARGE, METAL LOADING, AND CHEMICAL REACTIONS

By David L. Parkhurst¹

Lead and zinc ores were mined from the Picher Field in northeastern Oklahoma and southeastern Kansas (fig. D-2) from the turn of the 20th century until the 1960's. Sphalerite and galena were the major sulfide ores found in this carbonate-rock mining district. In addition, the mineralization produced chert, dolomite, and calcite. The mines were about 200 to 400 feet below land surface and almost all access was through vertical shafts. The major mine workings near Picher, Okla., form an interconnected maze within a region of about 20 square miles (fig. D-2). A description of the mines and associated geology is given in McKnight and Fischer (1970).

Mine dewatering was stopped after mining ceased and the mines subsequently filled with water. About 1980, mine water began to discharge from a few mine shafts and air shafts at land-surface altitudes of about 800 feet in the Tar Creek basin. Mine water has discharged intermittently since that time. This abstract reports estimates of the volume of water and the metal loading of Tar Creek due to mine-water discharge from January 1984 through March 1985. An analysis of the geochemical reactions that produced the chemistry of the mine water also is presented.

Water Discharge and Metal Loading

The mines filled with water, partly by surface-water inflow through two mine collapses that have captured streamflow in the northern reaches of the Tar Creek basin, and partly by ground water, although the quantity of ground water is unknown. A slight hydraulic gradient of less than 1 foot per mile is apparent from the north inflow points to the south discharge points (fig. D-2).

A continuous water-level recorder has been operated in an air shaft that penetrates the mine workings. The air shaft is on the Blue Goose lease, near the southern limit of the mines, about 1 mile west of the main discharge points (fig. D-2). Mine discharge has been estimated from the following

data: (1) the continuous water-level record in the air shaft, (2) a series of streamflow measurements at the mine discharge points, and (3) the continuous streamflow record at a gaging station on Tar Creek about 4 miles downstream from mine-discharge points.

Mine discharge at the major discharge points was measured on 9 days corresponding to a wide range of water levels in the air shaft. The sums of the point discharges for each day are plotted in figure D-3A. The curve relates mine discharge to the water level in the air shaft, analogous to the relation between discharge and gage height at a stream-gaging station. The mine discharge can be estimated for any given water level in the air shaft. The rating can be used for mine discharges ranging from about 1.5 to 50 cubic feet per second and water levels ranging from 800.0 to 803.2 feet in the air shaft. Mine discharge at water levels below 800 feet was assumed to be negligible relative to the total annual discharge from the mines.

Water levels in the air shaft have periodically exceeded 803.2 feet, the upper limit of this rating. The rating is curved steeply upward at its right end and cannot be extrapolated with confidence. Therefore, in an effort to estimate the mine discharge at higher water levels, a second rating was developed. From the rating curve established for the air shaft, mean-daily mine discharge was calculated for all days that the water level in the air shaft was less than 803.2 feet. The mine discharge for these days is plotted against Tar Creek discharge for the same days in figure D-3B. The data can be divided into two linear groups. The line with lesser slope corresponds to relatively dry periods, and that with the greater slope corresponds to wet periods with direct runoff from rainfall. The top line was extrapolated to estimate the mine discharge when the water level in the air shaft exceeded 803.2 feet.

The two ratings were used to calculate the mean-daily discharge of water from the mines from

¹U.S. Geological Survey, Oklahoma City, Oklahoma

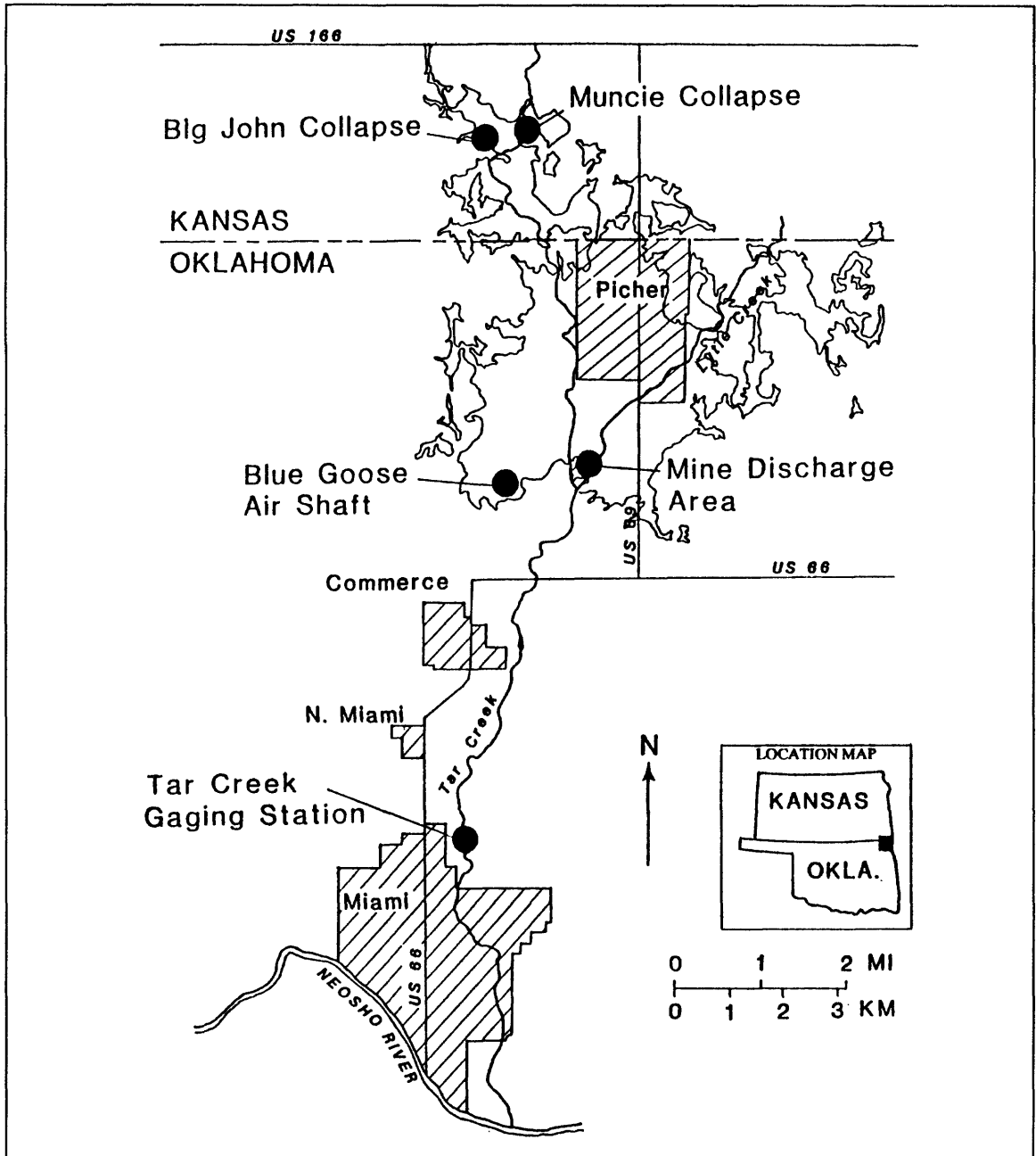


Figure D-2. — Location of mine workings of the Picher Field and selected features.

January 1984 through March 1985. The mean-daily discharge ranged from less than 1.5 to 225 cubic feet per second. The total volume of water discharged during the period was 5,600 acre-feet. The annual volume of mine discharge is estimated to be 3,400 acre-feet per year. To use all available data for the 15 months, the data were averaged by month of the year when data existed (for example, the

January 1984 and January 1985 data were averaged) and summed for all months to determine the value of 3,400 acre-feet per year. Assuming this value to be representative of the long-term average, and applying the known volume of the mine workings, 76,000 acre-feet (Oklahoma Water Resources Board, 1983), gives a residence time of about 22 years for water in the mines.

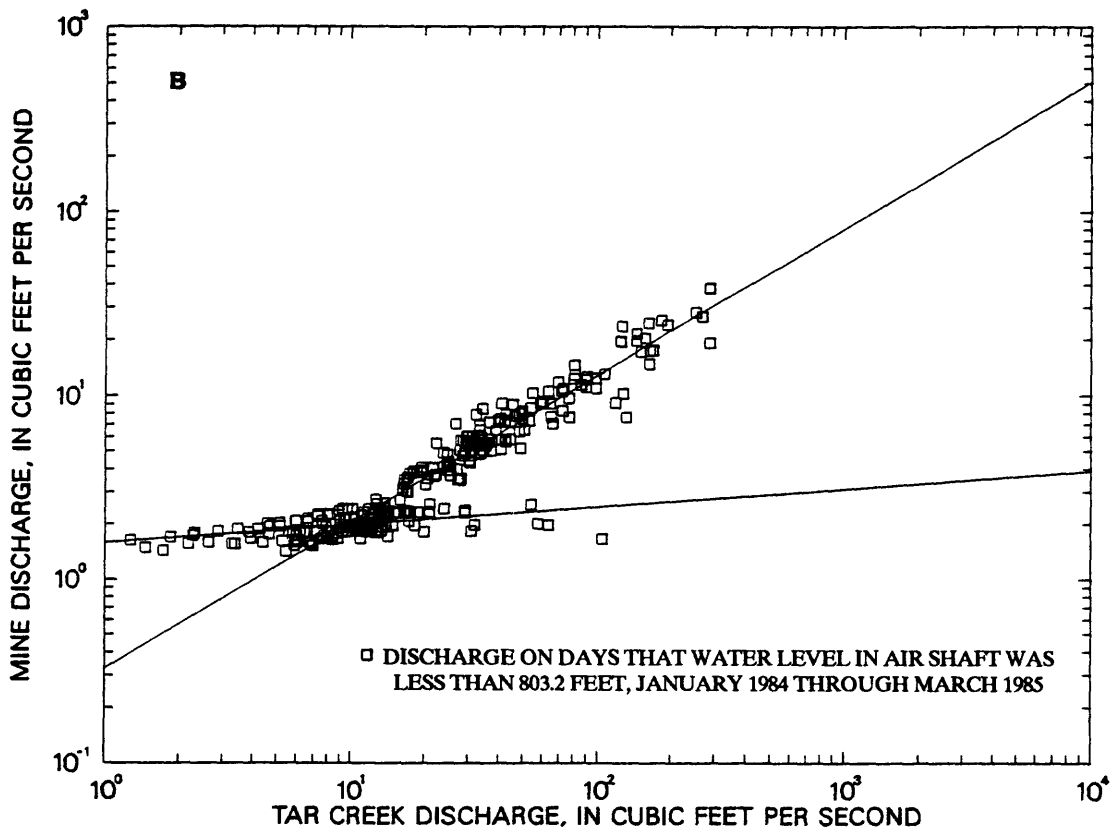
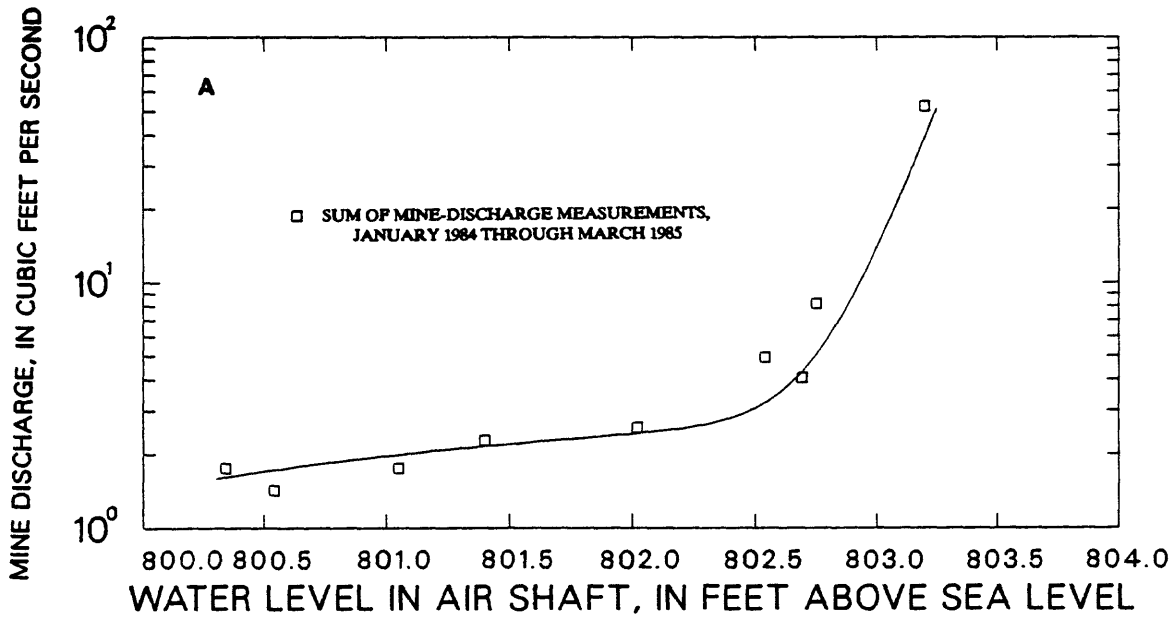


Figure D-3. — Plots of mine discharge against: (a) water level in air shaft, and (b) mean daily discharge of Tar Creek.

Typical concentrations and resulting yearly loads of metals in the mine discharge water are as follows:

Metal	Concentration (micrograms per liter)	Load (metric tons per year)
Cadmium	50	0.2
Iron	250,000	1,100
Lead	50	.2
Manganese	4,000	17
Zinc	120,000	500

Major Chemistry of the Mine Water

Chemical analyses of water samples from mine shafts, air shafts, and discharge points have been used to postulate the chemical reactions that produced the chemical composition of the water within the mines. The computer program PHREEQE (Parkhurst and others, 1980) was used to estimate the saturation indices of minerals that were assumed present in the mines or assumed likely to form in the mine environment. Calcite and dolo-

mite are undersaturated with respect to mine water and gypsum is nearly saturated. The saturation indices of ferric hydroxides cannot be reliably estimated. Pyrite and sphalerite are assumed to be undersaturated in the presence of oxygen.

Mass-balance models were generated by the computer program BALANCE (Parkhurst and others, 1982). The models calculated the quantities of each of a set of minerals that must react to evolve the mine water from rainwater (assumed to be pure water). The models were constrained to be consistent with the saturation-index calculations; that is, undersaturated minerals could only dissolve, and supersaturated minerals could only precipitate. No unique set of reactions could be found because the number of plausible reacting minerals exceeded the analytical constraints. (In other words, the number of unknowns was greater than the number of equations.)

Results of the mass-balance calculations are presented in figure D-4. This figure shows a histogram of an average reaction model based on 12

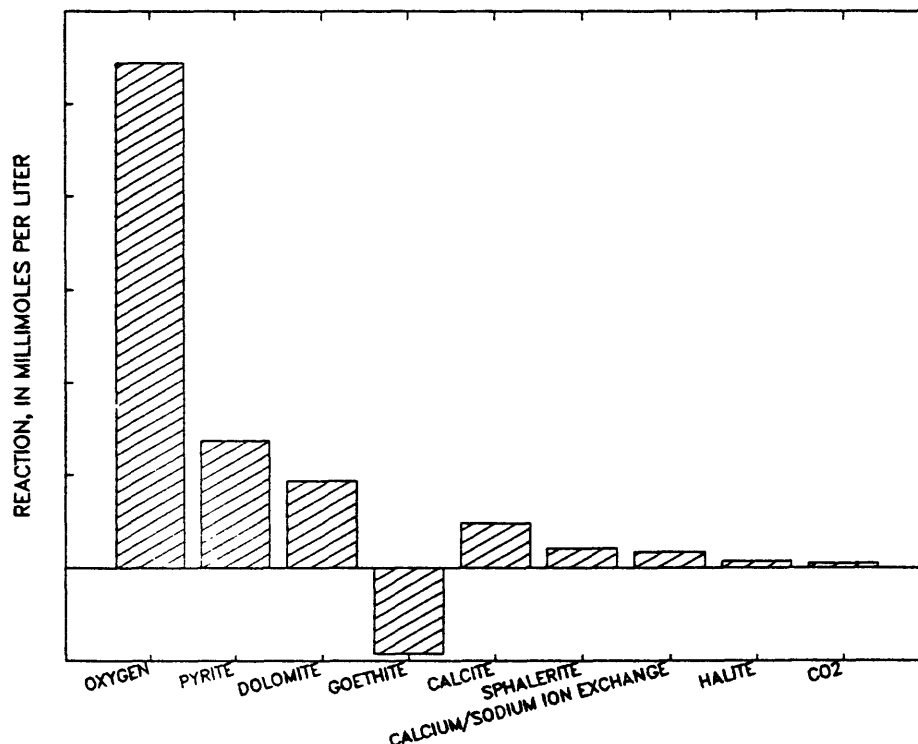
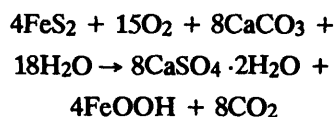


Figure D-4. — Amounts of minerals and gases that must react with rainwater to evolve the chemical composition of mine water. (Reaction is incomplete, as explained in text.)

mine-water samples, assuming oxygen, pyrite, dolomite, goethite, calcite, sphalerite, calcium-sodium ion exchange, halite, and carbon dioxide can account for all chemical reactions. The reaction of each mineral (dissolving or precipitating) is consistent with the saturation-index calculation. However, the reaction indicated by the histogram is incomplete. For example, the saturation index of gypsum is uniformly near saturation; which indicates that gypsum is involved in the reaction, but gypsum is not included in the reaction model. Similarly, many of the samples had carbon-dioxide bubbles evolving at the time of collection but carbon dioxide is negligible in the reaction model. These and other inconsistencies in the proposed reaction model can be resolved if some unknown degree of the following reaction has occurred:



To quantify the degree of this reaction that has occurred requires still another piece of analytical data; stable carbon-isotope data now being analyzed may place constraints on the extent of this reaction.

The proposed reactions are presented as net reactions, when, in fact, they must have occurred in two environments. The sulfide ores could dissolve only in the presence of oxygen, yet, the large concentrations of ferrous iron, undetectable concentrations of ferric iron, and small concentra-

tions of oxygen indicate a reducing environment. The water within the mines is thus the result of: (1) an oxidizing environment when the mines were open to the atmosphere during mining or as the mines were filling, and (2) a reducing environment when the mines filled with water and atmospheric contact was negligible.

REFERENCES CITED

- McKnight, E.T. and Fischer, R.P., 1970, *Geology and ore deposits of the Picher Field, Oklahoma and Kansas*: U.S. Geological Survey Professional Paper 588, 165 p.
- Oklahoma Water Resources Board, 1983, *Estimation of the quantity of water in the flooded underground lead-zinc mines of the Picher Field, Oklahoma and Kansas*: Oklahoma City, Tar Creek Field Investigation, Task I.3, Subtask I.3.D, 3 p.
- Parkhurst, D.L., Plummer, L.N., and Thorstenson, D.C., 1982, *BALANCE* – A computer program for calculating mass transfer for geochemical reactions in ground water: U.S. Geological Survey Water-Resources Investigations 82-14, 29 p.
- Parkhurst, D.L., Thorstenson, D.C., and Plummer, L.N., 1980, *PHREEQE* – A computer program for geochemical calculations: U.S. Geological Survey Water-Resources Investigations 80-96, 210 p.

DISTRIBUTION OF MICROORGANISMS AND SELECTED METALS IN MINE DRAINAGE, STREAM WATER, AND SEDIMENT

By Kathleen S. Smith¹, Lorraine H. Filipek², David M. Updegraff³, and Clara S.E. Papp¹

Tar Creek is the major stream draining a lead-zinc mining area in northeastern Oklahoma and southeastern Kansas (fig. D-1). Since 1980, water from abandoned and flooded mine workings near Picher, Okla., has been discharging from several boreholes and shafts. The discharge water, which is high in Cd, Fe, Pb, Zn, and other metals, flows into Tar Creek. The objective of the initial studies was to survey the microbial population and chemical characteristics of water and sediment in Tar Creek and the mine-discharge areas. This article presents some preliminary findings from: (1) sequential extractions performed on some Tar Creek sediments; (2) microbial enumerations and assays performed on stream and discharge water and sediments; and (3) biomass assays performed on some stream and discharge water samples.

The study area consists of prairie underlain predominantly by Pennsylvanian shales with some sandstone and limestone layers. The host rock for the ore deposits is the Boone Formation (Mississippian), which consists of chert, jasperoid, limestone, and dolomite. The principal ore minerals are sphalerite (ZnS) and galena (PbS) (McKnight and Fischer, 1970). A large part of the study area is overlain by mine and mill-waste materials, predominantly chert fragments called chat. Chat forms much of the Tar Creek sediment.

Water and sediment samples were collected from Tar Creek (fig. D-1) and from a mine-discharge stream referred to as the Mine Tributary (fig. D-5). The northernmost Tar Creek site (TC1, fig. D-1) serves as a background site and is in farmland north of the main mining area. Tar Creek sites TC2 and TC3 are north of the mine discharge in an area overlain by chat. Site TC4 is just downstream from the mine-discharge area (fig. D-5). Sites TC5 through TC7 (fig. D-1) are at increasing distances downstream from the

mine-discharge area. The Mine Tributary samples are a sequence of samples taken at increasing distances from a discharging borehole (site MT1, fig. D-5). The Mine Tributary consists almost entirely of mine-discharge water and has several ponded areas. The water becomes increasingly acidic as it approaches Tar Creek.

Some Tar Creek composite sediment samples (sites TC1, TC2, TC4, TC5, and TC6) have been examined by a selective chemical extraction procedure to determine the mode of occurrence and variation of trace metals within the sediments. It was necessary to grind the sediment samples to obtain a homogeneous aliquot. The sequential extraction scheme was as follows:

- (a) 1-M MgCl₂ at pH 7—releases exchangeable cations;
- (b) 1-M NaOAc at pH 5—dissolves carbonates;
- (c) 0.1-M NH₂OH·HCl in 0.01-M HNO₃—dissolves hydrous Mn oxides (Chao, 1972);
- (d) A 3:2 mixture of hot 50 percent H₂O₂ and 0.025-M HNO₃—dissolves metals associated with sulfides and organic material;
- (e) Warm 0.25-M NH₂OH·HCl in 0.025-M HCl—dissolves hydrous Fe oxides (Chester and Hughes, 1967);
- (f) Hot 25 percent HCl—dissolves crystalline iron phases and some clays; and
- (g) The residue and a separate whole-sediment aliquot were digested in a mixture of hot HF, HNO₃, and HClO₄.

The extracts were analyzed for Al, Ca, Fe, Mn, Pb, Zn, Ni, Cd, Cr, Co, and Cu by flame atomic absorption spectrophotometry with appropriate blanks and standards. Total S, total C, inorganic C, and organic C were also determined for each sample by a Leco⁴ sulfur-carbon analyzer. One duplicate sample was carried throughout the

¹U.S. Geological Survey, Denver, Colo.

²U.S. Geological Survey, Reston, Va.

³Department of Chemistry and Geochemistry, Colorado School of Mines, Golden, Colo.

⁴The use of tradenames in this report is for identification purposes only and does not constitute endorsement by the U.S. Geological Survey.

- Although total Cr, Co, Ni, Mn, and Fe appear to be diluted by the presence of chat in the sediment, the HCl-extractable concentrations (extraction f) of these elements are correlated with each other and increase to well above background levels at the farthest downstream site (TC6). This indicates coprecipitation of the trace metals with iron oxyhydroxide flocs that are observed in these sediments; it may also indicate an association of these metals with clays dissolved in the HCl extraction, although Al and Fe are known to coprecipitate as an Al-Fe oxyhydroxide phase. (Little or no Cr, Co, or Ni were found in extractions a through e at any site.)
- The ratio of Fe dissolved by extraction e to that dissolved by extraction f was highest at site TC4, just downstream from where the mine drainage enters, and decreases rapidly downstream, which suggests an increasing crystallinity of the Fe phases.
- Organic C and total S concentrations decreased downstream from site TC2.
- The partitioning patterns of Zn and Cd among the extractions are almost identical. The results suggest that most of the Zn and Cd are present as detrital sphalerite, with some minor carbonate phases.
- The Pb results are more difficult to interpret but suggest that much of the Pb is detrital galena.

Microbial enumerations and assays were conducted to yield information about the distribution and variation of microorganisms within water and sediment. Microbial growth media included nutrient agar, minimal yeast-extract agar, and thiosulfate-amended agar, which were intended to yield information about aerobic heterotrophs, aerobic chemolithotrophs and mixotrophs, and *Thiobacillus*, respectively. Assays for sulfate-reducing bacteria were performed to complement the *Thiobacillus* data. An initial statistical sampling was done to determine the magnitude of sampling and analytical errors in relation to actual variation in the study area. A hierarchical four-level analysis of variance design was used to quantify variation among (1) sampling sites, (2) duplicate composite samples collected from each site, (3) duplicate aliquots (which were used for

inoculation of microbial growth media) taken from each composite sample, and (4) duplicate microbial enumerations. Although local microbial variation is high, and the microbiological analytical procedures used incorporate a rather large error, the findings indicate that a two-level design that includes one composite sample per site and two aliquots per sample (each enumerated only once) is adequate to determine statistical differences between sites.

The difference between total aerobic viable enumerations on nutrient agar plates in water and sediment samples from Tar Creek in June 1984 and those in June 1985 are plotted in figure D-6. The enumerations are reported as colony-forming units (CFU). The differences among sites was far greater in 1984 than in 1985, which may be due to several factors:

- The contribution of mine discharge to the total flow of Tar Creek in 1984 was about twice that in 1985.
- The study area had received a large amount of rain just before the 1984 sampling, which might have washed out Tar Creek sediments and microbes.
- The range in pH among the sites was much greater in 1984 than in 1985 (3.6 to 7.8 in 1984; and 5.8 to 7.1 in 1985).

The trend in the 1984 population correlates with organic and total carbon, H₂O₂-extractable Fe and Pb (extraction d), residual Fe and Pb, and readily exchangeable Zn and Cd (extraction a) (when metal-extraction values are expressed as a percentage of the total concentration of the metal). Also, the microbial enumerations correlate with readily exchangeable Cd when Cd is expressed as the analytical concentration removed in the extraction. Warm acidified NH₂OH-HCl-extractable Fe (extraction e) is inversely correlated with the 1984 nutrient agar population. Extraction data for 1985 sediments are as yet unavailable.

Total June 1985 Tar Creek aerobic microbial enumerations on nutrient agar and minimal yeast-extract agar (0.13 g/L yeast extract) are plotted in figure D-7a. Both agars were amended with 25 percent Tar Creek water and adjusted to a pH close to the natural pH. The results indicate that more microorganisms will grow on the minimal

EXPLANATION

— 1985

- - 1984

▲ DATA POINTS--Error bars are used where data point does not span error region

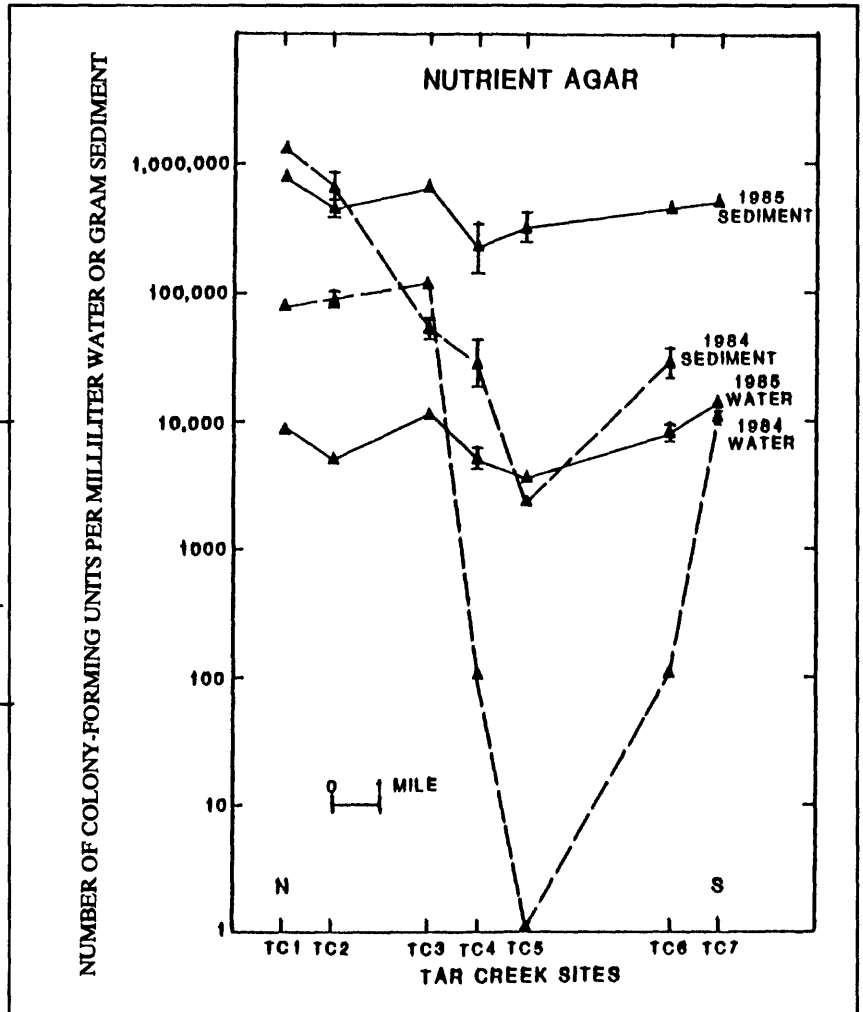


Figure D-6. — Total microbial counts in Tar Creek water and sediment on nutrient agar, 1984 and 1985.

agar than on the nutrient agar and suggest that many microbes in Tar Creek have a small organic carbon requirement and hence may use oxidizable inorganic compounds as an energy source. Sulfate-reducing bacteria in Tar Creek water exhibit a maximum value at site TC3 and minimum values at sites TC4 through TC6. The enumeration trend of thiosulfate-amended agar resembles nutrient agar enumerations.

Mine Tributary enumerations are plotted in figure D-7b. Sites MT5 and MT6 had the lowest pH values and the highest Eh values of the Mine Tributary samples. Sulfate-reducing bacteria in Mine Tributary waters are maximal at sites MT4 and MT5, and minimal at sites MT1 and MT6. Unlike the Tar Creek samples, the enumeration trend of thiosulfate-amended agar is opposite that of nutrient agar. All enumerations will be com-

pared with chemical data when such data are available.

Biomass (amount of living cellular material) determinations were performed on water samples from sites MT1, MT2, MT3, MT5, MT6, TC2, TC5, and TC6 with adenosine triphosphate (ATP) as an indicator. A method modified from Ehlke and others (1977) was used for this procedure. Amount of ATP in water decreased steadily downstream along Tar Creek, following the trend for organic C. The results for the Mine Tributary sites indicate that ATP increases to site MT3, decreases slightly at site MT5, and greatly increases at site MT6.

These preliminary data suggest several avenues for further investigation. First, the inverse correlation of warm acidified $\text{NH}_2\text{OH}\cdot\text{HCl}$ -extractable

NUMBER OF COLONY-FORMING UNITS PER MILLILITER WATER OR GRAM SEDIMENT

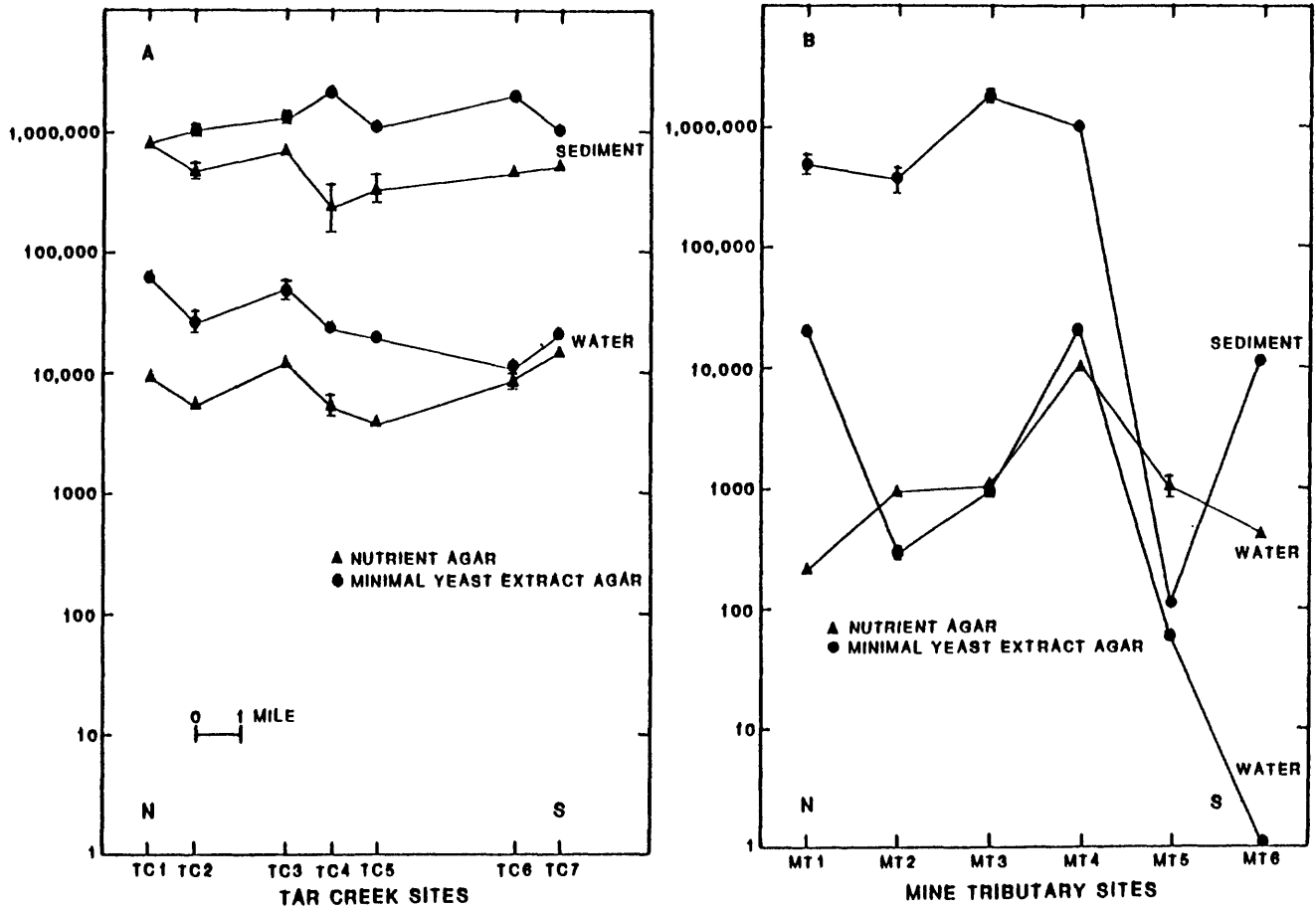


Figure D-7. — Total microbial counts in 1985 water and sediment on nutrient agar and minimal yeast extract agar: A. Tar Creek sites, and B. Mine Tributary sites.

Fe (extraction e) with microbial enumerations on nutrient agar suggests that microorganisms may be involved in the crystallization of iron phases. Second, the direct correlation of readily exchangeable Cd with microbial enumerations suggests that microbes are able to precipitate Cd. Finally, the correlation of the nutrient agar enumeration with organic and total C, H₂O₂-extractable Fe and Pb, residual Fe and Pb, and readily exchangeable Zn and Cd indicates a geomicrobiological process through which these variables may interact.

REFERENCES CITED

Adams, J.C., 1980, Tar Creek water quality reconnaissance regarding ground water discharge from abandoned lead and zinc mines of Picher Field, Ottawa County, Oklahoma: Oklahoma Water Resources Board Publication no. 100, 23 p.

Chao, T.T., 1972, Selective dissolution of manganese oxides from soils and sediments with acidified hydroxylamine hydrochloride: Soil

Science Society of America Proceedings, v. 36, p. 764-768.

Chester, Roy, and Hughes, M.J., 1967, A chemical technique for the separation of ferromanganese minerals, carbonate minerals and adsorbed trace elements from pelagic sediments: *Chemical Geology*, v. 2, p. 249-262.

Ehlke, T.A., Irwin, G.A., Liem, B.W., and Slack, K.V., eds., 1977, *Methods for collection and analysis of aquatic biological and microbiological samples*: U.S. Geological Survey Techniques of Water Resources Investigations, chapter A4, book 5, 332 p.

Krauskopf, K.B., 1979, *Introduction to geochemistry*, 2d ed.: New York, McGraw-Hill, 617 p.

McKnight, E.T., and Fischer, R.P., 1970, *Geology and ore deposits of the Picher Field, Oklahoma and Kansas*: U.S. Geological Survey Professional Paper 588, 165 p.

PROBLEMS ASSOCIATED WITH THE ANALYSIS OF PLANT SAMPLES IN THE TAR CREEK STUDY

By Barbara M. Erickson¹, Thelma F. Harms¹, and Lorraine H. Filipek¹

The lead-zinc mines in northeastern Oklahoma (fig. D-1), once an extremely productive mining area, were abandoned in the 1950's and 1960's. Since 1980, mine water high in Cd, Fe, Pb, and Zn has been discharging and entering Tar Creek (fig. D-8).

To determine whether the elevated heavy-metal concentrations and lowered pH of Tar Creek have had an effect on the surrounding plant communities and soils, samples of grass (*Festuca* sp.), sumac (*Rhus glabra* L.), and soil were collected in May 1984 at nine sites along Tar Creek from above the mining area (site 1, fig. D-8) to its confluence with the Neosho River (site 9, fig. D-8). Eight of the sites (2 through 9) were chosen in conjunction with studies on the microbiology (chapter IVB) and geochemistry (chapter IVA) of Tar Creek. Samples were also collected at four sites located at geometrically increasing distances from a major borehole discharge point close to site 4 (fig. D-9). In addition, samples of pasture grass (*Andropogon* sp.), wheat (*Triticum* sp.), and soil were collected at geometrically increasing distances along a traverse starting at site 6 (fig. D-8).

The plant samples were collected by clipping the terminal 18 to 30 cm of sumac and the above-ground portion of grass and wheat with stainless steel clippers and storing the plant materials in cloth bags. The unwashed plant materials were dried at 50 °C for 1 week in a forced air oven, ground with a standard Wiley² mill, and a split of the homogenized ground material was ashed at 450 °C.

Approximately one-third of the samples of each of the 3 sample sets (Tar Creek, 9 samples; borehole area, 4 samples; and traverse, 6 samples) were chosen randomly and split into two parts to determine variation due to analytical methods according to sampling design and statistical reduction of data procedures recommended by Miesch

(1976). The entire suite of samples was then randomized and submitted for analysis.

The soils were collected as close as possible to the sampled plants by first scrapping off the surface debris, then digging the next 12 cm of soil with a stainless steel trowel. The soils were also collected in cloth sample bags, and preparation for analysis is underway.

Major, minor, and selected trace elements of all vegetation samples were determined by inductively coupled plasma emission spectroscopy (ICP/ES), similar to methods developed by Motooka and Sutley (1982). After the plant ash was mixed to ensure homogeneity, 500 mg of ash was placed in a 150-mL beaker, and 10 mL of concentrated nitric acid was added. The samples were slowly evaporated to dryness on a low-temperature hot plate. The solubilized salts were dissolved in a 20.0 mL of 20 percent hydrochloric acid solution and filtered to remove any undissolved solids; the resulting solutions were analyzed by ICP/ES.

Analytical results for 24 elements are erratic and disappointing; duplicate analyses of the same samples are not comparable, as illustrated in table D-1.

Table D-1. — Analysis of two samples of vegetation and their duplicate by inductively coupled plasma-emission spectroscopy

[ppm = parts per million]

	Calcium, percent	Manga- nese, ppm	Lead, ppm	Zinc, ppm
Grass sample	25	448	288	> 4,000
Duplicate	40	226	< 8	281
Sumac sample	21	300	39	1,533
Duplicate	4	753	202	> 4,000

¹U.S. Geological Survey, Denver, Colo.

²The use of tradenames in this report is for identification purposes only and does not constitute endorsement by the U.S. Geological Survey.

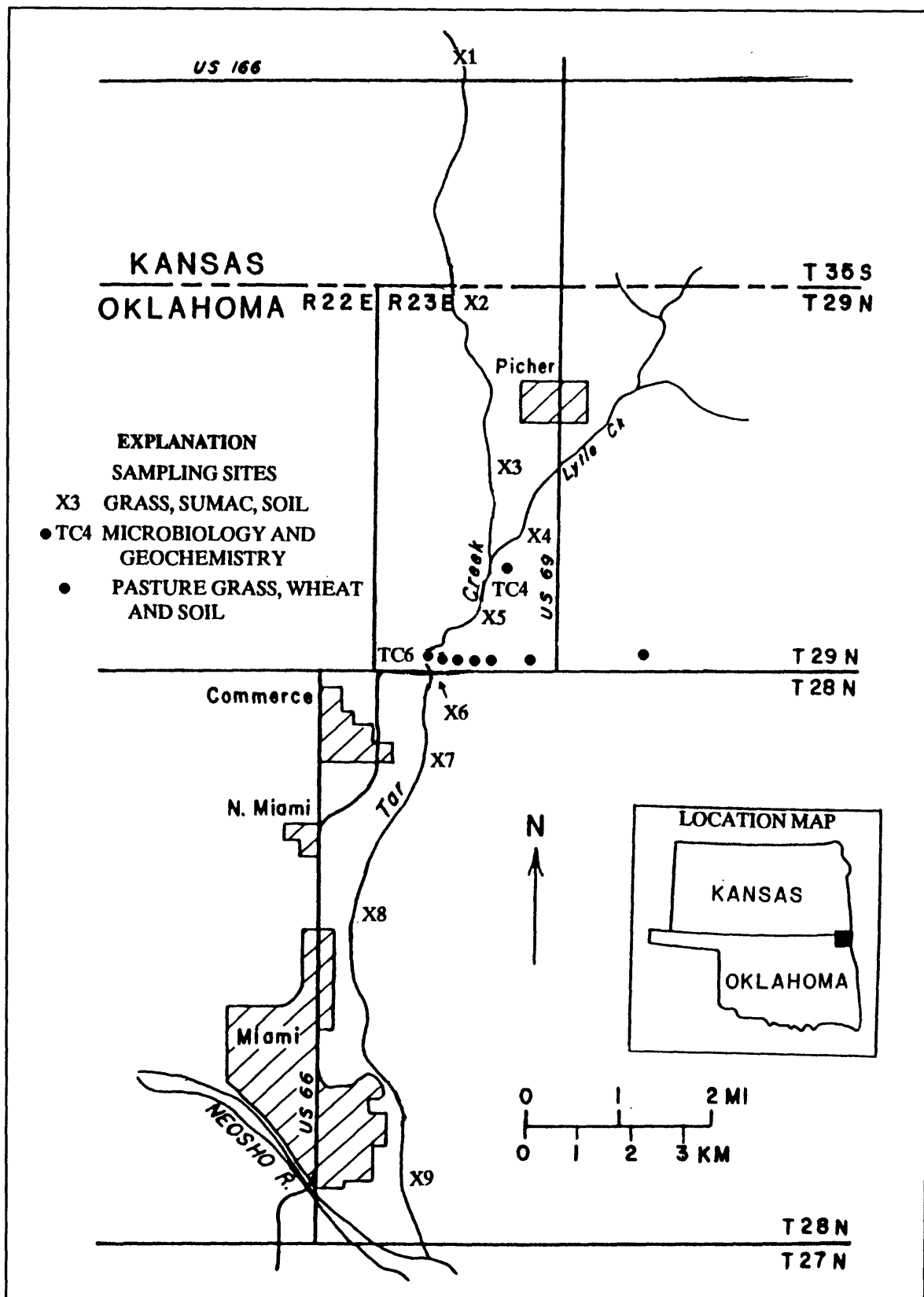


Figure D-8. – Tar Creek study area and location of sampling sites. (Modified from Adams, 1980.)

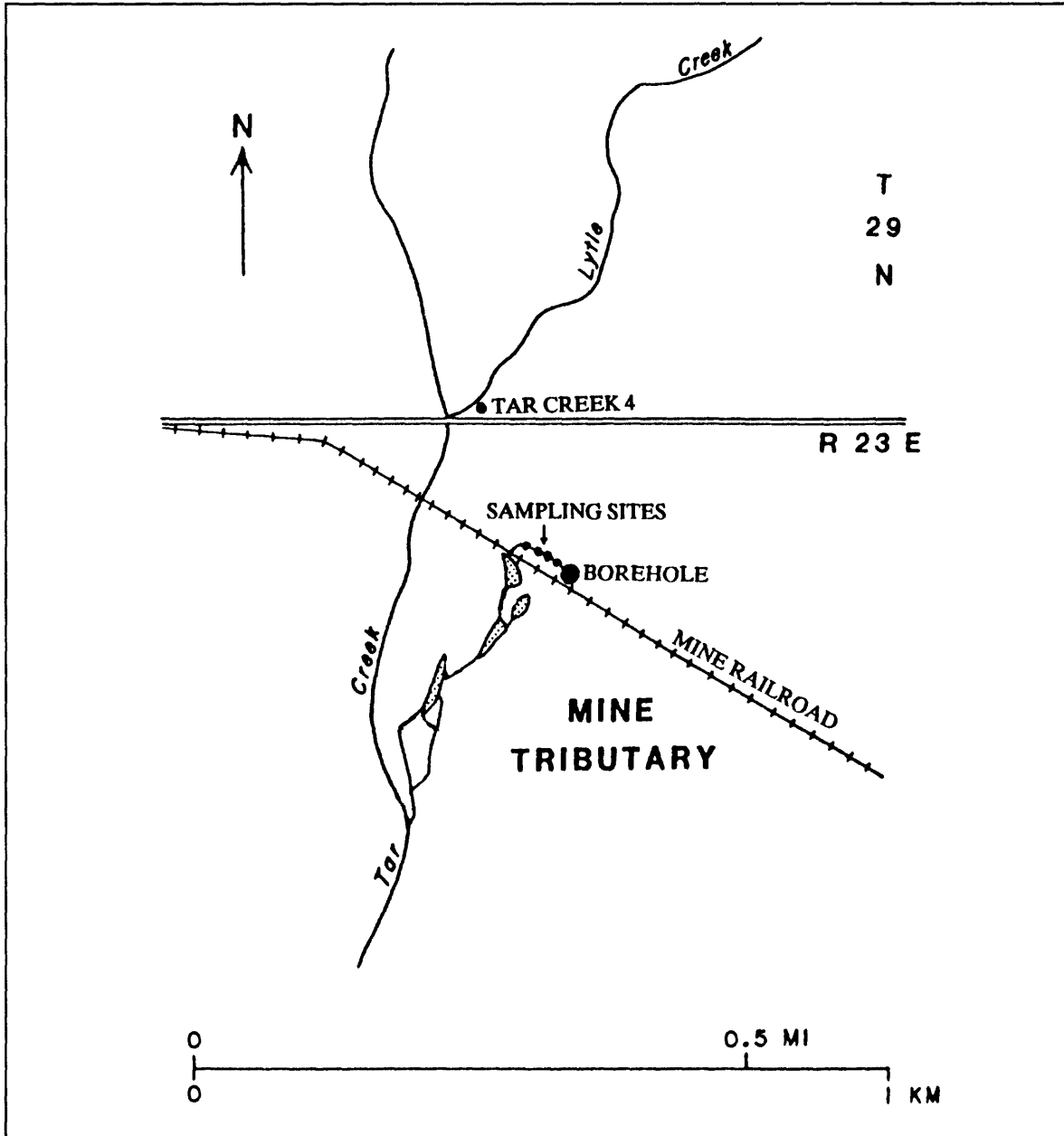


Figure D-9.— Location of sampling sites near borehole discharge.

The high zinc concentrations in some of the samples might be either contaminating and/or interfering with the ICP/ES; therefore, the use of atomic-absorption spectrophotometry (AAS) might increase precision (T. Harms, U.S. Geological Survey, oral commun., 1985). To test atomic absorption as a valid analytical method, a

subset of samples was chosen and a 25-mg sample of the plant ash weighed. Dilute nitric acid was added, and the samples were heated in a water bath for 1 hour. The samples were then cooled, diluted to 10.0 mL with water, mixed, centrifuged, and the amount of zinc measured. These duplicate samples show greater precision than the same

samples analyzed by ICP/ES (table D-2); the zinc analyses by AAS for all samples are pending. When all zinc results are complete, As, Cd, Co, Cu, Pb, Ni, Mo, Fe, Mg, and Mn concentrations will also be determined by AAS.

Table D-2.—Zinc analyses of three samples of grass, one sample of sumac, and their duplicates by atomic absorption spectrophotometry.

Sample	Zinc concentration, ppm
Grass	
Sample 1	18,000
Duplicate	13,000
Sample 2	270
Duplicate	290
Sample 3	5,300
Duplicate	5,200
Sumac	
Sample	3,400
Duplicate	3,100

In conclusion, zinc concentrations for grass and shrubs reported in the literature typically

average 690 and 1,560 ppm, respectively (Gough, 1979). Comparison of these averages with the high zinc values for grass and sumac in the Tar Creek area (table D-2) indicates that the water of Tar Creek has affected the surrounding vegetation. A complete assessment of this effect is underway.

REFERENCES CITED

- Adams, J.C., 1980, Tar Creek water quality reconnaissance regarding ground water discharge from abandoned lead and zinc mines of Picher Field, Ottawa County, Oklahoma: Oklahoma Water Resources Board Publication no. 100, 23 p.
- Gough, L.P., Shacklette, H.T., and Case, A.A., 1979, Element concentrations toxic to plants, animals, and man: U.S. Geological Survey Bulletin 1466, 80 p.
- Miesch, A.T., 1976, Geochemical survey of Missouri—Methods of sampling, laboratory analysis, and statistical reduction of data: U.S. Geological Survey Professional Paper 954-A, 39 p.
- Motooka, J.M., and Sutley, S.J., 1982, Analysis of oxalic acid leachates of geologic materials by inductively coupled plasma, atomic emission spectroscopy: *Applied Spectroscopy*, v. 36, no. 5, p. 524–533.

CHAPTER E. – METALS IN GROUND WATER

	Page
Geohydrologic setting of the Miami Wash-Pinal Creek acidic ground-water study area near Globe, Arizona, by J.H. Eychaner.....	E-3
Neutralization of acidic ground water in eastern Arizona, by K.G. Stollenwerk.....	E-7
Arsenic species in ground water and pore waters in stream sediments affected by mine drainage in Montana and Colorado, by W.H. Ficklin and J.L. Ryder.....	E-9
Arsenic in an alluvial-lacustrine aquifer, Carson Desert, western Nevada, by A.H. Welch and M.S. Lico.....	E-13
Hydrogeochemistry of uranium and associated elements at abandoned uranium mines in western North Dakota, by R.L. Houghton, R.L. Hall, J.D. Unseth, J.D. Wald, G.S. Anderson, and S.R. Hill.....	E-19

ILLUSTRATIONS

	Page
Figure	
E-1. Map showing major geographic features of Miami Wash-Pinal Creek study site near Globe, Arizona.....	E-4
E-2. Map showing locations of study sites on Clark Fork River, Montana, and Clear Creek, Colorado.....	E-10
E-3. Graph showing arsenic concentrations in pore water at 10-cm intervals in two sediment cores from Clark Fork River, Montana.....	E-11
E-4. Map showing location of Dodge Ranch site in Carson Desert, western Nevada.....	E-14
E-5. Map showing location of wells, piezometers, soil-water samplers, and staff gages at Dodge Ranch.....	E-15
E-6. Vertical section A-A' showing: (A) lithology with dissolved arsenic concentrations in February 1985, and (B) ground-water zones at Dodge Ranch.....	E-16
E-7. Map showing location of abandoned uraniumiferous lignite mines and associated uraniumiferous lignite deposits in Montana, North Dakota, and South Dakota.....	E-20
E-8. Gamma-ray log of subsurface in uraniumiferous lignite area, western North Dakota.....	E-22

TABLES

	Page
Table	
E-1. Speciation of elements in contaminated ground water.....	E-7
E-2. Concentration of radioactive and selected associated constituents in mine-affected and unaffected aquifer settings.....	E-21

CHAPTER E. — METALS IN GROUND WATER

GEOHYDROLOGIC SETTING OF THE MIAMI WASH-PINAL CREEK ACIDIC GROUND-WATER STUDY AREA NEAR GLOBE, ARIZONA

By James H. Eychaner¹

Water that contains elevated concentrations of dissolved metals and sulfate at pH 3.6 is moving through a shallow alluvial aquifer and interacting with surface streams near Globe, Ariz. (fig. E-1). The water has contaminated public water supplies, and discharge from the aquifer to a stream has the potential to degrade public supplies for Phoenix, Ariz., 130 km west of the study area. A major source of the contamination is leakage from acid ponds (Envirologic Systems, Inc., 1983, p. 10) through piles of copper-mine waste and tailings that are emplaced on the aquifer (fig. E-1).

The objectives of the study are to describe the physical and chemical characteristics of the system, to estimate the chemistry of future stream outflow, and to evaluate models of the transport of reactive constituents in ground water. The study began in May 1984 and is to be completed in March 1988.

The study area is in the Basin and Range province in a highland valley that drains to the north (Peterson, 1962). Quaternary alluvium 300 to 800 m wide, 17 km long, and as much as 50 m thick forms the valley floor. Gila Conglomerate (Tertiary and Quaternary age) underlies the alluvium and crops out on adjacent slopes. The conglomerate is 100 to 1,200 m thick and as much as 5 km wide. The alluvium and conglomerate form a single aquifer, which is structurally bounded by impermeable diabase, granite, and welded tuff. Extensive porphyry copper deposits are found in the granite southwest of the valley and have been mined for more than 70 years.

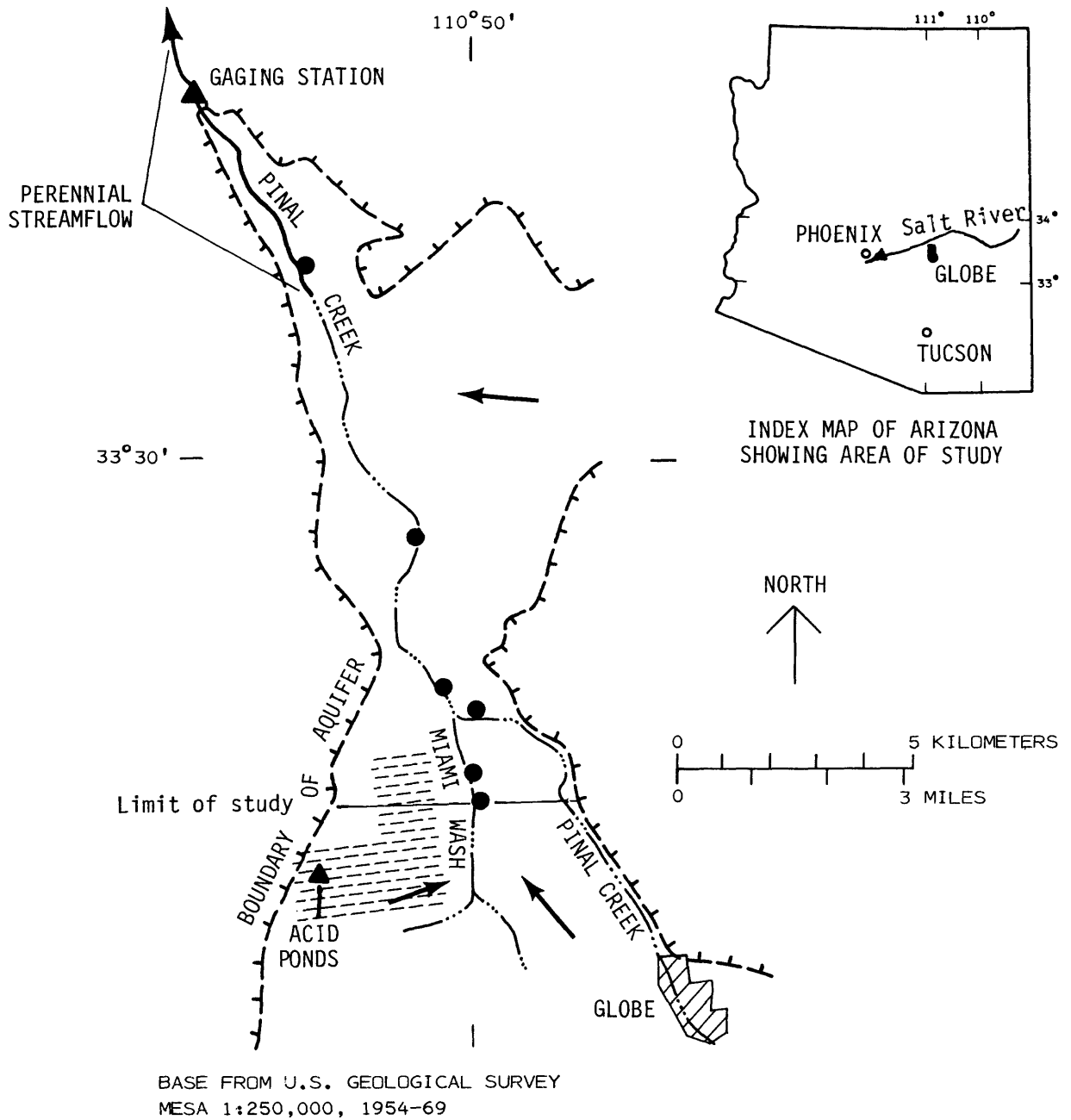
About 0.3 m³/s of water flows through the aquifer and forms a perennial stream at its downstream boundary. Dissolved-solids concentration of the outflow has increased about 70 mg/L annually since 1979 and reached 3,000 mg/L in 1984. This rate of increase is consistent with data from

ground-water samples collected nearby in 1942, 1963, and 1982. Dissolved manganese increased from 0.5 mg/L in 1979 to 15 mg/L in 1984. Ground-water samples in the upstream part of the area contain as much as 16,000 mg/L dissolved solids, including 10,400 mg/L sulfate, 3,200 mg/L iron, 150 mg/L copper, and 73 mg/L manganese. Cadmium, cobalt, lead, lithium, nickel, and vanadium are present, but arsenic, chromium, and molybdenum have not been detected. The contamination is primarily in the alluvium, although the conglomerate is also contaminated to an unknown depth below the alluvium. Water upgradient in the conglomerate is a sodium-calcium-bicarbonate type containing about 400 mg/L dissolved solids.

As the acidic water reacts with calcite and other minerals in the aquifer, pH rises, and many metals become less soluble. This neutralization can continue until the calcite supply in the affected flow tube is exhausted. The increased calcium level causes gypsum to precipitate. Where acidic water reaches the surface, ferric hydroxide precipitates and probably adsorbs other metals. Intermittent runoff in the sand channels of Miami Wash and Pinal Creek can transport the precipitate out of the study area. Manganese oxide precipitates have been found in the perennial-flow reach of Pinal Creek.

Streamflow in the upstream part of the area is generally ephemeral; two reaches contain interrupted flow. For the first 6 months of 1985, however, streamflow was continuous through the valley, and outflow was about 1.1 m³/s. Recharge to the aquifer during this period raised water levels in wells by as much as 3.5 m, and some levels rose to 1 m below land surface. Concurrent streamflow measurements and water samples were taken at 11 sites during high flow in March and again during low flow in August of 1985.

¹U.S. Geological Survey, Tucson, Arizona



EXPLANATION

- OBSERVATION-WELL SITE
- GENERALIZED DIRECTION OF GROUND-WATER FLOW
- WASTE AND TAILINGS PILES

Figure E-1.— Major geographic features of Miami Wash-Pinal Creek study site near Globe, Arizona.

Sixteen observation wells were drilled in October 1984 at five sites to depths ranging from 11 to 59 m. The wells were completed with 0.9-m screens and solvent-welded 102-mm PVC casing. Samples have been collected quarterly and analyzed for inorganic constituents. Additional drilling began in December 1985 to locate the bottom of the contaminated zone and to collect minimally disturbed samples of the aquifer.

The Miami Wash-Pinal Creek site is attractive for research because of the heavy contaminant load and the wide range of chemical and hydrologic conditions within a small area. Research topics that may be addressed in the study include (1) the local variability of neutralization capacity, (2) the effects of ground-water/surface-water

interactions on dispersion and neutralization of contaminants, (3) pathways for secondary removal of contaminants, and (4) evidence in woody vegetation of historically contaminated locations.

REFERENCES CITED

- Envirologic Systems, Inc., 1983, Mining activities and water quality report: Florence, Arizona, Central Arizona Association of Governments Mineral Extraction Task Force Report METF-7, 142 p.
- Peterson, N.P., 1962, Geology and ore deposits of the Globe-Miami district, Arizona: U.S. Geological Survey Professional Paper 342, 151 p.

NEUTRALIZATION OF ACIDIC GROUND WATER IN EASTERN ARIZONA

By Kenneth G. Stollenwerk¹

This discussion of chemical reactions occurring in the Miami Wash-Pinal Creek valley near Globe, Ariz., is a continuation of the preceding article.

Sulfate is the major constituent of the contaminated ground water at the Miami Wash-Pinal Creek valley site. Calculations made with the computer program PHREEQE (Parkhurst and others, 1980) show that sulfate complexes dominate the chemistry of contaminated ground water in the study area. (See table E-1.)

Table E-1. — *Speciation of elements in contaminated ground water*

Species	Percent
Ca ²⁺	54
CaSO ₄ ⁰	46
Mg ²⁺	55
MgSO ₄ ⁰	45
Na ⁺	93
NaSO ₄ ⁻	7
Al ³⁺	16
AlSO ₄ ⁺	39
Al(SO ₄) ₂ ²⁻	45
Fe ²⁺	58
FeSO ₄ ⁰	42
Mn ²⁺	56
MnSO ₄ ⁰	43
Cu ²⁺	53
CuSO ₄ ⁰	47
Ni ²⁺	54
NiSO ₄ ⁰	46
Co ²⁺	50
CoSO ₄ ⁰	50
Zn ²⁺	41
ZnSO ₄ ⁰	41
Zn(SO ₄) ₂ ²⁻	18
Cd ²⁺	32
CdSO ₄ ⁰	36
Cd(SO ₄) ₂ ²⁻	22

The solubility product is exceeded for the following minerals in the most contaminated part of the aquifer: alunite (KA₁₃(SO₄)₂(OH)₆), jurbanite (AlOHSO₄ • 5H₂O), jarosite (Na, K, H)Fe₃(SO₄)₂(OH)₆, gypsum (CaSO₄ • 2H₂O), chalcedony (SiO₂), and pryophyllite (Al₂Si₄O₁₀(OH)₂).

Initially, some question was raised as to whether all elements were in true solution. Oxyhydroxides of Al, Fe, and Mn often pass through a 0.45-μm filter (Hem and others, 1973; Kennedy and others, 1974). As a result, erroneously high concentrations may be measured. During the first sampling trip, ground water from each well was successively filtered through 0.4-μm, 0.1-μm, and 0.3-μm membranes and analyzed for dissolved constituents. No difference (within analytical error) was found in the concentration of Al, Fe, or Mn in any of the filtrates from any of the wells. Thus, any particulate Al, Fe, and Mn present in ground water from the study area is retained by the 0.4-μm filter. Sulfate complexes with Al, Fe, and Mn appear to be important in preventing formation of the colloidal oxyhydroxides noted in the studies cited above.

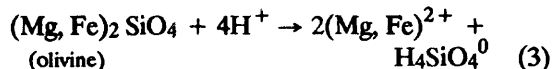
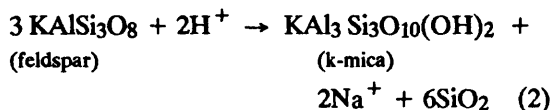
Constituents of the contaminated ground water that may adversely affect the environment, in addition to low pH, include high total dissolved solids, Al, Cu, Co, Cd, Fe, Ni, and Zn. Several reactions are important for removing these constituents from solution.

The following three types of reaction are important for neutralization of H⁺:

1. Reaction with carbonate minerals in alluvium:



2. Reaction with silicate minerals:



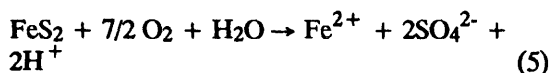
¹U.S. Geological Survey, Denver, Colorado

3. Reaction with bicarbonate in uncontaminated ground water:



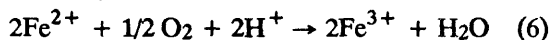
Neutralization of H^+ by carbonate minerals and HCO_3^- is relatively fast. Reaction of H^+ with silicate minerals proceeds at a much slower rate. Petrographic examination of alluvium from the contaminated zone shows extensive alteration of silicate minerals to clay minerals. The relative importance of reactions 1 through 4 is unknown at this time.

Because contaminated ground water contains high concentrations of iron, reactions involving iron have a significant effect on the composition of ground water in the study area. The original acidity of the ground water is a result of sulfide mineral oxidation:



Reaction 5 also provides a significant amount of the Fe^{2+} and SO_4^{2-} in contaminated ground water.

After ground water leaves the sulfide-rich source area, oxidation of Fe^{2+} is an additional, relatively continuous source of H^+ :



Two moles of H^+ are produced for every mole of Fe^{2+} oxidized and precipitated as $\text{Fe}(\text{OH})_3$. Contaminated ground water contains approximately 0.3 mmol/L H^+ . Oxidation of Fe^{2+} will result in an additional 116 mmol/L H^+ . Stumm and Morgan (1970) show that the rate of Fe^{2+} oxidation decreases as H^+ increases. Thus, unless the H^+ produced by reaction 7 is neutralized, reaction 6 becomes slow, and Fe^{2+} will persist in contaminated ground water, even in the presence of O_2 . Only 15 percent of the Fe^{2+} in ground water stored in plastic bottles in the laboratory (exposed to atmospheric O_2) was oxidized to Fe^{3+} in 140 days. The pH after 140 days had dropped to 2.5.

Sulfate and iron form about 75 percent of the dissolved solids in contaminated ground water. Calcium released from CaCO_3 during neutralization of H^+ reacts with SO_4^{2-} to form $\text{CaSO}_4 \bullet 2\text{H}_2\text{O}$. Gypsum crystals are abundant in alluvium collected from the contaminated part of the aquifer. The primary mechanism for removal of Fe from solution is oxidation to Fe^{3+} and precipitation of $\text{Fe}(\text{OH})_3$.

Aluminum sulfate minerals such as jurbanite and alunite control the concentration of Al in contaminated ground water. As pH increases and SO_4 decreases, kaolinite and gibbsite become important in limiting Al in solution. Cu, Co, Ni, Zn, and Cd are undersaturated with respect to the mineral phases tested in PHREEQE. Adsorption by, and coprecipitation with, oxyhydroxides are two likely controls on their concentration in contaminated ground water.

In addition to the aforementioned reactions, dilution could be a significant factor in reducing the acidity and concentration of constituents in the contaminant plume. The magnitude of this effect is not currently known, however.

REFERENCES CITED

- Hem, J.D., Roberson, C.E., Lind, C.J., and Polzer, W.L., 1973, Chemical interactions of aluminum with aqueous silica at 25 °C: U.S. Geological Survey Water-Supply Paper 1827-E, 57 p.
- Kennedy, V.C., Zellweger, G.W., and Jones, B.F., 1974, Filter pore-size effects on the analysis of Al, Fe, Mn, and Ti in water: *Water Resources Research*, v. 10, no. 4, p. 785-790.
- Parkhurst, D.L., Thorstenson, D.C., and Plummer, L.N., 1980, PHREEQE—A computer program for geochemical calculations: U.S. Geological Survey Water-Resources Investigations Report 80-96, 210 p.
- Stumm, Werner, and Morgan, J.J., 1970, *Aquatic chemistry*: New York, John Wiley and Sons, Inc., 583 p.

ARSENIC SPECIES IN GROUND WATER AND PORE WATERS IN STREAM SEDIMENTS AFFECTED BY MINE DRAINAGE IN MONTANA AND COLORADO

By Walter H. Ficklin¹ and Jean L. Ryder¹

Stream sediments have accumulated immediately upstream of a small hydroelectric dam on the Clark Fork River at the confluence of the Clark Fork and Blackfoot Rivers, Mont. (fig. E-2). The dam is the first obstruction along the Clark Fork. The small town of Milltown lies immediately across Interstate Highway 90 from the accumulated sediments. Arsenic (0.6 mg/L) was found in a sample of well water from a Milltown water supply; the source of the arsenic is the accumulated sediments in the reservoir upstream of the dam (Woessner and others, 1984).

The dissolution of the arsenic from these sediments into the ground water provides an ideal situation for the study of the mobility and stability of arsenic in the aqueous environment. Wood (1974) proposed a mechanism for methylation of arsenic in aquatic systems. In 1983, 20 ground-water samples from wells placed in the accumulated sediment were analyzed for total arsenic, arsenic (III), arsenic (V), and the two anticipated methylated arsenic compounds. No methylated arsenic compounds were detected. Arsenic (III) was the most abundant species, but arsenic (V) was present in all but one sample. One sample from a well beyond the accumulated sediments contained only arsenic (V). The highest concentration of total arsenic in the ground-water samples was 9.8 mg/L; the concentration of arsenic (III) in the same samples was 6.9 mg/L. The U.S. Environmental Protection Agency's recommended limit for arsenic in drinking water is 0.05 mg/L (Lederer and Fensterheim, 1983). Eight of the wells were sampled again in June 1985. A similar pattern of arsenic (III) and arsenic (V) was found in the water, but no organic arsenic acids were detected. Two sediment cores were also collected in June 1985; one (core 3) was 110 cm long; the other (core 5) was 120 cm long (fig. E-3). Each core was divided into 10-cm sections and the pore water extracted under nitrogen pressure.

Total arsenic concentration in the pore water of both cores increased with depth, then abruptly decreased (fig. E-3). The sulfate concentration in the pore water of core 5 was as great as 400 mg/L; that in core 3 was only 3 mg/L. Sulfate concentration in the well water showed a similar pattern; that is, the sulfate concentration seems to decrease in the direction of the ground-water flow.

Arsenic occurs in the pore water at the same depth at which iron concentrations increase. Arsenic (III) and arsenic (V) concentrations in the pore water were measured. The pore water of core 5 contained a mixture of arsenic (III) and arsenic (V), whereas water from core 3 contained a mixture of arsenic (III) and arsenic (V), but only to the depth at which arsenic concentration decreases; below that point all of the arsenic is arsenic (III).

One of the steps in the sequence of microbially mediated processes in aquatic systems is the reduction of iron (III) to iron (II) (Stumm and Morgan, 1981). When iron is reduced, adsorbed arsenic is released. The released arsenic may be partly reduced to arsenic (III), assuming that all released arsenic was originally present as arsenic (V). The concentration of each species may be controlled by the redox potential of the system.

Arsenic occurs in several types of mineral deposits and also in acid mine waters. The arsenic in the Milltown sediments may be an accumulation of products from acid mine drainage, adsorption of arsenic by iron hydroxides, and unoxidized mine tailings. Similar acid mine drainages occur in the Colorado mineral belt. This is closer to the U.S. Geological Survey's Central Laboratories and was judged appropriate for the study of the chemical nature of arsenic as it occurs in acid mine drainages and in the bottom material of streams in mining areas.

Chemical analysis of water flowing from three mines near Denver, Colo., (fig. E-2), and of other

¹U.S. Geological Survey, Denver, Colorado

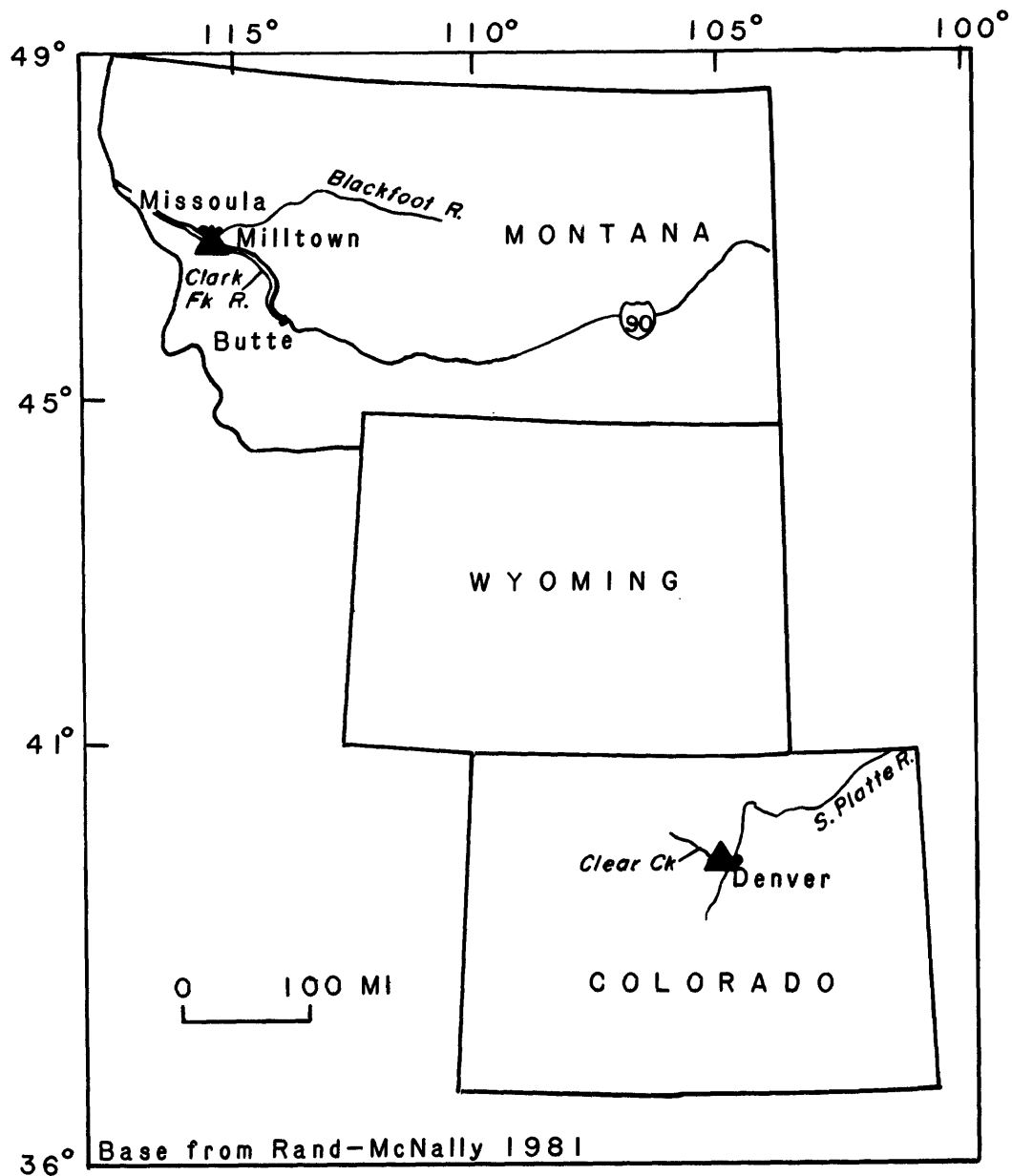


Figure E-2. — Locations of study sites on Clark Fork River, Montana, and Clear Creek, Colorado.

iron-rich waters, shows that all arsenic occurs as arsenic (III), even though the waters are highly oxidizing. Acid mine waters precipitate iron compounds. If the pH of the water is greater than 3.5, the precipitated iron compounds immediately beneath the water contain a mixture of arsenic (III) and arsenic (V) when the precipitate is dissolved

in 0.2 M ammonium oxalate/oxalic acid buffer. The precipitated iron compound (about 1 g) was placed in 50 mL of the buffer at the time of sample collection to prevent changes in the oxidation state of the arsenic from storage. The preweighed bottle of buffer was weighed again after addition of the sample. To obtain the dry weight of the

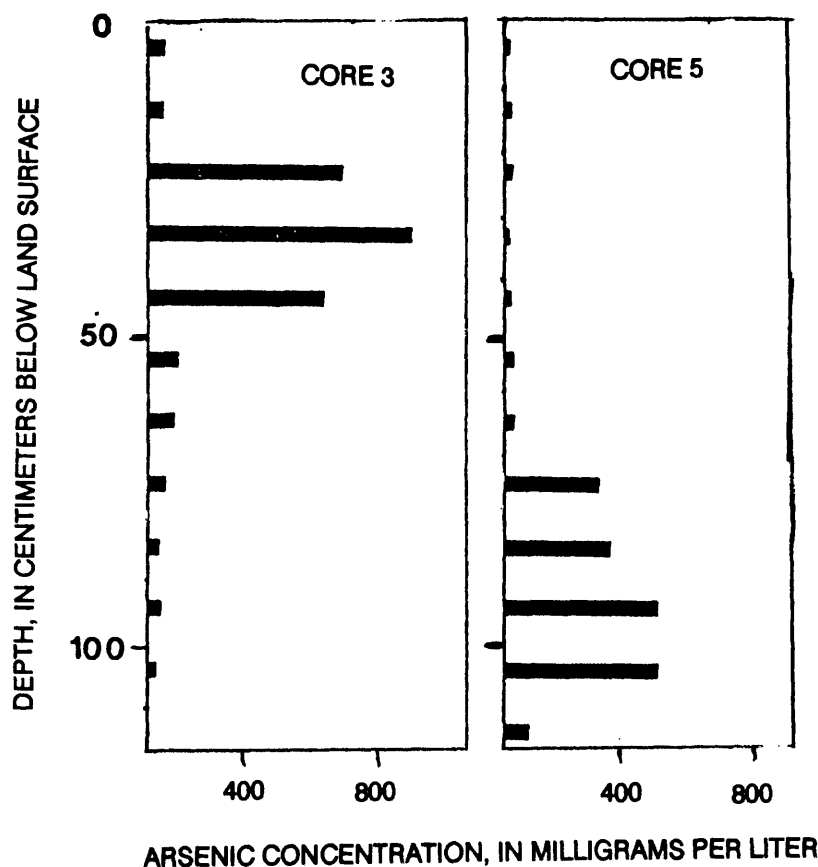


Figure E-3. — Arsenic concentrations in pore water at 10-cm intervals in sediment cores from Clark Fork River, Montana.

sample, an additional sample of the iron compound was collected and dried to determine the water content. The arsenic concentration in the buffer was determined after 24 hours of shaking.

Stream sediments in Clear Creek (Jefferson and Clear Creek Counties, Colo., fig. E-2) should be similar to those in the Clark Fork River, Mont. Clear Creek drains an extensive mining area where acid mine waters drain into the stream and where numerous piles of mine waste occur. Stream bed samples were collected from the stream along the 80-km reach from near its source to near its confluence with the South Platte River. "Available arsenic" concentrations as great as 10 mg/g and 20 mg/g total arsenic were found. The concentration of arsenic in the stream water was less than the detection limit of the analytical method used (2 mg/L). The bottom material contained no detectable methylarsonate or dimethylarsenite. Attempts to determine arsenic (III) in the same manner as the acid mine precipitates were un-

successful. Loss of arsenic (III) occurs within 24 hours when the oxalate buffer extract is spiked with arsenic (III). The same loss from the acid mine precipitates does not occur within 5 days.

REFERENCES CITED

- Lederer, W.H., and Fensterheim, R.J., 1983, Arsenic: New York, Van Nostrand Reinhold Co., p. 30.
- Stumm, Werner, and Morgan, J.J., 1981, Aquatic chemistry, 2d ed.: New York, John Wiley and Sons, p. 460.
- Woessner, W.W., Moore, J.N., Popoff, M.A., Sartor, L.C., and Sullivan, M.L., 1984, Arsenic source and water supply remedial action study, Milltown, Montana: Helena, Mont., Solid Waste Bureau, Montana Department of Health and Environmental Sciences.
- Wood, J.M., 1974, Biological cycles for toxic elements in the environment: Science, v.183, p. 1049.

ARSENIC IN AN ALLUVIAL-LACUSTRINE AQUIFER, CARSON DESERT, WESTERN NEVADA

By Alan H. Welch¹ and Michael S. Lico¹

Elevated arsenic concentrations (> 0.01 mg/L) are common in ground water of the western United States (Alaska, Arizona, California, Idaho, Nevada, Oregon, and Washington), as indicated by results of an exhaustive survey of available data bases and field sampling (Welch and others, 1985). Natural high concentrations of arsenic appear to be associated with one of four geological environments: alluvial-lacustrine deposits, geothermal systems, volcanic deposits and their derivatives, and mineralized (sulfide-rich) areas, notably gold-bearing deposits (Welch and others, 1985). The most extensively affected environment, in terms of total area, appears to be the alluvial-lacustrine type, where arsenic concentrations as high as several milligrams per liter are attained.

Studies of naturally occurring arsenic in ground water indicate that arsenic exists primarily as an hydroxide anion, either as an oxidized (arsenate) or a reduced (arsenite) species (Cherry and others, 1979, p. 378). Low-molecular-weight, organically bound arsenic compounds can occur naturally in ground water, but limited data indicate that their concentrations are small in comparison to the inorganic arsenic species (Irgolic, 1982, p. 100). The National interim primary drinking water standard for arsenic is 0.05 mg/L in the United States (U.S. Environmental Protection Agency, 1976), in terms of the total concentration of arsenic. Relative arsenic toxicities (oxidation states are in parentheses) are as follows: arsine (-3) $>$ organo-arsine compounds, arsenites (+3), and oxides (+3) $>$ arsenates (+5) and arsonium metals (+1) $>$ native arsenic (0) (Penrose, 1974).

The site selected for study is 90 km east of Reno, Nev., in the arid Carson Desert near Fallon, Nev. (fig. E-4). It is underlain by alluvial-lacustrine deposits and is referred to here as the Dodge Ranch site. The aquifer system at the site consists primarily of unconsolidated sand that is

complexly interbedded and interfingering with finer grained deposits (Morrison, 1964; Glancy, 1981; Olmsted and others, 1984). Glancy (1981) has documented wide local variation in water chemistry in the shallow alluvial aquifer (from land surface to a depth of about 15 m) and notes that dissolved-solids and arsenic concentrations differ greatly over very short distances, both laterally and with depth.

The 0.14-km² Dodge Ranch site consists of a flood-irrigated pasture bounded on three sides by irrigation ditches and drains that, except during irrigation, generally act as drains for the shallow ground water (fig. E-5). Ground-water flow is nearly parallel to the fourth, northern boundary of the roughly square pasture. A thick clay layer underlies the zone of active flow (fig. E-6A). Wells (open to depths of about 3, 6, and 9 m) and soil-moisture samplers were installed approximately along a flow line determined by water-level monitoring in shallow piezometers (open to a depth of about 3 m). Ten wells for sampling, 22 piezometers, 7 soil-moisture samplers, 3 staff gages, and 1 surface-water sampling site were established and monitored in the study area (fig. E-5). Before the application of irrigation water, which is every 2 to 3 weeks during the growing season, depths to the water table have ranged from at or near land surface to 5 m and greater.

The quality of ground water at Dodge Ranch ranges from a dilute type (about 550 mg/L dissolved solids) dominated by calcium and bicarbonate to a moderately saline water (more than 10,000 mg/L) dominated by sodium and chloride. Large changes in arsenic concentration—over 2 orders of magnitude—take place within a lateral distance of only 200 m (fig. E-6B). The residence time of ground water here is approximately 5 years (assuming plug flow). Four ground-water zones can be defined from the major-element chemistry and position in the flow system—the upper, recharge zone; the intermediate zone; the deep zone; and the shallow subsurface at distal end of

¹U.S. Geological Survey, Carson City, Nev.

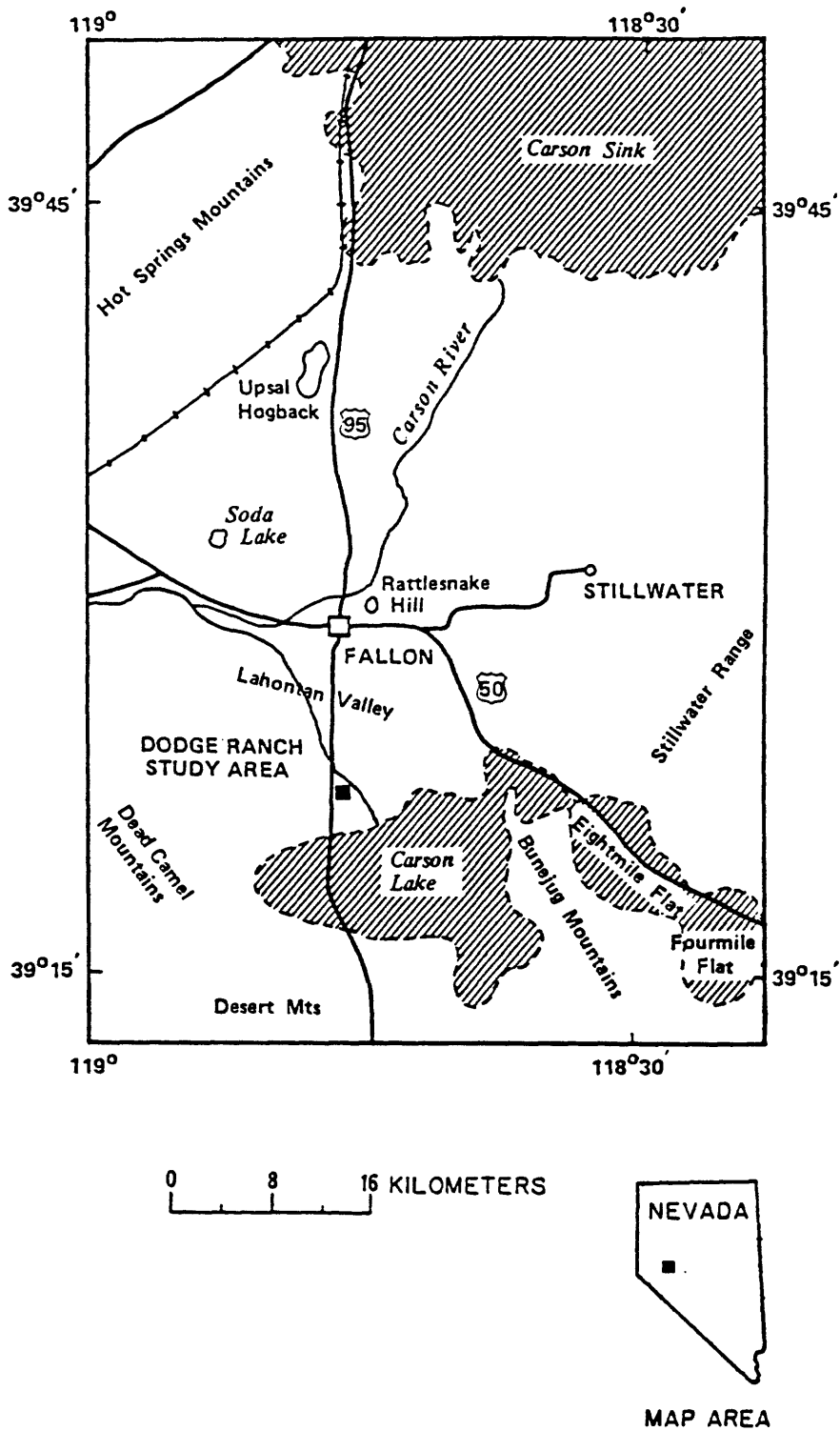


Figure E-4.—Location of Dodge Ranch study area in the southern Carson Desert, western Nevada.

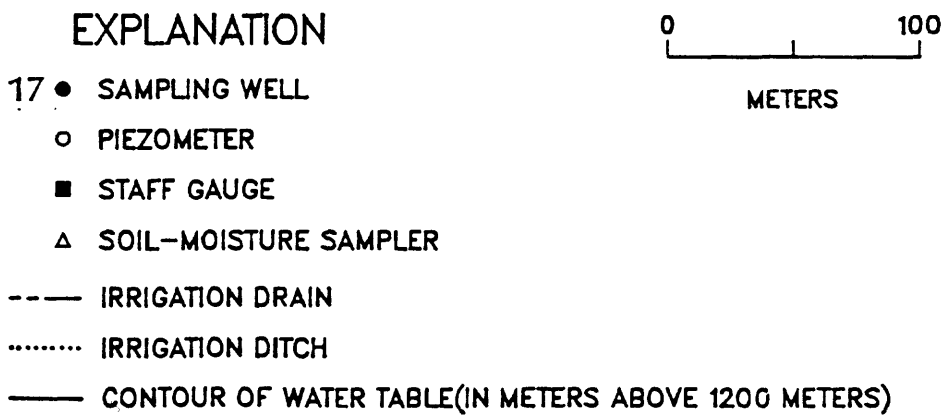
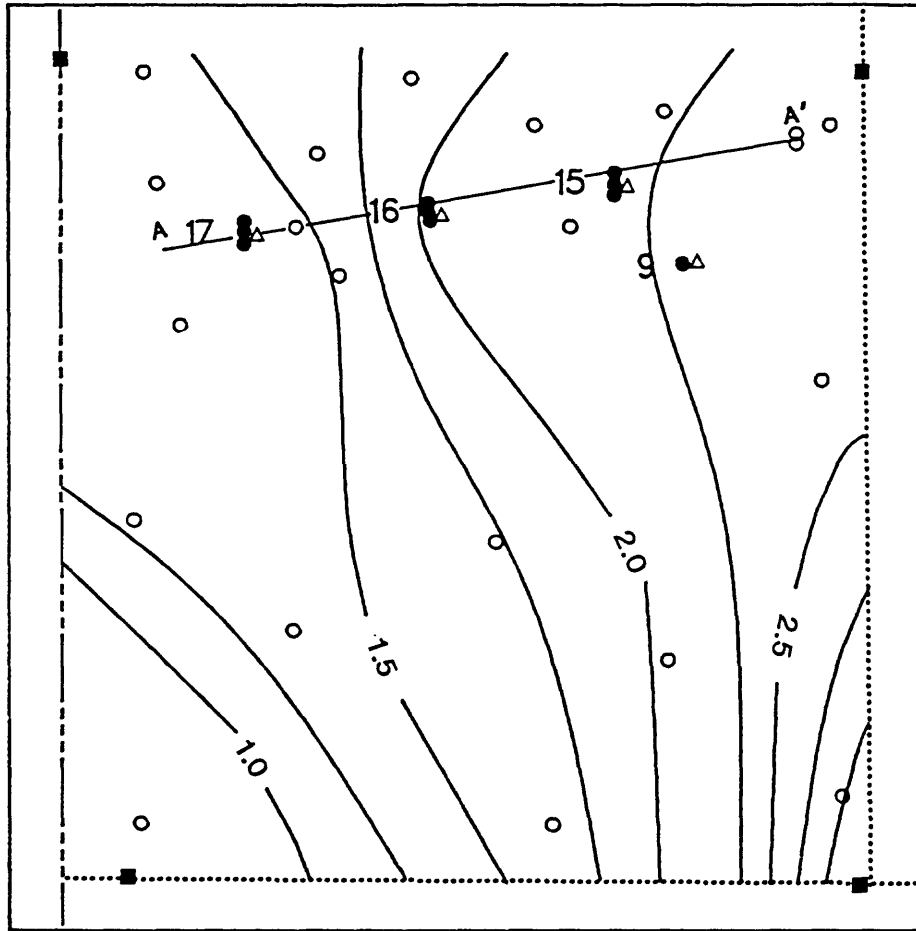


Figure E-5. — Location of wells, piezometers, soil-water samplers, and staff gages at Dodge Ranch.
 (Modified from Lico and others, 1986.)

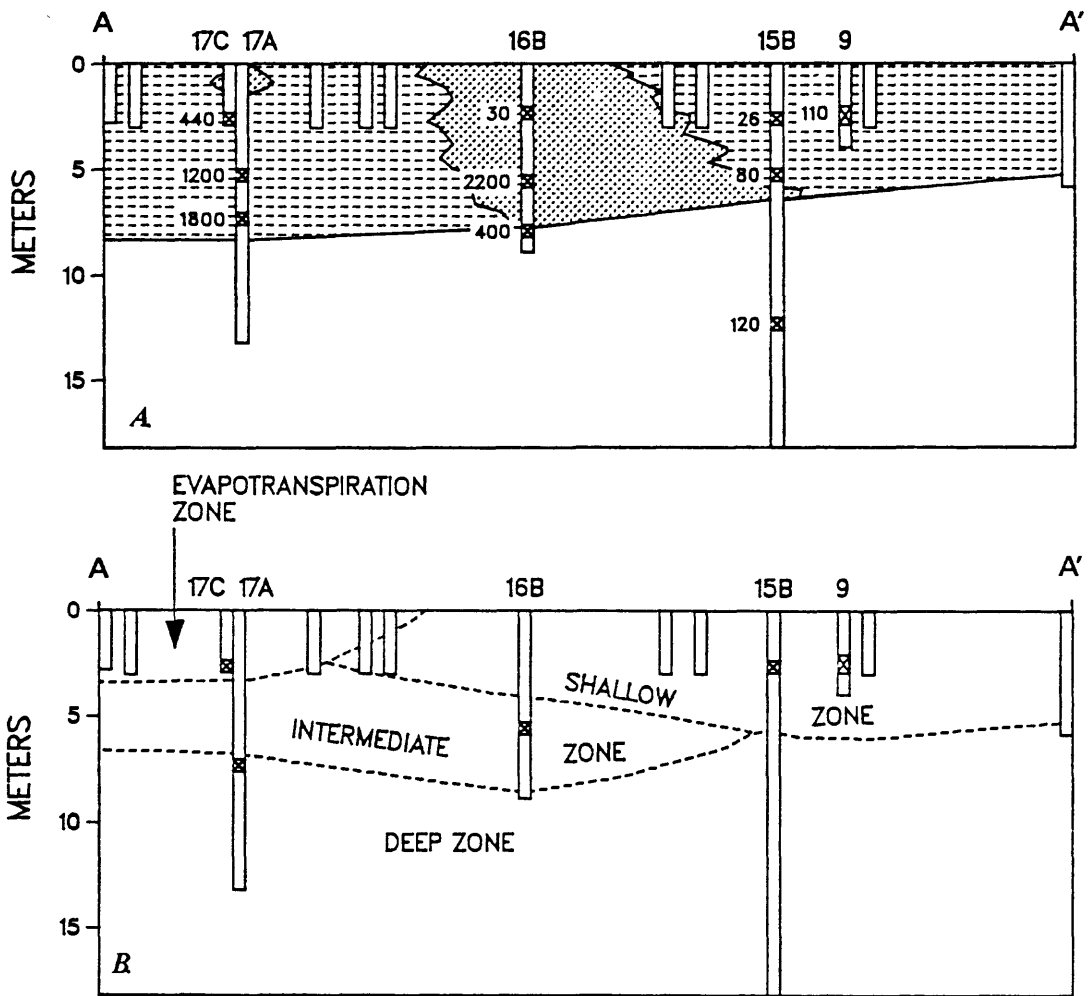


Figure E-6.— Vertical section A–A' showing: (A) lithology with dissolved arsenic concentrations in February 1985, and (B) ground-water zones at Dodge Ranch. Trace of vertical section is shown in figure E-5.

sampled area (fig. E-6). In the upper, recharge zone, the cation chemistry is controlled by exchange with smectite and by calcite solubility in the presence of high carbon-dioxide partial pressures (as high as 0.04 atmosphere and greater). The water in this zone is oxygenated and has arsenic concentrations as high as 0.1 mg/L. As water flows from the upper zone into the underlying intermediate-depth zone, the dissolved-oxygen concentrations decrease while arsenic concentrations remain about the same. The pH in this zone is increased, probably through hydrolysis of alumin-

silicate minerals, and is accompanied by a decrease in total inorganic carbon as a result of calcite precipitation. Within the deepest zone (generally 5 m below land surface), arsenic concentrations up to 2.2 mg/L have been measured. The fourth zone, in the shallow subsurface near the edge of the sampled area, has been affected by evapotranspiration and has arsenic concentrations as high as 0.7 mg/L.

Redox couples yield a fairly wide range in calculated electropotentials because the shallower

part of the system contains dissolved oxygen, and the deeper and more distal parts of the flow system contain dissolved sulfide, arsenite, and ferrous iron. In general, the agreement among the calculated redox values is poor. A systematic variation from the most oxidized to most reduced is: $\text{Fe}^{2+}/\text{Fe}^{3+}$ couple > $\text{As}^{3+}/\text{As}^{5+}$ couple > $\text{S}^{2-}/\text{SO}_4^{2-}$ couple. Platinum-electrode measurements, adjusted by the method of Thorstenson and others (1979), are greater than the values calculated from the arsenic and sulfur couples. The iron couple yields some values greater and some less than those measured with the electrode. The poor agreement between the measured and calculated values is not unusual when redox couples are not in equilibrium, as discussed in detail by Hostettler (1984) and Thorstenson (1984) and as considered by Lindburg and Runnels (1984) from field data. The agreement of the electrode measurements and the arsenic couple with the iron couple improves at higher iron concentrations (from about 0.06 to 0.24 mg/L), but not with higher total arsenic concentrations (which range up to 2.2 mg/L). The difference between the arsenic and iron couples is less (to within about 20 mv) at lower calculated Eh values. Differences calculated for arsenic versus sulfur and for iron versus sulfur decrease as the Eh becomes more negative, but the differences are all greater than 100 mv, with the smallest difference corresponding to the higher arsenic concentrations. Electrochemical disequilibrium obviously exists between the arsenic, iron, and sulfur couples. A consequence of this disequilibrium is that the measured Eh (or any of the other couples) cannot be used to predict the distribution of the inorganic arsenic species from analyses of total arsenic concentration. Analytical speciation is essential if the arsenic chemistry is to be quantitatively evaluated.

Analysis of the aquifer material indicates that arsenic concentrations are generally high (15 mg/L) except in the upper part of the flow system (Lico and others, 1986). X-ray diffraction has not revealed any arsenic minerals, although sulfides (probably as amorphous monosulfides) in the clay below the zone of active flow and ferric oxyhydroxide coatings have been observed visually. Total arsenic concentrations for selected grain sizes and for differing types of grains have been determined in an attempt to identify the sources

(and sinks) for arsenic. In general, grains smaller than very fine sand (.0625 mm) contain high concentrations of arsenic (reaching 20 mg/L); in contrast, the fine- to medium-sand fraction has relatively low concentrations (about 5 mg/L). The largest grain size examined, coarse sand, 0.5 mm, has arsenic concentrations similar to those in the fine-grained fractions. The coarse-sand particles were separated into four classes — quartz, feldspar, and dark and light lithic fragments. The arsenic content of the dark and light lithic fragments and of feldspar grains with ferric-hydroxide coatings was high (10 to 30 mg/L), whereas that of unstained quartz and feldspar was low (3 to 10 mg/L).

Processes that appear to be associated with high arsenic concentrations in the ground water at Dodge Ranch are (1) dissolution of ferric oxyhydroxide, (2) dissolution of manganese oxides, (3) evapotranspiration, (4) oxidation of sedimentary organic matter, and perhaps (5) desorption. Ferric oxyhydroxide and manganese oxides (birnesite, δMnO_2 ; MnOOH) can act as sinks for arsenic (Rai and Zachara, 1984, p. 5–1 to 5–10; Peterson and Carpenter, 1986). Dissolution of these minerals in the upper, recharge zone is indicated by high concentrations of dissolved iron and manganese. Within the intermediate and deep zone, dissolution of manganese oxides is thermodynamically favored, with rhodochrosite (MnCO_3) being at or near saturation. Thus, dissolution of manganese oxides, which were formed under differing geochemical conditions (such as during deposition of the sediments or during periods when the system was more oxidized as a result of a deeper water table) could release arsenic to solution, with the manganese concentrations limited by the precipitation of rhodochrosite. Iron concentrations are near saturation with respect to ferric oxyhydroxide and siderite, FeCO_3 . Dissolution of ferric oxyhydroxide in the two deeper zones may be occurring as a result of the precipitation of siderite (which would decrease the dissolved iron concentrations) due to the increasing greater dissolved inorganic carbon. The presence of high concentrations of dissolved inorganic and organic carbon, particularly in the two deeper zones, are consistent with release of arsenic from sedimentary organic matter.

Field and laboratory studies have led other investigators to conclude that adsorption on ferric oxyhydroxide (and perhaps smectite) can control concentrations of arsenic (Rai and Zachara, 1984, p. 5-1 to 5-10; Peterson and Carpenter, 1986). Laboratory studies suggest that arsenate adsorption is pH-dependent (for both ferric oxyhydroxide and smectite) but is difficult to predict in natural systems because of difficulty in defining the adsorbing phase, the effect of competing anions, and other factors. Phosphate and hydroxide compete with arsenic for adsorption sites on iron oxides and soils. Thus, the fairly high pH of the water at Dodge Ranch (about 7.8 to 9.2), along with arsenic concentrations above 0.4 mg/L and high concentrations of phosphate (about 1 to 9 mg/L as P), are favorable conditions for desorption of arsenic. Arsenic adsorption may, however, be a non-equilibrium process, thus the release of arsenic may require the dissolution of the oxides.

REFERENCES CITED

- Cherry, J.A., Suaikau, A.U., Tallman, D.E., and Nicholson, R.V., 1979, Arsenic species as an indicator of redox conditions in groundwater, *in* Back, William, and Stephenson, D.A., eds., *Contemporary hydrogeology*: Amsterdam, Elsevier, p. 373-392.
- Glancy, P.A., 1981, Geohydrology of the basalt and unconsolidated sedimentary aquifers in the Fallon area, Churchill County, Nevada: U.S. Geological Survey Open-File Report 80-2042, 105 p.
- Hostettler, J.D., 1984, Electrode electrons, aqueous electrons, and redox potentials in natural waters: *American Journal of Science*, v. 284, p. 734-759.
- Irgolic, K.J., 1982, Speciation of arsenic compounds in water supplies: U.S. Environmental Protection Agency Report 600/1-82-010, 107 p.
- Lico, M.S., Welch, A.H., and Hughes, J.L., 1986, Hydrologic, lithologic, and chemical data for sediment in the shallow alluvial aquifer at two sites near Fallon, Churchill County, Nevada, 1984-1985: U.S. Geological Survey Open-File Report 86-250, 43 p.
- Lindberg, R.D., and Runnells, D.D., 1984, Ground water redox reactions: An analysis of equilibrium state applied to Eh measurements and geochemical modeling: *Science*, v. 225, p. 925-927.
- Morrison, R.B., 1964, Lake Lahontan: Geology of southern Carson Desert, Nevada: U.S. Geological Survey Professional Paper 401, 153 p.
- Olnsted, F.H., Welch, A.H., VenDenburgh, A.S., and Ingegritsen, S.E., 1984, Geohydrology, aqueous geochemistry, and thermal regime of the Soda Lakes and Upsal Hogback geothermal systems, Churchill County, Nevada: U.S. Geological Survey Water-Resources Investigations Report 84-4054, 166 p.
- Penrose, W.R., 1974, Arsenic in the marine and aquatic environments: Analysis, occurrence and significance: *CRC Critical Reviews in Environmental Control*, v. 4, p. 465-482.
- Peterson, M.L., and Carpenter, R., 1986, Arsenic distributions in porewaters and sediments of Puget Sound, Lake Washington, the Washington coast and Saanich Inlet, B.C.: *Geochemica et Cosmochimica Acta*, v. 50, p. 353-369.
- Rai, D., and Zachara, J.M., 1984, Chemical attenuation rates, coefficients, and constants in leachate migration: *Electric Power Research Institute Report Ea-3356*, v. 1, 161 p.
- Thorstenson, D.C., 1984, The concept of electron activity and its relation to redox potentials in aqueous geochemical systems: U.S. Geological Survey Open-File Report 84-072, 67 p.
- Thorstenson, D.C., Fisher, D.W., and Croft, M.G., 1979, The geochemistry of the Fox Hills-Basal Hell Creek aquifer in southwestern North Dakota and northwestern South Dakota: *Water Resources Research*, v. 15, p. 1479-1498.
- U.S. Environmental Protection Agency, 1976, National interim primary drinking water regulations: Washington, D.C., U.S. Environmental Protection Agency Office of Water Supply, EPA-570/9-76-003.
- Welch, A.H., Lico, M.S., and Hughes, J.L., 1985, Arsenic in ground water of the western United States (abs.), *in* Second annual Canadian/American Conference on Hydrogeology: Banff, Alberta, June 1985, p. 81.

HYDROGEOCHEMISTRY OF URANIUM AND ASSOCIATED ELEMENTS AT ABANDONED URANIUM MINES IN WESTERN NORTH DAKOTA

By Robert L. Houghton¹, Rowland L. Hall¹, Joseph D. Unseth¹, James D. Wald¹, Garth S. Anderson², and Stephen R. Hill²

The uraniferous lignite deposits of the Paleocene Fort Union Formation of western North and South Dakota and eastern Montana (fig. E-7) were formed when infiltrating water leached uranium and associated elements from volcanic ash beds in the Miocene Arikaree Formation and deposited them in the first underlying, organic-rich, reducing zone encountered. The uranium content of these beds ranges from 0.001 percent to more than 2.1 percent as uranium oxide. In addition to uranium and its radioactive decay products, the lignites are enriched in arsenic, molybdenum, selenium, and vanadium. Oxidation of the uraniferous lignite after subsequent periods of erosion permitted remobilization of much of the uranium to form deposits of uranyl sulfate septahydrate salts in overlying sands (fig. E-8). In general, these highly soluble salts are more radioactive than the underlying lignite.

Between 1955 and 1967, approximately 590,000 lb of uranium oxide were recovered from 95,000 tons of lignite in at least 16 pits in western North Dakota. The overburden was stripped, and the lignite was burned in pit bottoms or nearby kilns to concentrate the uranium in its ash by a factor of about 10. Waste oil and old tires were used to facilitate combustion of the wet, Leonardite-grade lignite. The resultant ash was shipped to processing plants in other States for extraction of the uranium.

Because uranium salts in the overburden generally were not recovered during mining, spoils piles at abandoned mine sites have surface gamma-ray exposure levels as high as 500 microrentgens per hour, approximately 30 times local background levels. Infiltrating water leaches spoils and residual ash and introduces uranium and associated elements such as radium, arsenic, molybdenum, and selenium to water in the lignite

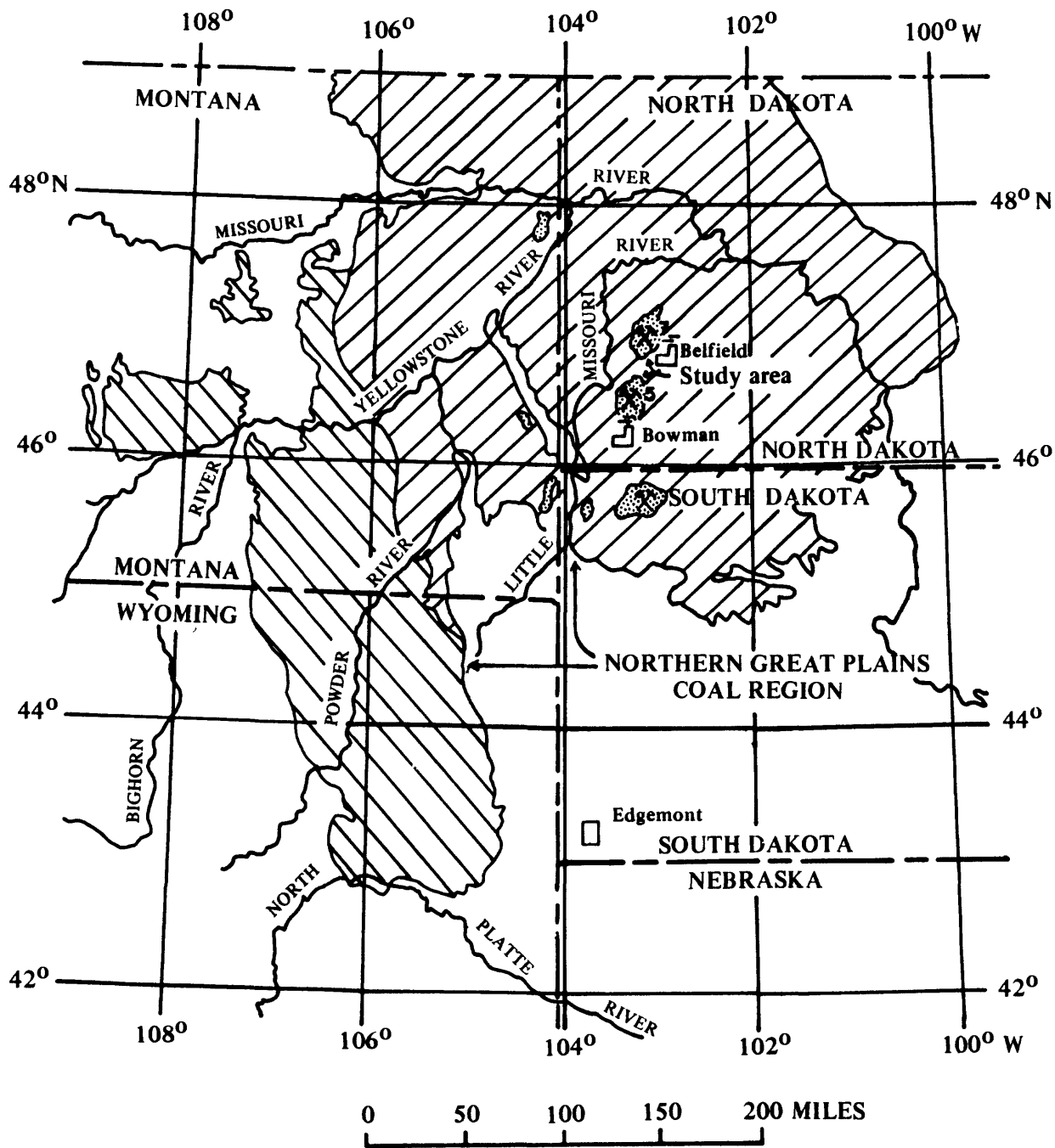
aquifers or exposed in the pits. Aquifer and pit water have uranium concentrations ranging from 12 to 19,000 mg/L and accompanying radium-226 concentrations ranging from 1 to 360 pCi/L (table E-2). Ground water in mine areas also commonly contains concentrations of arsenic, cadmium, manganese, and mercury in excess of Federal drinking-water standards (U.S. Environmental Protection Agency, 1986). Clays below the lignite range from 10 to 80 feet in thickness and generally prevent infiltration to underlying aquifers.

Although the area is sparsely populated, exposure to mine-derived contaminants has been widespread. For example, the mine lakes have long been popular for swimming and frequently have been stocked for fishing. Also, the lignite aquifer has been used locally for domestic and livestock supply; and uranium-rich, sandy spoils have been used in the construction of some new houses in the area, resulting in radon-exposure levels ranging from 10 to 40 times the Federal health standards (U.S. Environmental Protection Agency, 1983b).

Illegal dumping of oil-field wastes and concentrated hydrochloric acid in one mine pit has provided excellent tracers of potential uranium transport through the lignite aquifer. Chloride and gamma-radiation monitors suggest transport rates of 1.2 to 3.5 ft/d under acidic conditions, depending on the extent of fracturing in the lignite and the degree to which it has been oxidized. Availability of uranium to the aquifer for transport is controlled principally by the solubility of the uranium salts and the oxidation state of the system. The pH of reacting water controls uranium speciation in the aquifer but has little effect on the solubility of uranium salts.

¹U.S. Geological Survey, Bismarck, N.D.

²North Dakota Public Service Commission, Bismarck, N.D.



EXPLANATION

	Uraniferous lignite area		Processing mill
	Lignite region		Ashing kiln
	Sub-bituminous region		Abandoned uraniumiferous lignite mine area. Superscript indicates number of mines

Figure E-7. — Location of abandoned uraniumiferous lignite mines and associated uraniumiferous lignite deposits in Montana, North Dakota, and South Dakota.

Table E-2. -- Concentration of radioactive and selected associated constituents in mine-affected and unaffected aquifer settings

[Concentrations are in micrograms per liter except radium-226, which is in picocuries per liter. The drinking-water standard is based on the U.S. Environmental Protection Agency (1983a; 1986)]

Constituent	Number of samples	Minimum value	Maximum value	Mean value	Standard deviation	Drinking-water standard
Lignite aquifer within 4 miles of mine sites						
Arsenic	82	<1	1,500	320	310	50
Cadmium	98	<1	70	15	16	10
Manganese	98	1	23,000	1,120	3,670	50
Mercury	96	<.1	8	4	4	2
Molybdenum	98	1	3,100	203	521	--
Radium-226	98	.2	360	39	94	5
Selenium	98	.6	13	8	5	10
Uranium	98	.2	11,000	849	1,770	--
Vanadium	67	<4	143	16	11	--
Water in mine pits						
Arsenic	32	<1	2,100	340	480	50
Cadmium	32	<1	81	18	29	10
Manganese	32	110	26,000	13,000	5,920	50
Mercury	32	<.1	7	4	5	2
Molybdenum	32	3	1,690	198	265	--
Radium-226	32	.2	273	26	94	5
Selenium	32	11	30	24	5	10
Uranium	32	.8	19,000	3,310	5,780	--
Vanadium	32	<4	138	19	41	--
Lignite aquifers in the uraniferous lignite area more than 4 miles from mine sites						
Arsenic	500	<0.05	19	1.6	2.4	50
Cadmium	500	<1	22	8	10	10
Manganese	500	20	11,000	830	736	50
Mercury	500	<.1	2	.2	1.1	2
Molybdenum	500	<1	84	8.4	11	--
Radium-226	500	<.1	56	6.1	18	5
Selenium	500	<.2	28	.5	1.3	10
Uranium	500	<.02	756	17	51	--
Vanadium	500	<4	139	7.1	14	--

A pilot reclamation project was implemented at one abandoned pit 6 miles northwest of Bel-field, N.D., during the summer of 1985 (fig. E-7). Basically, the reclamation involved the selective replacement of spoils into the pit from which they had been removed. Analyses of drillhole cuttings

and cored spoils obtained from 2-foot depth increments on a 50-foot grid over the 8.2-acre spoils pile were used to identify spoils with radium-226 concentrations exceeding 5 pCi/g above background levels or with uranium concentrations exceeding 5 times background levels; and these were

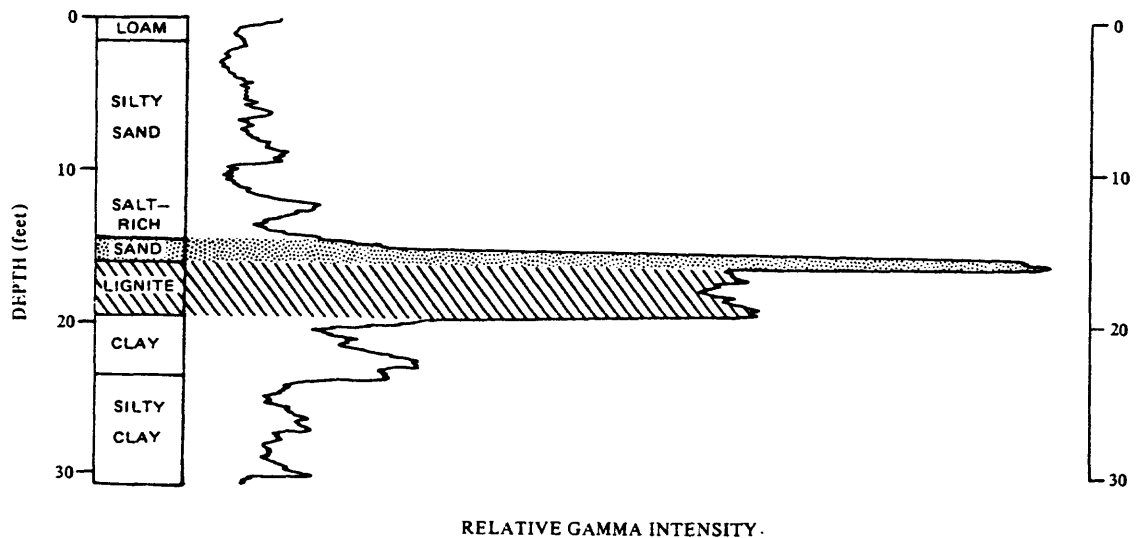


Figure E-8.—Gamma-ray log of subsurface in uraniumiferous lignite area, western North Dakota.

mapped in three dimensions. These "most-contaminated" spoils were replaced selectively in the mine pit above the water table to prevent dissolution of soluble uranium salts. Replaced spoils of high radioactivity and specific conductance also were capped with clay from the base of the pit, and the surface topography was mounded to minimize infiltration that might introduce radioactive and other soluble salts into the aquifer. A minimum of 4 feet of less contaminated spoils and topsoil were spread above the clay cap to minimize post-reclamation surface-radiation levels. Similarly, spoils with specific conductances greater than 5,000 $\mu\text{S}/\text{cm}$ were replaced at least 8 feet below the postreclamation land surface to promote revegetation but above the water table to prevent

the movement of dissolved solids to the aquifer. Preliminary monitoring indicates that all reclaimed areas were within 10 pCi/L of the background level before the topsoil was added.

REFERENCES CITED

- U.S. Environmental Protection Agency, 1983a, Standards for remedial actions at inactive uranium processing sites: Federal Register, v. 48, no. 3, p. 590-606.
- — — 1983b, National revised primary drinking water regulations: Federal Register, v. 48, no. 194, p. 45519-45520.
- — — 1986, Quality criteria for water 1986: EPA 440/5-86-001.

CHAPTER F. – ORGANIC COMPOUNDS IN GROUND WATER

	Page
Field comparison of ground-water sampling devices for recovery of purgeable organic compounds, by T.E. Imbrigiotta, Jacob Gibs, T.V. Fusillo, J.J. Hochreitter, and G.R. Kish	F-5
Recent developments in downhole samplers for organic and volatile compounds in ground water, by J.H. Fickin, W.H. Sonntag, and A.J. Boettcher	F-5
Screening for volatile organic compounds in ground water by gas chromatography with photoionization and hall detectors, by T.V. Fusillo, Jacob Gibs, J.A. Kammer, and T.E. Imbrigiotta	F-9
Application of the gas chromatographic/flame ionization detector analysis, by H.R. Feltz, J.A. Lewis, and F.L. Cardinali	F-11
Methodology	F-11
Detector sensitivity	F-11
Sample analysis, reporting procedures, and quality control	F-12
Application of GC/FID scans	F-13
Use of gas chromatograph/flame ionization detector to identify organic substances in ground water, by R.C. Buchmiller	F-17
Evaluation of four field-determined characteristics used as water-quality indicators during aquifer sampling for purgeable organic compounds, by Jacob Gibs and T.E. Imbrigiotta.....	F-19

ILLUSTRATIONS

	Page
Figure	
F-1. Photographs of samplers described in text:	
(A) Pump-type sampler	F-5
(B) Small-diameter flow-through sampler	F-6
(C) Small-diameter sampler that collects a sealed sample	F-7
F-2. Chromatograms showing comparison of detector sensitivity.....	F-13
F-3. Sample GC/FID analytical report: (A) chromatogram, and (B) table showing retention times (RT), peak (AREA), area integration codes (TYPE), compound identification number (CAL), calculated concentration ($\mu\text{g/L}$) (AMOUNT), and names of compounds present (NAME)	F-14
F-4. Graph showing Northern New Jersey well, August 14, 1984, purgeable organic compounds concentration time history during well purging.....	F-21

TABLES

	Page
Table	
F-1. Characteristics of gas-chromatographic detectors.....	F-12
F-2. Chemical quality of ground water at two sites in New Jersey	F-20

CHAPTER F – ORGANIC COMPOUNDS IN GROUND WATER

FIELD COMPARISON OF GROUND-WATER SAMPLING DEVICES FOR RECOVERY OF PURGEABLE ORGANIC COMPOUNDS

By Thomas E. Imbrigiotta¹, Jacob Gibs¹, Thomas V. Fusillo¹, Joseph J. Hochreiter¹, and George R. Kish¹

The increasing need to sample ground water for analysis for organic compounds has triggered the development and production of a wide variety of ground-water sampling devices. Environmental investigators have questioned the ability of all these devices to obtain equally representative samples for the analysis of purgeable organic compounds. Such compounds present special sampling and analytical difficulties because of their low molecular weights, low solubilities in water, low boiling points, and tendency to degas in open systems. Previous evaluations of sampler recovery efficiency have been conducted only under controlled laboratory conditions. This study compares the abilities of seven different ground-water sampling devices to recover purgeable "priority pollutants" under field conditions.

The seven samplers evaluated were: gear submersible pump, helical-rotor submersible pump, bladder pump, peristaltic pump, syringe sampler, open bailer, and point-source bailer. These sampling devices were tested in three wells of differing depth and varying combinations and concentrations of purgeable organic compounds. Fifteen to 28 replicate samples were collected at each well with each sampler and analyzed for all purgeable priority pollutants. For each purgeable organic compound detected at a site, a well-defined mean concentration obtained with each sampler was determined. Because the true concentrations of purgeable organic compounds in each well was unknown, percentage recoveries could not be calculated, and it was assumed that the highest concentration recovered was the most accurate. The mean concentrations were compared statistically through analysis-of-variance testing to determine whether the sampling devices differed significantly, at the 95-percent confidence level, in their ability to recover each purgeable organic compound.

¹U.S. Geological Survey, West Trenton, N.J.

Significant differences in sampler recovery concentrations were found for some purgeable organic compounds at each of the sites. The order of the samplers from most effective (highest) recovery to least effective (lowest) recovery varied among sites and among compounds detected at a site. A composite ranking of the sampling devices from highest to lowest recovery based on data from all three sites yielded the following order:

1. point-source bailer
2. gear submersible pump
3. open bailer
4. bladder pump
5. helical-rotor submersible pump
6. peristaltic pump
7. syringe sampler

An analysis of variance of the ranked mean data indicated that samplers 1 through 5 were not significantly different in their ability to recover purgeable organic compounds.

A similar test of the coefficients of variation found no significant difference between any of the sampling devices in the precision with which they recovered purgeable organics. However, the four samplers with the lowest coefficients of variation were pumping devices, whereas the three samplers with the highest coefficients of variation were grab-sampling devices. Coefficients of variation by compound averaged 18 percent for compounds with concentrations above 20 µg/L and 31 percent for compounds with concentrations below 20 µg/L.

For samples from wells screened in shallow, unconfined aquifers in which the plume of contaminated ground water was not extensive, a higher rate of pumping (10 gal/min) during well development gave higher recoveries of purgeable organic compounds than a lower rate of pumping

(1 gal/min). Additionally, the concentrations of recovered purgeable organics in the screened interval decreased within 1 hour after the pumping for well development stopped.

Operating conditions had a significant effect on the recoveries by several samplers. Ambient air temperature affected the recovery of purgeable organic compounds by the peristaltic pump. At an air temperature lower than the ground-water temperature (0 °C versus 16 °C), the peristaltic pump recovered purgeables as efficiently as any of the other samplers. Under identical conditions

but at a higher air temperature (30 °C), however, the peristaltic pump recovered significantly lower amounts than the other sampling devices. The bladder pump recovered significantly lower concentrations of purgeable organic compounds when the pump body was not submerged far enough below the water column surface to properly seat the top check valve. Pouring water samples from the top of a bailer rather than using a bottom-discharge device significantly lowered the recoveries of purgeable organic compounds.

RECENT DEVELOPMENTS IN DOWNHOLE SAMPLERS FOR ORGANIC AND VOLATILE COMPOUNDS IN GROUND WATER

By James H. Ficken¹, Wayne H. Sonntag², and Arnold J. Boettcher³

The need for the development of downhole water samplers to collect ground-water samples that are not contaminated or diluted is being addressed by the U.S. Geological Survey in several areas of application. Water samples can now be obtained in a manner that will prevent the escape of dissolved gases and volatile organic compounds, which easily escape from unsealed samples.

In response to requests by investigators for samplers having specialized characteristics and functions unavailable commercially, three sampler designs were developed and prototypes built to satisfy requirements of specific sampling endeavors.

A pump-type sampler of stainless steel, designed by K.E. Stevens and A.J. Boettcher, has a large-diameter (about 2 inch) and a small-diameter (about 1-1/4 inch) version. It operates from a geophysical logging tool and can retrieve water samples from water depths exceeding 2,000 feet. At these depths, other samplers allow water to enter the reservoir too rapidly, which allows gases to escape from solution and form bubbles.

The pump-type sampler (fig. F-1A) is lowered to the desired depth, and the logging tool is activated. This causes a reciprocating action that operates a piston to pump water up through a sample

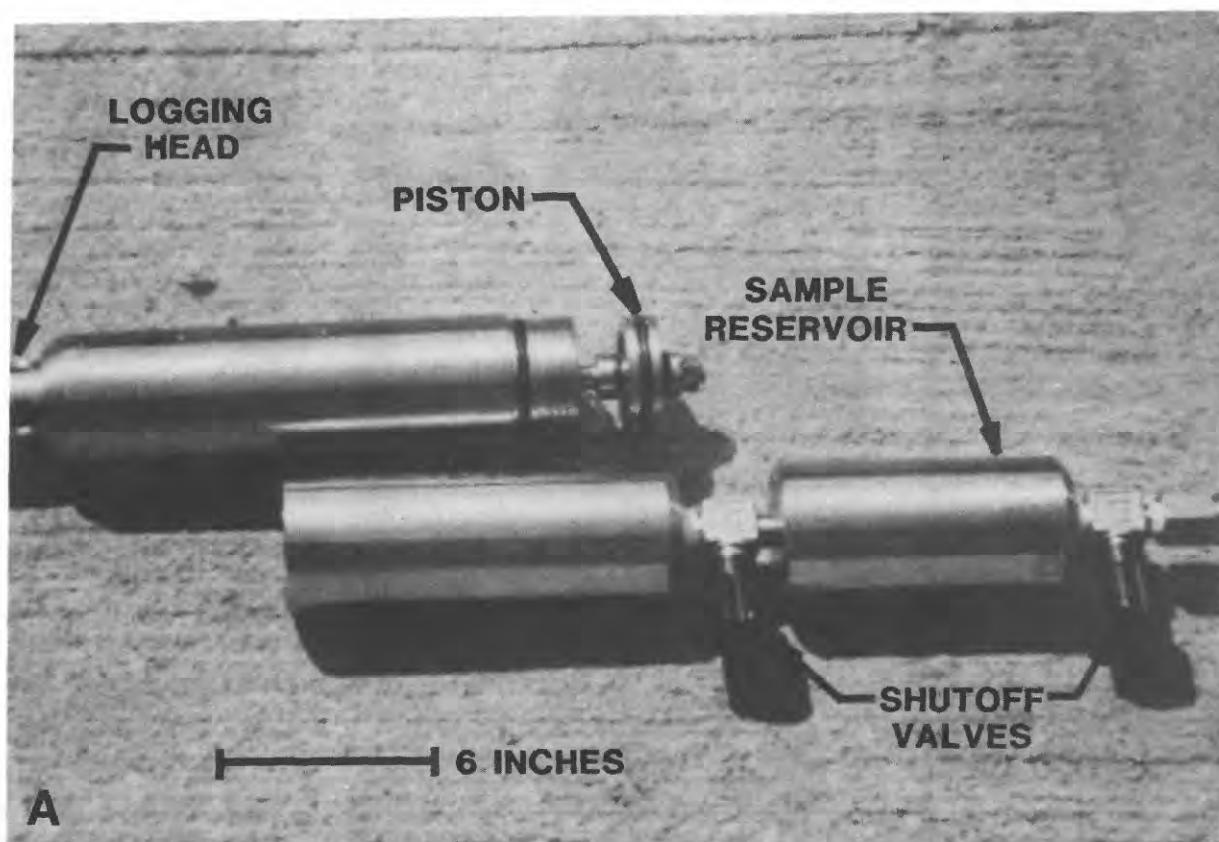


Figure F-1.—Samplers described in text: (A) pump-type sampler.

¹U.S. Geological Survey, Stennis Space Center, Miss.

²U.S. Geological Survey, Miami, Fla.

³U.S. Geological Survey, Denver, Colo.

cylinder or reservoir attached below the pump. After four or five cycles, the pump is stopped in a position that seals the sample reservoir. The sampler is then brought to the surface, shutoff valves are closed, and the sample reservoir is removed. The sample reservoir then can be shipped directly to the laboratory, without the transferral of the water sample to another container.

A flow-through sampler, designed by W.H. Sonntag, was developed in response to the need for

a flow-through sampler of small diameter that minimizes contact of oxygen with the sampled water. This sampler (fig. F-1B) consists of a stainless steel cylinder with a moveable center shaft and upper and lower piston seals. The sampler is opened and closed when a logging tool or head similar to the one used on the pump-type sampler is activated.

To obtain a water sample, the sampler is lowered "open" to the desired depth. The well is then pumped by a submersible pump positioned

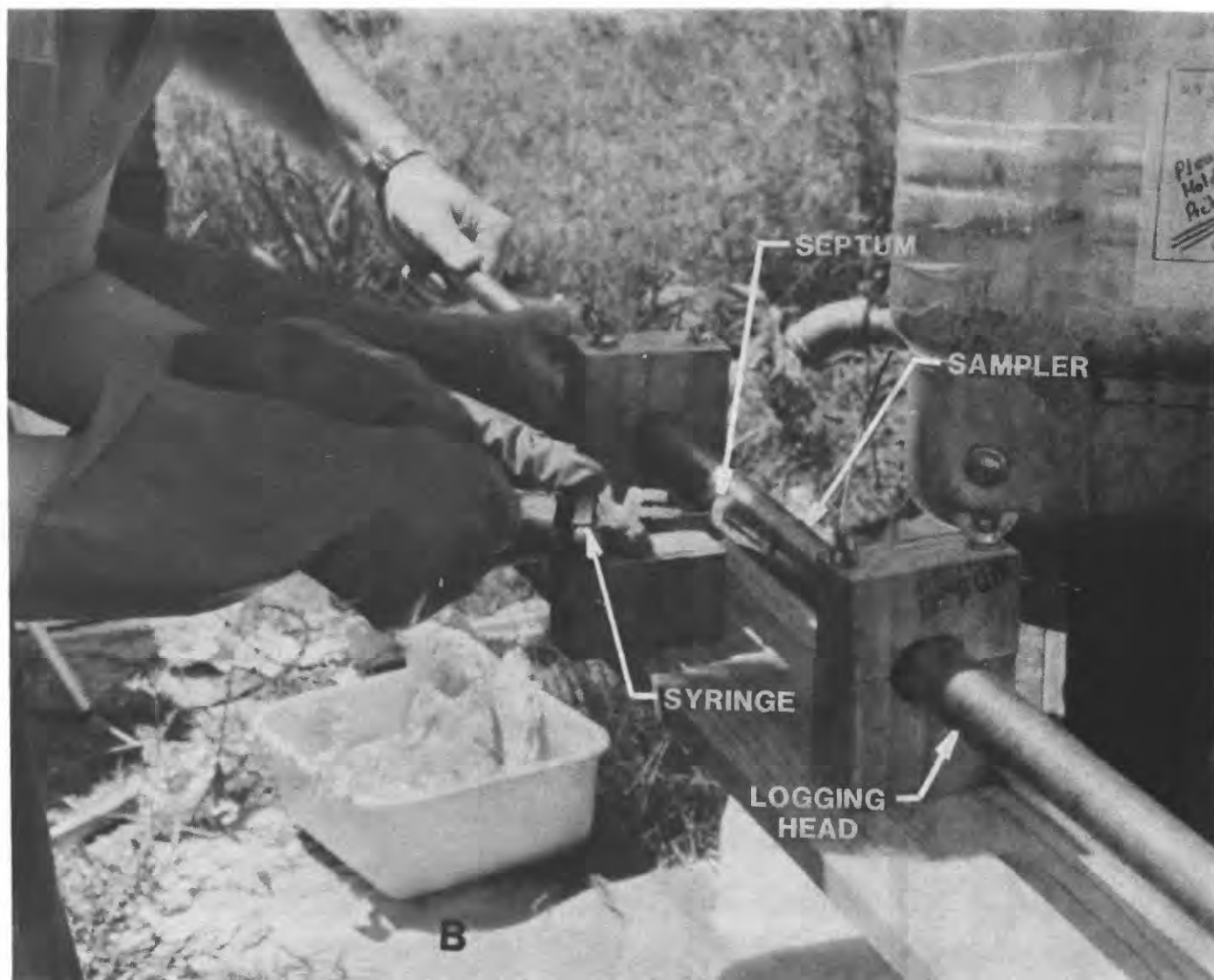


Figure F-1. — Samplers described in text: (B) small-diameter flow-through sampler.

above the sampler on a conventional pump at the surface. This allows water to flow through the sampler. The sampler is then closed when the logging head is activated. Samples are extracted at the surface with a syringe and needle inserted through a septum in the wall of the cylinder. The water sample then can be immediately analyzed or "fixed" for later analysis by reacting with agents placed in the syringe.

A third type of sampler, designed by J.H. Ficken, was developed in response to the needs of

the Toxic Waste Program for a sampler to go down a 2-inch well to depths of 200 feet and collect a sealed sample. The sampler (fig. F-1C) consists of a stainless steel tube about 30 inches long with a piston and piston rod attached to the suspending cable. A sample cylinder is attached to the bottom. The cylinder is prevented from moving down around the piston by a friction catch.

The sample cylinder is preloaded with distilled water and the sampler is lowered to the desired depth. A sharp tug on the suspending cable

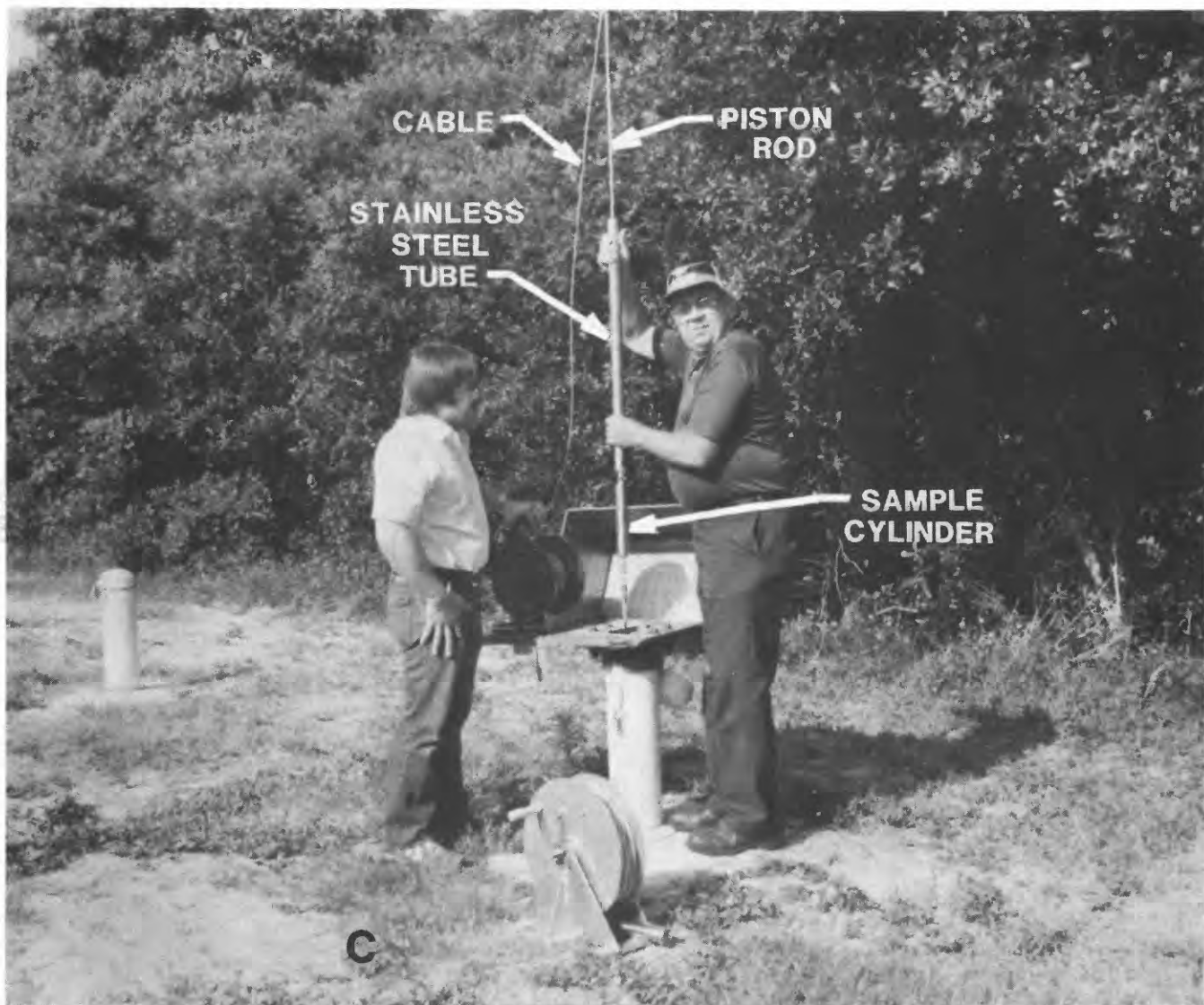


Figure F-1. — Samplers described in text: (C) small-diameter sampler that collects a sealed sample.

releases the friction catch, causing the sampler cylinder to move downward around the piston and water to move through the sample cylinder. After a short wait, the sampler is brought to the surface, the shutoff valves are closed, and the sample cylinder is removed. A sample cylinder has been developed with a piston in one end. A screw press

is used to force the water sample directly into analytical equipment or other containers.

These samplers help meet the need for specialized samplers not available currently from commercial sources and will likely find applications in future toxic-waste and other ground-water studies.

SCREENING FOR VOLATILE ORGANIC COMPOUNDS IN GROUND WATER BY GAS CHROMATOGRAPHY WITH PHOTOIONIZATION AND HALL DETECTORS

By Thomas V. Fusillo¹, Jacob Gibs¹, James A. Kammer¹, and Thomas E. Imbriotta¹

Volatile organic compounds (VOCs) are persistent contaminants in ground water, particularly in urban and industrial areas. In a ground-water reconnaissance where few data on VOCs are available, it may be desirable to analyze all samples for these compounds. High analytical costs and limited laboratory capacity often limit the numbers of samples that can be analyzed, however.

Many samples being analyzed by gas chromatography/mass spectrometry (GC/MS) contain no VOCs above the GC/MS detection limit, currently 3 µg/L. More than 80 percent of 900 ground-water samples collected during regional ground-water quality studies in New Jersey since 1979 contained no detectable concentrations of VOCs. In 1984, new laboratory instrumentation was installed at the U.S. Geological Survey's New Jersey District laboratory to scan water samples for VOCs. The scans were established as a screening procedure so that samples found to contain one or more VOCs at concentrations detectable by GC/MS could be identified and then submitted for GC/MS confirmation.

The analytical procedure used is specified by the U.S. Environmental Protection Agency (USEPA) methods 601 (purgeable halocarbons) and 602 (purgeable aromatics). The instrumentation consists of five components: a Tekmar² model ALS automatic sampler, which sequentially sparges up to 10 samples; Tekmar model LSC-2 automatic purge and trap concentrator; Tracor model 540 gas chromatograph with Hall electrolytic conductivity detector and photoionization detector; 8-ftx0.1-in. ID glass column packed with 1-percent SP-1000 on Carbopack B (60/80 mesh); and two Shimadzu model CR-3 computing integrators with a RS-232 computer interface.

Standard curves are developed for all "priority pollutant" volatile organic compounds, with emphasis on the concentration range from 0.5 to 5

µg/L. At least one surrogate compound is added to each sample. Each set of 10 analyses contains at least 1 blank and 1 spiked blank. Tentative compound identifications are made on the basis of retention time and relative response by the two detectors. The concentration range for a detected compound is estimated by applying the standard curve to the integrated peak area on the chromatogram.

The objective of the screening procedure is to identify samples that contain volatile organic compounds at concentrations high enough to be detected, identified, and quantified by GC/MS. The current minimum detection limit of 3 µg/L for volatile compounds serves as the guideline for submitting samples for GC/MS confirmation. Any sample that contains at least one compound at a concentration estimated at 3 µg/L or higher is recommended for further analysis.

Since implementation of this scan, the New Jersey Laboratory has analyzed 367 samples for volatile organic compounds. The results can be summarized as follows:

- 282 samples (77 percent) contained no organic compounds at concentrations above background on the GC (approximately 0.5 µg/L). Of these, 18 were submitted for GC/MS confirmation, and all were confirmed to contain no detectable compounds.
- 37 samples (10 percent) contained at least 1 compound at a concentration above 0.5 µg/L but no compounds above 3 µg/L. Of these, 18 were submitted for GS/MS confirmation, and 17 were confirmed to contain no compounds at concentrations above 3 µg/L.
- 48 samples (13 percent) contained at least 1 compound above 3 µg/L. Of these, 25 were submitted for GC/MS confirmation, and 22 had at least 1 compound confirmed above 3 µg/L.

¹U.S. Geological Survey, West Trenton, N.J.

²The use of brand names in this report is for identification purposes only and does not constitute endorsement by the U.S. Geological Survey.

The scanning of samples for VOCs has greatly reduced the number of samples that require analysis by GC/MS. It has also enabled the detection of non-priority pollutant volatile compounds, as well as some priority pollutant compounds, such as the dichlorobenzene isomers, that have not been routinely reported. The scans are also useful for quality assurance and have resulted in identification of data-entry errors such as incorrectly entered remarks codes or misidentified compounds.

Three problems have been identified in relation to the screening procedure. The first is the difficulty in completing the screening analysis in sufficient time to allow the submission of replicate samples for GC/MS analysis within the 14-day USEPA guideline. The second is the inability to store the GC scan data on WATSTORE. The third is equipment downtime, which has ranged from greater than 30 percent at startup to about 15 percent at present.

APPLICATION OF THE GAS CHROMATOGRAPHIC/FLAME IONIZATION DETECTOR ANALYSIS

By Herman R. Feltz¹, James A. Lewis², and F.L. Cardinali³

In an effort to reduce the cost of assessing the presence and concentration of organic substances in water and sediment, the U.S. Geological Survey's National Water Quality Laboratory in Denver, Colo., offers the gas chromatographic/flame ionization detector (GC/FID) analysis as a cost-effective and rapid screening procedure that complements the more expensive gas chromatographic/mass spectrometric (GC/MS) analysis for semivolatile organic compounds.

The GC/FID analysis, or "FID scan," provides semiquantitative data that may be used in reconnaissance or monitoring studies. Among the potential applications of the FID scan are: (1) screening a large number of samples from one or more sites for the presence of organic substances; (2) hydrocarbon "fingerprinting," where specific compounds such as nitrophenol, naphthalene, gasoline, or fuel oil may be a problem, or (3) as followup monitoring of specific organic compounds that have been identified by GC/MS analysis.

Methodology

Gas chromatography (GC) is an instrumental analytical technique used to separate components of a complex mixture of organic compounds. The ideal GS separation achieves a critical result—it resolves a complex mixture into discrete GC "peaks," where each peak represents a single component of the original mixture. The ideal gas chromatogram is rarely achieved, however, for several reasons. One is the nature of the original mixture. If the mixture is in a water matrix, the organic compounds must be extracted into an organic solvent (hexane, methylene chloride, diethyl ether, and so forth), and the extract must be free of residual water before the analysis can be performed. The choice of solvents and control of pH are impor-

tant considerations in achieving isolation of the compounds of interest. Polar organic compounds such as acetone, phenol, acetic acid, or pyridine will not be efficiently removed from a water sample when the solvent extraction is performed; thus some compounds present in the original sample may not be detected in the GC analysis because they are likely not extracted. On the other hand, numerous compounds that are extracted may not pass the injection port because of thermal degradation. Also, some nonideal GC results are related to the selectivity of detectors used with the chromatographs. Several detectors are used in gas chromatography, and each has its advantages and disadvantages. Detectors currently used in the U.S. Geological Survey's Laboratory include electron capture (ECD), flame photometric (FPD), alkali flame ionization (NPD), thermal conductivity (TCD), flame ionization (FID), and mass spectrometric (MS).

Detector Sensitivity

The sensitivity of a flame ionization detector to organic compounds may be shown by a comparison of FID data with data for other detectors (table F-1).

Examination of table F-1 indicates that the choice of detector depends on the compounds of interest in a given study. If compounds in the original sample are in concentrations below the detection limit of the detector being used, those compounds will not be detected, and the analytical report will include no information about them. For example, the FID is not the detector of choice for organochlorine and organophosphorus insecticides nor the triazine herbicides. The FID is highly sensitive to base/neutral/acid-extractable priority pollutant compounds, however.

¹U.S. Geological Survey, Reston, Va.

²U.S. Geological Survey, Denver, Colo.

³Centers for Disease Control, Atlanta, Ga.

Table F-1. — Characteristics of gas chromatographic detectors

Type of detector	Application (type of compounds)	Examples	Minimum concentration necessary for detection in water ($\mu\text{g/L}$)
Electron capture (ECD)	Chlorinated pesticides	DDT	0.01
		2,4-D	.01
		PCBs	.1
Flame photometric (FPD)	Organophosphate pesticides	Diazinon	.01
		Malathion	.01
Alkali flame ionization (NPD)	Triazine herbicides	Atrazine	.1
		Simazine	.1
Thermal conductivity (TCD)	Nearly all compounds that elute from the GC column.	N ₂ , O ₂ , CO ₂	1,000
Flame ionization (FID)	Nearly all organic compounds that elute from the GC column.		0.1 to 100, depending on type of compound.
Mass spectrometric (MS)	All organic substances or compounds that elute from the GC column.		1 to 1,000, depending on type of compound.

A 58-component base/neutral/acid-extractable standard at a concentration of 0.5 $\mu\text{g/L}$ per component was injected into a GC (fig. F-2). The GC/FID scan (upper chart) shows the three internal standards and some of the components in the standard, but the GC/MS scan (lower chart) shows only the three internal standards; everything else is "noise." This comparison illustrates why it is not always possible to detect (far less identify) peaks by MS even though the peaks are present in the FID scan. For GC/MS analysis, the unknown peak must, in general, represent a concentration greater than 2 $\mu\text{g/L}$ for water samples and 200 $\mu\text{g/kg}$ for sediment samples. The higher reporting value for sediment is necessitated by: (1) the presence of interfering organic compounds which are more prevalent in sediment, and (2) the need to extract the sample from only 50 grams of sediment to minimize interference from natural organic matter when synthetic substances are being sought.

Sample Analysis, Reporting Procedure, and Quality Control

Samples are prepared for GC/FID analysis by solvent extraction of water or sediment, followed by concentration of the resulting extract to a final volume of 1.0 mL. The extract is then analyzed by injecting 1.0 μL aliquot into a gas chromatograph. The GC/FID analytical report provided to the user (fig. F-3) includes a copy of the sample chromatogram and a table containing the GC retention times, peak areas, and concentrations of the unidentified compounds detected, which are estimated by comparison of the response (peak area) to the response of internal standards.

As part of its quality-control program, the laboratory adds a number of surrogates and internal standards to samples to monitor problems that may occur during the analytical procedure or that may be caused by "matrix effects" in the sample itself. (Surrogates and internal standards are compounds that do not occur naturally in the environment.)

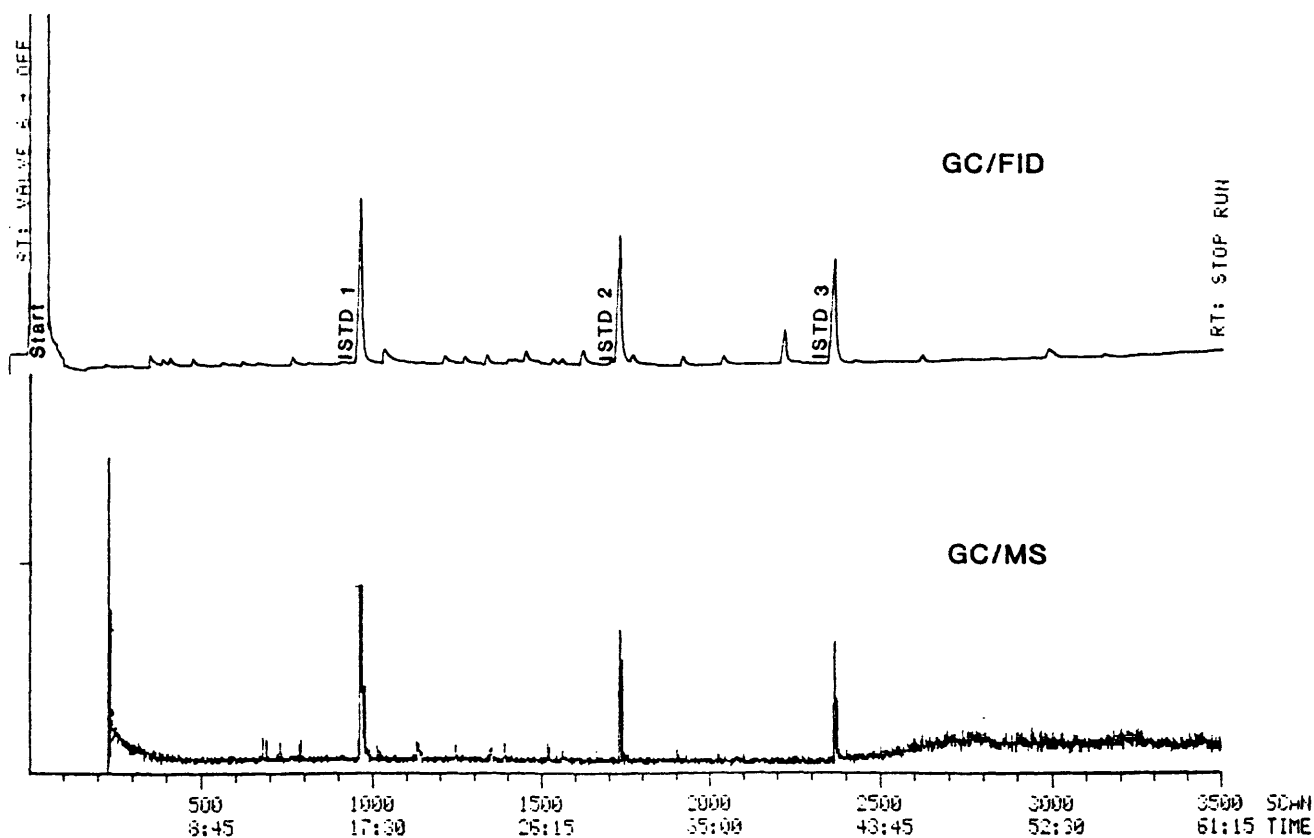


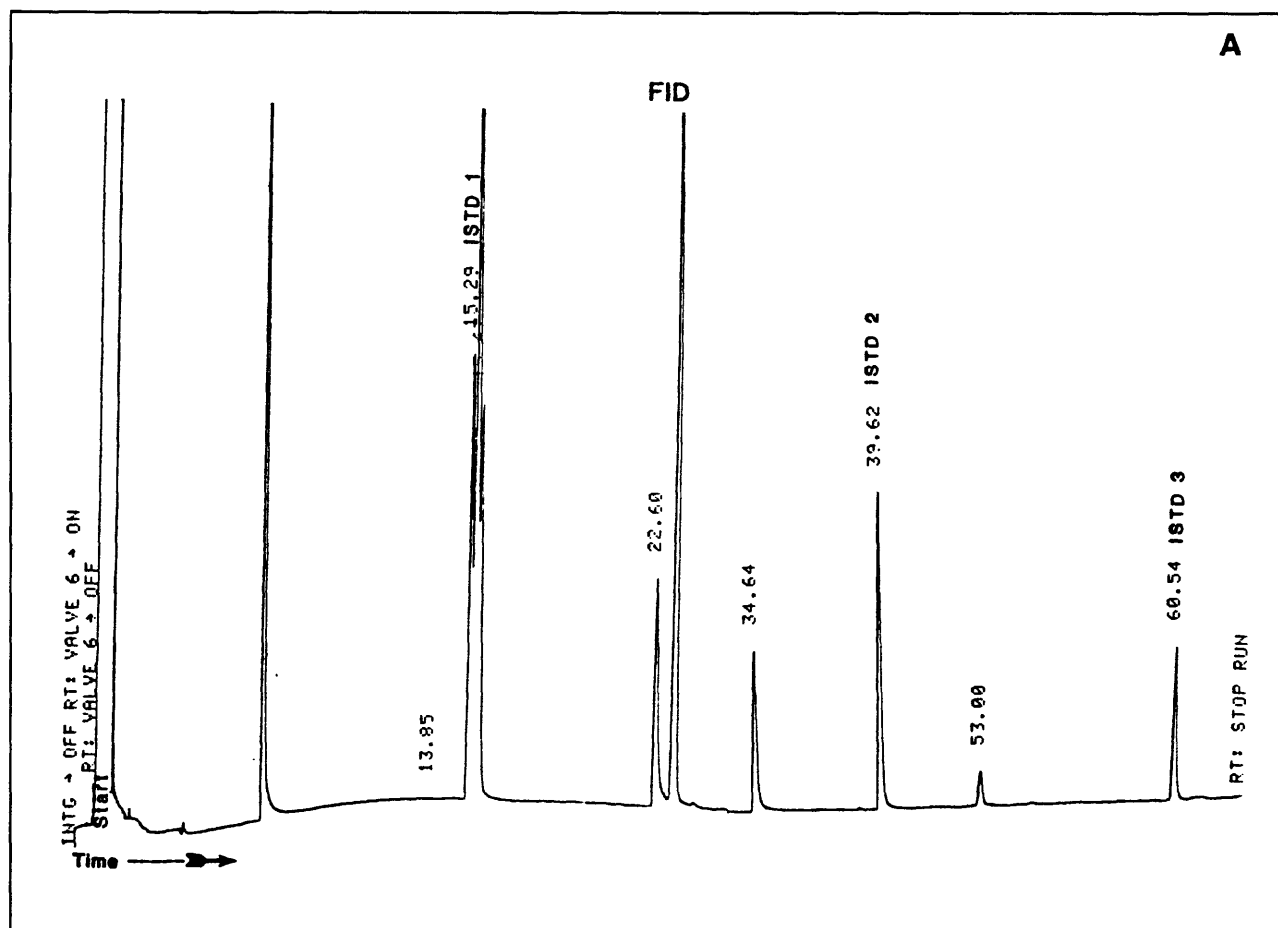
Figure F-2.—Comparison of detector sensitivity. Upper chromatogram, from gas chromatographic/flame-ionization detector, shows response to internal standard and some components of the added standard. Lower chromatogram, from gas chromatographic/mass spectrometric detector, shows response only to internal standards; the remainder is "noise."

Matrix effects can be evaluated by monitoring the recoveries of these compounds. If a problem is encountered, it is noted in the report for that sample. A typical surrogate/standard chromatogram is shown in figure F-3 with the corresponding table listing surrogates and internal standards.

Application of GC/FID Scans

Reconnaissance/Screening.—GC/FID scans can be used to screen samples for the presence of gas-chromatographable organic substances and, in some cases, to tentatively identify organic compounds. FID scans are far more informative than total organic carbon analyses but less informative than GC/MS.

The FID scan enables a large number of sites in a study area to be screened for detection of organic substances at a reasonable cost with quick turnaround time. Sites where substances have been detected can then be resampled for GC/MS analysis to identify individual compounds. Alternatively, the extract prepared for the initial FID scan can be recalled from cold storage and subsampled for followup GC/MS analysis if deemed appropriate. The quick turnaround on FID scans makes this possible by allowing a project leader time to evaluate results of "scan" data and request GC/MS analysis before the maximum holding time of 40 days after extraction is exceeded.



RT	AREA	TYPE	CAL	AMOUNT	NAME
7.29	487.93	BB	1	25.720	PHENOL-D6
13.85	0.03	BB		2.867E-02	
15.29	270.19+	BV	2	ISTD No. 1	NAPTHA-D8
15.49	579.23+	VV	3	21.021	1-FLUORONAPH
15.67	246.33	VB	4	23.075	P-DIBROMOBEN
22.60	180.03	BB	5	27.203	DIBROMOPHENO
23.33	572.86	BB	6	24.646	2-2DIFLUOROB
34.64	121.65	BB	7	24.751	2-4-6TRIBROM
39.62	231.88+	BB	8	ISTD No. 2	PHENANT-DI0
53.00	25.02	BB		25.023	
60.54	114.58+	BB	9	ISTD No. 3	CHRYSENE-D12

MULTIPLIER = 1
 ISDT 1 AMT = 10
 ISDT 2 AMT = 10
 ISDT 3 AMT = 10

B

Figure F-3.— Sample GC/FID analytical report: (A) chromatogram; and (B) table showing retention times (RT), peak (AREA), area integration codes (TYPE), compound identification number (CAL), calculated concentration ($\mu\text{g/L}$) (AMOUNT), and names of compounds present (NAME).

In summary, the FID scan indicates whether organic contamination is present, what the magnitude might be, and whether the peaks on the chromatogram might be identified by GC/MS.

Followup to GC/MS analysis for contaminant monitoring.— Samples may be submitted for GC/MS analysis for the purpose of identifying specific individual compounds. Depending on the nature of the sample, this can be tedious, time consuming, and expensive. After specific compounds at a sampling site are identified, followup analyses can be performed by the less expensive GC/FID analysis. Specific compounds of interest must be identified so that suitable standard mixtures can be prepared for GC/FID analysis. The GC/FID analysis is useful for monitoring the presence of the previously identified contaminants or for monitoring changes in their concentrations. Changes in hydrologic conditions may introduce compounds not present at the time of initial sampling, and these substances could interfere with compounds of interest. Therefore, periodic GC/MS confirmation of previously identified compounds is essential.

Fingerprinting.— This application is especially suited for studies at chemical or fuel-spill sites. The chromatographic pattern of organic com-

pounds can easily be observed from the GC/FID scan. No individual compound present in a fuel mixture is important in its own right, but the relative contribution of each component to the overall mixture is important and differs according to the source(s) of the fuel. Thus, the source of contamination can be identified and the movement of the organic plume through an aquifer system monitored. This is one of the best and most appropriate applications of the GC/FID analysis.

Quality assurance.— Another useful application of FID scans is the detection of sample contamination at sampling sites. The cost of drilling test wells and collecting samples is a considerable part of a project budget, and money is wasted if samples are contaminated by the equipment used in drilling and sampling. Augers, pipe, drilling muds, well casing, and tubing used to pump the sample can transfer some level of contamination to samples. As a field quality-control procedure, samples can be collected from these items with appropriate wash liquids. The wash samples can then be analyzed by FID scans to identify any contamination. This procedure is especially useful at chemical-waste disposal sites where cross-contamination is a major concern.

USE OF GAS CHROMATOGRAPH/FLAME IONIZATION DETECTOR TO IDENTIFY ORGANIC SUBSTANCES IN GROUND WATER

By Robert C. Buchmiller¹

An investigation to determine the occurrence of organic substances near areas where hazardous substances were disposed of or leaked from storage recently was completed at a military air base near Des Moines, Iowa, by the U.S. Geological Survey. Soil and water samples were collected from potentially contaminated areas, and three techniques that use gas chromatograph/flame ionization detector (GC/FID) scans were used to identify organic substances in these samples.

The first technique and primary use of the GC/FID scan was to screen all samples for additional gas chromatograph/mass spectrometer (GC/MS) analyses. Samples were selected for GC/MS analysis according to the shape of the GC/FID chromatograph and the number of peaks on the chromatograph that were greater than 10 percent of the peak of the internal standard per-deuteronaphthalene. GC/MS then was used to positively identify and quantify nonvolatile "priority pollutants" in selected soil and water samples and to provide tentative identification of other organic substances in the selected samples.

The second technique was used to extend the utility of the screening process because the num-

ber of GC/MS analyses was limited by the contract for this investigation. Results of GC/FID analyses were compared, and samples were selected for GC/MS analyses that appeared to contain a variety of organic substances. In this way a library of GC/FID scans with GC/MS-identified substances could be created to provide interpretation of samples for which GC/FID data existed.

The third technique used was a comparison of field soil- and water-sample GC/FID results with GC/FID results from reference samples of the hazardous wastes disposed of or actual disposal residues. Field samples that contained GC/FID results similar to those from the reference samples were interpreted to contain similar organic substances. The technique assumed that the GC/FID "fingerprint" for each substance was unique to the substance.

The GC/FID scan appears to be well suited to sample screening in certain types of field investigations and for limited qualitative interpretation. Additional experimentation and documentation of successful uses of this technique are needed to demonstrate its effectiveness, however.

¹U.S. Geological Survey, Iowa City, Iowa

EVALUATION OF FOUR FIELD-DETERMINED CHARACTERISTICS USED AS WATER-QUALITY INDICATORS DURING AQUIFER SAMPLING FOR PURGEABLE ORGANIC COMPOUNDS

By Jacob Gibs¹ and Thomas E. Imbrigiotta¹

A critical element of any ground-water sampling program is to ensure that the samples taken are representative. The sampling process needs to be monitored to determine when the initial fluctuations in concentrations of the dissolved constituents of interest during pumping reach a minimum level. After steady state is achieved, sampling may begin. Traditionally, measurements of pH, water temperature, dissolved oxygen, and specific conductance are used as indicators for monitoring the well-water discharge to establish when a representative sample may be taken. These characteristics are controlled primarily by the inorganic constituents and the physical characteristics of the aquifer, however, and thus may fail to indicate changes in the concentrations of purgeable organic compounds (POC) during pumping and determining when steady state occurs.

Tests were run at two wells to determine the best indicator for changes in POC concentrations as the well casing is flushed. Field measurements of chloride ion, ultraviolet absorbance at 254 nm, specific conductance, pH, dissolved oxygen, and water temperature were taken and compared. The chloride ion was measured by specific ion electrode. The ultraviolet (UV) absorbance instrumentation used was a single-beam spectrophotometer, Hitachi² model 100-20.

Both wells were screened in a shallow unconfined aquifer, had a 4-inch-diameter casing with a total depth of 24 feet, and a depth to water of approximately 6 feet. One well is in a glacial valley of northern New Jersey; the other is in the coastal plain of southern New Jersey. Both wells were sampled once a day for two consecutive days. The steady-state values of the water-quality measurements used in this study are listed in table F-2. A plot showing typical fluctuations in POC concen-

tration during the first well development of the northern New Jersey well is given in figure F-4. The transient part of the curve has larger changes in concentration than the steady-state part.

Trends in temperature and dissolved oxygen concentration did not follow those of the POC at either well. Water temperature varied only slightly (1.5°C), which was not large enough to plot against the POC concentrations. Dissolved oxygen concentrations in water from both wells were less than 1.5 mg/L. Inadvertent aeration of the sample can alter such values significantly. In the northern New Jersey well, the dissolved oxygen concentration increased with increasing specific compound concentrations during the well-development (transient) phase, but decreased with increasing specific compound concentration in the southern New Jersey well. Thus, dissolved oxygen is also not a reliable indicator for POC variations.

The pH decreased with increasing POC concentration in the transient phase of sampling at both wells, but the pH changes are not the exact inverse of those shown by specific compounds. Therefore, pH also is a poor indicator for the onset of steady-state POC concentrations. Specific conductance followed the trends of the POC concentrations at both wells, and chloride ion and ultraviolet absorbance followed the POC concentrations during the transient phase more closely than specific conductance. The ultraviolet absorbance followed the POC transient trends much more closely than the other field measurements at the southern New Jersey well, which contained purgeable organic aromatic compounds, but was not sensitive to changes in the northern New Jersey well, which contains no detectable purgeable organic compounds that absorb ultraviolet radiation at 254 nm.

¹U.S. Geological Survey, West Trenton, N.J.

²The use of brand names in this report is for identification purposes only and does not constitute endorsement by the U.S. Geological Survey.

Table F-2.—*Chemical quality of ground water at two sites in New Jersey*

[ND = not detected]

Steady-state field measurements	Northern New Jersey well		Southern New Jersey well	
	8-14-84	8-14-84	12-05-84	12-06-84
pH	6.5	6.38	6.05	6.09
Water temperature (°C)	18.4	18.9	15.5	16.0
Specific conductance	805	865	1,780	1,780
Dissolved oxygen (mg/L)	.48	.26	.21	.16
Chloride (mg/L)	140	145	560	640
Ultraviolet absorbance (at λ D = 254 nm)	.014	.035	.404	.559
Purgeable organic compounds (μ g/L)				
1,1-Dichloroethane	51	79	10.7	10.7
trans 1,2-Dichloroethylene	6.5	9.8	76	102
1,1-Dichloroethylene	37	53	ND	ND
1,1,1-Trichloroethane	698	941	ND	ND
Tetrachloroethylene	179	271	ND	ND
Vinyl chloride	ND	ND	64	70
Trichloroethylene	41	60	27	28
Chlorobenzene	ND	ND	21	204
Benzene	ND	ND	66	66
Ethylbenzene	ND	ND	25	27
Toluene	ND	ND	20	21
1,2-Dichlorobezene	ND	ND	14.7	14.2
1,3-Dichlorobezene	ND	ND	16.3	20.8
1,4-Dichlorobezene	ND	ND	7.3	9.0
Chloroform	ND	ND	10.3	14.8

Neither water temperature, pH, nor dissolved oxygen reflected the small fluctuations in POC concentrations during 10 hours of steady-state sampling. Ultraviolet absorbance followed the POC concentrations more closely than chloride ion where aromatic purgeable organic com-

pounds were present, and chloride ion followed the POC concentrations more closely than specific conductance under steady-state conditions. Thus, no reliable general field indicator for POC concentration variability was found in this study.

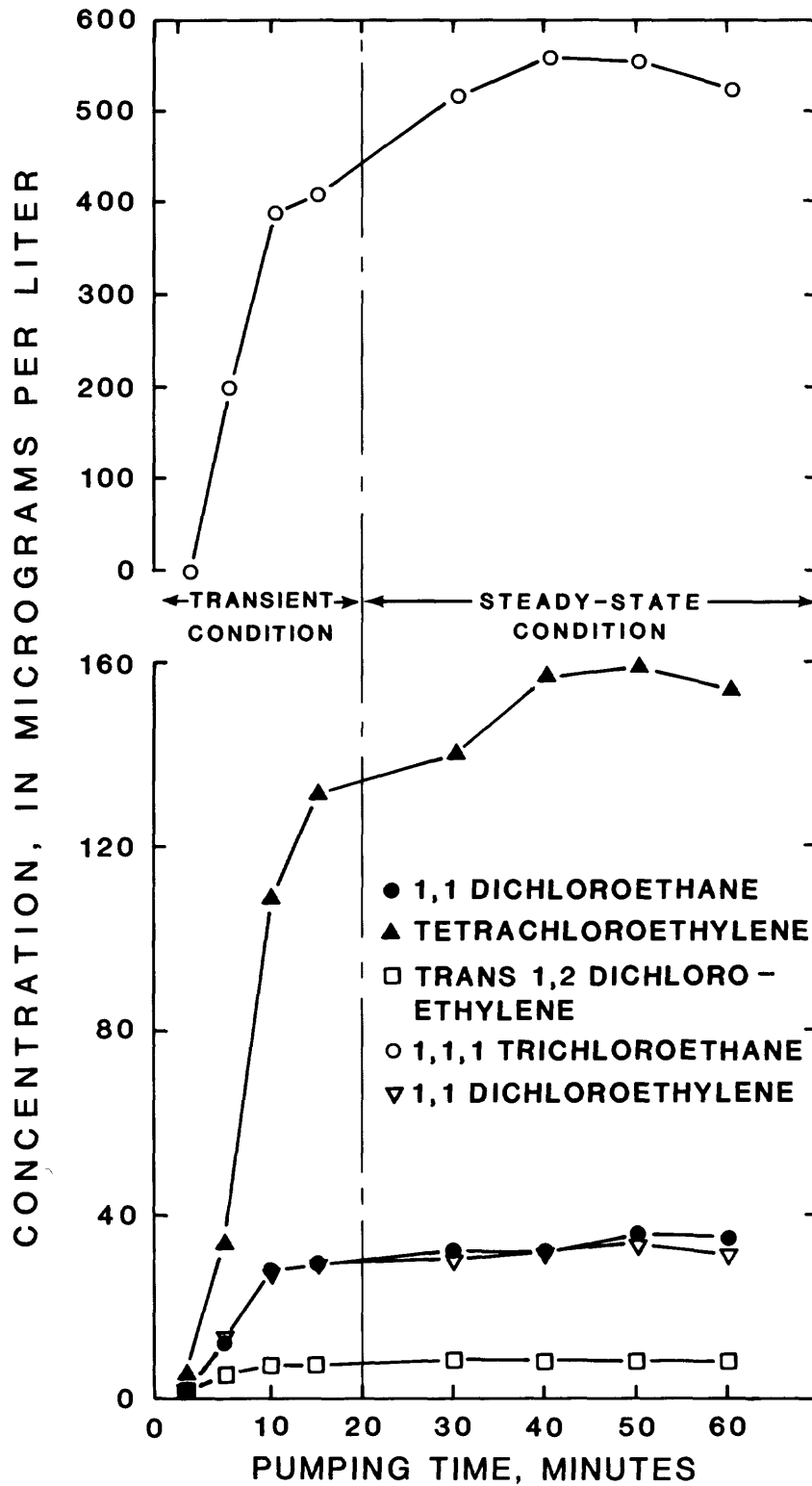


Figure F-4.—Northern New Jersey well, August 14, 1984, purgeable organic compounds concentration time history during well purging.